IN-HOST MODEL FOR THE CO-INFECTION DYNAMICS OF HIGH-RISK HUMAN PAPILLOMAVIRUS (HPV) AND HIV IN THE PRESENCE OF IMMUNE RESPONSE

by

ZVIITEYI CHAZUKA

submitted in accordance with the requirements

for the degree

DOCTOR OF PHILOSOPHY OF SCIENCE

in the subject of

APPLIED MATHEMATICS

at the

UNIVERSITY OF SOUTH AFRICA

SUPERVISOR: DR G.M. MOREMEDI

CO-SUPERVISOR: PROF E.RAPOO

26 SEPTEMBER 2021

Open Rubric

Abstract

HIV/AIDS continues to be a huge global burden having claimed million lives worldwide. It targets the immune system and defence mechanisms against infections such as the human papillomavirus(HPV). HPV can be classified as low-risk or high-risk, with high-risk types (16 and 18) mainly being responsible for cancers, such as cervical cancer in women. HPV is a very common sexually transmitted infection that is given less attention, with many men and women living and spreading infection through unsafe sexual practices. In this thesis we present a mathematical model for the transmission dynamics of HPV in-host in the presence of immune response represented by Cytotoxic T-Lymphocytes cells (CTL). The model presented considers the effects of latent HPV infections and the model dynamics are effectively analysed. The model presents two important reproduction numbers, that is the basic reproduction number $\mathcal{R}_0$ and the CTL reproduction number $\mathcal{R}_K$. The simulation dynamics of the HPV model are presented. We extend the model to include vaccination and it is established that, while immune response plays an important role in eradicating infection, it is not sufficient in totally eradicating HPV. The immune evasion dynamics of HPV are also analysed and conclusions drawn. Finally we also model the effects of HIV on the dynamics of HPV through the co-infection model. It is established that HIV through, immune-suppression, does make it easy for HPV to progress within the body. Simulations presented indicate the benefits of early initiation of antiretroviral therapy (cART/HAART) in the reduction of HPV prevalence. It is envisaged that the results presented in this thesis will motivate the widespread vaccination of women, girls and also boys, especially in developing countries where the HIV transmission rate is high. The study also aims to promote the uptake of HPV screening by women and girls and the practice of safe sexual practices to reduce infection.

Key terms: Human papillomavirus, Immune response, Mathematical model, Ordinary differential equations, Cytotoxic T-Lymphocytes, Reproduction number, Immune-suppression, Vaccination, Infection, High-risk, Low-risk.

Dedication

Dedicated to my best friend and little sister Ayandah Khahlamba, may this motivate you!

Preface

The work described in this thesis was carried out under the supervision of Dr G. M. Moremedi and Prof E. Rapoo, Department of Mathematical Sciences, University of South Africa, from March 2016 to June 2021.

This thesis represents original work by the author and has not otherwise been submitted in any form for any degree or diploma to any other University. Where use has been made of the work of others, it is duly acknowledged in the text.

Signed :

.....

Z. Chazuka (Student)

.....

Dr G.M. Moremedi (Supervisor)

.....

Prof E. Rapoo (Co-Supervisor)

Acknowledgements

Firstly, I would like to thank my Creator God in whom all things began, for giving me all the blessings to complete this work. I wish to thank Chinhoyi University of Technology, School of Natural Sciences and Mathematics for encouraging me to undertake doctoral research studies and supporting me through out my study. Many thanks to my supervisor, Dr G.M. Moremedi who from the beginning believed in my research idea and fully supported all my research activities and fought our so many "academic battles." I also thank my co-supervisor Prof E. Rapoo, for the advice, encouragement and guidance she gave me during my research visit. I am grateful for the facilities made available to me by the Department of Mathematical Sciences at the University of South Africa and UNISA finance for the bursary funding to cover my studies. I also would like to thank my parents Mr and Mrs Chazuka for encouraging me to "take the bull by the horn and conquer the world of mathematics". I also acknowledge the valuable inputs from Dr Morgan (Moffitt Cancer Institute), Dr Carmen Murall, Dr Isaac Segun Oke and Dr Chinwendu E. Madubueze for adding so much academic value to my work through comments, edits and suggestions. I am very grateful to my friend Bright Dodo who sacrificed his time and space in assisting me with my studies. Finally I would like to thank my best friend Modsen Muzira and all my friends spread all over the world for constantly 'nagging' me to complete the work and start something new, finally I have completed the work!

Publications

The following article is an extract from the thesis:

1. Chazuka Z., Moremedi G.M., Rapoo E. (2021) In-Host Dynamics of the Human Papillomavirus (HPV) in the Presence of Immune Response. In: Mondaini R.P. (eds) Trends in Biomathematics: Chaos and Control in Epidemics, Ecosystems, and Cells. BIOMAT 2020. Springer, Cham. https://$doi.org/10.1007/978-3-030-73241-7-6$

2. Z.Chazuka, G.M Moremedi and E.M. Rapoo, (2021). Stability analysis of an in-host high-risk human papillomavirus (HPV) vaccination model. Hindawi, Journal of Applied Mathematics [Under review].

Contents

List of Figures

List of Tables

Chapter 1

Introduction

Throughout the world cervical cancer, a disease that is mainly induced by the human papillomavirus (HPV) emerges as one of the top cancers that affect women. In 2018 cervical cancer was ranked as the fourth most common cancer prevalent among women after breast cancer(first with 2.1 million cases), colon cancer(second with 800 000 cases) and lung cancer (third with 700000 cases) [6]. HPV is one of the most common sexually transmitted viruses globally that is not given much attention with many men and women living and spreading infection daily through unsafe sexual practices. It is a unique circular double-strand deoxyribonucleic acid (DNA) virus [13], that normally enters the cell through the nucleus. Upon entrance, the virus unites its DNA with that of the cell, therefore, creating what is known as a hybrid cell [17]. When this happens, the functionality of the infected cell is seriously altered and it fails to respond well to signals. Sexual intercourse can cause abrasion and this may enable HPV entry into the epithelial cells within the stratified squamous epithelium. Normally epithelial cells are latently infected with HPV for a minimum of 60 days, depending on the severity of the HPV strain [90]. HPV can be classified as high-risk or low-risk. High-risk HPV types are those that can cause cancers such as cervical cancer, cancer of the vagina and vulva, penile cancer among other cancers. Low-risk HPV types are those that cause warts such as genital warts which normally are benign and not cancerous. High-risk HPV types normally have a certain period of latency where the cells are infected and yet do not produce virus while the low-risk types are either cleared by the immune system quickly or evolve into warts.

The human immune response system is made up of the innate immune system and the adaptive immune system. The innate immune system is defined as the general immune system of the body whose function mainly is to provide the body with the first line of defence against

infection [41]. The innate immune system is fast and is not specific as it responds in the same manner to all germs/ pathogens and foreign substances that harm the body. On the other hand, the adaptive immune system specifically targets the germs that causes a particular infection. This type of immune system is said to be specific and has the ability to 'recall" the type of germ/ pathogen it encounters[41]. However, such an immune system is slow to act because the identification mechanism of the pathogen causing the infection may not be easy and straightforward [41]. The interesting thing about the adaptive immune system is that, once it identifies a particular virus and gets rid of it, the next time that the body is attacked by the same virus, detection is easier (memory property) and therefore the response to pathogen is faster. Infections such as HPV however normally make it hard for the adaptive immune response system to identify them or recall their presence. This will be discussed in detail later in chapter 2.

A successful immune response will normally clear off most HPV infections [93, 34]. This is because, the moment that HPV infection enters the epithelial cells through abrasion, an active immune system will be alerted into action by the presence of HPV antigens, thereby prompting the recruitment and activation of the Cytotoxic T Lymphocytes (CTLs) or Natural killer T cells that combat the HPV infection. When the immune response is triggered, antibodies are released to neutralise and fight HPV within the tissues before the infection spreads. However, clearance of HPV does not guarantee that an individual will have permanent immunity. It only allows the individual to move from an infected to a susceptible. A delay in the immune response can cause persistence or a spread of infection to other healthy class cells. Re-infection of the cells can be either through continuous abrasion of the epithelium, through an infected partner, or through increasing the number of sexual partners an individual interacts with [38]. Although the persistence of HPV within the cells is pivotal in the development of cancer lesions, in the long run, there is strong evidence that immune suppression as a result of HIV also has a significant contribution [31]. Figure 1.1 is the world map indicating the distribution of HPV.

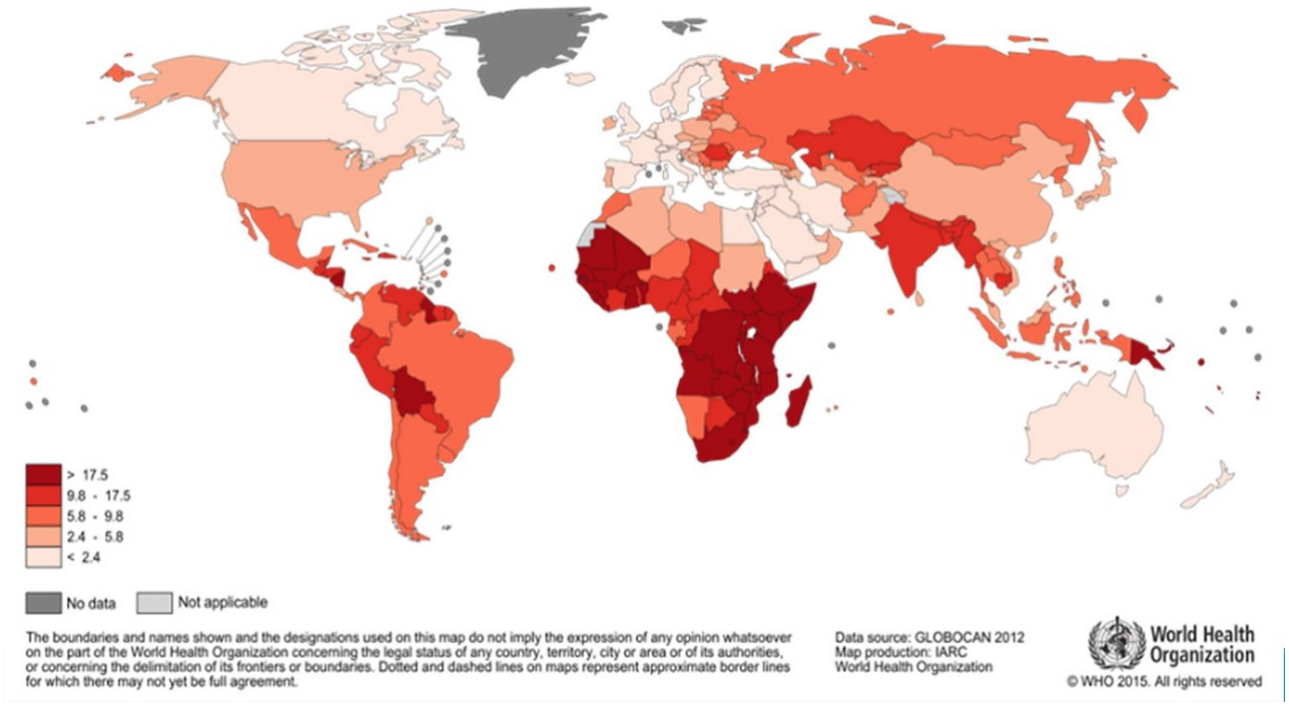

Figure 1.1: Distribution of HPV in the world Source: https://www.fightcancer.org/policy-resources/global-impact-cervical-cancer.

It can be seen that HPV is widely dominant in Africa and this could be attributed to poor health care systems and lack of proper screening methods. There is need for an increase in awareness and vaccine roll-out to reduce the burden of HPV in Africa. A reduction in the cost of acquiring the HPV vaccine would significantly reduce the burden of HPV in Africa and the developing world.

1.1 Classification of HPV types and intervention

There are more than 100 HPV types that are known in literature and out of these types, HPV-16 and HPV-18 are considered to contribute to about 70% of cervical cancer cases or precancerous lesions in women [13]. The other types mainly affect the skin (cutaneous), the lining of the mouth, throat, respiratory tract and anogenital epithelium (mucosal)[12] and may also be responsible for the occurrence of genital warts, head and neck cancers and respiratory tract infections. The various HPV types can be classified as low-risk-HPV types: 6, 11, 42, 43, and 44 or high-risk types: 16, 18, 31, 33, 34, 35, 39, 45, 51, 52, 56, 58, 59, 66, 68, and 70 [12], just to name a few. HPV genotypes are classified under the genus alpha type which is a group of all HPV types that contribute to sexually transmitted infections and cervical lesions or

carcinogens [71]. In this study, we are mainly interested in two high-risk types, i.e HPV-16 and HPV-18, which fall under the $(alpha - 9)$ and $(alpha - 7)$ species cervical carcinogens group [71]. HPV-16 has been found through research to be mainly responsible for cervical cancer lesions with 50% of cancer lesions while the other 20% is assumed to be caused by HPV-18 [84]. Currently, three vaccines are administered worldwide for the prevention of HPV infection; Cervarix, Gardasil and Gardasil-9. Cervarix is a bivalent vaccine that prevents infection against high-risk types, HPV-16 and HPV-18, while Gardasil is a quadrivalent vaccine that prevents infection caused by both high-risk and low-risk types i.e HPV-16, HPV-18, HPV-6 and HPV-11 [90] and Gardasil-9 is a nonavalent vaccine that protects against nine types of HPV which are HPV types, 6,11,16,18,31,33,45,52,58. Unfortunately, at the present moment, Gardasil-9 is only available in the United States of America because HPV vaccines are very expensive and the more strains it prevents against infection the more expensive it is. In Africa, there are a few countries that have successfully administered the vaccine to young girls and women between the ages of 13-26 years. However, governments are being encouraged to promote the vaccine uptake by women and girls as much as possible so as to reduce probable cervical cancer cases in Africa.

The human immune-deficiency virus (HIV) is a retrovirus that is classified under the *lentivirus* genus *retroviridae* group. It mainly targets the CD4+-cells [32, 91]. Immune suppression as a result of HIV infection increases the risk of HPV infection and increases the prevalence of HPV in both men and women [29]. HIV reduces the CD4+ T-cells levels and delays immune response to other infections. It alters the natural history of HPV infection, which then results in the rapid progression of HPV infection to cervical cancer lesions. Therefore clearance of HPV in an immune-compromised system becomes very difficult and individuals become highly susceptible to HPV-related cancers [32]. There is a need to model mathematically the co-infection dynamics of HIV/HPV, in the presence of immune response and intervention in order to ascertain how best at cellular and molecular level HPV infection can be combated in HIV-positive women and girls. Mathematical immunology makes it easier to understand the dynamics of infections within cells and from the results, we can relate it at population level. It follows that from modelling at population model we can find intervention methods and measures that work in reducing infection within a community. Mathematical modelling also helps to assess the community benefits of various intervention methods such as HPV vaccination and cancer screening in the reduction of co-infection in women living with HIV. In this particular study, the aim is to model the effects of interventions such as Combined Antiretroviral Therapy (cART)/Highly

Active Antiretroviral Therapy (HAART) and the HPV vaccine (quadrivalent). We will derive concepts from other mathematical models for HPV such as the work done by [90, 99, 79, 64] just to name a few. The study will make use of data parameters sourced from the literature on HPV and HIV.

1.2 The virology of the Human Papillomavirus (HPV)

The human papillomavirus belongs to a heterogeneous group or class of papillomaviruses. It is a non enveloped deoxyribonucleic acid (DNA) virus that is normally classified as either cutaneous (related to the skin) for instance HPV-6, HPV-11 HPV-42, HPV-43, HPV44, or mucosal (related to the mucosal membrane) for instance HPV types: 16, 18, H31, 33, 35, 39, 45, 51, 52, 56, 58, 59, 68, based on the particular tissue that they affect. HPV is known to be epitheliotropic (*has an affinity or is linked to the epithelium*), is about $(45 - 55)$ nanometer in diameter and can easily induce cell proliferation. There are more than 100 types of papillomaviruses that are known to affect humans. Half of these are known to infect the genital mucosa, making HPV a common sexually transmitted infection. Out of these, the high-risk types HPV-16 and HPV-18 are known to be one of the major causes of cervical cancer around the world. HPV spreads with the assistance of certain early proteins ($E1$ to $E7$) and late proteins ($L1$ and $L2$). The terms "early" and "late" simply indicate that the proteins are expressed "early" in infection or "late" in infection, respectively. The early proteins ($E1$ to $E7$) are expressed on the onset of HPV infection. The E proteins play a role in viral DNA replication, regulation of viral gene transcription, facilitation of viral assembly and release, inducing cell proliferation, inducing DNA synthesis and blocking or preventing cell differentiation [19]. Such early proteins are also responsible for inducing or inhibiting programmed cell death also known as *apoptosis*. On the other hand, the late proteins ($L1$ and $L2$) are responsible for viral amplification, assembly and release on the surface of the cell. Of these two proteins, the $L1$ protein is known as the major structural protein for HPV responsible for viral amplification while the $L2$ protein is the minor capsid protein responsible for the viral assembly and release.

The skin is made up of five layers that provide barriers to infection. The five layers are namely the cornified layer, granular layer, spinous layer, basal layer and the basement membrane. A detailed explanation of these layers is given in Figure 1.2 adapted from the work by Passmore *et al.* [73]. It is a diagram detailing how HPV enters through abrasion of the skin, the dynamics of HPV within epithelial cells and the effects of the different types of proteins mentioned above.

Normally sexual intercourse can cause some abrasion to occur in the genital mucosa and this

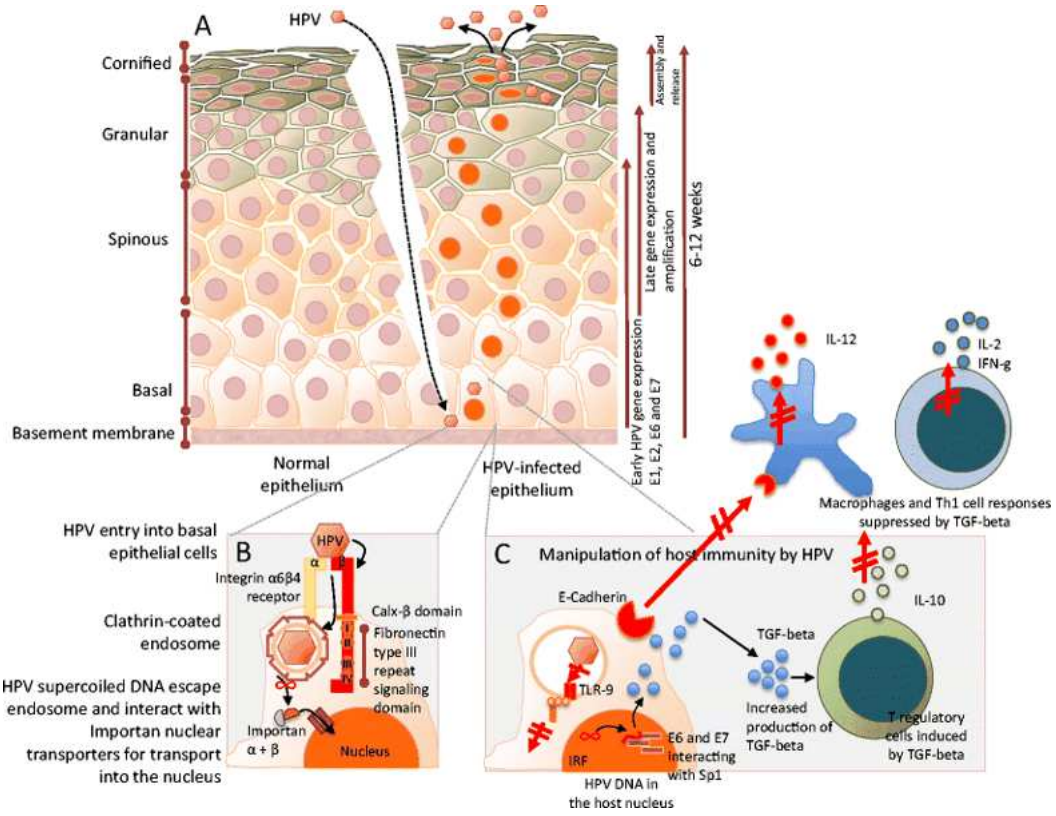

Figure 1.2: Schematic of HPV replication in-host, permission granted and figure adapted from the work by Passmore *et al.* [73].

will make it easy for infections such as HPV to enter through the skin. Figure 1.2 presents the infiltration of HPV in cells within the epithelium as a result of abrasion. The epithelium is made up of five layers and these include the *cornified layer*-which is the main protective barrier that is made up of about 30 layers of polyhedral corneocytes, the *granular layer*-which is a lipid layer barrier formed as a result of keratinocytes losing their nuclei, this barrier provides secondary protection after the cornified barrier, the *spinous layer*-which is a barrier made up of Langerhans cells and immune active cells that fight infection, the *basal layer*-which is a layer that is attached to the basement membrane and is made up of proliferating and non-proliferating keratinocytes. HPV normally targets the basal layer as indicated by **Figure 1.2, panel A.** HPV enters the epithelium through abrasion or tear during sexual intercourse. After this, viral replication occurs within the basal layer and early gene expression occurs, releasing the E-proteins namely $(E1, E2, E6, E7)$ while late gene expression will normally occur within the spinous layer to release the L-proteins ($L1$ and $L2$). The assembly and release of the HPV virions only occurs within the cornified layer as indicated. **Figure 1.2, panel B** presents how HPV enters the basal layer and the types of receptors it uses i.e ($alpha6$ and $beta4$) and the

transport dynamics of HPV DNA to the nucleus of the cell. **Figure 1.2, panel C** shows the immune evasion mechanisms of HPV. Through the expression of the early proteins, $E6$ and $E7$, there is increased production of the $TGF\text{-}\beta$ (the transforming growth factor-beta),which is a cytokine responsible for inhibiting macrophages and CD4+ T-cell responses to HPV infection [73]. **Figure 1.2** also shows the differences between a healthy epithelium and an HPV infected epithelium (left side of panel A(healthy epithelium) versus the right side of panel A (infected epithelium)).

1.3 Mathematical modelling of HIV/HPV co-infection dynamics

Mathematical epidemiology using non-linear ordinary differential equations emanated way back in 1927 when Kermark- Mckendrick developed the first SIR model for the cholera epidemic and since then various models have been developed by researchers using the same approach [45]. Mathematical modelling provides a good framework for understanding the dynamics of cancer and enables biological hypotheses to be tested and conclusions to be drawn through defining oncology in mathematical terms [33]. It helps researchers to understand factors that govern the outbreaks of infectious diseases or cause cancers. It also helps to identify the susceptible individuals in a population and come up with solutions or intervention programs to fight epidemics or pandemics. Modelling can help predict the future trends of an epidemic and therefore help relevant health authorities to prioritize the areas that need immediate health care.

Mathematically, several studies on HPV alone have been performed. Most of the models formulated centred mainly upon the role and effectiveness of HPV vaccines in the reduction and eradication of cervical cancer lesions among women [25, 27, 79, 90]. Igor *et al.* looked at an adaptive Markov chain Monte Carlo simulation model for HPV and from the model, they were able to develop a model for HPV 6/11 based on a Bayesian framework. The study used the posterior predictive inference method to demonstrate the impact of vaccination on the dynamics of HPV [49]. Ryser *et al.* carried out an in-host study on HPV clearance and investigated the role of stochasticity [80]. The results of this particular study indicated that incorporating stochasticity plays an important role in the elimination of HPV-infected cells. Smith? *et al.* developed an in-host HPV model that looked at the transmission dynamics of high-risk (HPV 16/18) and low-risk HPV (6/11) infection at the cellular level. Their model examined the long-

term outcome of the HPV vaccine and the possibility of co-infection within the cells. They also established that in the absence of vaccination there is a probable chance that low-risk and high-risk HPV types may coexist within an individual. However, using a vaccine that targets both low-risk and high-risk types such as a quadrivalent HPV vaccine can be beneficial in the reduction of the coexistence of HPV viral types [90]. The research by Smith? *et al.* encouraged the adoption of the quadrivalent HPV vaccine Gardasil that prevents the occurrence of low-risk and high-risk types in major parts of the developing world. The United States has however gone on to adopt the use of the nonavalent vaccine Gardasil-9 that targets 9 types of HPV.

In 2014 Noor Asir *et al.* developed a model for the development of cancer cells as a result of HPV infection. The results of this study indicated that there are behaviours that the model could exhibit based on the reproduction number, the proliferation rate of precancerous cells and mature rate of precancerous cells to cancerous cells. The simulation results indicated that there were two scenarios to consider that is either the solution of the model would converge to a stable equilibrium where the precancerous cells are under-long term control or the precancerous cells could grow without limit and this promotes malignancy [8]. However, their work did not take into consideration many other aspects that surround the creation of infected cells such as the role of immune response dynamics in the reduction of persistence of HPV. In terms of modelling HPV at population level, several interesting researches have been done. Among these, we have the work by Elbasha Elamin who formulated a two-sex HPV model that analysed the global stability dynamics of HPV in the presence of vaccination using the Lyapunov function approach [26]. The model looked at the interaction between males and females and the spread of HPV among heterosexual individuals. It also considered the role of HPV vaccination and the effects of breakthrough infections on the dynamics of HPV. The results of the study established that the disease-free and endemic equilibrium is only globally asymptotically stable provided that $R_0 < 1$ and $R_0 > 1$ respectively [26], where $\mathcal{R}_0$ is the reproduction number for the model. However, the results did not present any numerical simulations to back up the theoretical work done. Prior interesting works on HPV to follow up Elbasha Elamin include [27, 25]. In 2012, Ribassin-Majed *et al.* published a paper that modelled the transmission of HPV in the presence of vaccination. The authors analysed the dynamics of low-risk HPV types 6/11 which are mainly responsible for genital warts in the presence of a quadrivalent vaccine on French individuals. Results from the study indicated that non-oncogenic types of HPV such as HPV 6/11 could be eradicated provided that vaccine coverage was above 12% [78]. But, the work did not look at other infections that are caused by HPV 6/11 such as the

Recurrent Respiratory Papillomatosis (RRP) that normally affect young children and babies at birth. In another paper, Gurmu *et al.* presented work on a population model and optimal control of HPV with backward bifurcation [37]. In this particular work, the authors developed a deterministic model for HPV governed by ordinary differential equations. The bifurcation analysis of the model established that a backward bifurcation occurs when $\mathcal{R}_0 < 1$ hence, HPV infection can invade the population. The results of the analysis of the model showed that to effectively eradicate HPV within the community there is a need for the use of a combination of HPV screening and vaccination strategies. Their study also recommended that governments in developing countries should promote more education campaigns and programs on HPV. These will promote voluntary screening of HPV to reduce HPV infection through behaviour change [37]. Other most recent studies of note on the mathematical modelling of HPV include that of [111, 70, 2]

HIV/HPV co-infection is a complicated or complex nature of interaction as one infection increases the progression of the other and vice versa [47, 21]. These infections easily co-exist because they both favour an immune-compromised body. HPV normally targets HIV-positive individuals with a CD4+ T-cell count that is below 200 which is normally labelled as AIDS. HIV-negative women have a 4-10 times chance of clearing HPV naturally as compared to HIV-positive women [87]. Several clinical trials that analysed the co-infection dynamics of HIV/HPV have been carried out and most of the results point out the fact that without interventions such as vaccination and cART/HAART it is difficult for the ailing immune system to clear HPV infection and thus reduce the incidences of cervical cancer [87, 30, 48, 1, 58, 51]. Furthermore, studies have also revealed that due to similar modes of transmission via sexual interaction, HPV may also increase the risk of HIV infection in both men and women. The reason for this is that there is an increase in the inflammatory response that increases the recruitment of more susceptible cells that are at risk of HIV infection [24]. Lissouba *et al.* in their meta-analysis study established that individuals with any particular low-risk or high-risk type of HPV at any time within their lifetime have nearly twice the chance of getting infected with HIV as compared to those without any HPV strain [53]. There are preventative measures in place for reducing HIV/HPV infection and these include reducing the number of sexual partners, use of condoms($90 - 99\%$ chance of success), early start and adherence to cART/HAART (for those who are HIV-positive and know their status) and uptake of the HPV vaccine (preferably for those who have never engaged in sexual interaction before). From these measures, reduction of sexual partners and the use of condoms are more of behavioural change issues that have

slim chances of adherence. On the other hand cART/HAART uptake is highly recommended for all HIV-positive individuals in order to increase their CD4+ T-cell count thus there is a need for higher adherence. Currently, there is no conclusive data that supports the effects of HPV vaccination on the reduction of HIV/HPV co-infection, though clinical trials conducted have shown that the HPV vaccines are a safe prevention strategy for individuals with a viral load that is less than 200 cells/μL [46]. The mathematical modelling of the co-infection dynamics of HIV and high-risk HPV is an area that has not been done though biologically it has been proved that co-infection exists. Researches have mainly been devoted to studying the dynamics of HPV [59, 65, 89, 108, 29] just to name a few. In 2006, a meta-analysis study of HPV genotypes among HIV-infected women was done for 5 500 women and it was found that HIV-infected women had a high prevalence of HPV infection (36.3%) among those without any cervical cytological abnormalities[18]. These researches focused on studying the behaviour of HPV at both population and in-host(cellular level). They implored basic statistical analysis due to the nature of the research.

Most mathematical modellers have however prioritised the study of other types of co-infections such as co-infection of HIV-1 and TB [86, 11], HIV and hepatitis C co-infection [81] just to mention a few but none of them analysed the co-infection of HPV and HIV especially among women in Africa where the HIV prevalence is high and the implementations of HPV control measures are poor. It is in this regard that we would like to embark on the mathematical analysis of an HPV/HIV co-infection model that incorporates the effects of immune response and interventions such as vaccination and cART/HAART. In our present model, we are interested mainly in two important cases that is the dynamics of HPV in an immune-competent individual and the dynamics of HPV in an immune-compromised individual (HIV-infected individual). We will maintain in our work the terminology "HPV/HIV".

1.4 Research objectives

The main objective of this research is to develop an in-host mathematical model for the co-infection dynamics of high-risk HPV and HIV in the presence of latent HPV infections, immune response and intervention in the form of vaccination and cART/HAART. The specific objectives are:

1. To develop and analyse the basic in-host HPV model with immune response only;

2. Determine the equilibrium points and reproduction numbers for the basic model;

3. Carry out a bifurcation analysis for the model and establish local and global stabilities of the equilibrium points;

4. To extend the basic HPV model by incorporating vaccination as intervention;

5. To formulate the HPV/HIV co-infection model and analyse its dynamics in the presence of immune response;

6. Analyse through numerical simulations the dynamics of the HPV/HIV co-infection model with immune response, vaccination and treatment;

1.5 Significance of research

The human papillomavirus (HPV) is the main cause of cervical cancer in women worldwide. The susceptibility of the host to HPV is governed by several factors of which immune suppression as a result of HIV infection is chief among them. This necessitates the need to study the viral dynamics of HPV in the presence of an immune suppression caused by HIV. In this particular research, we will develop in-host mathematical models for HPV that incorporate latent infections, immune response and intervention through vaccination and antiretroviral therapy. This research is intended for a wider audience and it is hoped that several research articles will emerge from it. We hope from the results of this research to find ways to help women and girls fight HPV in a world that is HIV prevalent.

1.6 Methodology

We formulate an in-host HPV mathematical model with immune response and intervention in the form of vaccination. The mathematical methods that will be used in this research are:

- The next generation matrix approach to compute the reproduction number for the model [98]. The reproduction number, $\mathcal{R}_0$, is a critical threshold that measures the number of secondary infections that arise as a result of one infectious case.

- Bifurcation analysis will be carried out using the method by Castillo Chavez [15]. A bifurcation is defined as a change in the dynamical behaviour of a system due to changes in parameters or initial conditions. Bifurcations can be either forward (supercritical

bifurcation) or backward (sub-critical bifurcation). In this thesis, we use the Center Manifold Theory illustrated in [15] to establish the existence of a bifurcation for all the models formulated.

- Global stability analysis of the models will be done using the Lyapunov function stability methods. In particular, we will adopt Lyapunov functions from the works by [88, 3].
- Sensitivity analysis for the models developed will be done by computing the elasticity indices of $\mathcal{R}_0$ and also using PRCC methods outlined in [35] and the Tornado plots plotted with R-studio.
- Numerical simulations will be done using the fourth-order Runge Kutta methods embedded in Matlab using an ode45 solver.

1.7 Structure of the thesis

The thesis is arranged as follows: Chapter 2 presents the basics of in-host modelling, the differentiation of between-host modelling from in-host modelling, a brief explanation on the in-host modelling of viruses and finally a review of the work presented by [99] from whom we derive our mathematical model. The review presented carries out analysis of the model that Verma *et al.* did not carry out and this helps to map the modelling work in this thesis. In Chapter 3, the basic HPV model incorporating latency and the immune response is developed. The model is rigorously analysed and also numerical simulations are presented. Chapter 4 presents the co-infection model with which mathematical analysis is presented. Numerical simulations are carried out and discussed effectively to produce conclusions and recommendations in Chapter 5. In the same chapter we also present future work on HPV in-host modelling.

Chapter 2

Literature review

2.1 Between-host models for HPV

Mathematical modelling of infectious diseases plays a very important role in providing solutions to the fight against infection spread and persistence. Many mathematical biology research articles have clearly shown how modelling is an important tool in solving epidemiological issues that affect society. The modelling of HPV has been done both between-host (population level) and in-host (cellular level). Between-host models such as that of Gurmu *et al.* [37] presented the dynamics of HPV within a homogeneously mixing population. The study presented a mathematical model that was made up of the susceptible, the vaccinated, asymptomatic cases, infected cases, recovered cases and cancer cases. The reproduction number was found, local and global stability analysis were performed. Bifurcation analysis carried out proved that there existed a backward bifurcation for the model. The model was also extended to incorporate optimal control and the results showed that to eradicate HPV there was a need for a combination of prevention methods such as vaccination, cancer screening methods and treatment methods.

Elbasha *et al.* [27] formulated a model that assessed the epidemiological impact of administering vaccination strategies. The model compared the cost-effectiveness of vaccinating girls and women only over that of vaccinating both sexes. The results from the model indicated that while vaccinating girls and women only was cost-effective, including boys and men into the vaccination program proved to be more effective as it further reduces the incidences of genital warts, cervical cancer neoplasia and in the long run cervical cancer in women by $97\%, 91\%$ and 91%, respectively [27]. Elbasha again in 2008 [26] presented the global stability of a two-sex vaccination model. The compartmental model used was a basic SIR model and the effective

reproduction number was computed. It was concluded from the model that, when the effective reproduction number is greater than unity, there exists a locally unstable disease-free equilibrium and a globally stable endemic equilibrium and in the long run HPV can be eradicated within the population.

Another interesting population modelling research on HPV is that of Majed *et al.* [78] where they presented an SIS sex model for the transmission dynamics of HPV in the presence of vaccination. This model just like the work by Elbasha *et al.*, established that as long as the vaccinated reproduction number is less than unity, the disease-free equilibrium point is locally stable and therefore HPV can be eradicated [78]. All these models presented yielded interesting results that have made the complex nature of the HPV dynamics better understood. None of these models considered the possibility of latent HPV infections, which is an issue we take note of in our present in-host study.

2.2 In-host modelling

Mathematical models of in-host dynamics of infections such as HPV make it easy to understand the interactions necessary for viruses to spread within cells. Over the years, various in-host models have been presented through research articles, exploring the dynamics of some infections. Most of the pathogens or viruses that affect the body daily are intracellular and they normally affect susceptible target cells. In HPV, the pathogen or virus is the human papillomavirus, and it normally targets susceptible epithelial cells that are in the genital area (genital mucosa) or that are in the oral cavity area (oral mucosa). Upon entering and infecting an epithelial cell, HPV can exit the cell through a process called *lysis*. Lysis entails the destruction of the infected cells (cell death). Not all viruses cause infected cells to undergo lysis, some undergo what is known as *budding* (for example the HIV virus). In budding, the virus grows out of the entire infected cell, so portions of the cell are attached to the virus in the process. The in-host modelling of viruses such as HIV was first proposed by Perelson *et al.* in their work in 1993 [74]. The basic model presented considered susceptible target cells $T(t)$ interacting with infected HIV cells $I(t)$ and the HIV-free virus $V(t)$. The proposed basic model that has now

been extensively expanded to suit many other infections was given by

$$T'(t) = \Lambda - \kappa T(t)V(t) - dT(t),$$

$$I'(t) = \kappa T(t)V(t) - \delta I(t), \tag{2.1}$$

$$V'(t) = pI(t) - cV(t),$$

where Λ is the recruitment of healthy target cells, κ is the transmission rate, d is death rate of the susceptible target cells due to natural causes, δ is the virus induced death of infected cells, p is the production rate of infected cells and c is the natural clearance rate of the virus. The model(2.1) has a disease-free equilibrium given by

$$\mathcal{E}_0 = \left(\frac{\Lambda}{\mu}, 0, 0\right),$$

an endemic equilibrium given by

$$\mathcal{E}_1 = \left(\frac{\delta c}{\kappa p}, \frac{\Lambda\kappa p - d\delta c}{\kappa\delta c}, \frac{c[\Lambda\kappa p - d\delta c]}{\kappa p\delta c}\right),$$

and a basic reproduction number

$$\mathcal{R}_0 = \frac{p\Lambda\kappa}{dc\delta}.$$

In addition to this, stability analysis of the proposed model was done for the cases $\mathcal{R}_0 < 1$ and $\mathcal{R}_0 > 1$. Many other extensions to this basic model for infections such as cholera, malaria, HIV, HPV are further proposed in the literature by [10, 8, 75, 102, 90, 99, 63, 67, 68] just to name a few. These researches have presented rigorous mathematical analyses that establish the local and global stability of the disease-free and endemic equilibrium points. They have also presented the effects of increasing or decreasing the reproduction number $\mathcal{R}_0$, which is defined as the number of secondary infections produced by one infectious cell in the lifetime of the infection, through applying certain interventions. The extensions to the basic model (2.1) include the inclusion of latently infected cells, immune response: in the form of Cytotoxic T-cells (CTLs) and antibodies (B-cells). Such in-host models have also been used to explain the effects of interventions such as vaccination [99, 64] and cART/HAART treatment [106, 94].

Concerning the mathematical modelling of HPV, there a few in-host models as compared to between-host models presented in literature. Smith? *et al.* presented an in-host mathematical model that outlined the link between low-risk HPV and high-risk HPV types. The model considered the impact of vaccination, competition between HPV low-risk and high-risk

types within cells and the co-infection of high-risk and low-risk types on the HPV transmission dynamics. Results from the model showed that, if there is no vaccination, both the low-risk and high-risk viral types co-exist while with vaccination effective eradication is possible [90]. However, Smith? *et al.* did not explore the effect of immune responses in the presence of vaccination which is an important aspect in the dynamics of HPV within the body [90].

Hunt in his thesis presented a mathematical model for HPV in the presence of immune response without vaccination [40]. In this particular work, Hunt developed four models: a basic HPV model with immune response, an extended model with immune response, a memory model that incorporated immune response and delay and an HPV multi-strain model. In the basic HPV model, Hunt established that using the reproduction number one can determine the condition for eradication or persistence of infection. In the memory model, Hunt considered the possibility of developing memory cells after infection and the effect of such memory cells on the reproduction number, $\mathcal{R}_0$. The results indicated that, in the presence of memory cells, as long as the effective reproduction number $\mathcal{R}_e < 1$, HPV infection will eventually be cleared. It would be interesting to establish how memory cells can be activated naturally in all individuals or how they can be boosted. In the immune response delay model, Hunt presented a model that tried to address the effects of a delay in immune response on the onset of infection. The model included a time delay from the start of the infection till the immune response could detect HPV, but there was a flaw in the method because detection of HPV by the immune response is purely a random process [80] and probably a stochastic model would have been more appropriate. The results from the model established that there was a certain critical threshold that when reached meant that the immune response would be activated and viral clearance would drive the system to the disease-free equilibrium. The multi-strain model considered two competing types of HPV and the effect of cross-reactivity of similar types. It also investigated the possibility of competition of resources within cells that are co-infected by multi strains. Results from the study established that such a type of competition is not likely to occur within cells.

Another interesting research to note is that of Murall *et al.* [64] from which we build our work. In this particular work, they created an in-host model for HPV that specifically studied the dynamics of high-risk types in the presence of immune response and vaccination. The model formulated analysed two important aspects with regards to cell dynamics, which is oncogene expression and cell proliferation. In terms of high-risk HPV types, there are two main types of

oncogenes, $E6$ and $E7$, where the "E" stands for early genes that are expressed in the onset of HPV infection [9]. These particular oncogenes normally suppress two important tumour cell suppressor proteins "p53 and pRb" where the former (p53) stands for *(53 kilodalton protein)* named due to its molecular weight and the latter (pRb) is a *retinoblastoma protein* responsible for the prevention of excess cell growth of cancer cells. Oncogenes will normally initiate virus replication because they are responsible for stimulating cell cycle re-entry in the middle epithelial layers and hence facilitate genome amplification [64]. These oncogenes $E6$ and $E7$, when expressed, will block the action of the innate immune system which consequently delays the activation of the adaptive immune response against HPV infection, and therefore, promote persistence of infection. The higher the rate of oncogene expression as a result of HPV infection, the faster the conversion of infected HPV cells into self-proliferating or self-replicating cells. Results from the work by Murall *et al.* concluded that removing the ability of HPV to delay effector cell invasion consequently caused $\mathcal{R}_0 > 1$ for cell types with higher oncogene expression. The results also indicated that vaccine-imposed immunity could create higher oncogene expression which in turn has serious consequences on the host [64]. Furthermore, the model showed that high antibody response is an effective way of reducing the number of infected cells and consequently reduce the free HPV virions produced. They concluded that it may be important to consider if reducing HPV is better done using HPV vaccines that can increase oncogene expression and eventually cause a viral load increase or maybe to use other preventative medical health care mechanisms for the highly virulent types.

The final model under our consideration is that by Verma *et al.* who modified the model by Murall *et al.* to include the effects of immune suppression. The model presented a mechanistic model for the in-host dynamics of HPV in the presence of HIV within the oral mucosa. The model took into consideration cART/HAART as an intervention method. It also considered the effects of impaired HPV-specific effector cell responses due to the effects of HIV immune suppression. The model was further used to analyse the probable course of HPV in the presence of HIV though in this study they did not look at the effect of vaccination against HPV as a treatment option, an aspect we wish to take up in our study. The model identified the mechanisms by which HIV alters HPV infection within the oral mucosa. The results indicated that in the presence of cART/HAART, HPV infections can in the long run reduce due to the constant replenishment of CD4+ T cells and the protective immunity provided by cART/HAART. The discussion of aforementioned models discussed varies in terms of the purpose of research and model formulations. It can be seen that over the years there has been an improvement in the

in-host modelling dynamics of HPV with more meaningful conclusive results being obtained and published. However, all the above models did not take into consideration the effect of latent HPV infections which, if not taken into consideration, can become persistent HPV infections. This prompts us to develop a model that encompasses latent HPV infections, immune response and vaccination. We also extend the model created to assess the effect of immune suppression as a result of HIV.

It is important to note that "in-host" and " within-host" modelling are terms that mean the same thing in the modelling of infectious diseases. For the sake of consistency, we will use the term "in-host" throughout this research.

2.3 The role of immune response in HPV dynamics

High-risk human papillomaviruses $16, 18, 31, 45$, are major contributory causes of cervical cancer in women worldwide and about 80% of women are infected by HPV through sexual activities within their lifetime [82]. Due to infection and re-infection, some develop persistent HPV infections that lead to cancer lesions, while some can clear the HPV infection naturally provided it is detected by the immune system. A fully functional human body is well organized with great defences against infection and re-infection. It has the skin as the immediate defence mechanism since it has a tough layer of cells called (*keratinocytes*) that are constantly producing keratin. The skin is equipped with glands that secrete substances such as fatty acids and enzymes that break down bacteria. It is important to always keep the skin intact to avoid possible attacks by viruses. However, during sexual intercourse, viruses such as HPV take advantage of abrasion of the epidermal lining of the genital or oral mucosa [99] to enter into the body. A mucous membrane is a lining that covers the surface of internal organs such as the inside of the mouth (*oral mucosa*) [99], the inside of the nose (*nasal or respiratory mucosa*), the vagina and urethral (*genital mucosa*) just to name a few. If an infection is detected within the body, the immune system is prompted into action and fights the infection before it spreads throughout the body but this depends on how good the immune response of the body is to infection.

Most HPV cases in women are cleared naturally by the immune system within a year provided there is detection. A certain amount of the virus will lie dormant or latent until either it is cleared by the immune system or it develops into persistent HPV infection. HPV normally targets the squamous epithelial cells which are typically not immune cells but have immune

functions such epithelial tight junctions that limit the entry of HPV. The immune response plays an important role in clearing most infections that constantly affect us daily. It is the body's defence system that is prompted into action the moment a "foreign agent" is detected [92]. The immune system is classified as "innate" or adaptive, where the innate immune system is defined as the immediate line of defence that is prompted into action when abnormal cell growth or death is detected. It is made up of cytokines, phagocytes and soluble proteins that provide chemical signals of abnormalities within cells. The main function of the innate immune response is to trigger the adaptive immune response through creating inflammatory responses [92]. These inflammatory responses are only triggered by the damage of tissues as a result of infection and normally manifest in the form of signs of fever, swellings and redness of the skin among many other signs.

The innate immune response is the defence system that is made up of all the defence cells which include natural killer T-cells (*effector lymphocytes of the innate immune system that are responsible for the control of tumours and infections* [100]), keratinocytes cells (*cells that make up the epidermis*), Langerhans cells (*cells that are found in the basal and super basal layer of the epidermis and are responsible for antigen/toxin presentation on the epidermal surface for detection by the immune system [16]*), dendritic cells *(cells found in the skin and are responsible for antigen presentation and act as messengers between the innate and adaptive immune response [14])*, just to mention a few [92]. These cells create a link between the innate immune response system and the adaptive immune response, therefore, prompting T and B cells that attack viruses such as HPV [4]. Interestingly, viruses such as HPV are however very "clever" in concealing their presence within cells as they devise many ways of avoiding detection by the immune system thus creating an anti-inflammatory micro environment[4]. The simplest way HPV may evade the immune system is by infecting and replicating within the keratinocytes. The obvious reason for this being that keratinocytes have a short life span of approximately 30 days. Thus, invading such cells, the HPV virus avoids abnormal cell death that can be detected by the immune system. By hiding within the keratonicytes HPV succeeds in ensuring that there is no production of HPV virions, no abnormal cell death, no inflammation and consequently no detection. Abnormal cell death is crucial as it triggers inflammatory responses that prompt the adaptive immune response into action and this makes the survival of the virus within the body very difficult.

Invading the keratinocytes, however, is not the only way of evading the immune system used

by HPV, it can also happen through the $E6$ and $E7$ proteins [39]. The $E6$ protein is known as the major transformer protein for most papillomaviruses. It can change from one conformation to another and therefore automatically change its function. Due to this, the $E6$ protein subsequently interferes with the function of the $p53$ protein, which is a cellular tumour suppressor protein, and this promotes the growth of tumour cells [39]. The $p53$ protein is also responsible for temporarily blocking cell replication provided that there is a need for DNA repair within the body till the repair process is complete [47]. If there is HPV infection, the $E6$ and $E7$ proteins are responsible for inhibiting the action of the $p53$ protein and therefore cell replication becomes uncontrolled, promoting the occurrence of tumour cells. The effect of the $E6$ and $E7$ promoting rapid cell proliferation of infected cells is what we are considering in this model, based on the work by Verma *et al* [99].

HPV will evade the immune system through many other evasion mechanisms such as varying the expressions of cytokines (*substances that are secreted by cells and therefore induce inflammatory responses*) and chemo-attractants (*substances that attract mobile cells*). It can also promote the alteration of antigen presentation that facilitates the activation of T-cells. T-cells are lymphocytes or types of white blood cells that are responsible for cell-mediated immunity. These particular cells have a T-cell receptor on the cell surface that differentiates them from other cells such as B-cells and natural killer cells. So based on this little narration it is evident that persistent HPV infection is only deemed "successful" if the unique circular double-strand DNA virus manages, at all costs, to evade detection by the immune system. This leads to interesting mathematical modelling research of a little ''clever virus" in the presence of immune response which is the scope of this research.

2.4 A review of an HIV/HPV in-host co-infection model

The work under review presents an HIV/HPV co-infection model governed by ordinary differential which shows the effect of HIV/AIDS (*tat protein*), HPV oncogene expression and immune response on the dynamics of the spread of HPV within an HIV immune-compromised system. The mathematical models presented establish if there are any differences in terms of results obtained from solving the deterministic models formulated. For the sake of simplicity, the co-infection model is split into two sub-models that are analysed to establish the equilibrium points, the reproduction number, local and global stability. From the results of the sub-models, it is established that the co-infection model is locally and globally stable. The work by Verma

et al. [99] is reviewed as it is of interest to our HPV research. The model by Verma *et al.* is made up of two-sub models (HIV model and an HPV model) and is based on the work by Murall *et al.* [64]. This particular co-infection model was not analysed by the authors for the stability of equilibria, reproduction number and global stability analysis. To incorporate some of its aspects in our model we carry out a preliminary analysis on the model's equilibrium points. The results obtained will help us in the formulation of an HPV in-host model for this research.

2.4.1 Model formulation of HIV/HPV co-infection model.

The HIV/HPV co-infection model by Verma *et al.* made use of a simple basic HIV sub-model with treatment. It is assumed that: Healthy target cells, $T_h(t)$, are produced at a rate, s, and are assumed to die naturally at a rate, d. The transmission rate of HIV as a result of the interaction of the healthy target cells and the HIV virus $V_h(t)$, occurs at a rate, β. Infected target cells, $I_h(t)$, are cleared at rate, δ while N_1 is the burst size produced by the infected target cells and the HIV virions are cleared naturally at rate, c_1. In the presence of combined Anti-Retroviral Therapy (cART), the HIV model is modified to include the presence of the reverse transcriptase and protease inhibitor functions. The reverse transcriptase inhibitor, ϵ_{RT}, which is responsible for blocking the conversion of HIV RNA to HIV DNA while the protease inhibitor,ϵ_{PI}, is responsible for blocking new HIV virions from becoming mature HIV virions. This leads to the HIV sub-model given by the following differential equations

$$\begin{aligned} T_h'(t) &= s - dT_h - (1-\epsilon_{RT})\beta T_h V_h, \\ I_h'(t) &= (1-\epsilon_{RT})\beta T_h V_h - \delta I_h, \\ V_h'(t) &= (1-\epsilon_{PI})N_1 \delta I_h - c_1 V_h. \end{aligned} \tag{2.2}$$

Throughout the thesis the notation $T_h(t) = T_h$, $I_h(t) = I_h$ and $V_h(t) = V_h$ will be used to describe HIV cell classes.

The HPV sub model has the infected target cells $Y_1(t)$ where the rate of transmission of HPV virions, $W(t)$, through interaction with the healthy target cells is given by ψ. The cells die naturally at rate, μ, and are cleared at a CTL killing rate, a, and the HPV specific CTLs are represented by $E(t)$. The expansion rate of effector cells specific to HPV with carrying capacity, K is assumed to be, ω. Due to oncogene expression that occurs at a rate, ϵ, $Y_1(t)$ cells

are converted into transit amplifying cells $Y_2(t)$ that are self-proliferating. These cells grow at a rate $r\epsilon$ proportional to their densities, where r is the transit amplifying rate. Both $Y_1(t)$ and $Y_2(t)$ produce HPV virions $W(t)$ at a rate, k, and these virions are cleared at a rate c_2 due to antibody action. The model also assumes that $N_2 - Y_1$ represents the concentration of uninfected cells within the basal layer with an epithelial concentration of ϕ. This leads to the HPV sub model given by the following differential equations

$$\begin{aligned} Y_1'(t) &= \frac{\psi W(N_2 - Y_1)}{\phi + N_2 - Y_1} - Y_1(\epsilon + \mu + aE), \\ Y_2'(t) &= \epsilon Y_1 + Y_2(r\epsilon - \mu - aE), \\ W'(t) &= \mu k(Y_1 + Y_2) - c_2 W, \\ E'(t) &= \omega Y_2 E\left(\frac{E}{\bar{K}}\right). \end{aligned} \tag{2.3}$$

To maintain consistency throughout the thesis, we make the following changes to the HPV model presented; class $W(t)$ is renamed class $V(t)$, class $E(t)$ is renamed class $K(t)$, this is because the letters E, W have been used for different purposes throughout the thesis. The co-infection model under study is a complete model that incorporates the effect of trans-activator of transcription (*tat*) protein. HIV *tat* protein is a regulatory protein that enhances viral transcription. In relation to HIV/HPV dynamics, *tat* protein is secreted from the intra-epithelial immune cells. It disrupts the epithelial tight junctions that seal adjacent epithelial cells and restrict the easy flow of viruses such as HPV [5, 97, 99]. In the co-infection model, the total available epithelial cells are increased as a result of *tat* protein from the regular N_2 to $N_2(1+pV)$ where p is the effect of *tat* protein secreted by an HIV virion, V. This leads to the co-infection

model governed by the following differential equations

$$\begin{aligned}
T_h'(t) &= s - dT_h - (1-\epsilon_{RT})\beta T_h V_h, \\
I_h'(t) &= (1-\epsilon_{RT})\beta T_h V_h - \delta I_h, \\
V_h'(t) &= (1-\epsilon_{PI})N_1 \delta I_h - c_1 V_h, \\
Y_1'(t) &= \frac{\psi W(N_2(1+pV_h) - Y_1)}{\phi + N_2(1+pV_h) - Y_1} - Y_1(\epsilon + \mu + aE), \\
Y_2'(t) &= \epsilon Y_1 + Y_2(r\epsilon - \mu - aE), \\
W'(t) &= \mu k(Y_1 + Y_2) - c_2 W, \\
E'(t) &= \omega Y_2 E(1 - \frac{E}{\bar{K}}),
\end{aligned} \tag{2.4}$$

with initial conditions $T_h(0) = T_{h0}$, $I_h(0) = I_{h0}$, $V_h(0) = V_{h0}$, $Y_1(0) = Y_{10}$, $Y_2(0) = Y_{20}$, $W(0) = W_0$, and $E(0) = E_0$. System (2.4) is biologically feasible within the region

$$\Omega = \{(T_h, I_h, V_h, Y_1, Y_2, W, E) \in \mathcal{R}^{7+} : N(t) \leq \frac{s}{d}\}.$$

Model (2.4) represents cellular dynamics of human cells and viruses, and therefore we prove that for all time t, the solutions $(T_h, I_h, V_h, Y_1, Y_2, W, E)$ of system (2.4) with positive initial data are positive and bounded in Ω.

2.5 Positivity and boundedness of solutions

In the proof of positivity of solutions, we show that all solutions for model (2.4) remain positive for all time, t. Accordingly, we state and prove the following theorem below;

Theorem 1. *Let all parameters of system (2.4) be non-negative constants. A non-negative solution given by, $T_h(t), I_h(t), V_h(t), Y_1(t), Y_2(t), W(t), E(t)$ for system (2.4) exists for all the state variables with initial conditions given by $T_{h0} > 0, I_{h0} \geq 0, V_{h0} \geq 0, Y_{10} \geq 0, Y_{20} \geq 0, W_0 \geq 0, E_0 \geq 0 \ \forall \ t \geq 0$.*

Proof. To prove the above theorem we use the method outlined in [66]. Using the first equation to model system (2.4) we have

$$\begin{aligned} T_h'(t) &= s - dT_h - (1-\epsilon_{RT})\beta T_h V_h, \\ &> -(d + (1-\epsilon_{RT})\beta V_h)T_h. \end{aligned} \tag{2.5}$$

Using separation of variables to solve the above differential equation, we obtain

$$\frac{dT}{T_h} > -(d + (1-\epsilon_{RT})\beta V_h)T_h, \tag{2.6}$$

which by integration yields

$$T(t) = Ae^{-\int_0^t (d+(1-\epsilon_{RT})\beta V_h(s))ds}, \tag{2.7}$$

where A is a constant of integration. Taking initial conditions: at $t = 0, T_h(0) = T_{h0}$, such that it can be seen that $A = T_0$ and therefore it follows that

$$T_h(t) > T_{h0}e^{-\int_0^t (d+(1-\epsilon_{RT})\beta V_h(s))ds}, \tag{2.8}$$

which means that $T_h(t) > 0, \forall\ t > 0$. The solution for $T_h(t)$ is strictly positive for all $t \in [0, t^*)$. Similarly, it also follows that

$$\begin{aligned} I_h(t) &> I_h(0)e^{-\int_0^t \delta I_h(s)ds}, \\ V_h(t) &> V_h(0)e^{-\int_0^t c_1 V_h(s)ds}, \\ Y_1(t) &> Y_1(0)e^{-\int_0^t (\epsilon+\mu+aE(s))ds}, \\ Y_2'(t) &> Y_2(0)e^{-\int_0^t (aE(s)+\mu-r\epsilon)ds}, \\ W(t) &> W(0)e^{-\int_0^t c_2 W(s)ds}, \\ E(t) &> E(0)e^{-\int_0^t \frac{E(s)^2 \omega Y_2(s)}{K}ds} \end{aligned} \tag{2.9}$$

and this shows that $T_h(t) > 0,\ \ I_h(t) > 0,\ \ V_h(t) > 0\ \ Y_1(t) > 0,\ \ Y_2(t) > 0,\ \ W(t) > 0,\ \ E(t) > 0,\ \ \forall\ \ t \in [0, t)$. This completes the positivity proof. □

Theorem 2. *A solution to system (2.4) with initial conditions,* $T_{h0} > 0, I_{h0} \geq 0, V_{h0} \geq 0, Y_{10} \geq 0, Y_{20} \geq 0, W_0 \geq 0, \forall\ t \geq 0,$ *exists and is unique in* $\mathcal{R}_+^7, \forall\ t \geq 0.$

Existence of solutions in mathematical biology helps in ascertaining if a solution to the developed model exists and is unique. The existence of such a solution enables us to go ahead and find approximate solutions to the model and forecast the dynamics of infection spread. To prove existence, we state the following theorem by Derrick and Grossman [23]

Theorem 3. *Let Ω denote a region given by*

$$|t - t_0| \leq a, \| x - x_0 \| \leq 1, x = (x_1, x_2, ..., x_n), x_0 = (x_{10}, x_{20}, ...x_{n0}) \tag{2.10}$$

and suppose that $f(x,t)$ satisfies a Lipschitz condition given by

$$\| f(t, x_1) - f(t, x_2) \| \leq M \| x_1 - x_2 \|, \tag{2.11}$$

each time pairs (t, x_1) and (t, x_2) belong in Ω where M is a positive constant. Then, there exists a constant, $C \geq 0$, such that a unique continuous vector solution of $x(t)$ for model (2.4) within the interval of $(t - t_0) \leq C$ exists. The condition is satisfied by the requirement that the partial derivatives $\dfrac{\partial f_i}{\partial x_j}$ for $i, j = 1, 2, 3, ...$ are continuous and bounded in Ω.

A Lipschitz condition is defined to prove theorem (3) as follows

Definition 1. *Let $\mathbb{E}$ be an open subset of $\mathbb{R}^n$. Then, a function $f : \mathbb{E} \longrightarrow \mathbb{R}^n$ is said to satisfy a Lipschitz condition on $\mathbb{E}$ if there is a positive constant k_1 such that $\forall x, y \in \mathbb{E}$,*

$$| f(x) - f(y) | \leq k_1 | x - y | .$$

Therefore f is said to be locally Lipschitz on $\mathbb{E}$ for each point $x_0 \in \mathbb{E}$ if there is an $\epsilon-$ neighbourhood of x_0, $\eta_\epsilon(x_0)$ and a positive constant $k_0 > 0$ such that $\forall (x, y) \in \epsilon-$neighbourhood x_0,

$$| f(x) - f(y) | \leq k_0 | x - y | .$$

By an $\epsilon-$neighbourhood of x_0 and $\eta_\epsilon(x_0)$ we imply that an open ball of positive radius exists i.e.

$$\eta_\epsilon(x_0) = \{x \in \mathbb{R}^n | \ | x - x_0 | < \epsilon\}.$$

We define what is meant by *locally Lipschtz* and prove the following lemma as in the work by [76].

Lemma 1. *Let $\mathbb{E}$ be an open subset of $\mathbb{R}^n$ and let $f : \mathbb{E} \to \mathbb{R}^n$. Then if $f \in C^1(\mathbb{E})$, f is locally Lipschitz on $\mathbb{E}$.*

Proof. Provided that $\mathbb{E}$ is an open subset of $\mathbb{R}^n$ and given that $x_0 \in \mathbb{E}$, then it follows that $\exists\ \epsilon > 0$ such that $\eta_\epsilon(x_0 \subset \mathbb{E})$. Let $k_1 = \max_{|x-x_0| \leq \frac{\epsilon}{2}} \parallel Df(x) \parallel$ be the maximum of the continuous function $Df(x)$ on a compact set given by $\mid x - x_0 \mid \leq \frac{\epsilon}{2}$ and $\eta_{\frac{\epsilon}{2}}(x_0)$ be the $\frac{\epsilon}{2}-$ neighbourhood of x_0. For $x, y \in \eta_{\frac{\epsilon}{2}}(x_0)$, we set $u = x - y$ such that $x + su \in \eta_{\frac{\epsilon}{2}}(x_0)$ for $0 < s < 1$ since $\eta_{\frac{\epsilon}{2}}(x_0)$ is a convex set (this is a set such that for any two points within $\eta_{\frac{\epsilon}{2}}(x_0)$ the line joining the two points will always lie within the set $\eta_{\frac{\epsilon}{2}}(x_0)$. We define the function

$$F : [0, 1] \to \mathbb{R}^n$$

by $F(s) = f(x + su)$ and by differentiating $F(s)$, yields

$$F'(s) = u \times D(x + su), \tag{2.12}$$

which can be expressed as

$$F'(s) = u \times Df(x + su). \tag{2.13}$$

Hence

$$f(y) - f(x) = F(1) - F(0) \tag{2.14}$$

which implies that

$$\int_0^1 F'(s)ds = \int_0^1 u \times Df(x + su)ds \tag{2.15}$$

and

$$\begin{aligned} \mid f(y) - f(x) \mid \ &\leq \ \int_0^1 \mid u \times Df(x + su) \mid ds, \\ &\leq \int_0^1 \parallel Df(x + su) \parallel \mid u \mid ds, \\ &\leq k_1 \mid u \mid = k_1 \mid y - x \mid . \end{aligned} \tag{2.16}$$

This ends the proof of Lemma 1 and leads to the proof for existence of unique solutions for model system (2.4). □

Proof. Let model model system (2.4) be expressed as follows

$$\begin{aligned} f_1 &= s - dT_h - (1 - \epsilon_{RT})\beta T_h V_h, \\ f_2 &= (1 - \epsilon_{RT})\beta T_h(t) V_h - \delta I, \\ f_3 &= (1 - \epsilon_{PI}) N_1 \delta I_h - c_1 V_h, \end{aligned}$$

$$
\begin{aligned}
f_4 &= \frac{\psi W(N_2(1+pV_h)-Y_1)}{\phi+N_2(1+pV_h)-Y_1} - Y_1(\epsilon+\mu+aE),\\
f_5 &= \epsilon Y_1 + Y_2(r\epsilon-\mu-aE),\\
f_6 &= \mu k(Y_1+Y_2) - c_2 W,\\
f_7 &= \omega Y_2 E(1-\frac{E}{\bar{K}}).
\end{aligned} \tag{2.17}
$$

Finding the partial derivatives, we obtain

$$
\begin{array}{llll}
|\frac{\partial f_1}{\partial T_h}|=d<\infty, & |\frac{\partial f_1}{\partial I_h}|=0<\infty, & |\frac{\partial f_1}{\partial V_h}|=0<\infty, & |\frac{\partial f_1}{\partial Y_1}|=0<\infty,\\
|\frac{\partial f_1}{\partial Y_2}|=0<\infty, & |\frac{\partial f_1}{\partial W}|=0<\infty, & |\frac{\partial f_1}{\partial E}|=0<\infty, & |\frac{\partial f_2}{\partial T_h}|=0<\infty,\\
|\frac{\partial f_2}{\partial I_h}|=\delta<\infty, & |\frac{\partial f_2}{\partial V_h}|=0<\infty, & |\frac{\partial f_2}{\partial Y_1}|=0<\infty, & |\frac{\partial f_2}{\partial Y_2}|=0<\infty,\\
|\frac{\partial f_2}{\partial W}|=0<\infty, & |\frac{\partial f_2}{\partial E}|=0<\infty, & |\frac{\partial f_3}{\partial T_h}|=0<\infty, & |\frac{\partial f_3}{\partial I_h}|=0<\infty,\\
|\frac{\partial f_3}{\partial V_h}|=c_1<\infty, & |\frac{\partial f_3}{\partial Y_1}|=0<\infty, & |\frac{\partial f_3}{\partial Y_2}|=0<\infty, & |\frac{\partial f_3}{\partial W}|=0<\infty,\\
|\frac{\partial f_3}{\partial E}|=0<\infty, & |\frac{\partial f_4}{\partial T_h}|=0<\infty, & |\frac{\partial f_4}{\partial V_h}|=0<\infty, & |\frac{\partial f_4}{\partial Y_1}|=0<\infty,\\
|\frac{\partial f_4}{\partial Y_2}|=0<\infty, & |\frac{\partial f_4}{\partial W}|=0<\infty, & |\frac{\partial f_4}{\partial E}|=a<\infty, & |\frac{\partial f_5}{\partial T_h}|=0<\infty,\\
|\frac{\partial f_5}{\partial I_h}|=0<\infty, & |\frac{\partial f_5}{\partial V_h}|=0<\infty, & |\frac{\partial f_5}{\partial Y_1}|=\epsilon<\infty, & |\frac{\partial f_5}{\partial Y_2}|=|r\epsilon-\mu|<\infty,\\
|\frac{\partial f_5}{\partial W}|=0<\infty, & |\frac{\partial f_5}{\partial E}|=a<\infty, & |\frac{\partial f_6}{\partial T_h}|=0<\infty, & |\frac{\partial f_6}{\partial I_h}|=0<\infty,\\
|\frac{\partial f_6}{\partial V_h}|=0<\infty, & |\frac{\partial f_6}{\partial Y_1}|=k\mu<\infty, & |\frac{\partial f_6}{\partial Y_2}|=k\mu<\infty, & |\frac{\partial f_6}{\partial W}|=c_2<\infty,\\
|\frac{\partial f_6}{\partial E}|=0<\infty, & |\frac{\partial f_7}{\partial T_h}|=0<\infty, & |\frac{\partial f_7}{\partial I_h}|=0<\infty, & |\frac{\partial f_7}{\partial V_h}|=0<\infty,\\
|\frac{\partial f_7}{\partial Y_1}|=0<\infty, & |\frac{\partial f_7}{\partial Y_2}|=0<\infty, & |\frac{\partial f_7}{\partial E}|=0<\infty. &
\end{array} \tag{2.18}
$$

It can be seen that all the partial derivatives exist and are continuous. Therefore, by Lemma 1, there exists a unique solution for model (2.4) within the region Ω. □

2.6 Analysis of the sub-model for HIV

The HIV sub-model is given by

$$\begin{aligned} T_h'(t) &= s - dT_h - (1-\epsilon_{RT})\beta T_h V_h, \\ I_h'(t) &= (1-\epsilon_{RT})\beta T_h V_h - \delta I_h, \\ V_h'(t) &= (1-\epsilon_{PI})N_1 \delta I_h - c_1 V_h, \end{aligned} \tag{2.19}$$

with $T_h(0) = T_{h0} \geq 0, \quad I_h(0) = I_{h0} \geq 0, \quad V_h(0) = V_{h0} \geq 0$ as initial conditions and the total population of cells, $N(t) = T_h(t) + I_h(t)$, excluding the virus, is such that

$$\Omega_1 = \{(T_h, I_h, V_h) \in \mathcal{R}^{3+} : N(t) \leq \frac{s}{d}\}.$$

2.6.1 Equilibrium analysis and reproduction number $\mathcal{R}_{0H}$

The disease-free equilibrium for the sub-model is given by $\mathcal{E}_0 = \left(\frac{s}{d}, 0, 0\right)$. The basic reproduction number, $\mathcal{R}_{0H}$, is computed using the next generation method approach by [98] as follows

$$F_m = \begin{bmatrix} (1-\epsilon_{RT})\beta T_h V_h \\ 0 \end{bmatrix}, \tag{2.20}$$

and

$$V_m = \begin{bmatrix} \delta I_h \\ c_1 V_h - (1-\epsilon_{PI})N_1 \delta I_h \end{bmatrix}, \tag{2.21}$$

and then the F_m and V_m matrices are given by

$$\mathcal{F} = \begin{bmatrix} 0 & \frac{\beta s(1-\epsilon_{RT})}{d} \\ 0 & 0 \end{bmatrix}, \tag{2.22}$$

and

$$\mathcal{V} = \begin{bmatrix} \delta & 0 \\ -(1-\epsilon_{PI})N_1\delta & c_1 \end{bmatrix}, \tag{2.23}$$

such that the spectral radius $\rho(\mathcal{F}\mathcal{V}^{-1})$ is given by

$$\rho(\mathcal{F}\mathcal{V}^{-1})) = \mathcal{R}_{0H} = \frac{\beta s N_1 (1-\epsilon_{RT})(1-\epsilon_{PI})}{c_1 d}. \tag{2.24}$$

It is important to note that $\mathcal{R}_{0H}$ is strictly positive provided that $(1-\epsilon_{RT}) > 0$ and $(1-\epsilon_{PI}) > 0$. This reproduction number is also known as the effective reproduction number for the HIV treatment model.

Theorem 4. *The disease-free equilibrium for the HIV sub-model is locally asymptotically stable when* $\mathcal{R}_{0H} < 1$ *and unstable when* $\mathcal{R}_{0H} > 1$.

Proof. To prove local stability of the disease-free-equilibrium using the Jacobian method, we adopt the method outlined in [77] as follows

$$J(\mathcal{E}_0) = \begin{bmatrix} -d & 0 & -\dfrac{\beta s(1-\epsilon_{RT})}{d} \\ 0 & -\delta & \dfrac{\beta s(1-\epsilon_{RT})}{d} \\ 0 & N_1(1-\epsilon_{PI})\delta & -c_1 \end{bmatrix}, \tag{2.25}$$

and the sub matrix of the Jacobian corresponding to the infectious classes is given by

$$J(\epsilon_{01}) = \begin{bmatrix} -\delta & \dfrac{\beta s(1-\epsilon_{RT})}{d} \\ N_1(1-\epsilon_{PI})\delta & -c_1 \end{bmatrix}. \tag{2.26}$$

The determinant of $J(\epsilon_{01})$ is given by

$$\begin{aligned} Det(J(\epsilon_{01})) &= \delta c_1 - \frac{\beta s N_1 \delta (1-\epsilon_{RT})(1-\epsilon_{PI})}{d}, \\ &= \delta c_1 \left[1 - \frac{\beta s N_1 (1-\epsilon_{RT})(1-\epsilon_{PI})}{c_1 d}\right], \\ &= \delta \left[1 - \mathcal{R}_{0H}\right]. \end{aligned} \tag{2.27}$$

It can be seen that $tr(J(\epsilon_{01})) = -\delta - c_1 < 0$ and when $\mathcal{R}_{0H} < 1$, $Det(J(\epsilon_{01})) > 0$ and when $\mathcal{R}_{0H} > 1$, $Det(J(\epsilon_{01})) < 0$ hence the eigenvalues of $J(\epsilon_{01})$ have negative real parts implying that $\mathcal{E}_0$ is locally asymptotically stable when $\mathcal{R}_{0H} < 1$. □

2.6.2 Global stability of the disease-free equilibrium

The disease-free equilibrium, $\mathcal{E}_0$, is locally stable provided that $\mathcal{R}_{0H} < 1$. It is important to establish global stability of the disease-free equilibrium . Shuai *et al.* [88] presented two global stability methods for compartmental models using a Lyapunov function approach. The first method presented was the matrix-theoretic method for proving global stability of the disease-free equilibrium. The second method presented is the graph-theoretic method for proving global stability of the endemic equilibrium. In this research, we outline and use the matrix-theoretic method to prove global stability of the disease-free equilibrium. The method entails the use of the $\mathcal{F}$ and $\mathcal{V}$ matrices obtained from the computation of the reproduction number through the next generation matrix approach by Van den Driessche and Watmough [98]. Let

$$x' = \mathcal{F}(x, y) - \mathcal{V}(x, y), \tag{2.28}$$

where, $\mathcal{F}(x,y) = (\mathcal{F}_1, \mathcal{F}_2, \mathcal{F}_3.....\mathcal{F}_n)^T$ and $\mathcal{V}(x,y) = (\mathcal{V}_1, \mathcal{V}_2, \mathcal{V}_3.....\mathcal{V}_n)^T$, are the rate of appearance of new infections and the transition terms respectively. Let

$$y' = g(x,y), \tag{2.29}$$

where

$$\begin{aligned} x &= (x_1, x_2, x_3, ...x_n)^T \in \mathbb{R}^n, \\ g &= (g_1, g_2, g_3, ...g_m)^T \in \mathbb{R}^m, \\ y &= (y_1, y_2, y_3, ...y_m)^T \in \mathbb{R}^m, \end{aligned} \tag{2.30}$$

are the different populations for the infected and healthy compartments. In order to perform the matrix-theoretic method first set

$$f(x,y) = (\mathcal{F} - \mathcal{V})x - \mathcal{F}(x,y) + \mathcal{V}(x,y) \tag{2.31}$$

From equation (2.28) it follows that equation (2.31) becomes

$$f(x,y) = (\mathcal{F} - \mathcal{V})x - x' \tag{2.32}$$

and therefore

$$x' = (\mathcal{F} - \mathcal{V})x - f(x,y) \tag{2.33}$$

and we assume that $f(0,y) = 0$. Let $u^T \leq 0$ be the left eigenvector for the non-negative matrix $\mathcal{V}^{-1}\mathcal{F}$ that relates to the eigenvalue $\rho(\mathcal{F}\mathcal{V}^{-1}) = \mathcal{R}_{0H} = \rho(\mathcal{V}^{-1}\mathcal{F})$. The Perron eigenvector for model (2.28) is given by the following theorem;

Theorem 5. *Let $\mathcal{F}, \mathcal{V}$ and $f(x,y)$ be defined. If $f(x,y) \geq 0$ in $\Omega \in \mathbb{R}^{m+n}_+$, $\mathcal{F} \geq 0$, $\mathcal{V}^{-1} \geq 0$ and $\mathcal{R}_{0H} \leq 1$ then the Lyapunov function $\mathcal{L} = u^T\mathcal{V}^{-1}x$ can be used for the disease model (2.28) on Ω, where x represents the infectious components of the model.*

Proof. Let

$$\mathcal{L} = u^T\mathcal{V}^{-1}x, \tag{2.34}$$

and so by differentiation $\mathcal{L}$ along solutions of model (2.28) yields

$$\begin{aligned} \mathcal{L}'|_{(2.28)} &= u^T\mathcal{V}^{-1}x' = u^T\left[\mathcal{V}^{-1}(\mathcal{F} - \mathcal{V})x - f(x,y)\right] = u^T\mathcal{V}^{-1}(\mathcal{F} - \mathcal{V})x - u^T\mathcal{V}^{-1}f(x,y) \\ &= (\mathcal{R}_{0H} - 1)u^Tx - u^T\mathcal{V}^{-1}f(x,y). \end{aligned} \tag{2.35}$$

If $\mathcal{R}_{0H} \leq 1$, then it follows that $\mathcal{L}' \leq 0$ in Ω and hence $\mathcal{L}$ is an appropriate Lyapunov function for model (2.28). □

The set Ω in theorem 5 is chosen as a compact subset of $\mathbb{R}_+^{m+n}$ such that $(0, y_0) \in \Omega$ and Ω is positively invariant with respect to model (2.28). The Lyapunov function constructed in theorem 5 can be used to prove the global stability of the disease-free equilibrium, uniform persistence and it can also be used to establish existence of the endemic equilibrium [88].

Theorem 6. *Let $\mathcal{F}, \mathcal{V}$ and $f(x, y)$ be defined and let $\Omega \subset \mathbb{R}_+^{m+n}$ be compact such that $(0, y_0) \in \Omega$ and Ω is positively invariant with respect to model (2.28). Suppose that $f(x, y) \geq 0$ and $f(x, y_0) = 0$ in Ω, $\mathcal{F} \geq 0, \mathcal{V}^{-1} \geq 0$ and $\mathcal{V}^{-1}\mathcal{F}$ is irreducible. Assume that the disease-free represented by system $y' = g(0, y)$ has a unique equilibrium given by $y = y_0 > 0$, that is it is globally asymptotically stable in $\mathbb{R}_+^m$ provided that the following conditions hold;*

1. *$\mathcal{R}_{0H} < 1$, the disease-free equilibrium is globally asymptotically stable,*
2. *$\mathcal{R}_{0H} > 1$, the disease-free equilibrium is unstable such that model system (2.28) is uniformly persistent and there exists at least one endemic equilibrium.*

From the above theorem 6 we define an the following terms;

Definition 2. ***Permutation matrix [52].*** *A permutation matrix is a binary matrix that has exactly one entry that is equal to one in each row and column and is zero everywhere else. Such a matrix represents a permutation of n elements which when used to multiply a matrix A produces a permutation in the rows or columns of A.*

Definition 3. ***Reducible matrix [52].*** *A matrix is said to be reducible if, for some permutation,P, it follows that*

$$PAP^T = \begin{bmatrix} A_0 & 0 \\ A_1 & A_2 \end{bmatrix} \tag{2.36}$$

where A_0, A_1, A_2 are square matrices. Based on these definitions, we state without proof, the Perron-Frobenius theorem as follows

Theorem 7. ***The Perron-Frobenius Theorem*** *[52]. Let $A \geq 0$ be an $n \times n$ real matrix then the following results hold;*

1. *The spectral radius of A given by $\rho(A)$ is an eigenvalue of matrix A with respect to a non-negative eigenvector.*

2. *If matrix A is irreducible , then $\rho(A)$ is a simple eigenvalue and the associated eigenvector is positive.*

We adopt the method by [88] to prove global stability of HIV model (2.2) and state the following theorem;

Theorem 8. *The disease-free equilibrium,$\mathcal{E}_0$, is globally stable provided that $\mathcal{R}_{0H} < 1$.*

Proof. The method of a Lyapunov function for an in-host model by [103] is used and so recall that for the HIV sub-model, $\mathcal{R}_{0H} = \dfrac{\beta s N_1(1-\epsilon_{RT})(1-\epsilon_{PI})}{c_1 d}$. It can clearly be shown that the $\mathcal{F}$ and $\mathcal{V}^{-1}$ are non-negative and theorem 7 states that the non-negative matrix $\mathcal{V}^{-1}\mathcal{F}$ should have a non-negative left eigenvalue u corresponding to $\mathcal{R}_{0H} = \rho(\mathcal{V}^{-1}\mathcal{F}) = \rho(\mathcal{F}\mathcal{V}^{-1})$, meaning that $u^T\rho(\mathcal{V}^{-1}\mathcal{F}) = u^T\mathcal{R}_{0H}$. Let $X = (I, V)^T$, represent the infected and virus classes for the HIV sub-model. From the computation of $\mathcal{R}_{0H}$ we obtain,

$$\mathcal{F} = \begin{bmatrix} 0 & \dfrac{\beta s(1-\epsilon_{RT})}{d} \\ \\ 0 & 0 \end{bmatrix}, \quad \mathcal{V} = \begin{bmatrix} \delta & 0 \\ \\ -(1-\epsilon_{PI})N_1\delta & c_1 \end{bmatrix}. \tag{2.37}$$

Using $\mathcal{F}$ and $\mathcal{V}$ we check if $\mathcal{V}^{-1}\mathcal{F}$ is reducible or irreducible as follows

$$\mathcal{V}^{-1} = \begin{bmatrix} \dfrac{1}{\delta} & 0 \\ \\ \dfrac{(1-\epsilon_{PI})N_1}{c_1} & \dfrac{1}{c_1} \end{bmatrix}, \quad \mathcal{V}^{-1}\mathcal{F} = \begin{bmatrix} 0 & \dfrac{\beta s(1-\epsilon_{RT})}{\delta d} \\ \\ 0 & \dfrac{\beta N_1 s(1-\epsilon_{RT})(1-\epsilon_{PI})}{c_1 d} \end{bmatrix}. \tag{2.38}$$

It can be seen that matrix $\mathcal{V}^{-1}\mathcal{F}$ is reducible since the second column is the only non-zero column and thus theorem 6 fails and hence $u^T x \neq 0$. To prove the global stability however we construct a Lyapunov function of the form

$$\begin{aligned} \mathcal{L} &= u^T\mathcal{V}^{-1}x = \frac{(1-\epsilon_{PI})N_1}{c_1}I + \frac{1}{c_1}V, \\ &= \frac{\mathcal{R}_{0H}d}{\beta s(1-\epsilon_{RT})}I + \frac{\mathcal{R}_{0H}d}{\beta s N_1(1-\epsilon_{RT})(1-\epsilon_{PI})}V = \frac{\mathcal{R}_{0H}d}{\beta s(1-\epsilon_{RT})}\left[I + \frac{1}{N_1(1-\epsilon_{PI})}V\right] \end{aligned} \tag{2.39}$$

where $u^T = (0, 1)^T$. It follows from theorem 5 that

$$\mathcal{L}' = u^T\mathcal{V}^{-1}x' = (\mathcal{R}_{0H} - 1)u^T x - u^T V^{-1} f(x, T), \tag{2.40}$$

where $f(x,T) = (1-\epsilon_{RT})\beta V(T_0 - T)$. It follows that

$$\mathcal{L}' = (\mathcal{R}_{0H} - 1)V - \frac{\mathcal{R}_{0H} d}{s} V\left[T_0 - T\right] \leq 0, \tag{2.41}$$

provided that $\mathcal{R}_{0H} < 1$ and $\mathcal{L}' = 0$ implies that $T_0 = T$ or $V = 0$. The invariant set on which $L' = 0$, contains only one point $\left(\frac{s}{d}, 0, 0\right)$ and by applying LaSalle's invariant principle [50] it can be concluded that the disease-free equilibrium is globally asymptotically stable when $\mathcal{R}_{0H} < 1$. This concludes the proof. □

2.6.3 The endemic equilibrium for the HIV sub-model

The endemic equilibrium for (2.19) is given by

$$\begin{aligned} T^e &= \frac{c_1}{N_1\beta(1-\epsilon_{RT})(1-\epsilon_{PI})}, \\ I^e &= \frac{s}{\delta}\left[1 - \frac{1}{\mathcal{R}_{0H}}\right], \\ V^e &= s(1-\epsilon_{PI})N_1\left[1 - \frac{1}{\mathcal{R}_{0H}}\right] \end{aligned} \tag{2.42}$$

2.7 Analysis of the HPV sub-model

The HPV model is given by

$$\begin{aligned} Y_1'(t) &= \frac{\psi W(N_2 - Y_1)}{\phi + N_2 - Y_1} - Y_1(\epsilon + \mu + aE), \\ Y_2'(t) &= \epsilon Y_1 + Y_2(r\epsilon - \mu - aE), \\ W'(t) &= \mu k(Y_1 + Y_2) - c_2 W, \\ E'(t) &= \omega Y_2 E(1 - \frac{E}{\bar{K}}), \end{aligned} \tag{2.43}$$

with $Y_1(0) = y_{10} \geq 0$, $Y_2(0) = y_{20} \geq 0$, $W(0) = W_0 \geq 0$, $E(0) = E_0 \geq 0$, as initial conditions and the total population of cells $N_2(t) = Y_1(t) + Y_2(t)$ such that

$$\Omega_2 = \{(Y_1, Y_2, W, E) \in \mathcal{R}^{4+}.$$

2.7.1 Equilibrium points and stability analysis

The disease-free equilibrium point for (2.43) is given by $\mathcal{Q} = (0, 0, 0, \bar{K})$. The reproduction number is calculated using the next generation matrix approach [98] as follows

$$F_v = \begin{bmatrix} \frac{\psi W(N_2 - Y_1)}{\phi + N_2 - Y_1} \\ 0 \\ 0 \\ 0 \end{bmatrix}, \tag{2.44}$$

and

$$V_v = \begin{bmatrix} Y_1(\epsilon + \mu + aE) \\ Y_2(\mu + aE - r\epsilon) - \epsilon Y_1 \\ c_2 W - \mu k(Y_1 + Y_2) \\ -\omega Y_2 E(1 - \frac{E}{\bar{K}}) \end{bmatrix}, \tag{2.45}$$

and the $\mathcal{F}$ and $\mathcal{V}$ matrices are given by

$$\mathcal{F} = \begin{bmatrix} 0 & 0 & \frac{N_2\psi}{N_2 + \phi} \\ 0 & 0 & 0 \\ 0 & 0 & 0 \end{bmatrix}, \tag{2.46}$$

and

$$\mathcal{V} = \begin{bmatrix} (\epsilon + \mu + a\bar{K}) & 0 & 0 \\ -\epsilon & (\mu + a\bar{K} - r\epsilon) & 0 \\ -\mu k & -\mu k & c_2 \end{bmatrix}. \tag{2.47}$$

The system reduces to a 3-D system because the immune response class, E has a zero row and column when the equilibrium point is substituted and therefore has no effect on the reproduction number calculation. Inclusion of this class will result in a determinant of zero or a singular matrix. Based on this the spectral radius $\rho(\mathcal{F}\mathcal{V}^{-1})$ is given by

$$\rho(\mathcal{F}\mathcal{V}^{-1}) = \mathcal{R}_1 = \frac{N_2\psi\mu k(\mu + \epsilon + a\bar{K} - r\epsilon)}{c_2(\epsilon + \mu + a\bar{K})(\mu + a\bar{K} - r\epsilon)(N_2 + \phi)}, \tag{2.48}$$

It can be seen that $\mathcal{R}_1$ is positive provided that $\mu > r\epsilon$ and this becomes the biologically feasible region for $\mathcal{R}_1$.

Theorem 9. *The disease-free equilibrium for the HPV model is locally asymptotically stable when $\mathcal{R}_1 < 1$ and unstable when $\mathcal{R}_1 > 1$.*

Proof. The Jacobian sub matrix of the infectious classes of (2.4) is given by

$$J(\mathcal{Q}) = \mathcal{F} - \mathcal{V} = \begin{bmatrix} -(\epsilon+\mu+a\bar{K}) & 0 & \frac{N_2\psi}{N_2+\phi} \\ \epsilon & (r\epsilon-\mu-a\bar{K}) & 0 \\ \mu k & \mu k & -c_2 \end{bmatrix}, \tag{2.49}$$

and the determinant is given by

$$\begin{aligned} Det(J(\mathcal{Q})) &= -(\epsilon+\mu+a\bar{K})\left[c_2(\mu+a\bar{K}-r\epsilon)\right] + \frac{N_2\psi}{N_2+\phi}\left[\epsilon\mu k + \mu k(\mu+a\bar{K}-r\epsilon)\right], \\ &= -c_2(\mu+aE-r\epsilon)(\epsilon+\mu+a\bar{K}) + \frac{N_2\psi\mu k}{N_2+\phi}\left[\epsilon+\mu+a\bar{K}-r\epsilon\right], \\ &= c_2(r\epsilon-\mu-a\bar{K})(\epsilon+\mu+a\bar{K})\left[1-\mathcal{R}_1\right]. \end{aligned} \tag{2.50}$$

It can be seen that $tr(J(\mathcal{Q})) = -\epsilon - 2\mu - 2a\bar{K} - c_2 + r\epsilon < 0$ and when $R_1 < 1$, $Det(J(\mathcal{Q})) > 0$ and when $R_1 > 1$, $Det(J(\mathcal{Q})) < 0$. Therefore, the eigenvalues of $J(\mathcal{Q})$ have negative real parts which imply that the disease-free equilibrium is locally asymptotically stable when $\mathcal{R}_1 < 1$ and unstable when $\mathcal{R}_1 > 1$. □

2.7.2 Global stability analysis of the disease-free equilibrium, $\mathcal{Q}$

Theorem 10. *The disease-free equilibrium is globally stable provided that $\mathcal{R}_1 < 1$ around $\mathcal{Q}$.*

Proof. We recall that

$$\mathcal{R}_1 = \frac{N_2\psi\mu k(\mu+\epsilon+a\bar{K}-r\epsilon)}{c_2(\epsilon+\mu+a\bar{K})(\mu+a\bar{K}-r\epsilon)(N_2+\phi)}$$

and let $X = (Y_1, Y_2, W, E)^T$. From the computation of $\mathcal{R}_1$ using the next generation matrix approach we have

$$\mathcal{F} = \begin{bmatrix} 0 & 0 & \frac{N_2\psi}{N_2+\phi} \\ 0 & 0 & 0 \\ 0 & 0 & 0 \end{bmatrix}, \mathcal{V} = \begin{bmatrix} (\epsilon+\mu+a\bar{K}) & 0 & 0 \\ -\epsilon & (\mu+a\bar{K}-r\epsilon) & 0 \\ -\mu k & -\mu k & c_2 \end{bmatrix} \tag{2.51}$$

and so we check if $V^{-1}F$ is irreducible as follows;

$$\mathcal{V}^{-1} = \begin{bmatrix} \dfrac{1}{(\epsilon+\mu+a\bar{K})} & 0 & 0 \\ \dfrac{\epsilon}{(\epsilon+\mu+a\bar{K})(\mu+a\bar{K}-r\epsilon)} & \dfrac{1}{(\mu+a\bar{K}-r\epsilon)} & 0 \\ \dfrac{\mu k(\epsilon+\mu+a\bar{K}-r\epsilon)}{c_2(\epsilon+\mu+a\bar{K})(\mu+a\bar{K}-r\epsilon)} & \dfrac{\mu k}{c_2(\mu+a\bar{K}-r\epsilon)} & \dfrac{1}{c_2} \end{bmatrix}. \tag{2.52}$$

It follows that

$$\mathcal{V}^{-1}\mathcal{F} = \begin{bmatrix} 0 & 0 & \dfrac{N_2\psi}{(N_2+\phi)(\epsilon+\mu+a\bar{K})} \\ 0 & 0 & \dfrac{N_2\psi\epsilon}{(N_2+\phi)(\epsilon+\mu+a\bar{K})(\mu+a\bar{K}-r\epsilon)} \\ 0 & 0 & \dfrac{N_2\psi\mu k\epsilon}{c_2(N_2+\phi)(\epsilon+\mu+a\bar{K})(\mu+a\bar{K}-r\epsilon)} \end{bmatrix}. \tag{2.53}$$

It can be seen that $\mathcal{V}^{-1}\mathcal{F}$ is reducible because the third column is the only non-zero column and hence theorem 6 fails. So we construct a Lyapunov function of the form

$$\begin{aligned} \mathcal{W} &= u^T\mathcal{V}^{-1}X, \\ &= \frac{\mu k(\epsilon+\mu+a\bar{K}-r\epsilon)}{c_2(\epsilon+\mu+a\bar{K})(\mu+a\bar{K}-r\epsilon)}Y_1 + \frac{\mu k}{c_2(\mu+a\bar{K}-r\epsilon)}Y_2 + \frac{1}{c_2}W, \\ &= \frac{\mathcal{R}_1(N_2+\phi)}{N_2\psi}Y_1 + \frac{\mathcal{R}_1(N_2+\phi)(\epsilon+\mu+a\bar{K})}{N_2\psi(\mu+\epsilon+a\bar{K}-r\epsilon)}Y_2 + \frac{\mathcal{R}_1(N_2+\phi)(\epsilon+\mu+aK)(\mu+a\bar{K}-r\epsilon)}{N_2\psi\mu k(\mu+\epsilon+a\bar{K}-r\epsilon)}W \\ &= \frac{\mathcal{R}_1(N_2+\phi)}{N_2\psi}\left[Y_1 + \frac{(\epsilon+\mu+a\bar{K})}{(\mu+\epsilon+a\bar{K}-r\epsilon)}Y_2 + \frac{(\epsilon+\mu+a\bar{K})(\mu+a\bar{K}-r\epsilon)}{\mu k(\mu+\epsilon+a\bar{K}-r\epsilon)}W\right], \end{aligned} \tag{2.54}$$

where $u^T = (0,0,1)^T$ is the left eigenvector for the matrix $V^{-1}F$. From theorem 5 we obtain

$$\mathcal{W}' = u^T\mathcal{V}^{-1}X' = (\mathcal{R}_1 - 1)u^TX - u^TV^{-1}f(X,S) \tag{2.55}$$

where $S = N_2 - Y_1$, these are the susceptible epithelial cells and at disease-free equilibrium $S = S_0$. Hence $f(X,S) = \dfrac{\psi W(S_0 - S)}{(\phi + S_0 - S)}$ such that

$$\mathcal{W}' = (\mathcal{R}_1 - 1)u^T X - u^T V^{-1}\left[\frac{\psi W(S_0 - S)}{(\phi + S_0 - S)}\right],$$

$$= (\mathcal{R}_1 - 1)W - \frac{\mathcal{R}_1(N_2 + \phi)}{N_2\psi}\left[\frac{\psi W(S_0 - S)}{(\phi + S_0 - S)}\right], \tag{2.56}$$

$$= W\left[(\mathcal{R}_1 - 1) - \frac{\mathcal{R}_1(N_2 + \phi)}{N_2}\left[\frac{(S_0 - S)}{(\phi + S_0 - S)}\right]\right] \leq 0,$$

provided that $\mathcal{R}_1 < 1$. It also follows that $\mathcal{W}' = 0$, implies that $W = 0$ or $S_0 = S$. Therefore there exists an invariant set where $W = 0$ and $S_0 = S$ which is the disease-free equilibrium $\mathcal{Q}$ and by LaSalle's invariance principle [50] the disease-free equilibrium is globally asymptotically stable in Ω_2. This concludes the proof.

□

2.7.3 Endemic equilibrium analysis

The HPV sub-model presents two endemic equilibrium points which are the CTL-inactive endemic and the CTL-active endemic. The CTL-inactive endemic is the equilibrium point where $E = 0$ and is presented in terms of Y_2^* as follows

$$Y_1^* = \frac{\mu - r\epsilon}{\epsilon}Y_2^*, \quad W^* = \frac{\mu k(\mu + \epsilon - r\epsilon)}{c_2}Y_2^*, Y_2^* = Y_2^*, \quad E^* = 0. \tag{2.57}$$

The CTL-activated endemic equilibrium point is for the case $E \neq 0$ and is expressed Y_1^* and the reproduction number $\mathcal{R}_1$ as follows;

$$W^* = Y_1^*\left[\frac{\mu k(\epsilon + \mu + a\bar{K} - r\epsilon)}{c_2(\mu + a\bar{K} - r\epsilon)}\left(\frac{1}{\mathcal{R}_1}\right) + \frac{1}{N_2}\right] - \frac{Y_1^{*2}(\epsilon + \mu + a\bar{K})}{\psi N_2},$$

$$Y_2^* = Y_1^*\left[\frac{(\epsilon + \mu + a\bar{K} - r\epsilon)}{(\mu + a\bar{K} - r\epsilon)}\left(\frac{1}{\mathcal{R}_1}\right) + \frac{c_2 Y_1^*}{\psi N_2 \mu k}\right] + \frac{c_2 Y_1^*}{N_2 \mu k} - 1, \tag{2.58}$$

$$E^* = \bar{K}, \quad Y_1^* = Y_1^*$$

The endemic equilibrium points for an in-host HPV model are rather complex in nature. The stability of the above endemic equilibrium points can be performed through the creation of suitable Lyapunov functions or numerical simulations.

2.8 Analysis of the Co-infection model

The co-infection model is given by

$$\begin{aligned}
T_h'(t) &= s - dT_h - (1-\epsilon_{RT})\beta T_h V_h, \\
I_h'(t) &= (1-\epsilon_{RT})\beta T_h V_h - \delta I_h, \\
V_h'(t) &= (1-\epsilon_{PI})N_1 \delta I_h - c_1 V_h, \\
Y_1'(t) &= \frac{\psi W(N_2(1+pV_h)-Y_1)}{\phi + N_2(1+pV_h)-Y_1} - Y_1(\epsilon+\mu+aE), \\
Y_2'(t) &= \epsilon Y_1 + Y_2(r\epsilon - \mu - aE), \\
W'(t) &= \mu k(Y_1+Y_2) - c_2 W, \\
E'(t) &= \omega Y_2 E\left[1 - \frac{E}{\bar{K}}\right].
\end{aligned} \tag{2.59}$$

2.8.1 Equilibrium points and stability analysis.

The disease-free equilibrium for the co-infection model is given by

$$\mathcal{Q}_0 = \left(\frac{s}{d}, 0, 0, 0, 0, 0, \bar{K}\right).$$

The reproduction number, $\mathcal{R}_0$, is computed using the next generation matrix approach by [98]. To come up with the relevant matrices we only consider the infected and viral production classes that is I_h, V_h, Y_1, Y_2, W and therefore the matrices are found as follows

$$\mathbb{F} = \begin{bmatrix} (1-\epsilon_{RT})\beta T_h V_h \\ 0 \\ \dfrac{\psi W(N_2(1+pV_h)-Y_1)}{\phi + N_2(1+pV_h)-Y_1} \\ 0 \\ 0 \end{bmatrix}, \tag{2.60}$$

and

$$\mathbb{V} = \begin{bmatrix} \delta I_h \\ c_1 V_h - (1-\epsilon_{PI}) N_1 \delta I_h \\ Y_1(\epsilon + \mu + aE) \\ Y_2(\mu + aE - r\epsilon) - \epsilon Y_1 \\ c_2 W - \mu k(Y_1 + Y_2) \end{bmatrix}. \tag{2.61}$$

The $\mathcal{F}$ and $\mathcal{V}$ matrices are given by

$$\mathcal{F} = \begin{bmatrix} 0 & \frac{\beta s(1-\epsilon_{RT})}{d} & 0 & 0 & 0 \\ 0 & 0 & 0 & 0 & 0 \\ 0 & 0 & 0 & 0 & \frac{N_2\psi}{(N_2+\phi)} \\ 0 & 0 & 0 & 0 & 0 \\ 0 & 0 & 0 & 0 & 0 \end{bmatrix}, \tag{2.62}$$

and

$$\mathcal{V} = \begin{bmatrix} \delta & 0 & 0 & 0 & 0 \\ -N_1\delta(1-\epsilon_{PI}) & c_1 & 0 & 0 & 0 \\ 0 & 0 & (\epsilon + \mu + a\bar{K}) & 0 & 0 \\ 0 & 0 & -\epsilon & (\mu + a\bar{K} - r\epsilon) & 0 \\ 0 & 0 & -\mu k & -\mu k & c_2 \end{bmatrix}. \tag{2.63}$$

The dominant eigenvalues for $\mathcal{F}\mathcal{V}^{-1}$ are

$$\begin{aligned} \mathcal{R}_{0H} &= \frac{\beta s N_1 (1-\epsilon_{RT})(1-\epsilon_{PI})}{c_1 d} \quad \textit{and} \\ \mathcal{R}_1 &= \frac{N_2 \psi \mu k (\mu + \epsilon + a\bar{K} - r\epsilon)}{c_2(\epsilon + \mu + a\bar{K})(\mu + a\bar{K} - r\epsilon)(N_2 + \phi)}, \end{aligned} \tag{2.64}$$

such that the reproduction number,$\mathcal{R}_0$, is given by

$$\mathcal{R}_0 = max\{\mathcal{R}_{0H}, \mathcal{R}_1\}.$$

Provided that the conditions set on the HIV and HPV sub-models are met, $\mathcal{R}_0$ is strictly positive. This leads to the following theorem on local stability of (2.59).

Theorem 11. *The disease-free equilibrium for the HIV/HPV model (2.59) is locally asymptotically stable when* $\mathcal{R}_0 < 1$ *and unstable when* $\mathcal{R}_0 > 1$.

Proof. We find the Jacobian of the infectious classes evaluated at the disease-free equilibrium $\mathcal{J}(\mathcal{Q}_0)$ given as

$$\mathcal{J}(\mathcal{Q}_0) = \begin{bmatrix} -\delta & \frac{\beta s(1-\epsilon_{RT})}{d} & 0 & 0 & 0 \\ N_1\delta(1-\epsilon_{PI}) & -c_1 & 0 & 0 & 0 \\ 0 & 0 & -(\epsilon+\mu+a\bar{K}) & 0 & \frac{N_2\psi}{(N_2+\phi)} \\ 0 & 0 & \epsilon & -(\mu+a\bar{K}-r\epsilon) & 0 \\ 0 & 0 & \mu k & \mu k & -c_2 \end{bmatrix}. \tag{2.65}$$

The determinant of the Jacobian matrix, $\mathcal{J}(\mathcal{Q}_0)$, is given by;

$$\begin{aligned} |\mathcal{J}(\mathcal{Q}_0)| &= -\left[c_2(\epsilon+\mu+a\bar{K})(\mu+a\bar{K}-r\epsilon) - \frac{N_2\psi\mu k(\epsilon+\mu+a\bar{K}-r\epsilon)}{N_2+\phi}\right] \\ &\times \left[\frac{\beta s N_1\delta(1-\epsilon_{RT})(1-\epsilon_{PI}) - \delta c_1 d}{d}\right] \\ &= \delta c_1 c_2(\epsilon+\mu+a\bar{K})(r\epsilon-\mu-aE)(1-\mathcal{R}_1)(1-\mathcal{R}_0). \end{aligned} \tag{2.66}$$

It can be seen that

$$Tr(\mathcal{J}(\mathcal{Q}_0)) = -\delta - c_1 - (\epsilon+\mu+aE) - (\mu+aE-r\epsilon) - c_2,$$

which implies that the system is locally asymptotically stable since when $\mathcal{R}_0 < 1$, $Det(\mathcal{J}(\mathcal{Q}_0)) > 0$ and when $\mathcal{R}_0 > 1$, $Det(\mathcal{J}(\mathcal{Q}_0)) < 0$ and the system is unstable. □

2.9 Conclusion on the chapter

The work presented is on the viral dynamics of HPV by Verma *et al.* [99, 64]. The authors of the work did not present any preliminary analysis that showed that the model built was biologically feasible, locally and globally stable. We presented global stability analysis using the Lyapunov approach by Shuai *et al.* [88] and this consequently will assist us in our analysis for the basic model with latency presented in chapter 3. This chapter built up the base of our new work on HPV as it presented the HPV dynamics. The work presented is tallied with the simulation work done by the authors. It will assist in building up a model that shall be presented in chapter 3. There are some possible modifications that we hope to incorporate in

our new model. Our new model will consider the immune evasion property of HPV and how it affects the overall dynamics of HPV. In the next chapter, we present the basic deterministic in-host model for HPV in the presence of immune response and latency. The model presented will be thoroughly analysed to assess the effects of immune response.

Chapter 3

The basic in-host mathematical model for HPV with immune response

3.1 Introduction

This chapter presents the basic mathematical model for HPV based on the work done by Verma *et al.* [99, 64]. The model incorporates latency and immune responses. Theoretical results for the global and local stability dynamics of the model are established. Numerical simulations indicate that the disease-free and endemic equilibrium points are globally asymptotically stable, provided certain conditions are met.

3.2 Model formulation

In the model formulation, the model considers susceptible basal layer cells of the epithelium within the genital mucosa which are constantly at risk of HPV infection during sexual intercourse as a result of abrasion. The mathematical model is made up of susceptible target cells denoted by $T_s(t)$ which represent healthy cells that are at risk of getting infected upon abrasion of the epithelium. These cells are assumed to die naturally at rate, μ. When HPV enters or infects a healthy target cell, $T_s(t)$, it merges its DNA with that of the cell such that the cell is altered and no longer operates as a normal cell. Infection of the healthy target cells is assumed to occur at a rate given by

$$\frac{\beta V}{\gamma + T_s}, \tag{3.1}$$

and where β is the transmission rate of HPV, $V(t)$ is the free HPV virions, $T_s(t)$ is the total number of uninfected epithelial cells that are susceptible to infection and γ is the concentra-

tion of the epithelial cells where the infection is considered half-maximal [99, 64]. The model incorporates latently infected cells. Viral latency represents the presence of viral DNA within the body in the absence of infection [55]. Infections such as HPV can lie dormant within the skin or epithelial cells [62]. We assume that latently infected cells, $L(t)$, are target cells within the basal layer that lie dormant or do not show any cytological changes for a certain period before they either clear HPV infection or become infectious target cells. We define "clearance" of HPV infection from latently infected cells to be the spontaneous loosing of viral DNA during cell division as suggested by Ryser *et al.* [80], or the cells can expel the viral DNA , which can be assumed to be some form of innate immunity. In this model we assume "clearance" of HPV infection occurs at rate, ϕ, and cells cleared of infection do not die but go back to the susceptible class, $T_s(t)$. Normally, changes in immune response status (usually immune suppression) can cause latently infected cells to be reactivated, persistent infections, or to mature into infected cells [55]. The inclusion of latently infected cells takes into account the undetectable HPV infection that, in the long run, can develop into persistent HPV, if not cleared. In a review paper, Gravitt *et al.* states that new HPV infection is not necessarily a result of sexual activities or sexual partner acquisition, but can also be as a result of the recurrent latent infections [36]. Therefore, incorporating latency into the HPV model is important in understanding the dynamics of HPV progression within a community. We assume that natural death of latently infected cells also occurs at rate, μ. Infectious target cells for the model are denoted by $I_1(t)$. The model assumes that, after a certain period, the latently infected cells can subsequently mature into infectious target cells at rate ψ, and therefore progress to the $I_1(t)$ class. Natural death of the $I_1(t)$ cells occurs at rate μ. Throughout the model, clearance of HPV infection as a result of immune response is assumed to occur at rate, θ, within all infected cell classes $I_1(t)$ and $I_2(t)$. Due to oncogene expression at rate, $\epsilon \in [0, 1]$, $I_1(t)$ cells are converted into transit amplifying cells, $I_2(t)$, that trigger immune response due to unusual cell activity [99, 64]. These cells are assumed to self-proliferate at rate, $r\epsilon$, where r is the transit amplifying cells recruitment rate [99, 64] with$r\epsilon \leq \mu$ and $0 \leq r \leq 1$. $I_2(t)$ cells are cleared naturally at rate, μ, and release free virions due to bursting. Free virion production within the model is assumed to occur at rate, $N_2\mu(I_1 + I_2)$ where N_2 is the burst size that is due to virus particles produced by the $I_1(t)$ and $I_2(t)$ cells in a lifetime. Free virions are assumed to die naturally at a rate, δ. Immune response in the form of cytotoxic target cells (CTLs), $K(t)$, is assumed to be initiated by a rapid and unusual growth of $I_2(t)$ cells indicating an abnormality within the system. The reason why only the $I_2(t)$ class is considered in the generation of immune response is because, HPV is an intra-epithelial infection and therefore, such infection is not passed on to the blood

stream. HPV will also at all costs evade detection by the immune system and therefore, the only signal that can be detected is that of unusual cell growth or death, which is through the proliferation of $I_2(t)$ cells as explained by [63]. The other reason is that of CTL-response being only activated through the detection of the oncogene protein $E6$, which is only activated through the presence of $I_2(t)$ cells [63]. The immune response cells dock on to $I_1(t)$ cells or $I_2(t)$ cells and kill the infected cell. The model assumes that the proliferation rate of CTLs occurs at a rate, σ, [99, 64] and that immune response cells die naturally at a rate, ν. This leads to the following flow diagram for the basic HPV model with latency and immune response: The

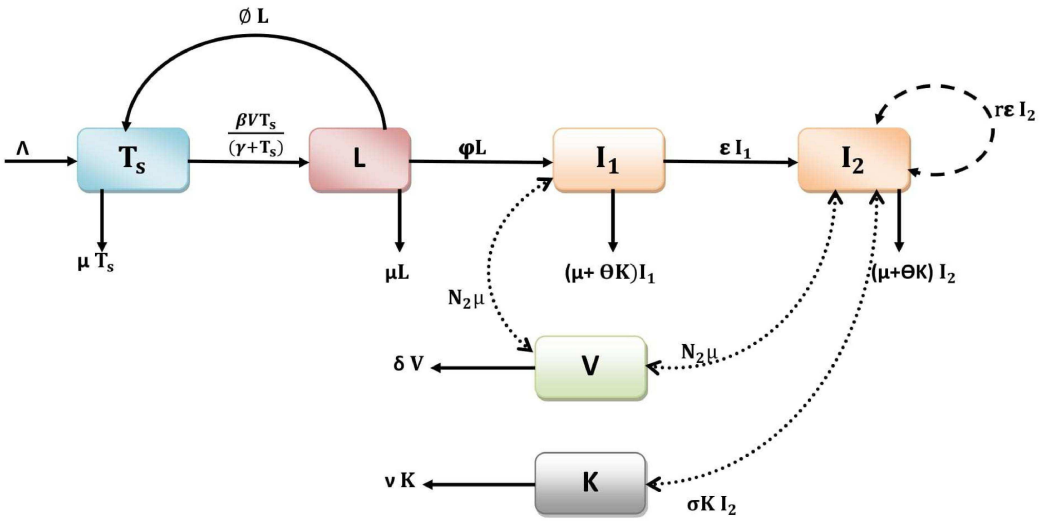

Figure 3.1: Flow diagram for the in-host dynamics of HPV in the presence of latency and immune response.

model flow diagram leads to the following model equations:

$$\begin{aligned}
T_s' &= \Lambda + \phi L - \left(\frac{\beta V}{(\gamma + T_s)} + \mu\right) T_s, \\
L' &= \frac{\beta V T_s}{(\gamma + T_s)} - (\mu + \psi + \phi) L, \\
I_1' &= \psi L - (\epsilon + \mu + \theta K) I_1, \\
I_2' &= \epsilon I_1 + r\epsilon I_2 - (\mu + \theta K) I_2, \\
V' &= N_2 \mu (I_1 + I_2) - \delta V, \\
K' &= \sigma I_2 K - \nu K,
\end{aligned} \tag{3.2}$$

with initial conditions given by $T_s(0) = T_{s0}, L(0) = L_0, I_1(0) = I_{10}, I_2(0) = I_{20}, V(0) = V_0$ and $K(0) = K_0$. A summary of parameters, classes and descriptions used in the model are presented in Table (3.1).

Table 3.1: Table of parameters

Parameter	**Description**
$T_s(t)$	Susceptible target epithelial cells that have been uncovered by abrasion during sexual intercourse.
$L(t)$	Latently infected cells that have been exposed to infection but are not yet producing the virus.
$I_1(t)$	Infected cells that are virus producing.
$I_2(t)$	Infected cells that are self-proliferating as a result of oncogene expression.
$V(t)$	Virus particles that infect the susceptible target epithelial cells.
$K(t)$	Immune response cells triggered by $I_2(t)$.
β	HPV infection transmission rate [99].
ϕ	Natural clearance of HPV within the latently infected cells as a result of natural healing of cells.
δ	Virion death rate.
μ	Natural cell death rate for $T_s(t), L(t), I_1(t), I_2(t)$ cells [64].
N_2	HPV burst size [99].
θ	HPV clearance rate as a result of immune response action [90, 63]. Such cells are docked by the immune cells and undergo cell death.
γ	Epithelial cell concentration for infection half maximal [64].
ψ	Mature rate of latently infected cells into infectious cells $I_1(t)$ that produce virus [40].
σ	CTL expansion rate in the presence of HPV viral proteins [64, 40]
ν	CTL natural death rate.
ϵ	Oncogene expression rate [64].
r	Transit amplifying cells recruitment rate [64].

3.3 Mathematical analysis of the basic model

3.3.1 Positivity and boundedness of solutions

Model system (3.2) describes the dynamics of high-risk HPV in human cells within the gential mucosa and it is important to prove that all the state variables, $T_s(t), L(t), I_1(t), I_2(t), V(t), K(t)$ are non-negative for all time $t > 0$. A mathematical model is said to be well posed provided that it has a unique solution for every point or initial condition for the model system. Model

system (3.2) should be well posed in order for it to be mathematically accepted and biologically feasible. This leads to the following important theorem and its proof;

Theorem 12. *Let the initial conditions of (3.2) satisfy* $T_{s0} > 0, L_0 > 0, I_{10} > 0, I_{20} > 0, V_0 > 0, K_0 > 0$. *The solutions of model (3.2),* $T_s(t), L(t), I_1(t), I_2(t), V(t), K(t)$, *are bounded and remain positive* $\forall t \in [0, t_0]$ *provided that the unique solutions for system (3.2) exist on an interval* $[0, t_0]$ *for some* $t_0 > 0$.

Proof. The method by [107] is adopted and we first prove that $T_s(t)$ is positive for $t \geq 0$, otherwise there exists a positive t_0 such that $T_s(t) > 0$ for $t \in [0, t_0)$ and $T_s(t_0) = 0$. Using the first equation of model (3.2), given by

$$T_s' = \Lambda + \phi L - \left(\frac{\beta V}{(\gamma + T_s)} + \mu \right) T_s, \tag{3.3}$$

it is noted that $T_s(t)$ is strictly positive $\forall\ t \in [0, t_0)$. Assuming that on the contrary let $t_0 > 0$, be the first time that $T_s(t_0) = 0$ and $T_s'(t_0) \leq 0$ then from equation (1) of model (3.2) we obtain $T_s(t_0) = \Lambda + \phi L > 0$, which is a contradiction. So, we conclude that $T_s(t) > 0$, $\forall\ t \in [0, t_0)$. Based on this, we also have the following

$$\begin{aligned}
L'|_{L=0} &= \frac{\beta V T_s}{(\gamma + T_s)} \geq 0, \\
I_1'|_{I_1=0} &= \psi L \geq 0, \\
I_2'|_{I_2=0} &= \epsilon I_1 \geq 0, \\
V'|_{V=0} &= N_2 \mu (I_1 + I_2) \geq 0, \\
K'|_{K=0} &= 0.
\end{aligned} \tag{3.4}$$

It can clearly be seen that $L(t) \geq 0, I_1(t) \geq 0, I_2(t) \geq 0, V(t) \geq 0, K(t) \geq 0,\ \ \forall\ t \in [0, t_0)$ which means that any solution within, $T_s(t), L(t), I_1(t), I_2(t), V(t), K(t)$ of model (3.2) is positive for all $t \geq 0$.

Furthermore we prove that the system is dissipative, that is all solutions are uniformly bounded in a proper subset of $\Omega \subset \mathbb{R}^6_+$. To do this, we state the following lemma;

Lemma 2. *Let* $T_s(t) > 0,\ L(t) \geq 0,\ I_1(t) \geq 0,\ I_2(t) \geq 0,\ V(t) \geq 0,\ K(t) \geq 0$. *Then, there exists a* $T_{sM}(t), L_M(t), I_{1M}(t), I_{2M}(t), V_M(t), K_M(t)$ *such that for* $T_s(t), L(t), I_1(t), I_2(t), V(t),$

$K(t), \limsup_{t\to\infty}(T_s(t)) \leq T_{sM}, \limsup_{t\to\infty}(L(t)) \leq L_M, \limsup_{t\to\infty}(I_1(t)) \leq I_{1M}, \limsup_{t\to\infty}(I_2(t)) \leq I_{2M}$, $\limsup_{t\to\infty}(V(t)) \leq V_M, \limsup_{t\to\infty}(K(t)) \leq K_M, \forall t \in [0, t_0]$.

Recall that the presence of HPV viral infection decreases the number of healthy T_s cells such that initially at $t = 0$, we expect that the number of healthy target cells should be close to the total cell population. Therefore if the system is disease-free, it means that all other equations of system (3.2) reduce to zero except for

$$T_s' = \Lambda + \phi L - \left(\frac{\beta V}{(\gamma + T_s)} + \mu\right) T_s, \tag{3.5}$$

which reduces to

$$T_s' \leq \Lambda - \mu T_s, \tag{3.6}$$

when evaluated at disease-free equilibrium . From equation (3.6), we can find an expression for $T_s'(t)$ as follows

$$T_s' + \mu T_s \leq \Lambda, \tag{3.7}$$

which can easily be solved using the integrating factor approach to obtain

$$T_s(t) \leq \frac{\Lambda}{\mu} + Ae^{-\mu t}, \tag{3.8}$$

where A is a constant of integration. By inputting the initial conditions $T_s(0) = T_{s0}$, we obtain the following result

$$T_s(t) = \frac{\Lambda}{\mu} + \left(T_{s0} - \frac{\Lambda}{\mu}\right) e^{-\mu t}. \tag{3.9}$$

Taking limits on equation (3.9), yields

$$\begin{aligned} \limsup_{t\to\infty} T_s(t) &\leq \limsup_{t\to\infty} \left[\frac{\Lambda}{\mu} + (T_{s0} - \frac{\Lambda}{\mu})e^{-\mu t}\right] \\ &\leq \frac{\Lambda}{\mu}. \end{aligned} \tag{3.10}$$

This means that the population of cells will grow towards $\frac{\Lambda}{\mu}$. To show that all other cells of (3.2) are also bounded, we recall that all constants for the system are positive and it follows that

$$T_s'(t) + L(t) + I_1'(t) + I_2'(t) = \Lambda - \mu(T_s + L + I_1 + I_2) + r\epsilon I_2 - \theta K(I_1 + I_2), \tag{3.11}$$

and this can be rewritten as

$$T_s'(t) + L'(t) + I_1'(t) + I_2'(t) \leq \Lambda - \mu(T_s + L + I_1 + I_2), \tag{3.12}$$

which when solved using the integrating factor approach yields

$$\int e^{\mu t} d(T_s + L + I_1 + I_2) \leq \int \Lambda e^{\mu t} dt, \tag{3.13}$$

which is equal to

$$(T_s + L + I_1 + I_2) \leq \frac{\Lambda}{\mu} + C_0 e^{-\mu t}, \tag{3.14}$$

where C_0 is a constant of integration. Taking lim sup on both sides of equation (3.14) yields

$$\limsup_{t\to\infty}(T_s + L + I_1 + I_2) \leq \limsup_{t\to\infty} \frac{\Lambda}{\mu} + C_0 e^{-\mu t} = \frac{\Lambda}{\mu}. \tag{3.15}$$

Let $T_{sM}(t) = L_M(t) = I_{1M}(t) = I_{2M}(t) = \dfrac{\Lambda}{min\{\mu\}}$ such that it can be established that $(T_s + L + I_1 + I_2)$ is bounded and so is $T_s(t), L(t), I_1(t), I_2(t)$, since

$$T_s(t), L(t), I_1(t), I_2(t) \leq (T_s + L + I_1 + I_2)(t). \tag{3.16}$$

So, $T_s(t) \leq T_{sM}$, $L(t) \leq L_M$, $I_1(t) \leq I_{1M}$ and $I_2(t) \leq I_{2M}$, $\forall t \in [0, t_0]$. Now considering the virus population, we recall that

$$\frac{dV}{dt} = N_2\mu(I_1 + I_2) - \delta V.$$

But $(I_1 + I_2) \leq T_s$ and this implies that $(I_1 + I_2) \leq \dfrac{\Lambda}{\mu}$. Hence, it can be seen that

$$\frac{dV}{dt} \leq N_2\Lambda - \delta V,$$

which leads to the following solution using the integrating factor approach

$$e^{\delta t}\frac{dV}{dt} \leq e^{\delta t} N_2\Lambda,$$

and this can be simplified as

$$V(t) \leq \frac{N_2\Lambda}{\delta} + C_1 e^{-\delta t},$$

where C_1 is a constant of integration. Therefore using the initial conditions $V(0) = V_0$, we have

$$V(t) \leq \frac{N_2\Lambda}{\delta} + (V_0 - \frac{N_2\Lambda}{\delta})e^{-\delta t}.$$

Taking lim sup limits both sides of the above equation yields

$$\limsup_{t\to\infty} V(t) \leq \limsup_{t\to\infty} \left[\frac{N_2\Lambda}{\delta} + (V_0 - \frac{N_2\Lambda}{\delta})e^{-\delta t}\right] = \frac{N_2\Lambda}{\delta}$$

and we choose $V_M = \dfrac{N_2\Lambda}{\delta}$ such that $V(t) \leq V_M$. Since I_1 and I_2 are bounded, it suffices that $V(t)$ is also bounded for all $t \in [0, t_0]$. Therefore, all feasible solutions to model system (3.2) are positively bounded by

$$\Omega = \{T_s(t), L(t), I_1(t), I_2(t), V(t), K(t) \in \mathbb{R}^6_+ \mid T_s \leq \frac{\Lambda}{\mu}\}.$$

The region is considered of biological interest and is positively invariant and attracting. This concludes the proof. □

3.3.2 Existence and Uniqueness of solutions

As an initial step, it is important to show that a solution to the initial value problem presented within the basic HPV model does exist and the solution is unique. We adopt the approach by [76] and use it to explain the existence and uniqueness theorem. The theorem is given as;

Theorem 13. *Let $t_0 > 0$ and from model system (3.2) if the initial conditions are such that $T_s(0) > 0, \quad L(0) > 0, \quad I_1(0) > 0, \quad I_2(0) > 0, \quad V(0) > 0, \quad K(0) > 0$ then $\forall t \in \mathbb{R}^n$, $T_s(t), \quad L(t), \quad I_1(t), \quad I_2(t), \quad V(t), \quad K(t)$ will exist in $\mathbb{R}^6_+$.*

Proof. To prove existence and uniqueness, we adopt the method for an in-host model outlined in [107]. We can show that $f : \mathbb{R}^6_+ \to \mathbb{R}^6_+$ where the model system (3.2) can be represented as follows;

$$\mathbf{x} = [T_s, L, I_1, I_2, V, K]^T \tag{3.17}$$

and

$$f(x) = [T_s', L', I_1', I_2', V', K']^T \tag{3.18}$$

and from the definition of a locally Lipschitz function stated in Lemma 1 in chapter 2 it can be seen that f is locally Lipschitz in its $\mathbf{x}$ argument. So we can directly deduce this from the Jacobian matrix given by

$$\nabla f = \begin{bmatrix} \frac{\beta V T_s - (T_s+\gamma)\beta V}{(T_s+\gamma)^2} - \mu & \phi & 0 & 0 & -\frac{\beta T_s}{(T_s+\gamma)} & 0 \\ \frac{\beta V(\gamma+T_s) - \beta V T_s}{(T+\gamma)^2} & -(\mu+\psi+\psi) & 0 & 0 & \frac{\beta T_s}{(T_s+\gamma)} & 0 \\ 0 & \psi & -(\epsilon+\mu+\theta K) & 0 & 0 & -\theta I_1 \\ 0 & 0 & \epsilon & r\epsilon - (\mu + \theta K) & 0 & -\theta I_2 \\ 0 & 0 & N_2\mu & N_2\mu & -\delta & 0 \\ 0 & 0 & 0 & \sigma K & 0 & \sigma I_2 - \nu \end{bmatrix}. \tag{3.19}$$

The Jacobian is bounded for every $\mathbf{x} \in \mathbb{R}^6_+$. Hence, f has a continuous bounded derivative on any compact subset of $\mathbb{R}^6_+$ and is therefore Lipschitz in $\mathbf{x}$. Based on the existence and uniqueness theorem by [76], there exists a unique, positive and bounded solution to the differential equation system (3.2) on the interval $[0, t_0]$ for some $t_0 > 0$. This concludes the proof. □

3.4 Equilibrium points and the reproduction number $\mathcal{R}_0$

To fully understand the behaviour of a basic model system we compute the equilibrium points and the basic reproduction number. The reproduction number is defined as the number of secondary infections produced by each infectious cell during its lifetime. In this work, we present two reproduction numbers of interest i.e. (the basic reproduction number and the CTL-reproduction number). The model system (3.2) also presents or exhibits three equilibrium points of interest that is the disease-free, the CTL-inactive endemic equilibrium and the CTL-active endemic equilibrium. The stability analysis of the model based on these three equilibrium points is established to show the stability of the entire system and explore the dynamics of the model.To establish disease-free equilibrium point, we solve model system (3.2) as follows

$$\begin{aligned}
0 &= \Lambda + \phi L - \left(\frac{\beta V}{(\gamma + T_s)} + \mu\right) T_s, \\
0 &= \frac{\beta V T_s}{(\gamma + T_s)} - (\mu + \psi + \phi) L, \\
0 &= \psi L - (\epsilon + \mu + \theta K) I_1, \\
0 &= \epsilon I_1 + r\epsilon I_2 - (\mu + \theta K) I_2, \\
0 &= N_2 \mu (I_1 + I_2) - \delta V, \\
0 &= \sigma I_2 K - \nu K.
\end{aligned} \tag{3.20}$$

Considering that all infectious compartments $\{L, I_1, I_2, V\}$ are all equal to zero, it follows that (3.20) yields a disease-free equilibrium given by

$$\mathcal{E}_0 = \left(\frac{\Lambda}{\mu}, 0, 0, 0, 0, 0\right). \tag{3.21}$$

3.4.1 Calculation of the basic reproduction number, $\mathcal{R}_0$.

The basic reproduction number $\mathcal{R}_0$, is defined as the number of secondary cases produced by a single infectious cell during its entire infectious period. We are interested in knowing mathematically if HPV in the long run will invade the whole epithelial cell population and probably if there will be persistence. R_0 is computed using the next generation matrix approach by

Van den Driessche and Watmough [98]. The method requires that we sort out the compartments of model system (3.2) such that the first compartments correspond to the infectious classes of the model followed by the uninfected compartments, where $x = (x_1, x_2, ...n)$ provided $x_i \geq 0, \quad i = 1, 2, ...n$ are all the individuals in the model while $x = (x_1, x_2, ...m)$ are infected individuals within the compartments. We also define X_{DFE} to be the set of all disease-free states where

$$X_{DFE} = \{x \geq 0 | x_i = 0, \quad i = 1, 2, ...m\}$$

. Let $F_i(x)$ be the rate of appearance of new infections within the infected compartments i and $V_i(x)$ be the difference between the transfer rate of individuals out of compartment i through all other means and the transfer of individuals into compartment i through all other means where $F_i(x),\ V_i(x) \in \mathcal{C}^2$. We proceed to define matrices

$$\begin{aligned} \mathcal{F} &= \left[\frac{\partial F_i(x_0)}{\partial x_j}\right], \\ \mathcal{V} &= \left[\frac{\partial V_i(x_0)}{\partial x_j}\right], \end{aligned} \tag{3.22}$$

for $i \geq 1, \quad j \leq m$ [98]. We take note that $\mathcal{F}$ is strictly a non-negative matrix and $\mathcal{V}$ is a non-singular matrix and the reproduction number is given by

$$\mathcal{R}_0 = \rho(\mathcal{F}\mathcal{V}^{-1}), \tag{3.23}$$

where ρ is the spectral radius or the dominant eigenvalue for the matrix $\mathcal{F}\mathcal{V}^{-1}$. We construct the $\mathcal{F}$ and $\mathcal{V}$ matrices for system (3.2) and of particular note is that the two matrices are made up of the infectious classes only that is $L(t), I_1(t), I_2(t), V(t)$ and exclude the susceptible and immune response classes, $T_s(t)$ and $K(t)$. Therefore we have the following matrices evaluated at the disease-free equilibrium point;

$$\mathcal{F} = \begin{bmatrix} 0 & 0 & 0 & \dfrac{\Lambda\beta}{(\Lambda + \gamma\mu)} \\ 0 & 0 & 0 & 0 \\ 0 & 0 & 0 & 0 \\ 0 & 0 & 0 & 0 \end{bmatrix}, \mathcal{V} = \begin{bmatrix} (\mu + \psi + \phi) & 0 & 0 & 0 \\ -\psi & (\epsilon + \mu) & 0 & 0 \\ 0 & -\epsilon & \mu - r\epsilon & 0 \\ 0 & -N_2\mu & -N_2\mu & \delta \end{bmatrix} \tag{3.24}$$

and

$$\mathcal{V}^{-1} = \begin{bmatrix} \frac{1}{(\mu+\psi+\phi)} & 0 & 0 & 0 \\ \frac{\psi}{(\mu+\phi+\psi)(\epsilon+\mu)} & \frac{1}{(\epsilon+\mu)} & 0 & 0 \\ \frac{\psi\epsilon}{(\mu+\phi+\psi)(\epsilon+\mu)(\mu-r\epsilon)} & \frac{\epsilon}{(\mu-r\epsilon)(\epsilon+\mu)} & \frac{1}{\mu-r\epsilon} & 0 \\ \frac{N_2\mu\psi(\mu+\epsilon-r\epsilon)}{\delta(\mu+\phi+\psi)(\epsilon+\mu)(\mu-r\epsilon)} & \frac{N_2\mu(\mu+\epsilon-r\epsilon)}{\delta(\mu-r\epsilon)(\epsilon+\mu)} & \frac{N_2\mu}{\delta(\mu-r\epsilon)} & \frac{1}{\delta} \end{bmatrix} \tag{3.25}$$

such that the spectral radius $\rho(FV^{-1})$ is given by

$$\mathcal{R}_0 = \frac{\beta\Lambda\psi N_2\mu(\mu+\epsilon-r\epsilon)}{\delta(\gamma\mu+\Lambda)(\psi+\phi+\mu)(\mu-r\epsilon)(\epsilon+\mu)} \tag{3.26}$$

with $\mu - r\epsilon > 0,\ 0 < r < 1$ and $0 < \epsilon < 1$. The assumption being that as oncogene expression, ϵ, increases $(\mu - r\epsilon)$ decreases and when oncogene expression, ϵ, decreases $(\mu - r\epsilon)$ approaches μ. Hence, the reproduction number is positive as required. Interpretation of $\mathcal{R}_0$ is as follows: $N_2\mu$ represents the number of virus particles produced by an infectious cell, $\frac{1}{\delta}$ is the average life of HPV, $\frac{\psi}{(\phi+\mu+\psi)}$ is the proportion of latently infected cells that mature into actively infected cells I_1, $\frac{\epsilon}{(\mu+\epsilon)(\mu-r\epsilon)}$ is the proportion of I_1 cells that are converted to I_2 cells due to oncogene expression and $\frac{1}{\mu+\epsilon}$ is the proportion of I_2 cells that self proliferate. From the reproduction number, $\mathcal{R}_0$ we want to establish when $\mathcal{R}_0 < 1$, then the disease-free equilibrium will be locally asymptotically stable. This means that HPV cannot invade the population of cells and if $\mathcal{R}_0 > 1$, the disease-free equilibrium is unstable and total invasion of cells by HPV is possible. $\mathcal{R}_0 < 1$, the desired threshold, implies that an infectious cell will produce less than one infectious cell such that HPV infection will not spread among cells.

Theorem 14. *The disease-free equilibrium for model* (3.2) *is locally asymptotically stable provided that* $\mathcal{R}_0 < 1$ *and unstable when* $\mathcal{R}_0 > 1$.

Proof. To prove the local stability of the disease-free equilibrium of (3.2), we find the Jacobian for the system and evaluate it at the disease-free equilibrium. The Jacobian for the system

evaluated at the disease-free equilibrium is given by

$$J(\mathcal{E}_0) = \begin{bmatrix} -\mu & \phi & 0 & 0 & -\dfrac{\Lambda\beta}{(\Lambda+\gamma\mu)} & 0 \\ 0 & -(\mu+\psi+\phi) & 0 & 0 & \dfrac{\Lambda\beta}{(\Lambda+\gamma\mu)} & 0 \\ 0 & \psi & -(\epsilon+\mu) & 0 & 0 & 0 \\ 0 & 0 & \epsilon & -(\mu-r\epsilon) & 0 & 0 \\ 0 & 0 & N_2\mu & N_2\mu & -\delta & 0 \\ 0 & 0 & 0 & 0 & 0 & -\nu \end{bmatrix}, \tag{3.27}$$

We need to show that the eigenvalues produced by the Jacobian (3.27), all have negative real parts. We split and rearrange the Jacobian matrix (3.27) as shown in matrix (3.28) where the first row represents the susceptible cells and the second row represents the immune response cells while the bottom (right block) represents the infectious classes (L, I_1, I_2, V) as shown;

$$J(\mathcal{E}_0) = \left[\begin{array}{cc|ccc|c} -\mu & \phi & 0 & 0 & -\dfrac{\Lambda\beta}{(\Lambda+\gamma\mu)} & 0 \\ 0 & -\nu & 0 & 0 & 0 & 0 \\ \hline 0 & 0 & -(\psi+\phi+\mu) & 0 & 0 & \dfrac{\Lambda\beta}{(\Lambda+\gamma\mu)} \\ 0 & 0 & \psi & -(\mu+\epsilon) & 0 & 0 \\ 0 & 0 & 0 & \epsilon & -(\mu-r\epsilon) & 0 \\ 0 & 0 & 0 & N_2\mu & N_2\mu & -\delta \end{array}\right]. \tag{3.28}$$

By finding the eigenvalues of the first sub-matrix, we establish that the eigenvalues are $\lambda = -\mu$ and $\lambda = -\nu$. The eigenvalues of the next sub-matrix for the infected class produce a fourth degree polynomial equation given by

$$P(\lambda) = \lambda^4 + a_1\lambda^3 + a_2\lambda^2 + a_3\lambda + a_4, \tag{3.29}$$

where λ is the eigenvalue and

$$\begin{aligned} a_1 &= 3\mu + \psi + \phi + \epsilon(1-r) + \delta > 0, \\ a_2 &= \delta(3\mu + \epsilon(1-r) + \psi + \phi) + (\mu+\psi+\phi)(2\mu + \epsilon(1-r)) + (\epsilon+\mu)(\mu - r\epsilon) > 0, \\ a_3 &= \delta(\mu+\psi+\phi)(2\mu + \epsilon(1-r)) + (\epsilon+\mu)(\mu-r\epsilon)(\delta+\mu+\psi+\phi) > 0, \\ a_4 &= \delta(\mu+\epsilon)(\mu+\psi+\phi)(\mu-r\epsilon)\left[1-\mathcal{R}_0\right] > 0. \end{aligned} \tag{3.30}$$

The polynomial (3.29) requires further mathematical probing. It is important to know if all the eigenvalues for the polynomial equation $P(\lambda)$ have negative real parts (implying stability of the

disease-free equilibrium) or positive real parts (implying that the disease-free equilibrium might not be stable). To do this, we state the Routh Hurwitz Criterion for a fourth-order polynomial as follows

Theorem 15. *Given that a polynomial*

$$P(x) = x^n + a_1x^{n-1} + a_2x^{n-2} + a_3x^{n-3} + ... + a_{n-1}x + a_n$$

where a_i *for* $(i = 1, 2, 3, ..., n)$ *are real constants and we define the nth Hurwitz matrix* H_n *as*

$$H_n = \begin{bmatrix} a_1 & 1 & 0 & 0 & ..... & 0 \\ a_3 & a_2 & a_1 & 1 & ..... & 0 \\ a_5 & a_4 & a_3 & a_2 & ..... & 0 \\ . & . & . & . & ..... & 0 \\ . & . & . & . & ..... & 0 \\ . & . & . & . & ..... & 0 \\ 0 & 0 & 0 & 0 & ..... & a_n \end{bmatrix} \tag{3.31}$$

where $a_i = 0$ *if* $j > n$. *All the roots of the polynomial* $P(x)$ *have negative real parts if and only if the determinants of all the Hurwitz matrices are positive:* $det(H_j) > 0, \quad j = 1, 2, 3, ..., n$ *[107].*

Using theorem 15 we state without proof the following lemma for criterion for polynomials of fourth degree.

Lemma 3. *The eigenvalues of the fourth degree polynomial* $P(\lambda) = \lambda^4 + a_1\lambda^3 + a_2\lambda^2 + a_3\lambda + a_4$ *have negative real parts provided that* $a_1 > 0, \quad a_2 > 0, \quad a_3 > 0, a_4 > 0$, $a_1a_2 > a_3$ *and* $a_3(a_1a_2 - a_3) - a_1^2a_4 > 0$ *where* $a_0, \quad a_1, \quad a_2, \quad a_3, a_4$ *are given by equation (3.30).*

Proof. To show that the Routh Hurwitz condition is satisfied, let:

$$\alpha = (3\mu + \psi + \phi + \epsilon(1 - r) + \delta), \ \alpha_1 = (\mu + \psi + \phi), \ \alpha_2 = (2\mu + \epsilon(1 - r))$$

and $\alpha_3 = (\epsilon + \mu)(\mu - r\epsilon)$ Hence,

$$\begin{aligned} a_1a_2 - a_3 &= \alpha + \delta^2\delta\alpha^2 + \alpha_3\alpha_2 + \alpha\alpha_1\alpha_2 > 0, \\ a_3(a_1a_2 - a_3) &= \delta^3\alpha\alpha_1\alpha_2 + \delta^2\alpha_3(\alpha_1 + \alpha^2 + \alpha\alpha_1 + \alpha) + \delta\alpha_3\alpha_2(\alpha_2\alpha_1 + \alpha_3\alpha_2) \\ &+ \delta\alpha_1\alpha(\alpha\alpha_3 + \alpha_1\alpha_2^2) + \alpha_1\alpha_2\alpha_3(\alpha_3 + \alpha\alpha_1) \end{aligned} \tag{3.32}$$

and

$$a_1^2 a_4 = (1 - \mathcal{R}_0)\left[\delta^3\alpha_3\alpha_1 + 2\delta^2\alpha\alpha_1\alpha_3 + \delta\alpha^3\alpha_1\alpha^2\right], \tag{3.33}$$

such that

$$\begin{aligned} a_3(a_1a_2 - a_3) - a_1^2a_4 \quad &= \quad \delta^3\alpha_2(\alpha_3 + \alpha\alpha_1) + \delta^2\alpha_3(\alpha_1 + \alpha\alpha_2) + \delta\alpha_2\alpha_3(\alpha_2\alpha_1 + \alpha_3 + \alpha\alpha_1) \\ &+ \quad \delta\alpha_1^2\alpha\alpha_2^2 + \alpha_1\alpha_2\alpha_3(\alpha_3 + \alpha\alpha_1) + \mathcal{R}_0\alpha_1\alpha_3\left[\delta\alpha^2 + \delta^3 + 2\delta^2\alpha\right] > 0. \end{aligned} \tag{3.34}$$

The Routh Hurwitz condition is satisfied and this implies that the quartic polynomial has roots with negative real parts. Thus, the disease-free equilibrium is locally asymptotically stable when $\mathcal{R}_0 < 1$ and unstable otherwise. This completes the proof. □

□

3.4.2 Global stability analysis of the disease-free equilibrium

The disease-free equilibrium, $\mathcal{E}_0$, is locally stable provided that $\mathcal{R}_0 < 1$. We adopt the work done by Wang *et al.* [103] and Shuai and Van den Driessche*et al.* [88] to prove the global stability of model system (3.2).

Theorem 16. *The disease-free equilibrium, $\mathcal{E}_0$, for system* (3.2) *is globally stable provided that* $\mathcal{R}_0 < 1$.

Proof. We prove global stability of model system (3.2) through following the work by Shuai and Van den Driessche [88]. Recall that from our model

$$\mathcal{R}_0 = \frac{\beta\Lambda\psi N_2\mu(\mu + \epsilon - r\epsilon)}{\delta(\gamma\mu + \Lambda)(\psi + \mu + \phi)(\mu - r\epsilon)(\epsilon + \mu)}. \tag{3.35}$$

The Perron-Frobenius theorem states that every non-negative matrix can be obtained as a limit of positive matrices. Therefore, there exists an eigenvector with non-negative parts and the corresponding eigenvalue is non-negative and will be greater or equal in its absolute value to all other eigenvalues of the matrix [60]. In simpler terms the theorem simply states that since we have the non-negative matrix $\mathcal{V}^{-1}\mathcal{F}$, it should have a non-negative left eigenvalue u corresponding to

$$\mathcal{R}_0 = \rho(\mathcal{V}^{-1}\mathcal{F}) = \rho(\mathcal{F}\mathcal{V}^{-1}),$$

which implies that

$$u^T\rho(\mathcal{V}^{-1}\mathcal{F}) = u^T\mathcal{R}_0.$$

Recall that

$$\mathcal{F} = \begin{bmatrix} 0 & 0 & 0 & \dfrac{\beta T_{s0}}{(\gamma + T_{s0})} \\ 0 & 0 & 0 & 0 \\ 0 & 0 & 0 & 0 \\ 0 & 0 & 0 & 0 \end{bmatrix}, \mathcal{V} = \begin{bmatrix} (\mu + \psi + \phi) & 0 & 0 & 0 \\ -\psi & (\epsilon + \mu) & 0 & 0 \\ 0 & -\epsilon & \mu - r\epsilon & 0 \\ 0 & -N_2\mu & -N_2\mu & \delta \end{bmatrix}, \tag{3.36}$$

where $T_{s0} = \dfrac{\Lambda}{\mu}$ and

$$\mathcal{V}^{-1} = \begin{bmatrix} \dfrac{1}{(\mu + \psi + \phi)} & 0 & 0 & 0 \\ \dfrac{\psi}{(\mu + \psi + \phi)(\epsilon + \mu)} & \dfrac{1}{(\epsilon + \mu)} & 0 & 0 \\ \dfrac{\psi\epsilon}{(\epsilon + \mu)(\mu + \psi + \phi)(\mu - r\epsilon)} & \dfrac{\epsilon}{(\epsilon + \mu)(\mu - r\epsilon)} & \dfrac{1}{\mu - r\epsilon} & 0 \\ \dfrac{N_2\mu\psi(\mu + \epsilon - r\epsilon)}{\delta(\psi + \phi + \mu)(\mu - r\epsilon)(\epsilon + \mu)} & \dfrac{N_2\mu(\mu + \epsilon - r\epsilon)}{\delta(\mu - r\epsilon)(\epsilon + \mu)} & \dfrac{N_2\mu}{\delta(\mu - r\epsilon)} & \dfrac{1}{\delta} \end{bmatrix}, \tag{3.37}$$

so that

$$\mathcal{V}^{-1}\mathcal{F} = \begin{bmatrix} 0 & 0 & 0 & \dfrac{\beta T_{s0}}{(\gamma + T_{s0})(\mu + \psi + \phi)} \\ 0 & 0 & 0 & \dfrac{\beta\psi T_{s0}}{(\gamma + T_{s0})(\mu + \psi + \phi)(\epsilon + \mu)} \\ 0 & 0 & 0 & \dfrac{\beta\psi\epsilon T_{s0}}{(\gamma + T_{s0})(\mu + \psi + \phi)(\epsilon + \mu)(\mu - r\epsilon)} \\ 0 & 0 & 0 & \dfrac{\beta N_2\mu\psi(\mu + \epsilon - r\epsilon)T_{s0}}{\delta(\gamma + T_{s0})(\mu + \psi + \phi)(\epsilon + \mu)(\mu - r\epsilon)} \end{bmatrix}. \tag{3.38}$$

It can be seen that $\mathcal{V}^{-1}\mathcal{F}$ is reducible since the last column is the only no-zero column and therefore theorem 6 stated in chapter 2 fails. Therefore we construct a Lyapunov function of the form

$$\mathcal{Z} = u^T\mathcal{V}^{-1}\mathcal{X}, \tag{3.39}$$

where $u^T = (0,0,0,1)$ and $\mathcal{X} = (L, I_1, I_2, V)^T$. Therefore equation (3.39) becomes

$$\mathcal{Z} = \begin{bmatrix} 0 & 0 & 0 & 1 \end{bmatrix} \begin{bmatrix} \frac{1}{(\mu+\psi+\phi)} & 0 & 0 & 0 \\ \frac{\psi}{(\mu+\psi+\phi)(\epsilon+\mu)} & \frac{1}{(\epsilon+\mu)} & 0 & 0 \\ \frac{\psi\epsilon}{(\epsilon+\mu)(\mu+\psi+\phi)(\mu-r\epsilon)} & \frac{\epsilon}{(\epsilon+\mu)(\mu-r\epsilon)} & \frac{1}{\mu-r\epsilon} & 0 \\ \frac{N_2\mu\psi(\mu+\epsilon-r\epsilon)}{\delta(\psi+\phi+\mu)(\mu-r\epsilon)(\epsilon+\mu)} & \frac{N_2\mu(\mu+\epsilon-r\epsilon)}{\delta(\mu-r\epsilon)(\epsilon+\mu)} & \frac{N_2\mu}{\delta(\mu-r\epsilon)} & \frac{1}{\delta} \end{bmatrix} \begin{bmatrix} L \\ I_1 \\ I_2 \\ V \end{bmatrix}. \tag{3.40}$$

Equation (3.40) leads to

$$\begin{aligned} \mathcal{Z} &= \frac{N_2\mu\psi(\mu+\epsilon-r\epsilon)}{\delta(\psi+\phi+\mu)(\mu-r\epsilon)(\epsilon+\mu)}L + \frac{N_2\mu(\mu+\epsilon-r\epsilon)}{\delta(\mu-r\epsilon)(\epsilon+\mu)}I_1 + \frac{N_2\mu}{\delta(\mu-r\epsilon)}I_2 + \frac{1}{\delta}V, \\ &= \frac{\mathcal{R}_0(\gamma\mu+\Lambda)}{\beta\Lambda}\left[L + \frac{(\mu+\psi+\phi)}{\psi}I_1 + \frac{(\mu+\psi+\phi)(\epsilon+\mu)}{\psi(\mu+\epsilon-r\epsilon)}I_2 + \frac{(\mu+\psi+\phi)(\epsilon+\mu)(\mu-r\epsilon)}{N_2\mu\psi(\mu+\epsilon-r\epsilon)}V\right]. \end{aligned} \tag{3.41}$$

Using theorem 5 stated in chapter 2, we obtain the derivative of $\mathcal{Z}$ as

$$\mathcal{Z}' = u^T\mathcal{V}^{-1}(\mathcal{F}-\mathcal{V})\mathcal{X} - u^T\mathcal{V}^{-1}f(x,T_s) \tag{3.42}$$

where

$$u^T\mathcal{V}^{-1} = \begin{bmatrix} 0 & 0 & 0 & 1 \end{bmatrix} \begin{bmatrix} \frac{1}{(\mu+\psi+\phi)} & 0 & 0 & 0 \\ \frac{\psi}{(\mu+\psi+\phi)(\epsilon+\mu)} & \frac{1}{(\epsilon+\mu)} & 0 & 0 \\ \frac{\psi\epsilon}{(\epsilon+\mu)(\mu+\psi+\phi)(\mu-r\epsilon)} & \frac{\epsilon}{(\epsilon+\mu)(\mu-r\epsilon)} & \frac{1}{\mu-r\epsilon} & 0 \\ \frac{N_2\mu\psi(\mu+\epsilon-r\epsilon)}{\delta(\psi+\phi+\mu)(\mu-r\epsilon)(\epsilon+\mu)} & \frac{N_2\mu(\mu+\epsilon-r\epsilon)}{\delta(\mu-r\epsilon)(\epsilon+\mu)} & \frac{N_2\mu}{\delta(\mu-r\epsilon)} & \frac{1}{\delta} \end{bmatrix}, \tag{3.43}$$

which gives

$$u^T\mathcal{V}^{-1} = \left(\frac{N_2\mu\psi(\mu+\epsilon-r\epsilon)}{\delta(\psi+\phi+\mu)(\mu-r\epsilon)(\epsilon+\mu)}, \frac{N_2\mu(\mu+\epsilon-r\epsilon)}{\delta(\mu-r\epsilon)(\epsilon+\mu)}, \frac{N_2\mu}{\delta(\mu-r\epsilon)}, \frac{1}{\delta}\right) \tag{3.44}$$

and

$$(\mathcal{F}-\mathcal{V})\mathcal{X}=\begin{bmatrix} -(\mu+\psi+\phi) & 0 & 0 & \dfrac{\beta T_{s0}}{(\gamma+T_{s0})} \\ \psi & -(\epsilon+\mu) & 0 & 0 \\ 0 & \epsilon & -(\mu-r\epsilon) & 0 \\ 0 & N_2\mu & N_2\mu & -\delta \end{bmatrix}\begin{bmatrix} L \\ I_1 \\ I_2 \\ V \end{bmatrix}, \tag{3.45}$$

which gives

$$(\mathcal{F}-\mathcal{V})\mathcal{X}=\left[\frac{\beta T_{s0}}{(\gamma+T_{s0})}V-(\mu+\phi+\psi)L,\ \psi L-(\epsilon+\mu)I_1,\ \epsilon I_1-(\mu-r\epsilon)I_2,\ N_2\mu(I_1+I_2)-\delta V\right]^T, \tag{3.46}$$

therefore with little manipulation we obtain

$$u^T\mathcal{V}^{-1}(\mathcal{F}-\mathcal{V})\mathcal{X}=(\mathcal{R}_0-1)V, \tag{3.47}$$

we also have

$$f(x,T_s)=(\mathcal{F}-\mathcal{V})\mathcal{X}-F(x,T_s)+V(x,T_s).$$

and so

$$f(x,T_s)=\begin{bmatrix} \dfrac{\beta V T_{s0}}{(\gamma+T_{s0})}-(\mu+\psi+\phi)L \\ \psi L-(\epsilon+\mu)I_1 \\ \epsilon I_1+r\epsilon I_2-\mu I_2 \\ N_2\mu(I_1+I_2)-\delta V \end{bmatrix}-\begin{bmatrix} \dfrac{\beta T_s}{(\gamma+T_s)} \\ 0 \\ 0 \\ 0 \end{bmatrix}+\begin{bmatrix} (\mu+\psi+\phi)L \\ (\epsilon+\mu+\theta K)I_1-\psi L \\ (\mu+\theta K)I_2-\epsilon I_1-r\epsilon I_2-\mu I_2 \\ \delta V-N_2\mu(I_1+I_2) \end{bmatrix}. \tag{3.48}$$

which yields

$$f(x,T_s)=\begin{bmatrix} \dfrac{\beta V T_{s0}}{(\gamma+T_{s0})}-\dfrac{\beta V T_s}{(\gamma+T_s)} \\ \theta K I_1 \\ \theta K I_2 \\ 0 \end{bmatrix} \tag{3.49}$$

such that

$$u^T\mathcal{V}^{-1}f(x,T_s)=\frac{\mathcal{R}_0(\gamma+T_{s0})}{T_{s0}}\left[\frac{T_{s0}}{\gamma+T_{s0}}-\frac{T_s}{\gamma+T_s}\right]V+\frac{\mathcal{R}_0(\gamma+T_{s0})(\mu+\psi+\phi)\theta K}{\beta\psi T_{s0}}\left[I_1+\frac{\mu+\epsilon}{\mu+\epsilon-r\epsilon}I_2\right]. \tag{3.50}$$

Therefore

$$\mathcal{Z}' = (\mathcal{R}_0 - 1)\, V - \frac{\mathcal{R}_0(\gamma + T_{s0})}{T_{s0}} \left[\left(\frac{T_{s0}}{\gamma + T_{s0}} - \frac{T_s}{\gamma + T_s} \right) V + \frac{B}{\beta\psi} \left(I_1 + \frac{\mu + \epsilon}{\mu + \epsilon - r\epsilon} I_2 \right) \right] \tag{3.51}$$

where $B = (\mu + \psi + \phi)\theta K$. Provided that $\mathcal{R}_0 \leq 1$, then it follows that $\mathcal{Z}' \leq 0$ and it can also be seen that $\mathcal{Z}' = 0$ is satisfied when $V = I_1 = I_2 = K = 0$ and $T_{s0} = T_s$. Therefore it can be established that the only largest compact invariant set in $(T_s, L, I_1, I_2, V, K) \in \mathbb{R}^6_+ : \mathcal{Z}' = 0$ is the singleton $\{\mathcal{E}_0\}$. Based on LaSalle's invariance principle [50], it suffices to state that the singleton $\{\mathcal{E}_0\}$ is globally asymptotically stable in Ω when $\mathcal{R}_0 < 1$ and this concludes the proof. □

3.4.3 The endemic equilibrium

As stated earlier, model system (3.2) has two endemic equilibrium points namely the CTL-inactive endemic equilibrium, $\mathcal{E}_1^e$ and the CTL-active endemic equilibrium, $\mathcal{E}_2^e$. The CTL-inactive endemic equilibrium point is given by

$$\mathcal{E}_1^e = \{T_s^e, L^e, I_1^e, I_2^e, V^e, K^e\}$$

where

$$\begin{aligned}
T_s^e &= \frac{\Lambda\gamma}{\mu[\mathcal{R}_0\gamma\mu + \Lambda(\mathcal{R}_0 - 1)]} > 0, \\
L^e &= \frac{\Lambda(\mathcal{R}_0 - 1)(\gamma\mu + \Lambda)}{(\mu + \psi)[\mathcal{R}_0\gamma\mu + \Lambda(\mathcal{R}_0 - 1)]} > 0, \\
I_1^e &= \frac{\Lambda\psi(\mathcal{R}_0 - 1)(\gamma\mu + \Lambda)}{(\mu + \psi)(\epsilon + \mu)[\mathcal{R}_0\gamma\mu + \Lambda(\mathcal{R}_0 - 1)]} > 0, \\
I_2^e &= \frac{\Lambda\psi\epsilon(\mathcal{R}_0 - 1)(\gamma\mu + \Lambda)}{(\mu + \psi)(\mu - r\epsilon)(\epsilon + \mu)[\mathcal{R}_0\gamma\mu + \Lambda(\mathcal{R}_0 - 1)]} > 0, \\
V^e &= \frac{\mathcal{R}_0(\mathcal{R}_0 - 1)(\mu + \psi + \phi)(\Lambda + \gamma\mu)^2}{(\mu + \psi)[\mathcal{R}_0\gamma\mu + \Lambda(\mathcal{R}_0 - 1)]} > 0, \\
K^e &= 0.
\end{aligned} \tag{3.52}$$

The CTL activated endemic equilibrium is given by

$$\mathcal{E}_2^e = \{T_s^{ee}, L^{ee}, I_1^{ee}, I_2^{ee}, V^{ee}, K^{ee}\}$$

where

$$
\begin{aligned}
T_s^{ee} &= \frac{\Lambda\sigma\epsilon\psi - \nu\alpha_1(\alpha_2+\theta K^{ee})(\alpha_3+\theta K^{ee})}{\sigma\epsilon\psi\mu}, \\
L^{ee} &= \frac{\nu(\alpha_2+\theta K^{ee})(\alpha_3+\theta K^{ee})}{\sigma\epsilon\psi}, \\
I_1^{ee} &= \frac{\nu(\alpha_3+\theta K^{ee})}{\sigma\epsilon}, \\
I_2^{ee} &= \frac{\nu}{\sigma}, \\
V^{ee} &= \frac{N_2\nu\mu(\alpha_4+\theta K^{ee})}{\delta\sigma\epsilon}, \\
K &= K^{ee},
\end{aligned}
\tag{3.53}
$$

where $\alpha_1 = (\mu+\psi)$, $\alpha_2 = (\mu+\epsilon)$, $\alpha_3 = (\mu - r\epsilon)$, $\alpha_4 = (\mu+\epsilon-r\epsilon)$ and $\alpha_5 = (\mu+\psi+\phi)$ and K^{ee} is found using the following quartic polynomial given by

$$
M(K^{ee}) = a_0 K^{ee4} + a_1 K^{ee3} + a_2 K^{ee2} + a_3 K^{ee} + a_4 = 0 \tag{3.54}
$$

with

$$
\begin{aligned}
a_0 &= \theta^4\delta\alpha_1\alpha_5\nu^2 > 0, \\
a_1 &= \theta^3\nu^2\alpha_1\left[2\delta\alpha_5(\alpha_2+\alpha_3) - \beta N_2\mu\psi\right], \\
a_2 &= \theta^2\left[\delta\nu^2\alpha_1\alpha_5(2\alpha_2\alpha_3+\alpha_2+\alpha_3) - \delta\nu\alpha_5\delta\epsilon\psi(\Lambda+\gamma\mu) - \beta N_2\mu\psi\nu^2\alpha_1(\alpha_4+\alpha_2+\alpha_3)\right], \\
a_3 &= \theta\left[\delta\nu^2\alpha_5\alpha_1\alpha_2\alpha_3(1+\alpha_2+\alpha_3) + \beta N_2\mu\psi\nu(\psi\Lambda\epsilon\sigma - \alpha_1\alpha_2\alpha_3 + \alpha_4(\alpha_2\alpha_1+\alpha_3\alpha_1))\right], \\
a_4 &= \delta\epsilon\psi\nu\sigma\alpha_2\alpha_5\alpha_3(\Lambda+\gamma\mu)\left[\mathcal{R}_0 - 1\right] - \delta\nu^2\alpha_1\alpha_5\alpha_2^2\alpha_3^2\left[1 - \frac{\mathcal{R}_0(\Lambda+\gamma\mu)}{\Lambda}\right].
\end{aligned}
\tag{3.55}
$$

From equation (3.55) (coefficient equations) it can be clearly seen that $a_0 > 0$ always since all parameters used in the model are positive. It can also be seen that coefficient a_1 is positive when $2\delta\alpha_5(\alpha_2+\alpha_3) > \beta N_2\mu\psi$ and negative when $2\delta\alpha_5(\alpha_2+\alpha_3) < \beta N_2\mu\psi$ which leaves us to determine the signs for the remaining coefficients of interest. To do this, we use Descartes rule of signs [40] for a quartic polynomial as shown in the Table 3.2.

Table 3.2: Descartes table of signs

No.	a_0	a_1	a_2	a_3	a_4	Sign Changes	Roots
1.	+	+	+	+	+	0	0
2.	+	−	+	+	+	2	0, 2
3.	+	−	−	+	+	2	0, 2
4.	+	−	−	−	+	2	0, 2
5.	+	−	−	−	−	1	1
6.	+	+	−	+	+	2	0, 2
7.	+	+	−	−	+	2	0, 2
8.	+	+	−	−	−	1	1
9.	+	+	+	−	+	2	0, 2
10.	+	+	+	−	−	1	1
11.	+	+	+	+	−	1	1
12.	+	−	+	+	−	3	1, 3
13.	+	−	+	−	+	4	0, 4
14.	+	+	−	+	−	3	1, 3
15.	+	−	+	−	−	3	1, 3
16.	+	−	−	+	−	3	1, 3

From the results from Table 3.2, we state the following lemma;

Lemma 4. *The quartic polynomial* $M(K^{ee}) = a_0K^{ee4} + a_1K^{ee3} + a_2K^{ee2} + a_3K^{ee} + a_4$ *has*

1. *one unique positive root provided that cases* $5, 8, 10, 11$ *hold for the coefficients of interest.*

2. *more than one positive root provided that cases* $1, 2, 3, 4, 6, 7, 9, 12, 13, 14, 15, 16$ *hold for the coefficients of interest.*

3.4.4 The CTL activated reproduction number, $\mathcal{R}_K$.

There exists a CTL activated immune response reproduction number that indicates the number of infected cells each immune cell can kill. Therefore, the greater the CTL reproduction number the smaller the infected cell population. The mean lifetime of CTL cells for the model is given by $\frac{1}{\nu}$ and when infection reaches a steady state of I_2^e the average amount of CTL produced will be σI_2^e. Based on model (3.2) (for $\sigma I_2 - \nu \leq 0$) the CTL immune response reproduction

number is given by

$$\mathcal{R}_K = \frac{\sigma I_2}{\nu} = \frac{\Lambda\sigma\psi\epsilon(\mathcal{R}_0 - 1)(\gamma\mu + \Lambda)}{\nu(\mu + \psi)(\mu - r\epsilon)(\epsilon + \mu)[\mathcal{R}_0\gamma\mu + \Lambda(\mathcal{R}_0 - 1)]}. \tag{3.56}$$

If $\mathcal{R}_K > 1$ then the CTL-active endemic equilibrium $\mathcal{E}_2^e$ exists. We state the following lemma;

Lemma 5. *The conditions governing the CTL-inactive/ activated equilibrium are;*

1. *If $\mathcal{R}_0 > 1$ and $\mathcal{R}_K < 1$, then the CTL-inactive endemic equilibrium $\mathcal{E}_1^e$ is globally asymptotically stable.*

2. *If $\mathcal{R}_0 > 1$ and $\mathcal{R}_K > 1$, then the CTL-inactive endemic equilibrium $\mathcal{E}_1^e$ is unstable while the CTL-active equilibrium $\mathcal{E}_2^e$ is globally asymptotically stable.*

The CTL-inactive endemic equilibrium point, $\mathcal{E}_1^e$, presents a situation where there is HPV infection among cells but the innate immune response is not responsive, or may not be required, or is suppressed [107], while the CTL-active endemic equilibrium, $\mathcal{E}_2^e$, on the other hand is the equilibrium where CTL response is prompted into action as it docks on to the infected cell and kills it. It is important to establish the local and global stability of these points, however the equilibrium point, $\mathcal{E}_2^e$, is rather too complex as it contains a quartic polynomial that is rather difficult to solve analytically. The global stability analysis will be presented using numerical simulations.

3.4.5 Local stability analysis of the endemic equilibrium $\mathcal{E}_1^e$

We investigate the local stability of the endemic equilibrium $\mathcal{E}_1^e$ using the Center Manifold theory [15]. This is to establish if there exists a forward bifurcation that implies the stability of the endemic near $\mathcal{R}_0 = 1$.

Theorem 17. *Model system (3.2) has a unique stable endemic equilibrium point given by $\mathcal{E}_1^e$ whenever $\mathcal{R}_0 > 1$ and is unstable otherwise.*

Proof. To investigate the probable existence of a forward bifurcation and the local stability of

the endemic equilibrium, $\mathcal{E}_1^e$, let

$$\begin{aligned}
\dot{x}_1 &= f_1 = \Lambda + \phi x_2 - \left[\frac{\beta x_5}{(\gamma + x_1)} + \mu\right] x_1, \\
\dot{x}_2 &= f_2 = \frac{\beta x_5 x_1}{(\gamma + x_1)} - (\mu + \psi + \phi) x_2, \\
\dot{x}_3 &= f_3 = \psi x_2 - (\epsilon + \mu + \theta x_6) x_3, \\
\dot{x}_4 &= f_4 = \epsilon x_3 + r\epsilon x_4 - (\mu + \theta x_6) x_4, \\
\dot{x}_5 &= f_5 = N_2 \mu (x_3 + x_4) - \delta x_5, \\
\dot{x}_6 &= f_6 = \sigma x_4 x_6 - \nu x_6,
\end{aligned} \tag{3.57}$$

where $T_s = x_1$, $L = x_2$, $I_1 = x_3$, $I_2 = x_4$, $V = x_5$, $K = x_6$. We consider the case where the bifurcation parameter of interest is the transmission rate $\beta = \beta^*$ and solving for β^* given that $\mathcal{R}_0 = 1$ yields

$$\begin{aligned}
1 &= \frac{\beta \Lambda \psi N_2 \mu (\mu + \epsilon - r\epsilon)}{\delta(\gamma\mu + \Lambda)(\mu + \psi + \phi)(\mu - r\epsilon)(\epsilon + \mu)}, \\
\beta^* &= \frac{\delta(\gamma\mu + \Lambda)(\mu + \psi + \phi)(\mu - r\epsilon)(\epsilon + \mu)}{\Lambda \psi N_2 \mu (\mu + \epsilon - r\epsilon)}.
\end{aligned} \tag{3.58}$$

The Jacobian of model system (3.2) evaluated at the disease-free equilibrium and with $\beta = \beta^*$ is given by

$$J^* = \begin{bmatrix}
-\mu & \phi & 0 & 0 & -\dfrac{\delta(\mu + \psi + \phi)(\mu - r\epsilon)(\epsilon + \mu)}{\psi N_2 \mu (\mu + \epsilon - r\epsilon)} & 0 \\
0 & -(\mu + \psi + \phi)) & 0 & 0 & \dfrac{\delta(\mu + \psi + \phi)(\mu - r\epsilon)(\epsilon + \mu)}{\psi N_2 \mu (\mu + \epsilon - r\epsilon)} & 0 \\
0 & \psi & -(\epsilon + \mu) & 0 & 0 & 0 \\
0 & 0 & \epsilon & -(\mu - r\epsilon) & 0 & 0 \\
0 & 0 & N_2\mu & N_2\mu & -\delta & 0 \\
0 & 0 & 0 & 0 & 0 & -\nu
\end{bmatrix}. \tag{3.59}$$

It has been established in theorem (11) that the Jacobian matrix (3.59) evaluated at the disease-free equilibrium has eigenvalues with negative real parts and it has a zero eigenvalue when $\mathcal{R}_0 = 1$. Based on this, we can apply the Center Manifold Theorem [15] which is stated as follows:

Theorem 18 (Center Manifold Theory,adopted from, Castillo Chavez and Song [15]). *Consider the following general system of ordinary differential equation equations with a parameter* ϕ

$$\frac{dx}{dt} = F(x, \phi), F : \mathbb{R}^n \times \mathbb{R} \text{ and } F \in \mathbb{C}^2(\mathbb{R}^n \times \mathbb{R}) \tag{3.60}$$

where 0 *is an equilibrium of the system that is* $f(0, \phi) = 0$ *for all* ϕ *and assume that*
A1*:* $A = D_x F(0,0) = \left(\frac{\partial f_i}{\partial x_j}(0,0)\right)$ *is the linearisation of system (3.2) around the equilibrium point with* ϕ *evaluated at* 0.

A2*: Zero is a simple eigenvalue of A and other eigenvalues of A have negative real parts.*

A3*: Matrix A has a right eigenvalue given by* ω *and a left eigenvalue given by* v *that correspond to the zero eigenvalue.*

Let f_k *be the* k^{th} *component of* f *and*

$$\begin{cases} a &= \sum_{k,i,j=1}^{n} v_k \omega_i \omega_j \frac{\partial^2 f_k}{\partial x_i \partial x_j}(0,0), \\ \\ b &= \sum_{k,i=1}^{n} v_k \omega_i \frac{\partial^2 f_k}{\partial x_i \partial \phi}(0,0). \end{cases} \tag{3.61}$$

The local dynamics of the system around 0 *are totally governed by* a *and* b.

i. $a > 0$, $b > 0$. *When* $\phi < 0$ *with* $|\phi| \ll 1$, *0 is locally asymptotically stable, and there exists a positive unstable equilibrium; when* $0 \leq \phi \ll 1$, *0 is unstable and there exists a negative and locally asymptotically stable equilibrium;*

ii. $a < 0$, $b < 0$. *When* $\phi < 0$ *with* $|\phi| \ll 1$, *0 unstable; when* $0 \leq \phi \ll 1$, *0 is locally asymptotically stable, and there exists a positive unstable equilibrium;*

iii. $a > 0$, $b < 0$. *When* $\phi < 0$ *with* $|\phi| \ll 1$, *0 is unstable, and there exists a locally asymptotically stable negative equilibrium; when* $0 \leq \phi \ll 1$, *0 is stable, and a positive unstable equilibrium appears;*

iv. $a < 0$, $b > 0$. *When* ϕ *changes from negative to positive, 0 changes its stability from stable to unstable. Correspondingly a negative unstable equilibrium becomes positive and locally asymptotically stable.*

Applying the Center Manifold Theorem to our model, we let $\mathbf{W} = (\omega_1, \omega_2, \omega_3, \omega_4, \omega_5, \omega_6)$ be the right eigenvector associated with the zero eigenvector and $\mathbf{V} = (v_1, v_2, v_3, v_4, v_5, v_6)$ be the left

eigenvector associated with the zero eigenvector. We multiply the Jacobian matrix (3.59) by the right eigenvector as follows

$$\begin{pmatrix} -\mu & \phi & 0 & 0 & -\frac{\delta(\mu+\psi+\phi)(\mu-r\epsilon)(\epsilon+\mu)}{\psi N_2\mu(\mu+\epsilon-r\epsilon)} & 0 \\ 0 & -(\mu+\psi+\phi) & 0 & 0 & \frac{\delta(\mu+\psi+\phi)(\mu-r\epsilon)(\epsilon+\mu)}{\psi N_2\mu(\mu+\epsilon-r\epsilon)} & 0 \\ 0 & \psi & -(\epsilon+\mu) & 0 & 0 & 0 \\ 0 & 0 & \epsilon & -(\mu-r\epsilon) & 0 & 0 \\ 0 & 0 & N_2\mu & N_2\mu & -\delta & 0 \\ 0 & 0 & 0 & 0 & 0 & -\nu \end{pmatrix} \begin{pmatrix} \omega_1 \\ \omega_2 \\ \omega_3 \\ \omega_4 \\ \omega_5 \\ \omega_6 \end{pmatrix} = \begin{pmatrix} 0 \\ 0 \\ 0 \\ 0 \\ 0 \\ 0 \end{pmatrix} \tag{3.62}$$

This yields the following right eigenvectors

$$\omega_1 = -\frac{1}{\mu}, \quad \omega_2 = \frac{1}{(\mu+\psi)}, \quad \omega_3 = \frac{\psi}{(\epsilon+\mu)(\mu+\psi)}, \quad \omega_4 = \frac{\epsilon\psi}{(\epsilon+\mu)(\mu+\psi)(\mu-r\epsilon)}, \tag{3.63}$$
$$\omega_5 = \frac{N_2\mu\psi(\mu+\epsilon-r\epsilon)}{\delta(\mu+\psi)(\mu+\epsilon)(\mu-r\epsilon)}, \quad \omega_6 = 0$$

and the left eigenvectors are found by

$$\begin{pmatrix} v_1 \\ v_2 \\ v_3 \\ v_4 \\ v_5 \\ v_6 \end{pmatrix}^T \begin{pmatrix} -\mu & 0 & 0 & 0 & -\frac{\delta(\mu+\psi+\phi)(\mu-r\epsilon)(\epsilon+\mu)}{\psi N_2\mu(\mu+\epsilon-r\epsilon)} & 0 \\ 0 & -(\mu+\psi+\phi) & 0 & 0 & \frac{\delta(\mu+\psi+\phi)(\mu-r\epsilon)(\epsilon+\mu)}{\psi N_2\mu(\mu+\epsilon-r\epsilon)} & 0 \\ 0 & \psi & -(\epsilon+\mu) & 0 & 0 & 0 \\ 0 & 0 & \epsilon & -(\mu-r\epsilon) & 0 & 0 \\ 0 & 0 & N_2\mu & N_2\mu & -\delta & 0 \\ 0 & 0 & 0 & 0 & 0 & -\nu \end{pmatrix} = \begin{pmatrix} 0 \\ 0 \\ 0 \\ 0 \\ 0 \\ 0 \end{pmatrix} \tag{3.64}$$

which yields the following left eigenvectors

$$v_1 = 0, \quad v_2 = v_2, \quad v_3 = \frac{(\mu+\psi+\phi)}{\psi}v_2, \quad v_4 = \frac{(\epsilon+\mu)(\mu+\psi+\phi)}{\psi(\mu+\epsilon-r\epsilon)}v_2,$$
$$v_5 = \frac{(\epsilon+\mu)(\mu+\psi+\phi)(\mu-r\epsilon)}{N_2\mu\psi(\mu+\epsilon-r\epsilon)}v_2, \quad v_6 = 0 \tag{3.65}$$

where v_2 is given by solving the equation $\mathbf{V}\,.\,\mathbf{W} = 1$ as follows

$$1 = \frac{v_2}{(\mu+\psi)} + \frac{v_2(\mu+\phi+\psi)}{(\epsilon+\mu)(\mu+\psi)} + \frac{\epsilon(\mu+\psi+\phi)v_2}{(\mu+\epsilon-r\epsilon)(\mu-r\epsilon)(\mu+\psi)} + \frac{(\mu+\psi+\phi)v_2}{\delta(\mu+\psi)},$$

so that

$$v_2 = \frac{\delta(\epsilon+\mu)(\mu+\psi)(\mu-r\epsilon)(\mu+\epsilon-r\epsilon)}{\delta(\mu-r\epsilon)(\mu+\epsilon-r\epsilon)\left[2\mu+\psi+\epsilon+\phi\right] + (\mu+\psi+\phi)(\epsilon+\mu)\left[\epsilon\delta+(\mu+\epsilon-r\epsilon)(\mu-r\epsilon)\right]}. \tag{3.66}$$

We observe that $v_2 > 0$ provided that $(\mu - r\epsilon) > 0$. The bifurcation coefficients a and b are found as follows

$$a = \sum_{k,i,j=1}^{n} v_k\omega_i\omega_j\frac{\partial^2 f_k}{\partial x_i\partial x_j}(0,0),$$

$$b = \sum_{k,i=1}^{n} v_k\omega_i\frac{\partial^2 f_k}{\partial x_i\partial\beta^*}(0,0). \tag{3.67}$$

The bifurcation coefficient a is evaluated at the disease-free equilibrium and upon substitution of v_2, ω_1, ω_5 we obtain

$$\begin{aligned} a &= 2v_2\omega_5\omega_1\frac{\partial^2 f_2}{\partial x_5\partial x_1}(0,0) = 2v_2\omega_5\omega_1\frac{\beta^*\mu^2\gamma}{(\mu\gamma+\Lambda)} \\ &= \frac{-2v_2\mu\gamma(\mu+\psi+\phi)}{\Lambda(\mu+\psi)}. \end{aligned} \tag{3.68}$$

Hence,

$$a = \frac{-2\mu\gamma\left[\delta(\epsilon+\mu)(\mu+\psi)(\mu-r\epsilon)(\mu+\epsilon-r\epsilon)\right]}{\Lambda\left[\left[\delta(\mu-r\epsilon)(\mu+\epsilon-r\epsilon)\right]\left[2\mu+\psi+\epsilon+\phi\right] + (\mu+\psi+\phi)(\epsilon+\mu)\left[\epsilon\delta+(\mu+\epsilon-r\epsilon)(\mu-r\epsilon)\right]\right]}. \tag{3.69}$$

It can be seen that $a < 0$, provided that $\mu - r\epsilon > 0$.

Finding b yields

$$b = \sum_{k,i=1}^{n} v_k\omega_i\frac{\partial^2 f_k}{\partial x_i\partial\beta^*}(0,0) = v_2\omega_5\frac{\partial^2 f_2}{\partial x_5\partial\beta^*}(0,0) = \frac{v_2}{\beta^*}. \tag{3.70}$$

Hence,

$$b = \frac{\delta(\epsilon+\mu)(\mu+\psi)(\mu-r\epsilon)(\mu+\epsilon-r\epsilon)}{\beta^*\left[\delta(\mu-r\epsilon)(\mu+\epsilon-r\epsilon)\left[2\mu+\psi+\epsilon+\phi\right]+(\mu+\psi+\phi)(\epsilon+\mu)\left[\epsilon\delta+(\mu+\epsilon-r\epsilon)(\mu-r\epsilon)\right]\right]}, \tag{3.71}$$

where $\beta^* > 0$ and therefore $b > 0$ provided $\mu - r\epsilon > 0$. □

We state the following theorem,

Theorem 19. *Model system (3.2) exhibits a unique locally asymptotically stable endemic equilibrium provided that $a < 0$ and $b > 0$. When $\beta^* < 0$, it implies that there is a negative endemic equilibrium state and when $\beta^* > 0$ a positive stable endemic equilibrium exists.*

When $a < 0$ and $b > 0$, there exists a forward transcritical bifurcation that occurs at $\mathcal{R}_0 = 1$ as indicated in Figure (3.2). Such a bifurcation is one where there is an exchange of stability between the disease-free equilibrium and endemic equilibrium states. It ensures that the endemic equilibrium is locally asymptotically stable whenever $\mathcal{R}_0 > 1$ but close to 1. Theorem (19) explains that the control of HPV highly depends on the initial sizes of the sub-populations of the model system (3.2). The bifurcation exhibited here is a forward transcritical bifurcation and this means that the control of HPV does not necessarily depend on the number of people that are initially infected but on a host of other possibilities. In such a case HPV can be eradicated/eliminated from the body when $\mathcal{R}_0 < 1$ while it persists when $\mathcal{R}_0 > 1$. Figure 3.2 illustrates the forward bifurcation for model (3.2), for $a < 0$ and $b > 0$.

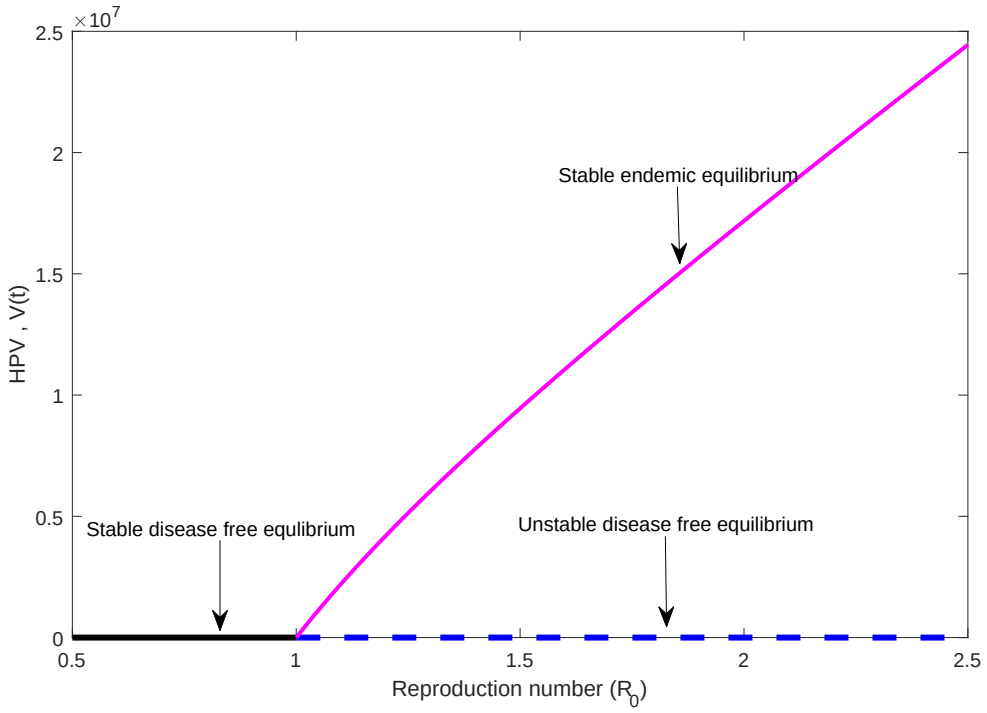

Figure 3.2: Forward bifurcation plot for the dynamics of HPV in-host showing the relationship between $\mathcal{R}_0$, given in equation (3.26) and the virus population endemic value, $V^e(t)$, obtained in equation (3.52).

3.4.6 Global stability analysis of the endemic equilibrium

We prove mathematically that the endemic equilibrium is globally stable using the Lyapunov function approach. In 1920 Volterra formulated the very first Lyapunov function for proving the global stability analysis of a predator-prey model. Since then, the Lyapunov has proven to be the most successful method used in proving global stability of an equilibrium state especially the endemic equilibrium. The Lyapunov function however is not easily constructed as it requires some level of mathematical skill and works by [25, 27] demonstrate such skills. Such a function is said to be positive definite everywhere except at the endemic equilibrium where it is zero. This leads to the following important definition of a positive definite function by Savari [83] given below,

Definition 4. *A real-valued continuously differentiable function f is said to be positive definite on a neighbourhood of the origin $\mathcal{D}$, if $f(0) = 0$ and $f(x) > 0$ for every non zero $x \in \mathcal{D}$. [83]*

The Lyapunov function has derivatives along the trajectories that are semi-negative definite within the invariant set of the model under consideration. Provided that one is able to suc-

cessfully construct a particular epidemic model, the global stability analysis of the equilibrium points will follow directly from the LaSalle's invariance principle which is given by the following theorem,

Theorem 20. *(LaSalle's Invariant Principle [50]) Assuming that V is a Lyapunov function for a model system governed by differential equations on $\mathbb{G}$. Define $\mathbb{S} = \{x \in \mathbb{G} \cap \Omega : \dot{V}(x) = 0\}$ and let $\mathbb{M}$ be the largest invariant set in $\mathbb{S}$, then every bounded trajectory of the system that remains in $\mathbb{G}$ approaches the set $\mathbb{M}$ as $t \to +\infty$.*

The Lyapunov function method is explained as follows: Consider a system given by

$$\frac{dx}{dt} = f(x), \tag{3.72}$$

where in the case of model (3.2), $f : \Omega \subseteq \mathbb{R}^6_+ \to \mathbb{R}^6_+$ is continuous. We create a Lyapunov function V on some $\mathbb{G} \subseteq \Omega$ provided that

- V is continuous on $\mathbb{G}$.
- V is not continuous at $\bar{x} \in \bar{\mathbb{G}}$ (which is defined as the closure of $\mathbb{G}$) such that $\lim_{x \to \bar{x}} V(x) = +\infty (x \in \mathbb{G})$
- $\dot{V} = gradV \cdot f \leq 0$ on $\mathbb{G}$.

Based on the above explanation of what a Lyapunov function is, we construct a Lyapunov function for model system (3.2) by stating the following theorem,

Theorem 21. *The CTL-inactive endemic equilibrium, $\mathcal{E}_1$, is globally asymptotically stable provided that $\mathcal{R}_0 > 1$ and $\mathcal{R}_K \leq 1$.*

Proof. To prove theorem (20), we construct a simple Lyapunov function of the form

$$\begin{aligned} \mathcal{W}(T_s, L, I_1, I_2, V, K) &= \left(T_s - T_s^e \ln \frac{T_s}{T_s^e}\right) + A\left(L - L^e \ln \frac{L}{L^e}\right) + B\left(I_1 - I_1^e \ln \frac{I_1}{I_1^e}\right) \\ &+ C\left(I_2 - I_2^e \ln \frac{I_2}{I_2^e}\right) + D\left(V - V^e \ln \frac{V}{V^e}\right) + EK, \end{aligned} \tag{3.73}$$

where A, B, C, D, E are constants to be found. Taking the time derivative along the solutions of model (3.2), we obtain

$$\begin{aligned} \frac{d\mathcal{W}}{dt} &= \dot{T}_s\left(1 - \frac{T_s^e}{T_s}\right) + A\dot{L}\left(1 - \frac{L^e}{L}\right) + B\dot{I}_1\left(1 - \frac{I_1^e}{I_1}\right) + C\dot{I}_2\left(1 - \frac{I_2^e}{I_2}\right) \\ &+ D\dot{V}\left(1 - \frac{V^e}{V}\right) + E\dot{K} \end{aligned} \tag{3.74}$$

and by substitution of $\dot{T}_s, \dot{L}, \dot{I}_1, \dot{I}_2, \dot{V}, \dot{K}$, we obtain

$$\begin{aligned}\frac{d\mathcal{W}}{dt} = & \left(\Lambda + \phi L - \left(\frac{\beta V}{(\gamma + T_s)} + \mu\right) T_s\right)\left(1 - \frac{T_s^e}{T_s}\right) + A\left(\frac{\beta V T_s}{(\gamma + T_s)} - (\mu + \psi + \phi)L\right)\left(1 - \frac{L^e}{L}\right) \\ & + B(\psi L - (\epsilon + \mu + \theta K)I_1)\left(1 - \frac{I_1^*}{I_1}\right) + C(\epsilon I_1 + r\epsilon I_2 - (\mu + \theta K)I_2)\left(1 - \frac{I_2^e}{I_2}\right) \\ & + D(N_2\mu(I_1 + I_2) - \delta V)\left(1 - \frac{V^*}{V}\right) + E(\sigma I_2 K - \nu K). \end{aligned} \tag{3.75}$$

Expanding equation (3.75) yields

$$\begin{aligned}\frac{d\mathcal{W}}{dt} = & \Lambda + \phi L - \left(\frac{\beta V}{(\gamma + T_s)} + \mu\right) T_s - \frac{T_s^e}{T_s}(\Lambda + \phi L) + T_s^e\left(\frac{\beta V T_s}{(\gamma + T_s)} + \mu\right) + A\left(\frac{\beta V T_s}{(\gamma + T_s)}\right) \\ & - A(\mu + \psi + \phi)L - \frac{AL^e}{L}\frac{\beta V T_s}{(\gamma + T_s)} + AL^e(\mu + \psi + \phi) + B(\psi L - (\epsilon + \mu + \theta K)I_1) \\ & - \frac{BI_1^e}{I_1}\psi L + BI_1^e(\epsilon + \mu + \theta K) + C(\epsilon I_1 + r\epsilon I_2 - (\mu + \theta K)I_2) - \frac{CI_2^e}{I_2}\epsilon I_1 - CI_2^e(r\epsilon - \mu - \theta K) \\ & + D(N_2\mu(I_1 + I_2) - \delta V) - \frac{DV^e}{V}N_2\mu(I_1 + I_2) + DV^e\delta + EK(\sigma I_2 - \nu). \end{aligned} \tag{3.76}$$

Cancelling out common terms and grouping terms without the subscript (e) simplifies to

$$\begin{aligned}\frac{d\mathcal{W}}{dt} = & \Lambda - \mu T_s - \frac{T_s^e}{T_s}(\Lambda + \phi L) + T_s^e\left(\frac{\beta V T_s}{(\gamma + T_s)} + \mu\right) - \frac{AL^e}{L}\frac{\beta V T_s}{(\gamma + T_s)} + AL^e(\mu + \psi + \phi) - B\theta K I_1 \\ & - \frac{BI_1^e}{I_1}\psi L + BI_1^e(\epsilon + \mu + \theta K) - \frac{CI_2^e}{I_2}\epsilon I_1 - CI_2^e(r\epsilon - \mu - \theta K) - D\delta V - \frac{DV^e}{V}N_2\mu(I_1 + I_2) \\ & + DV^e\delta + EK(\sigma I_2 - \nu) + \frac{\beta V T_s}{(\gamma + T_s)}(A - 1) + L(\phi + B\psi - A(\mu + \psi + \phi)) \\ & + I_1(C\epsilon - B(\epsilon + \mu) + N_2\mu D) + I_2(C(r\epsilon - \mu) + N_2\mu D) + I_2 K(E\sigma - C\theta). \end{aligned} \tag{3.77}$$

To find the constants A, B, C, D, E, we let

$$(A - 1) = 0, \quad (\phi + B\psi - A(\mu + \psi + \phi)) = 0, \quad (C(r\epsilon - \mu) + N_2\mu D) = 0, \quad (E\sigma - C\theta) = 0,$$

and $C\epsilon - B(\epsilon + \mu) + N_2\mu D = 0$. By simple calculation we obtain

$$A = 1, \ B = \frac{(\mu + \psi)}{\psi}, \ C = \frac{(\mu + \psi)(\mu + \epsilon)}{\psi(\mu + \epsilon - r\epsilon)}, \ D = \frac{(\mu + \psi)(\mu + \epsilon)(\mu - r\epsilon)}{N_2\mu\psi(\mu + \epsilon - r\epsilon)}, \ E = \frac{\theta(\mu + \psi)(\mu + \epsilon)}{\sigma\psi(\mu + \epsilon - r\epsilon)}.$$

At the endemic equilibrium, $\mathcal{E}_1^e$, we obtain,

$$\Lambda = (\mu + \psi)L^e + \mu T_s^e, \quad \frac{\beta V^e T_s^e}{(\gamma + T_s^e)} = (\mu + \psi + \phi)L^e, \quad N_2\mu(I_1^e + I_2^e) = \delta V^e.$$

By substitution into $\mathcal{W}'$ and by simplification, we obtain

$$\begin{aligned}
\frac{d\mathcal{W}}{dt} &\leq \mu T_s^e\left(2-\frac{T_s}{T_s^e}-\frac{T_s^e}{T_s}\right)+(\mu+\psi)L^e\left(2-\frac{T_s^e}{T_s}-\frac{I_1^eL}{L^eI_1}\right)+\phi L^e\left(1-\frac{T_s^eL}{T_sL^e}\right)\\
&+ \frac{V^e\delta(\mu+\psi)(\mu+\epsilon)(\mu-r\epsilon)}{N_2\mu\psi(\mu+\epsilon-r\epsilon)}\left(1-\frac{V}{V^e}\right)+\frac{(\mu+\psi)I_1^e\theta K}{\psi}\left(1-\frac{I_1}{I_1^e}\right)-\frac{(\mu+\psi)(\mu+\epsilon)I_2^e\epsilon}{\psi(\mu+\epsilon-r\epsilon)}\\
&+ \frac{(\mu+\psi)(\mu+\epsilon)(\mu-r\epsilon)I_2}{\psi(\mu+\epsilon-r\epsilon)}-\frac{(\mu+\psi)(\mu+\epsilon)(\mu-r\epsilon)V^e}{V\psi(\mu+\epsilon-r\epsilon)}(I_1+I_2)+\frac{K\theta\nu(\mu+\psi)(\mu+\epsilon)}{\sigma\psi(\mu+\epsilon-r\epsilon)}(\mathcal{R}_K-1)\\
&\leq \mu T_s^e\left(2-\frac{T_s}{T_s^e}-\frac{T_s^e}{T_s}\right)+(\mu+\psi)L^e\left(2-\frac{T_s^e}{T_s}-\frac{I_1^eL}{L^eI_1}\right)-\frac{(\mu+\psi)(\mu+\epsilon)I_2^e\epsilon}{\psi(\mu+\epsilon-r\epsilon)}\\
&- \frac{(\mu+\psi)(\mu+\epsilon)(\mu-r\epsilon)V^e}{V\psi(\mu+\epsilon-r\epsilon)}(I_1+I_2)+\frac{K\theta\nu(\mu+\psi)(\mu+\epsilon)}{\sigma\psi(\mu+\epsilon-r\epsilon)}(\mathcal{R}_K-1). \qquad (3.78)
\end{aligned}$$

The arithmetic mean (AM) and geometric mean (GM) relationship states that

$$AM=\frac{b_1+b_2+b_3+.....+b_n}{n}\geq\sqrt{b_1b_2b_3....b_n}=GM.$$

This is satisfied provided that the inequalities given by

$$\left(2-\frac{T_s}{T_s^e}-\frac{T_s^e}{T_s}\right)\leq 0,\quad \left(2-\frac{T_s^e}{T_s}-\frac{I_1^eL}{L^eI_1}\right)\leq 0$$

hold. Therefore, when $\mathcal{R}_0>1$ and $\mathcal{R}_K<1$ we notice that the inequality given by $\frac{d\mathcal{W}}{dt}\leq 0$ holds. For $\frac{d\mathcal{W}}{dt}=0$, it means that $T_s=T_s^e,\quad L=L^e,\quad I_1=I_1^e,\quad I_2=I_2^e, V=V^e,\quad K=0$. Hence, the largest invariant set for $\left((T_s,L,I_1,I_2,V,K)|\frac{d\mathcal{W}}{dt}=0\right)$ is a singleton, $\mathcal{E}_1$. Therefore by LaSalle's invariant principle [50], we conclude that the CTL-inactive endemic equilibrium, $\mathcal{E}_1$, is globally asymptotically stable provided that $\mathcal{R}_0>1$ and $\mathcal{R}_K\leq 1$. This concludes the proof. □

Theorem 22. *The CTL-active endemic equilibrium, $\mathcal{E}_2^e$, is globally asymptotically stable provided that $\mathcal{R}_0>1$ and $\mathcal{R}_K\geq 1$.*

Proof. We construct the following Lyapunov function to prove the global stability of the CTL-active endemic equilibrium.

$$\mathcal{Q} = T_s-T_s^*-\int_{T_s^*}^{T_s}\frac{(\mu+\psi+\phi)L^*}{\left(\frac{\beta V^*u}{u+\gamma}\right)}du+L-L^*-L^*\ln\frac{L}{L^*}+\frac{(\mu+\psi+\phi)}{\psi}\left[I_1-I_1^*-I_1^*\ln\frac{I_1}{I_1^*}\right]$$

$$+ \quad \frac{(\epsilon+\mu)(\mu+\psi+\phi)}{\epsilon\psi}\left[I_2 - I_2^* - I_2^*\ln\frac{I_2}{I_2^*}\right] + \frac{(\epsilon+\mu)(\mu+\psi+\phi)(\mu-r\epsilon)(1+\theta K^*)}{N_2\mu\epsilon\psi}$$

$$\times \quad \left[V - V^* - V^*\ln\frac{V}{V^*}\right] + \frac{\theta}{\sigma}\left(\frac{(\mu+\psi+\phi)}{\psi}\right)\left[K - K^* - K^*\ln\frac{K}{K^*}\right]. \tag{3.79}$$

Differentiating $\mathcal{Q}$ gives

$$\begin{aligned}
\mathcal{Q}' &= T_s'\left[1-(\mu+\psi+\phi)L^*\left(\frac{T_s+\gamma}{\beta V^* T_s}\right)\right] + L'\left[1-\frac{L^*}{L}\right] + \frac{(\mu+\psi+\phi)}{\psi}\left[1-\frac{I_1^*}{I_1}\right]I_1' \\
&+ \frac{(\epsilon+\mu)(\mu+\psi+\phi)}{\epsilon\psi}\left[1-\frac{I_2^*}{I_2}\right]I_2' + \frac{(\epsilon+\mu)(\mu+\psi+\phi)(\mu-r\epsilon)}{N_2\mu\epsilon\psi}[1+\theta K^*]\left[1-\frac{V^*}{V}\right]V' \\
&+ \frac{\theta}{\sigma}\frac{(\mu+\psi+\phi)}{\psi}\left[1-\frac{K^*}{K}\right]K'.
\end{aligned} \tag{3.80}$$

By substituting $T_s', L', I_1', I_2', V', K'$, we obtain

$$\begin{aligned}
\mathcal{Q}' &= \left[1-(\mu+\psi+\phi)L^*\left(\frac{T_s+\gamma}{\beta V^* T_s}\right)\right]\left[\Lambda+\phi L - \left(\frac{\beta V}{(\gamma+T_s)}+\mu\right)T_s\right] + \left[1-\frac{L^*}{L}\right] \\
&\times \left[\frac{\beta V T_s}{(\gamma+T_s)} - (\mu+\psi+\phi)L\right] + \frac{(\mu+\psi+\phi)}{\psi}\left[1-\frac{I_1^*}{I_1}\right][\psi L - (\epsilon+\mu+\theta K)I_1] \\
&+ \frac{(\epsilon+\mu)(\mu+\psi+\phi)}{\epsilon\psi}\left[1-\frac{I_2^*}{I_2}\right][\epsilon I_1 + r\epsilon I_2 - (\mu+\theta K)I_2] + \frac{(\epsilon+\mu)(\mu+\psi+\phi)(\mu-r\epsilon)}{N_2\mu\epsilon\psi} \\
&\times [1+\theta K^*]\left[1-\frac{V^*}{V}\right][N_2\mu(I_1+I_2) - \delta V] + \frac{\theta}{\sigma}\frac{(\mu+\psi+\phi)}{\psi}\left[1-\frac{K^*}{K}\right][\sigma I_2 K - \nu K].
\end{aligned}$$

(3.81)

Recall that at the endemic equilibrium

$$\Lambda = (\mu+\psi)L^* + \mu T_s^*, \quad \beta V^* T_s^* = (\mu+\psi+\phi)L^*(\gamma+T_s^*), \quad \frac{\psi L^*}{I_1^*} = \frac{(\epsilon+\mu)}{\psi} + \frac{\theta K^*}{\psi},$$

and by expansion and simplification we obtain

$$\begin{aligned}
\mathcal{Q}' &= \Lambda + \phi L - \frac{\beta V T_s}{(\gamma + T_s)} - \mu T_s - (\mu + \psi + \phi) L^* \left(\frac{T_s + \gamma}{\beta V^* T_s}\right) \left[\Lambda + \phi L - \frac{\beta V T_s}{(\gamma + T_s)} - \mu T_s\right] \\
&+ \frac{\beta V T_s}{(\gamma + T_s)} - \frac{\beta V L^* T_s}{L(\gamma + T_s)} + (\mu + \psi + \phi) L^* - \frac{(\mu + \psi + \phi)(\epsilon + \mu + \theta K)}{\psi} I_1 \\
&- \frac{(\mu + \psi + \phi) L I_1^*}{I_1} + \frac{(\mu + \psi + \phi)(\epsilon + \mu + \theta K) I_1^*}{\psi} + \frac{(\epsilon + \mu)(\mu + \psi + \phi)}{\epsilon \psi} [\epsilon I_1 + r\epsilon I_2 - (\mu + \theta K) I_2] \\
&- \frac{(\epsilon + \mu)(\mu + \psi + \phi)}{\epsilon \psi} \left[\frac{\epsilon I_1 I_2^*}{I_2} + r\epsilon I_2^* - (\mu + \theta K) I_2^*\right] + \frac{(\epsilon + \mu)(\mu + \psi + \phi)(\mu - r\epsilon)}{N_2 \mu \epsilon \psi} [1 + \theta K^*] \\
&\times [N_2 \mu (I_1 + I_2) - \delta V] - \frac{(\epsilon + \mu)(\mu + \psi + \phi)(\mu - r\epsilon)}{N_2 \mu \epsilon \psi} [1 + \theta K^*] \left[\frac{N_2 \mu (I_1 + I_2) V^*}{V} - \delta V^*\right] \\
&+ \frac{\theta}{\sigma} \frac{(\mu + \psi + \phi)}{\psi} [\sigma I_2 K - \nu K] - \frac{\theta}{\sigma} \frac{(\mu + \psi + \phi)}{\psi} [\sigma I_2 K^* - \nu K^*]. \qquad (3.82)
\end{aligned}$$

For further simplification, we use the following substitution:
$\Lambda - \mu T_s = (\mu + \psi) L^* + \mu T_s^* - \mu T_s, \quad \beta V^* T_s^* = (\mu + \psi + \phi) L^* (\gamma + T_s^*)$, such that

$$\begin{cases}
\Lambda + \phi L - \frac{\beta V T_s}{(\gamma + T_s)} - \mu T_s - (\mu + \psi + \phi) L^* \left(\frac{T_s + \gamma}{\beta V^* T_s}\right) \left[\Lambda + \phi L - \frac{\beta V T_s}{(\gamma + T_s)} - \mu T_s\right] \\
= (\mu + \psi) L^* + \mu T_s^* - \mu T_s + \phi L - \frac{\beta V T_s}{(\gamma + T_s)} - (\mu + \psi + \phi) L^* \left(\frac{T_s + \gamma}{\beta V^* T_s}\right) \\
\times \left[(\mu + \psi) L^* + \mu T_s^* - \mu T_s + \phi L - \frac{\beta V T_s}{(\gamma + T_s)}\right] \\
= \mu T_s^* \left[1 - \frac{T_s}{T_s^*} - \frac{T_s^*}{T_s} \left(\frac{T_s + \gamma}{T_s^* + \gamma}\right) + \left(\frac{T_s + \gamma}{T_s^* + \gamma}\right)\right] + ((\mu + \psi) L^* + \phi L) \left[1 - \frac{T_s^*}{T_s}\right] - \frac{\beta V T_s}{(T_s + \gamma)},
\end{cases} \qquad (3.83)$$

and

$$\begin{cases} \dfrac{\beta V T_s}{(\gamma+T_s)} - \dfrac{\beta V L^* T_s}{L(\gamma+T_s)} + (\mu+\psi+\phi)L^* = \dfrac{\beta V T_s}{(\gamma+T_s)} + \dfrac{\beta V^* T_s^*}{(\gamma+T_s^*)}\left[1 - \dfrac{V}{V^*}\dfrac{L^*}{L}\right] \\ = \dfrac{\beta V T_s}{(\gamma+T_s)} + (\mu+\psi+\phi)L^*\left[1 - \dfrac{V}{V^*}\dfrac{L^*}{L}\right], \\ \\ \phi L\left[1 - \dfrac{T_s^*}{T_s}\right] + \phi L^*\left[1 - \dfrac{V}{V^*}\dfrac{L^*}{L}\right] = \phi L^*\left[1 - \dfrac{V}{V^*}\dfrac{L^*}{L} - \dfrac{T_s^*}{T_s}\dfrac{L}{L^*}\right], \\ \\ -\dfrac{(\mu+\psi+\phi)(\epsilon+\mu+\theta K)}{\psi} I_1 - \dfrac{(\mu+\psi+\phi)LI_1^*}{I_1} + \dfrac{(\mu+\psi+\phi)(\epsilon+\mu+\theta K)I_1^*}{\psi} \\ = \dfrac{(\mu+\psi+\phi)(\epsilon+\mu+\theta K)}{\psi} I_1^*\left[1 - \dfrac{I_1}{I_1^*}\right] = 0, \\ \\ \dfrac{(\epsilon+\mu)(\mu+\psi+\phi)}{\epsilon\psi}[\epsilon I_1 + r\epsilon I_2 - (\mu+\theta K)I_2] - \dfrac{(\epsilon+\mu)(\mu+\psi+\phi)}{\epsilon\psi}\left[\dfrac{\epsilon I_1 I_2^*}{I_2} + r\epsilon I_2^* - (\mu+\theta K)I_2^*\right] \\ = \dfrac{(\epsilon+\mu)(\mu+\psi+\phi)}{\psi} I_1\left[1 - \dfrac{I_2^*}{I_2}\right] + \dfrac{(\epsilon+\mu)(\mu+\psi+\phi)(\mu+\theta K)}{\epsilon\psi}[\mu - r\epsilon + \theta K]I_2^*\left[1 - \dfrac{I_2}{I_2^*}\right] = 0, \\ \\ \dfrac{\theta\nu}{\sigma}\dfrac{(\mu+\psi+\phi)}{\psi} I_2\left[K - K^*\right] + \dfrac{\theta(\mu+\psi+\phi)}{\psi}\left[K^* - K\right] = 0. \end{cases} \tag{3.84}$$

Substituting (3.83) and (3.84) into $\mathcal{Q}'$ and simplifying yields

$$\begin{aligned} \mathcal{Q}' &= \mu T_s^*\left[1 - \frac{T_s}{T_s^*} - \frac{T_s^*}{T_s}\left(\frac{T_s+\gamma}{T_s^*+\gamma}\right) + \left(\frac{T_s+\gamma}{T_s^*+\gamma}\right)\right] + (\mu+\psi)L^*\left[2 - \frac{T_s^*}{T_s} - \frac{V}{V^*}\frac{L^*}{L} - \frac{LI_1^*}{I_1 L^*}\right] \\ &+ \phi L^*\left[1 + \frac{L}{L^*} - \frac{L^*}{L}\frac{V}{V^*} - \frac{L}{L^*}\frac{T_s^*}{T_s} - \frac{LI_1^*}{I_1 L^*}\right]. \end{aligned} \tag{3.85}$$

Since the arithmetic mean is greater than the geometric mean, it follows that

$$1 - \frac{T_s}{T_s^*} - \frac{T_s^*}{T_s}\left(\frac{T_s+\gamma}{T_s^*+\gamma}\right) + \left(\frac{T_s+\gamma}{T_s^*+\gamma}\right) \leq 0, \quad 2 - \frac{T_s^*}{T_s} - \frac{V}{V^*}\frac{L^*}{L} - \frac{LI_1^*}{I_1 L^*} \leq 0$$

and $1+\frac{L}{L^*}-\frac{L^*}{L}\frac{V}{V^*}-\frac{L}{L^*}\frac{T_s^*}{T_s}-\frac{LI_1^*}{I_1L^*}\leq 0$, which means that $\mathcal{Q}'\leq 0$, provided that $T_s=T_s^*, L=L^*, I_1=I_1^*, I_2=I_2^*, V=V^*, K=K^*$. Therefore, it follows by LaSalle's invariance principle [50] that the CTL-active endemic equilibrium is globally asymptotically stable. This completes the proof. □

3.5 Sensitivity analysis of the in-host HPV model

Sensitivity analysis is carried out to establish which control methods are effective in the reduction of the spread of HPV in-host. This analysis helps us to identify those particular parameters that have an impact on $\mathcal{R}_0$. The best measure of sensitivity is the calculation of the elasticity index otherwise known as the normalized sensitivity index and it is given by [7] as,

$$\Gamma_p^{\mathcal{R}_0}=\frac{\partial\mathcal{R}_0}{\partial p}\times\frac{p}{\mathcal{R}_0}. \tag{3.86}$$

where p is the parameter of interest in relation to the reproduction number $\mathcal{R}_0$. Using the parameters in Table 3.3, the following normalised sensitivity indices are calculated and tabulated,

$$\Gamma_\beta^{\mathcal{R}_0}=\frac{\partial\mathcal{R}_0}{\partial\beta}\times\frac{\beta}{\mathcal{R}_0}=1,\ \Gamma_{N_2}^{\mathcal{R}_0}=\frac{\partial\mathcal{R}_0}{\partial N_2}\times\frac{N_2}{\mathcal{R}_0}=1,\ \Gamma_\delta^{\mathcal{R}_0}=\frac{\partial\mathcal{R}_0}{\partial\delta}\times\frac{\delta}{\mathcal{R}_0}=-1,\ \Gamma_\Lambda^{\mathcal{R}_0}=\frac{\partial\mathcal{R}_0}{\partial\Lambda}\times\frac{\Lambda}{\mathcal{R}_0}=0.5714.$$

$$\Gamma_\psi^{\mathcal{R}_0}=\frac{\partial\mathcal{R}_0}{\partial\psi}\times\frac{\psi}{\mathcal{R}_0}=0.9558,\ \Gamma_\phi^{\mathcal{R}_0}=\frac{\partial\mathcal{R}_0}{\partial\phi}\times\frac{\phi}{\mathcal{R}_0}=-0.8850,\ \Gamma_\mu^{\mathcal{R}_0}=\frac{\partial\mathcal{R}_0}{\partial\mu}\times\frac{\mu}{\mathcal{R}_0}=-0.6613,$$

$$\Gamma_\epsilon^{\mathcal{R}_0}=\frac{\partial\mathcal{R}_0}{\partial\epsilon}\times\frac{\epsilon}{\mathcal{R}_0}=0.0191,\ \Gamma_r^{\mathcal{R}_0}=\frac{\partial\mathcal{R}_0}{\partial r}\times\frac{r}{\mathcal{R}_0}=0.0145,\ \Gamma_\gamma^{\mathcal{R}_0}=\frac{\partial\mathcal{R}_0}{\partial\gamma}\times\frac{\gamma}{\mathcal{R}_0}=-0.5714. \tag{3.87}$$

This leads to Table 3.4 that summarises the calculations above and displays the sensitivity indices. The most sensitive parameters of the model are β, N_2, ψ and δ. The results indicate that a 10% increase on the transmission rate, β and the burst size, N_2 will result in a 10% increment in $\mathcal{R}_0$ while an increase by 10% of the natural viral death δ, will result in a decrease in $\mathcal{R}_0$ by 10%. It can also be seen that an increase in the epithelial cell concentration by 5.7% will consequently decrease $\mathcal{R}_0$ by 5.7% an increase in the mature rate of latently infected cells by 9.5% will increase $\mathcal{R}_0$ by 10%. Oncogene expression, $\epsilon=0.1$, has little effect on $\mathcal{R}_0$ though increasing its value also increases $\mathcal{R}_0$ and finally the transit-amplifying rate,r, has the least significant effect on $\mathcal{R}_0$. These two parameters,ϵ and r are highly dependent on each other and by this, we mean that the proliferation of I_1 into I_2 is dependent on the oncogene expression rate. So, the higher the oncogene expression rate the more significant effect on $\mathcal{R}_0$.

Table 3.3: Table of parameters.

Parameter	**Value**	**Description**	Source
Λ	36000 cells per ml per day	$CD4^+$ Epithelial cell recruitment rate	[63]
β	0.0067 virions per day	HPV infection rate.	[99]
δ	0.05 cells per day	Virion death rate.	Est.
μ	0.048 per day	Cells death rate.	[64]
N_2	1000 virions per cell	HPV burst size.	[99]
θ	0.01 per day	HPV clearance rate.	[90]
γ	10^6	Epithelial cell concentration for infection half maximal.	[64]
ψ	0.03	Mature rate of latently infected cells.	[40]
σ	0.001 cells per ml	CTL expansion rate.	Est.
ν	0.5 cells per ml	CTL death rate.	Est.
ϵ	varied between $0-1$	Oncogene expression.	[64]
r	0.01	Transit amplifying cells recruitment rate.	[64]
ϕ	0.6	Natural clearance of HPV as a result of healing of cells.	[40]

We also carried out sensitivity analysis using the partial rank correlation coefficient method (PRCCs). The PRCC method we adopted is explained in Gomero [35]. The method tests each parameter while holding other parameters at the median value and the results are ranked by the amount of the effect on the outcome. The PRCCs and the corresponding p-values are computed using the Rstudio package. Computed PRCC values were found to be bounded between the closed interval $[-1, 1]$ and due to this the sampling distribution of some of the parameters of interest was skewed. to correct this the Fisher Transformation method as indicated in [56] and given by

$$z_{score} = \frac{1}{2} \ln \left(\frac{1+\rho}{1-\rho} \right) \tag{3.88}$$

Table 3.4: Table of sensitivity indices for $\mathcal{R}_0$

Parameter	**Sensitivity**	**Parameter**	**Sensitivity**
β	100%	ϕ	-88.5%
N_2	100%	μ	-66.13%
δ	-100%	ϵ	1.9%
Λ	57.14	r	1.45%
ψ	95.58%	γ	-54.14%

where ρ is the computed Pearson correlation coefficient for each parameter. The Fisher transformation transforms the skewed distribution into a normal distribution. The P-values computed from the Fisher transformation are adjusted using the False-Discovery-Rate (FDR) approach by Benjamini and Hochberg outlined in [42]. The false discovery rate is defined as an expected fraction of the false positives among all other positives that results in the rejection of the null hypothesis [42]. The adjusted PRCC values and the corresponding P-values are given in Table 3.5. The PRCCs of parameters that are greater than zero are said to have a *positive correlation*

Table 3.5: Table of PRCC significance (for FDR-adjusted P-values)

Parameter	**PRCC**	**P-value**	**Significant?**
β	0.44956	0	$True$
Λ	0.01829	0.5653	$False$
μ	-0.15806	9.06×10^{-7}	$True$
γ	-0.15929	8.83×10^{-7}	$True$
ψ	0.64249	0	$True$
ϵ	-0.02897	0.4530	$False$
r	-0.02599	0.4598	$False$
ϕ	-0.60327	0	$True$
δ	-0.67998	0	$True$
N_2	0.11319	5.04×10^{-4}	$True$

and so increasing such parameters will also increase $\mathcal{R}_0$. On the other hand, PRCCs that are less than zero are said to have a *negative correlation* and increasing such parameters with a negative PRCC will imply a decrease in $\mathcal{R}_0$. From the PRCC plots we establish the important parameters of interest and therefore know what intervention methods to use to increase or decrease the impact of these parameters. Figure 3.3 presents the PRCC plot for the basic HPV

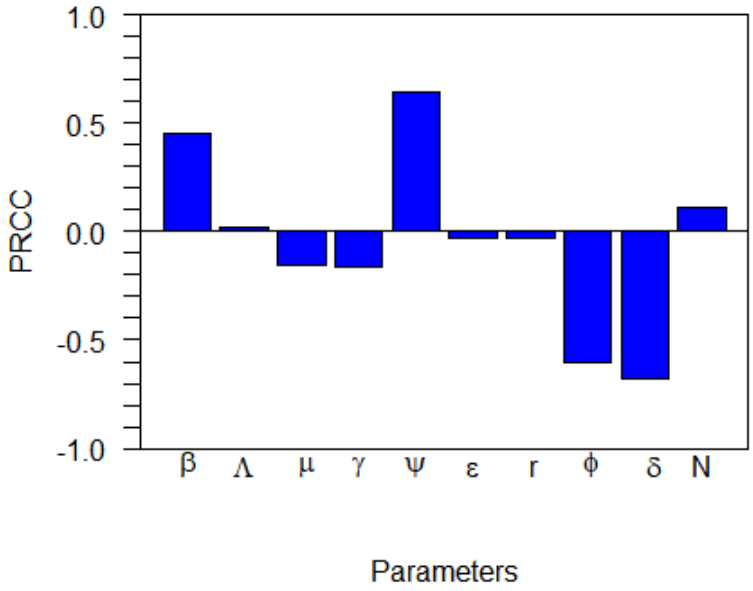

Figure 3.3: Sensitivity analysis of the basic reproduction number $\mathcal{R}_0$ given in equation (3.26), for the basic HPV in-host model, with all other parameters as in Table 3.3.

model that exhibits the effect of the parameters on $\mathcal{R}_0$. The simulations indicate that parameters β, ψ have a positive correlation and increasing these parameters will effectively increase $\mathcal{R}_0$, thus making the transmission rate and the mature rate of latently infected cells parameters of biological interest. The transmission rate, β, can be reduced through intervention methods such as the reduction of sexual partners [63] and condom use, while the mature rate of latently infected cells, ψ, can be decreased through an increase in antibodies that target HPV (introduction of a vaccine). The parameters that have a negative correlation are, $\phi, \delta, \gamma, \mu$ and increasing these parameters will effectively decrease $\mathcal{R}_0$. Of these parameters, the parameters that make sense when it comes to decreasing $\mathcal{R}_0$ are the clearance rate, ϕ, and the rate of virion death, δ, while increasing the epithelial cell concentration,γ, and the natural death rate, μ, might not be biological feasible. So based on this we can suggest that to increase clearance of HPV, we can find interventions such as the use of Virus-Like-Particle (VLP) vaccines such as Gardasil that increase HPV antibody generation or other immune response boosting mechanisms against HPV. The Monte Carlo simulations for the parameters with high PRCC magnitudes against the reproduction number, $\mathcal{R}_0$, are presented in Figure 3.4.

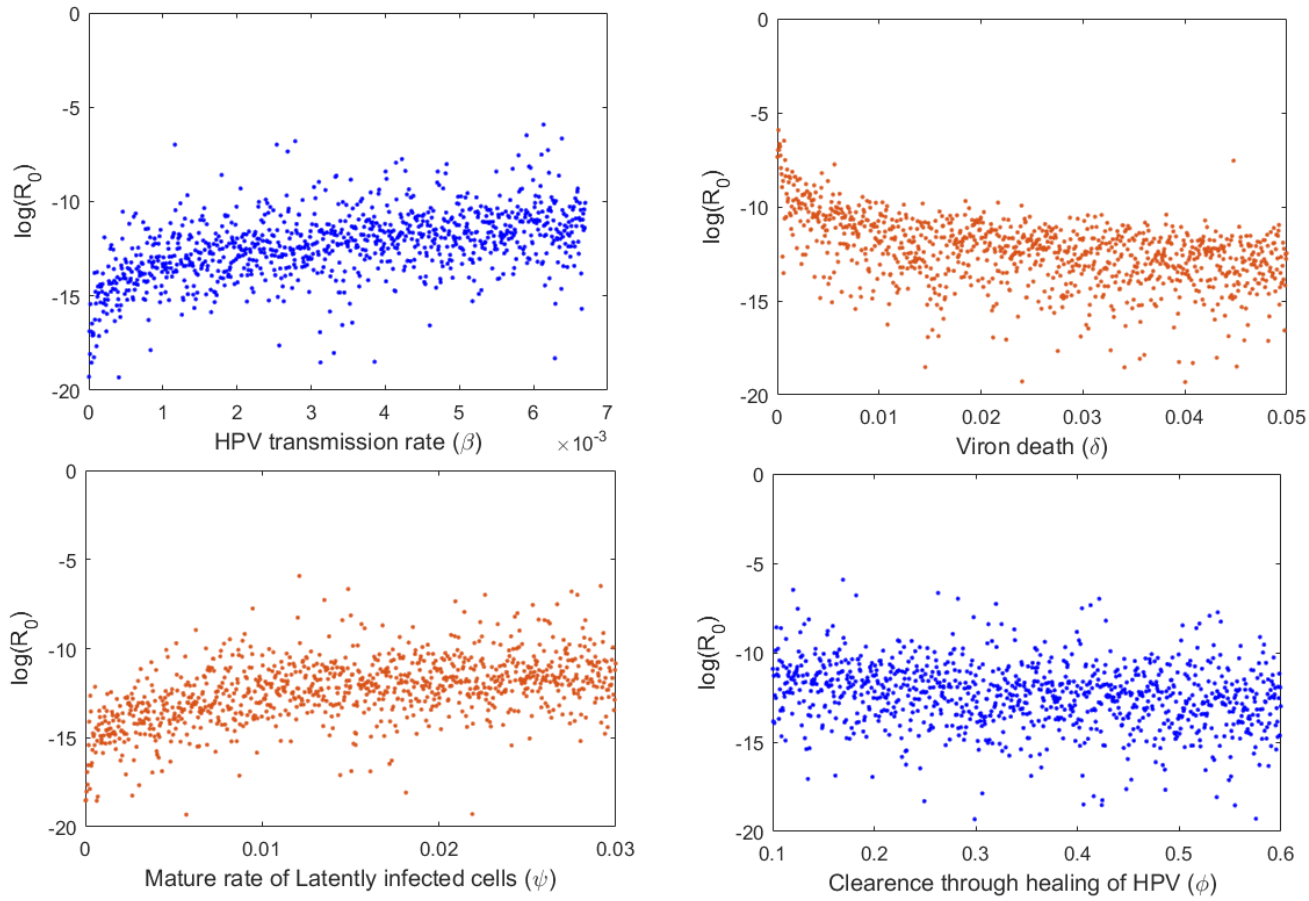

Figure 3.4: The Monte Carlo simulations for parameters with large PRCC magnitude, using $\mathcal{R}_0$ given by equation (3.26) and its associated parameters. Parameters values used for the simulations are taken from Table 3.3. The simulations performed are 1000 per run.

The Monte Carlo simulations indicate that the transmission rate, β, and the mature rate of latently infected cells, ψ, have a positive correlation with the spread of HPV among cells and so increasing these parameters consequently increases $\mathcal{R}_0$ as supported by the sensitivity indices in Table 3.4. The virion death rate, δ, has a negative correlation with the spread of HPV among cells and so increasing the virion death consequently decreases $\mathcal{R}_0$ as indicated by the sensitivity indices in Table 3.4. The scatter plots also indicate that the natural clearance of HPV, ϕ, within latently infected cells reduces the spread of HPV among cells.

In addition to the computation of the PRCC values and the corresponding P-values, we also carried out a pairwise comparison of all the parameters whose P-values were less than 0.05, as illustrated by [69, 43]. The results presented are for both the unadjusted P-values and FDR-adjusted, presented in Table 3.7 and Table 3.6 respectively. The pairwise comparison is performed on parameters whose P-value is less than 0.05 only. With the comparisons we identify the parameters that have a higher promotion of the spread of HPV in-host. Table

3.8 further indicates if the parameters are significantly different ("True") or not significantly different, ("False"). The comparison establishes if there are any significant differences between the parameters that are being compared. It is observed that the effect of natural death of epithelial cells and epithelial cell concentration is not significantly different while the rest of the parameters are significantly different in relation to their influence on the spread of HPV in-host.

Table 3.6: Pairwise PRCC Comparison for unadjusted P-values

	β	μ	γ	ψ	ϕ	δ	N
β		0	0	6.023×10^{-10}	0	0	2.2×10^{-16}
μ			0.9976	0	0	0	1.284×10^{-9}
γ				0	0	0	1.078×10^{-9}
ψ					0	0	0
ϕ						0.003646	0
δ							0
N							

Table 3.7: Pairwise PRCC Comparison for FDR-adjusted P-values

	β	μ	γ	ψ	ϕ	δ	N
β		0	0	7.696×10^{-10}	0	0	2.914×10^{-16}
μ			0.9976	0	0	0	1.419×10^{-9}
γ				0	0	0	1.258×10^{-9}
ψ					0	0	0
ϕ						0.003828	0
δ							0
N							

Table 3.8: Are the parameters different after FDR adjustment?

	β	μ	γ	ψ	ϕ	δ	N
β	True	True	True	True	True	True	True
μ			False	True	True	True	True
γ				True	True	True	True
ψ					True	True	True
ϕ						True	True
δ							True
N							

3.6 Numerical Simulations

Numerical simulations presented show the infection dynamics of HPV in the presence of latency and immune response. The simulations show the stability of the disease-free and endemic equilibrium states which support the theoretical work done within this chapter. Parameter values used in the simulations are taken from the literature and given in the Table 3.3. We first look at the stability analysis of the disease-free equilibrium, $\mathcal{E}_0$. All simulations are run in Matlab. Figure 3.5 indicates that the disease-free equilibrium given by $\mathcal{E}_0 = (7.5 \times 10^5, 0, 0, 0, 0, 0)$ is globally asymptotically stable therefore supporting theorem (16). The figure indicates that the infected classes will converge to zero over time while the healthy cells class T_s will converge to 7.5×10^5 cells showing that the disease-free is stable when $\mathcal{R}_0 = 0.1591 < 1$.

The phase portraits for the disease-free equilibrium are given by Figure 3.6. The phase plots support the stability of the disease-free equilibrium as it can be seen that Figure 3.6(a) indicates that when HPV is introduced as a result of the abrasion of the epithelial cells, the healthy cells T_s gradually decrease relative to the virus population increasing. This continues until the virus reaches a viral load peak, then we suddenly observe a gradual decrease in the virus till it reaches zero. Though $\mathcal{R}_0 < 1$ and $\mathcal{R}_K < 1$, the trend can be as a result of the immune system which can suppress the viral load at some point within the infection provided there is some detection of abnormal cell behaviour. The remaining phase plots, Figures 3.6(b-d) support the existence of a globally asymptotically stable disease-free equilibrium provided that $\mathcal{R}_0 < 1$ and $\mathcal{R}_K < 1$.

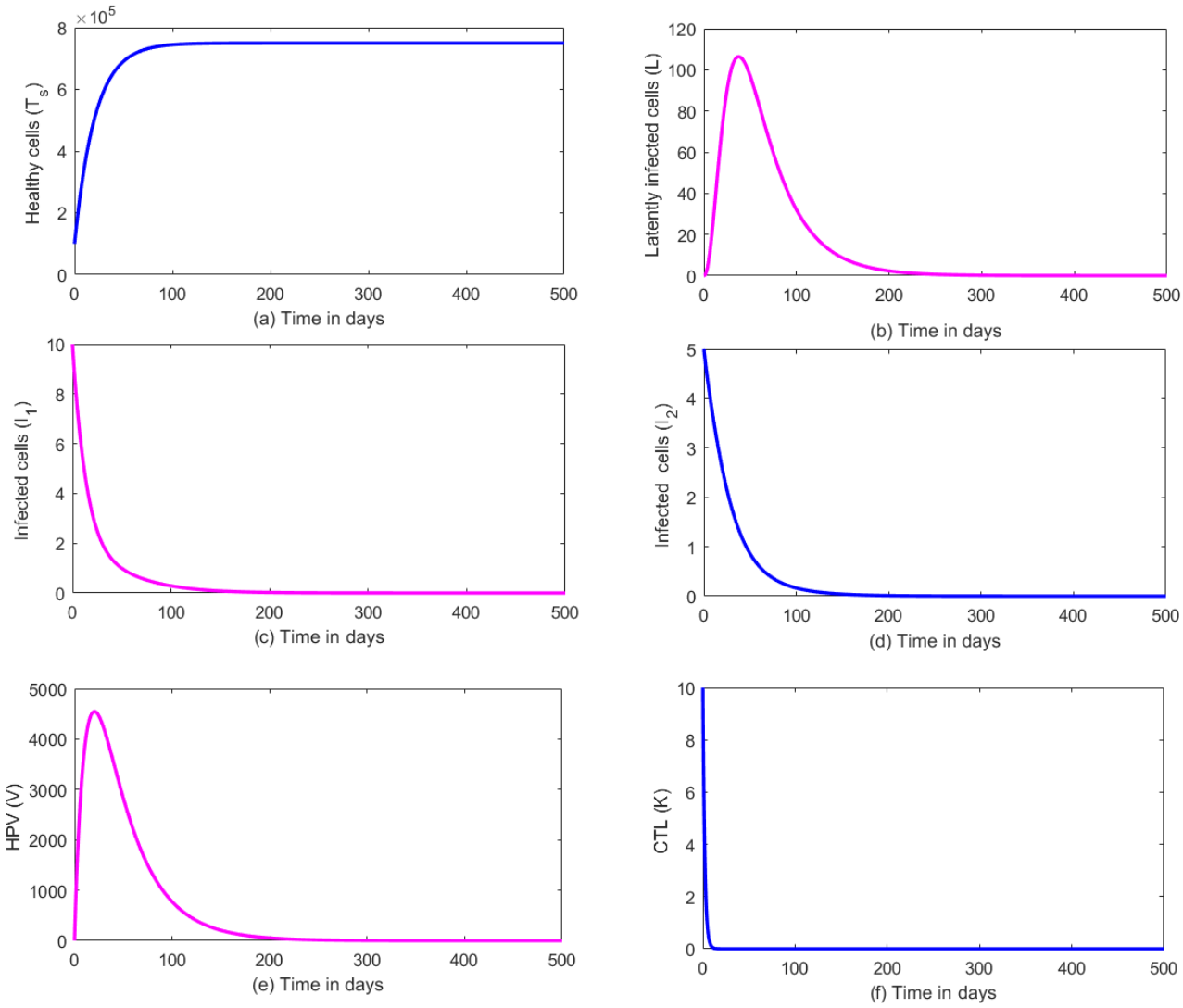

Figure 3.5: In-host dynamics of the basic HPV model (3.2) for classes $T_s(t), L(t), I_1(t), I_2(t), V(t), K(t)$ and $\mathcal{R}_0 = 0.1591 < 1$, with $\epsilon = 0.01$ and all other parameters taken from Table 3.3. The initial conditions used are $T_s(0) = 10^5, L(0) = 0, I_1(0) = 10, I_2(0) = 5, V(0) = 0.01$ and $K(0) = 10$.

The dynamics of the first endemic equilibrium point, $\mathcal{E}_1^e$, also known as the CTL-inactive endemic equilibrium are given by the simulations in Figure 3.7. The simulations, Figure 3.7(a-d), show the dynamics of HPV in the absence of CTL action as a probable result of immune response evasion. The figures also indicate that in the absence of immune response, infected cells increase while the susceptible healthy cells decrease to a minimal value. Figure 3.7 (b-e) specifically shows some form of delay in the increase of infected cells and virus cells in the early days between $0 - 150$ days. This is due a delay in the maturation of latently infected cells. The simulations

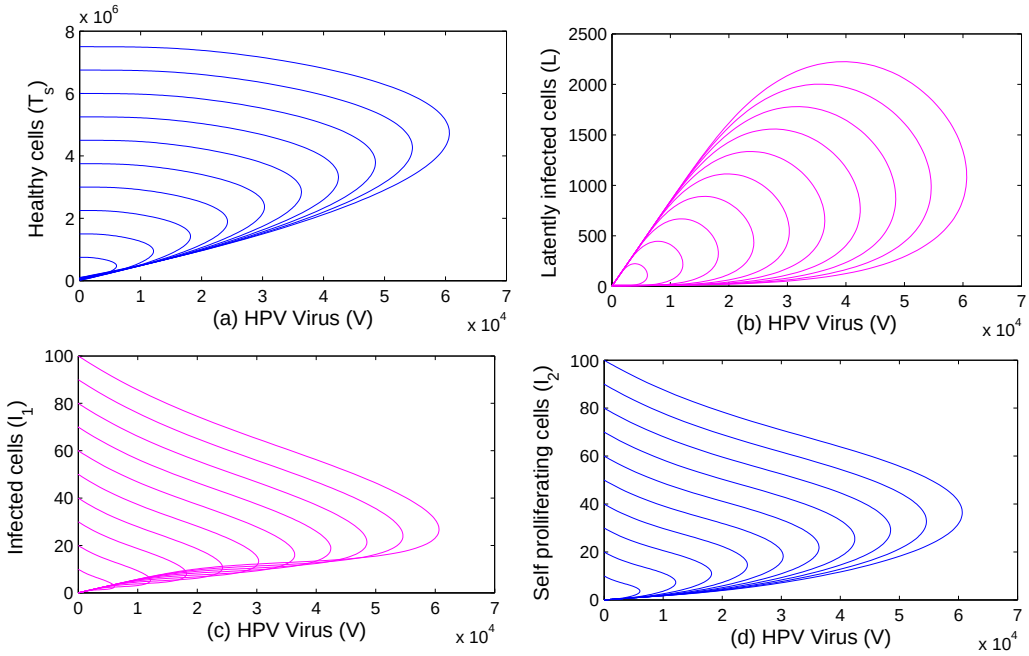

Figure 3.6: Phase plots for the in-host dynamics of the basic HPV model (3.2) for classes $T_s(t), L(t), I_1(t), I_2(t)$ versus HPV (V(t)) and $\mathcal{R}_0 = 0.1591 < 1$, with $\epsilon = 0.01$, and all other parameters as in Table 3.3.

indicate that classes $T_s(t), L(t), I_1(t), I_2(t), V(t), K(t)$, converge to the CTL-inactive endemic equilibrium given by $\mathcal{E}_1^e = (3.2 \times 10^4, 4.418 \times 10^5, 2.419 \times 10^4, 2.183 \times 10^5, 2.932 \times 10^8, 0)$ with $\mathcal{R}_0 = 13.8090 > 1$ and $\mathcal{R}_K = 0.0563 < 1$. The simulations support theorem 22, which states that the endemic equilibrium $\mathcal{E}_1^e$ is globally asymptotically stable when $\mathcal{R}_0 > 1$ and $\mathcal{R}_K < 1$. The corresponding phase portraits for the endemic point, $\mathcal{E}_1^e$ are given in Figure 3.8. These phase portraits for the case $\mathcal{R}_0 = 13.809 > 1, \mathcal{R}_K = 0.0563 < 1$, clearly indicate that upon the introduction of HPV, healthy cells will gradually reduce as the viral load increases while latently infected cells, infected cells and self-proliferating cells will gradually increase. This will eventually prompt a situation where self-proliferating cells (I_2) will exceed the number of infected cells (I_1) and this promotes the spread of the virus within the cells as long as there is no immune response. Clearly, the phase portraits indicate that the endemic equilibrium point, $\mathcal{E}_1^e$, is globally asymptotically stable when $\mathcal{R}_0 > 1, \mathcal{R}_K < 1$. Figure 3.8 supports the existence of the equilibrium point, $\mathcal{E}_1^e$, and as HPV increases there is a decrease in susceptible epithelial cells, an increase in: latently infected cells (L) , infected cells (I_1) and self-proliferating cells (I_2). We observe that in the absence of CTL response there is a possibility of persistence of infection as it becomes uncontrolled and exhibits a divergent behaviour as seen in Figure 3.8(a-d). The next set of simulations present the dynamics of HPV in the presence of immune response

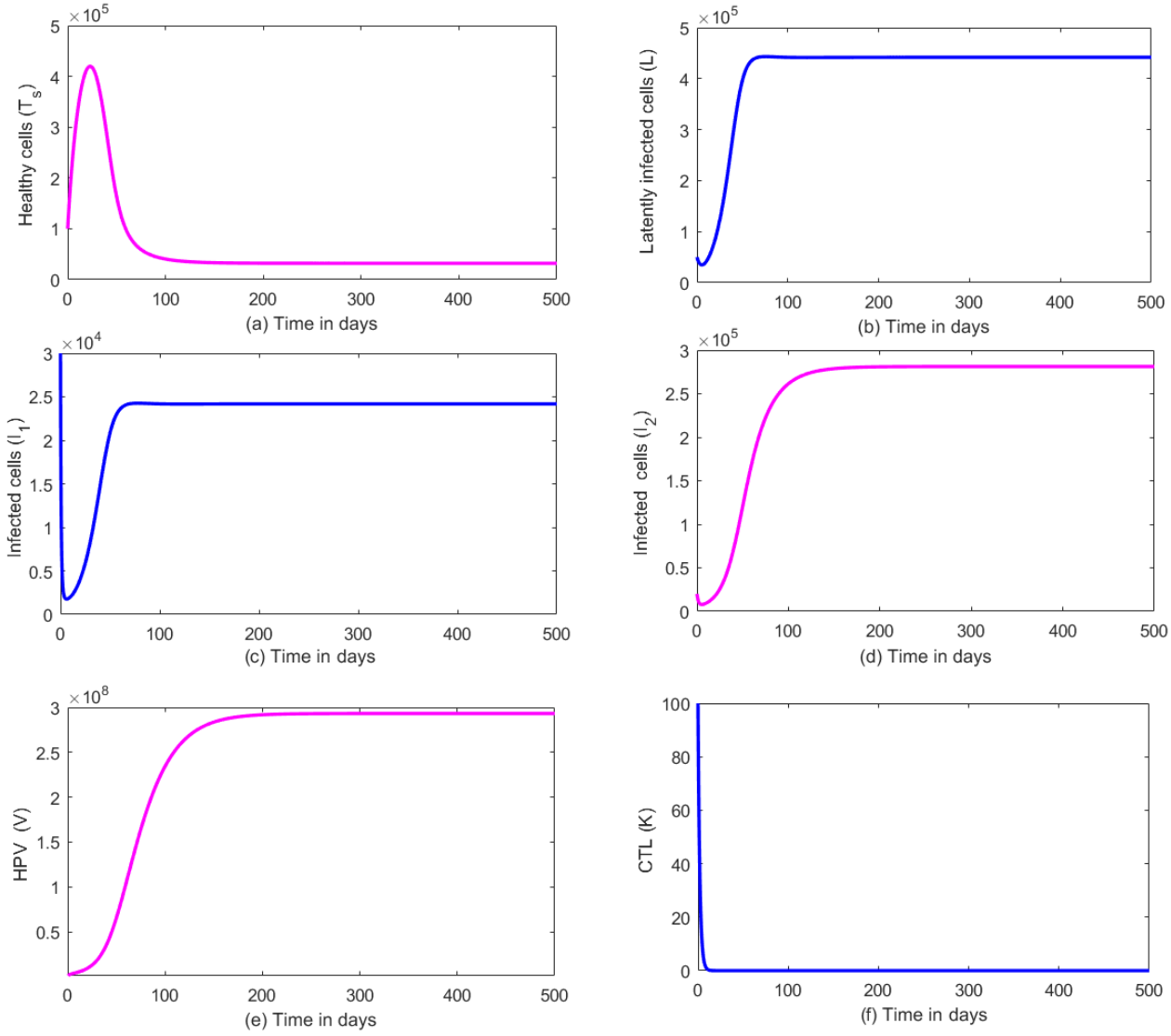

Figure 3.7: In-host dynamics of the basic HPV model (3.2) in the absence of immune response for classes $T_s(t), L(t), I_1(t), I_2(t), V(t), K(t)$ and $\mathcal{R}_0 = 13.8090 > 1, \mathcal{R}_K = 0.0563 < 1$, with parameters $\epsilon = 0.5$, $\sigma = 10^{-6}$ and all other parameters taken from the Table 3.3. Initial conditions used are $T_s(0) = 10^5, L(0) = 5 \times 10^4, I_1(0) = 3 \times 10^4, I_2(0) = 2 \times 10^4, V(0) = 10^3$ and $K(0) = 100$.

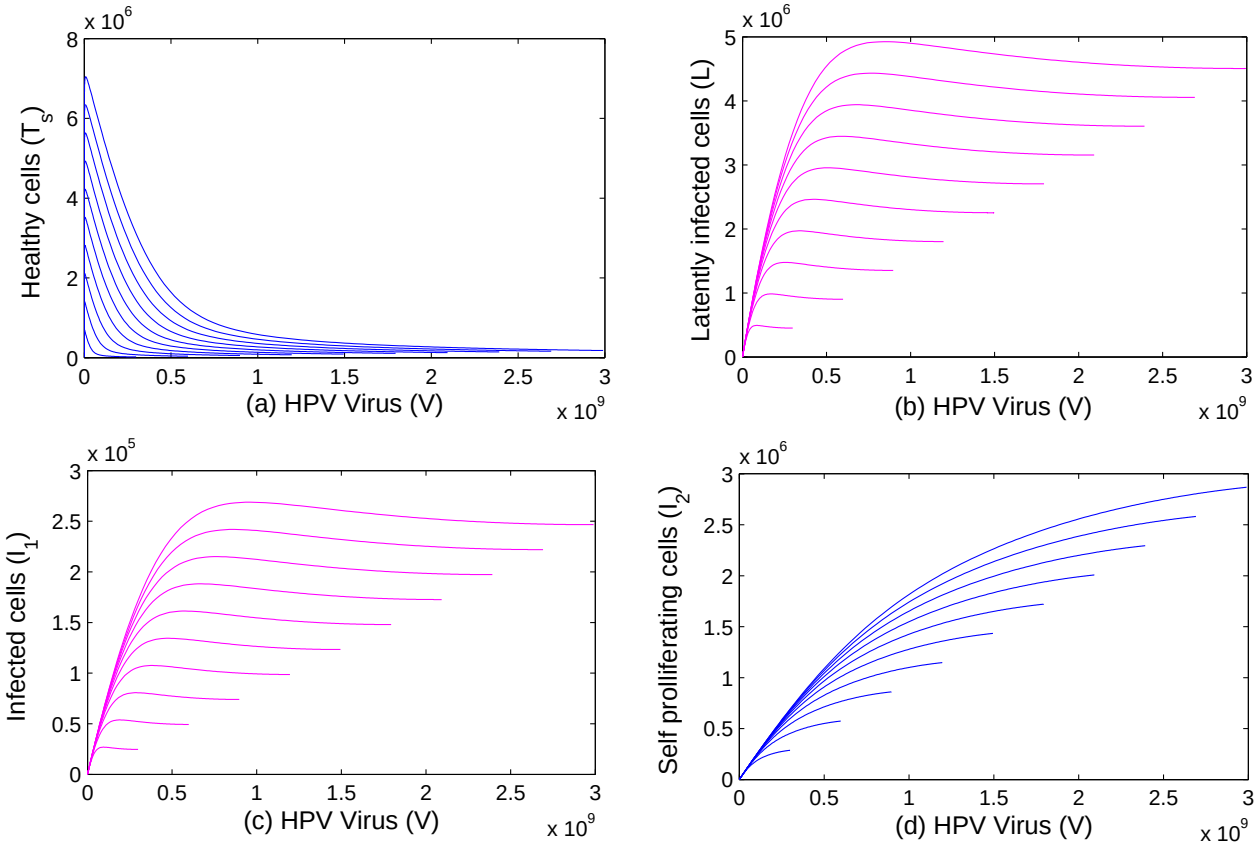

Figure 3.8: Phase portraits for the in-host dynamics of the basic HPV model (3.2), in the absence of immune response for classes $T_s(t), L(t), I_1(t), I_2(t)$ and $\mathcal{R}_0 = 13.809 > 1, \mathcal{R}_K = 0.0563 < 1$, with $\epsilon = 0.5$, and all other parameters as in Table 3.3.

when $\mathcal{R}_0 > 1, \mathcal{R}_K > 1$. This is presented in Figure (3.9). The simulations in Figure 3.9(a-e) show the dynamics of HPV in the presence of CTL action. The simulations indicate that in the presence of immune response, susceptible healthy cells gradually decrease to a constant rate that is higher than that of the case where there was no immune response (see Figure 3.7(a)). This shows that in the presence of immune response we have more susceptible healthy cells due to better viral clearance. We also note that due to healing of some latently infected cells, the healthy cells do not approach zero rather they approach a constant value greater than zero, due to replenishment of some cells.

The simulation dynamics compare the case where there is no CTL action ($\theta = 0$) and the case where there is CTL action ($\theta > 0$). It can be seen that when there is CTL action the susceptible epithelial cells reach an equilibrium value of 8.534×10^4 up by 6.608×10^4 cells from the CTL inactive equilibrium of 1.926×10^4 cells, about 77% increase. The infected equilibrium reduces by 4.07×10^4 cells (about 9%) for the latently infected class, by $6,69 \times 10^3$ (about 27%) for the infected class I_1 and by $2,362 \times 10^5$ (about 83%) for the infected class I_2. It can be seen that the self-proliferating cells, I_2 which are responsible for the activation of the CTL action are marginally decreased when the CTL action is present. Similarly, we observe that in the presence of CTL action the HPV viral load reduces by 2.3278×10^8 (78 %) which supports the biological theory that the immune response plays a pivotal role in the reduction of HPV infection. HPV will try to evade detection by the immune system by all means. The epidermal stroma junction is made up of T-cells, natural killer cells and B-cells. There are various mechanisms that HPV will use to evade the immune response. Among them;

1. Hiding in the keratinocytes (cells that are already for programmed cell death). Then the immune system can not detect abnormal cell death and, due to this, there are no inflammatory responses created to alert the immune system of a possible attack.

2. HPV will remain in the epithelium and avoid the induction of viremia, abnormal cell death or inflammation.

3. HPV will also evade the immune responses directly through the secretion of the E5 protein which is responsible for the down-regulation of the MHC class molecules. The secretion of the E5, E6 and E7 oncoproteins by high-risk HPV types will promote the success of the immune response evasion by HPV.

The simulations support theorem 23 that states that the CTL-active endemic equilibrium, $\mathcal{E}_2^e$, is

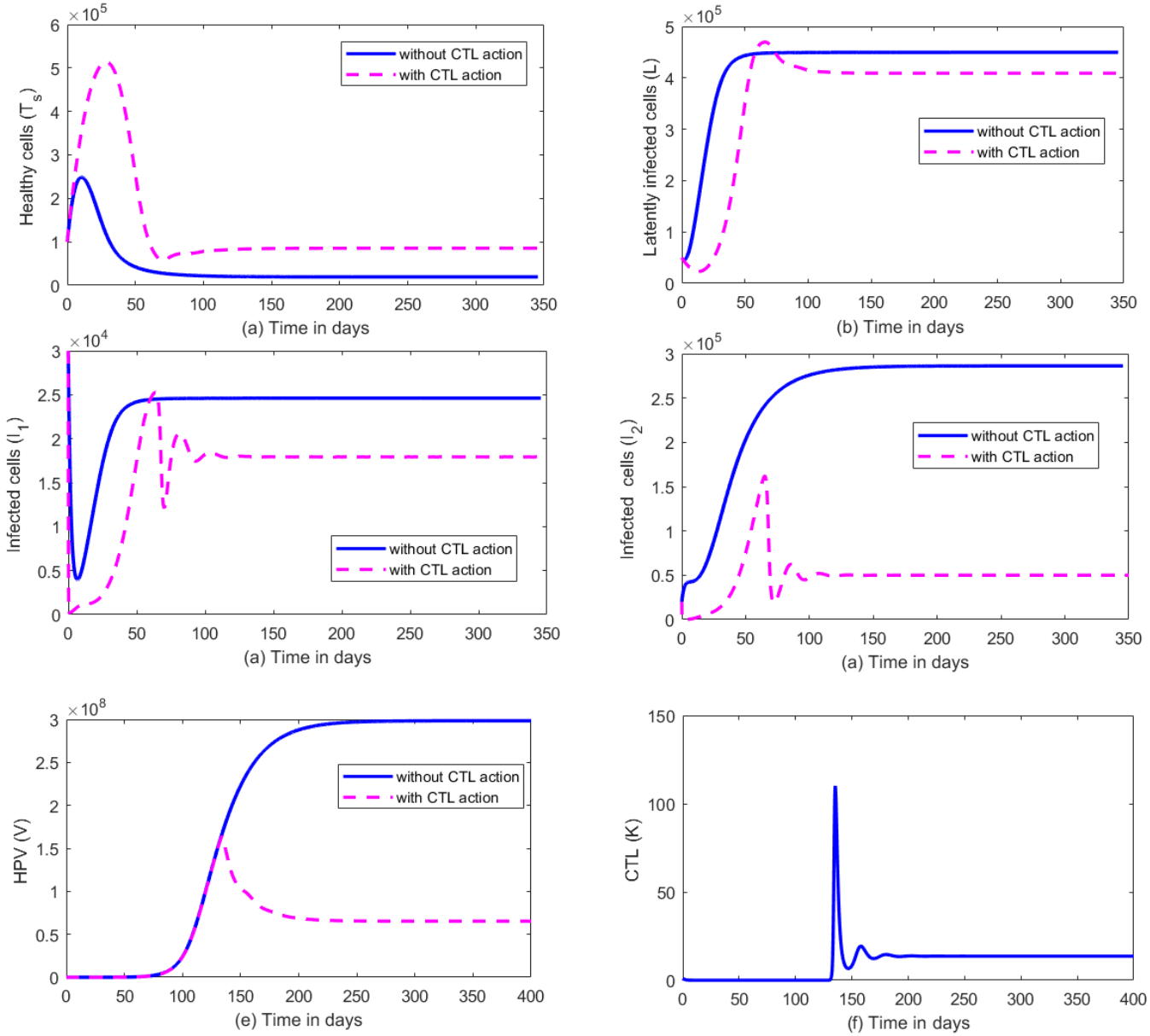

Figure 3.9: In-host dynamics of the basic HPV model (3.2), in the presence of immune response for classes $T_s(t), L(t), I_1(t), I_2(t), K(t)$ and $\mathcal{R}_0 = 22.6862 > 1, \mathcal{R}_K = 5.7251 > 1$, with $\epsilon = 0.5$, $\sigma = 0.00001$, varying CTL killing rate θ and all other parameters taken from Table 3.3.

globally asymptotically stable when $\mathcal{R}_0 > 1$ and $\mathcal{R}_K > 1$. The simulations in Figure 3.9 clearly show the effect of immune response evasion by HPV. The phase portraits for the endemic equilibrium point, $\mathcal{E}_2^e$, also indicate that the endemic equilibrium is globally asymptotically stable and attracting as shown in Figure 3.10.

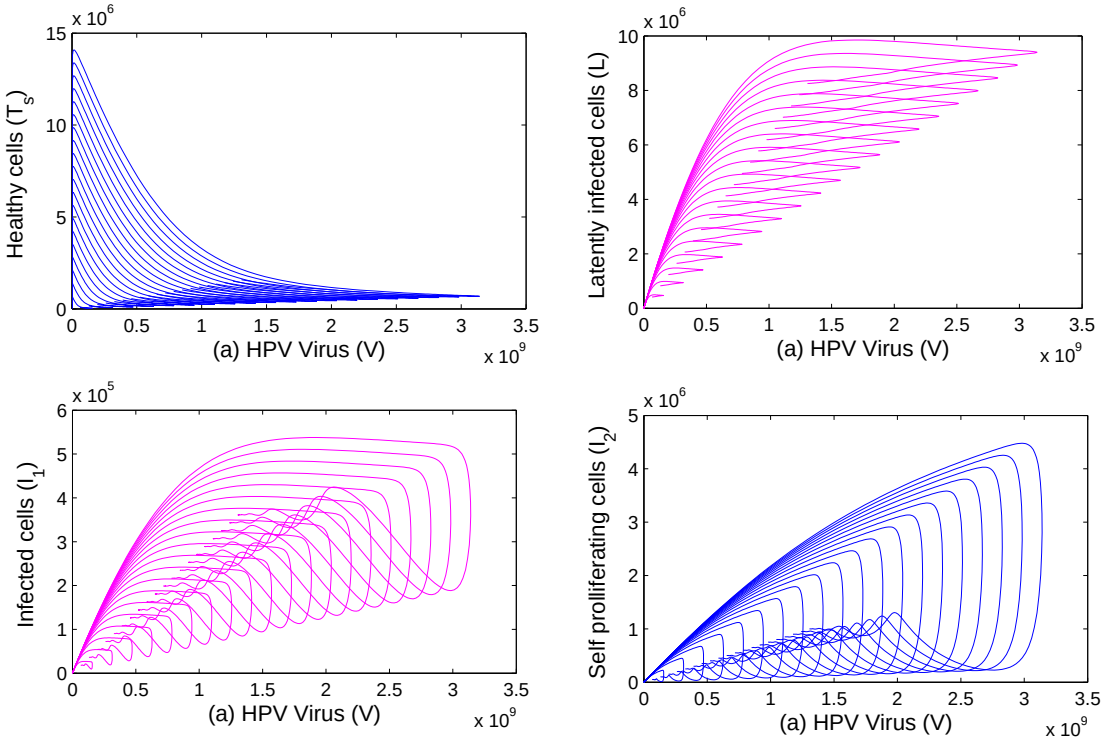

Figure 3.10: Phase portraits for the in-host dynamics of the basic HPV model (3.2, in the presence of immune response for classes $T_s(t), L(t), I_1(t), I_2(t)$ and $\mathcal{R}_0 = 22.6862 > 1, \mathcal{R}_K = 5.7251 > 1$, with $\epsilon = 0.5, \quad \sigma = 0.00001$ and all other parameters are taken from Table 3.3.

Effects of oncogene expression on the dynamics of HPV infection

The effects of oncogene expression on the dynamics of the infected cells I_1, self-proliferating cells, I_2 and HPV,$V(t)$, for $\mathcal{R}_0 > 1$ as shown in Figure 3.11. Results indicated by the Figures 3.11(a-c) show that as oncogene expression increases, there is a decrease in I_1 cells as these cells begin to undergo cell proliferation and are converted to I_2 cells which ,consequently, increases I_2 cells. It is interesting to note that when $\epsilon = 0$, we have no I_2 cells, rather there is a gradual increase in I_1 as indicated in Figure 3.11(a). In terms of HPV, $V(t)$, we observe an increase in the production of the virus by I_1 and I_2 cells as oncogene expression increases. As oncogene expression increases, we also observe an increase in the production of the virus by I_1 and I_2 cells. Of interesting note is that, when $\epsilon = 0$, we still have a production of the HPV virions.

This is because, while there may be no proliferating cells I_2, mature I_1 cells may continue to burst and release virions as a result of abnormal cell death, hence increasing the viral load.

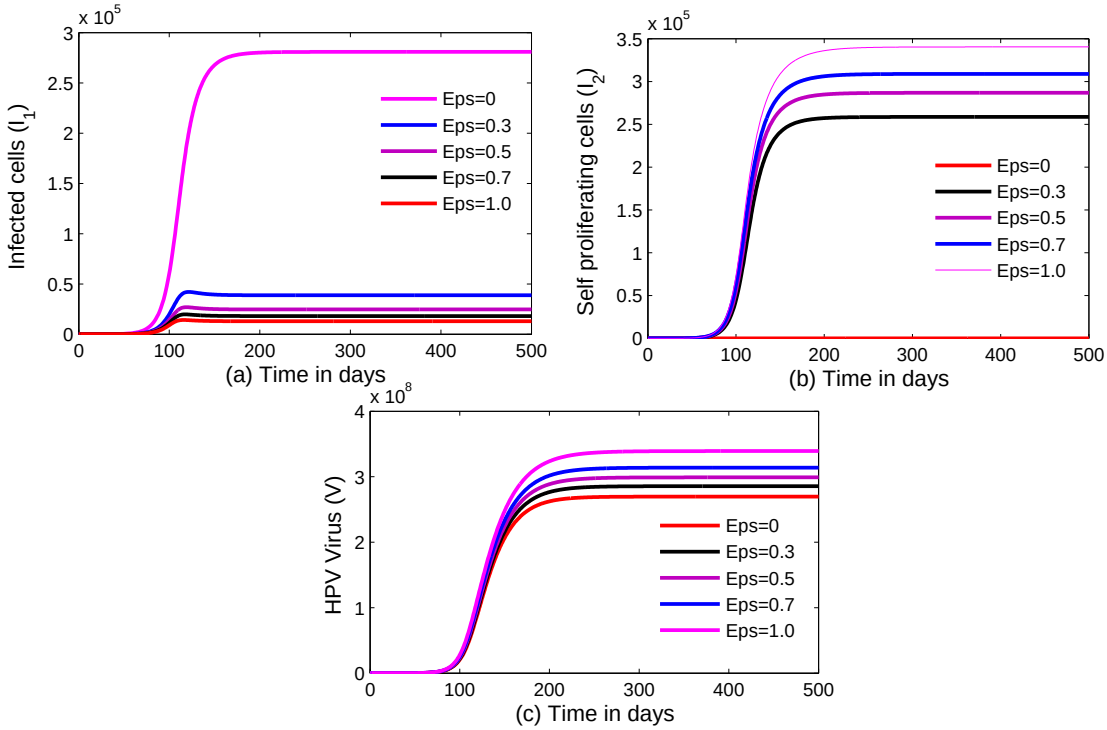

Figure 3.11: Dynamics of HPV infection for varying oncogene expression rates, $Eps = \epsilon$ and $\mathcal{R}_0 > 1$, for the classes $I_1(t), I_2(t), V(t)$ from model system (3.2) and all other parameters are as in Table 3.3.

Dynamics of HPV in the presence of vaccination

We extend the basic HPV model (3.2) to include the inhibition of infection as a result of vaccination. HPV vaccines are known to prevent HPV infection in sexually inactive or active women. It is advisable that the vaccine be taken before an individual is sexually active for better protection against certain high-risk HPV types. These vaccines are made up of virus-like particles (VLPs) that offer safe protection against HPV [101]. The VLPs are not infectious since they do not possess the viral DNA though they resemble the virus [101]. Their presence within the body generates antibodies that fight the HPV infection and this achieves the purpose of the vaccine. Currently, three vaccines are used to prevent HPV in women, that is, Gardasil, Cervarix and Gardasil-9. Gardasil is a quadrivalent vaccine that protects against four HPV strains (HPV 6,11,16,18), Cervarix is a bivalent vaccine, that protects against two HPV strains (HPV 16,18) and Gardasil-9 is a vaccine that protects against nine HPV strains that is (HPV 6,11,16,18,31,33,45,52,58) [95]. At the moment, only the United States of America is currently

using Gardasil-9 while other countries are using Gardasil and Cervarix [110]. In developing countries especially those in Africa, the HPV vaccines are very expensive making them not accessible to most women and girls. The HPV vaccines in use, unfortunately, do not offer immunity against other sexually transmitted infections and they do not clear any prevailing HPV infections within the body. Therefore, they are known as prophylactic vaccines [95]. The current HPV vaccines are known to have a high efficacy towards persistent HPV infections, with Gardasil-9 having the highest efficacy of nearly a hundred percent [72]. In terms of modelling the dynamics of HPV in the presence of a vaccine, Smith? *et al.* [90] developed a model that assessed the effects of vaccinating using Cervarix (for low-risk types) and Gardasil (for high-risk types). Their model included the inhibition effects of the vaccine, modelled through an inhibition parameter in the force of infection. The results of their study indicated that Cervarix clears only low-risk types while Gardasil clears both low and high-risk types implying that, in the presence of co-infection, Gardasil acts better at preventing HPV than Cervarix. Murall *et al.* [64] in their work on HPV looked at the effects of vaccination by including a higher viral clearance rate and a higher CTL proliferation rate. These increased effects were due to the effects of an increase in antibodies as a result of the HPV vaccine. In our extended model, we adopt the work done by Smith? *et al.* [90] and present the HPV vaccination model which considers the effect of a quadrivalent vaccine such as Gardasil in the prevention of high-risk HPV infections. The extended model assumes that the vaccine will inhibit the interaction between the virus and the susceptible healthy target cells. Inhibition of the virus through the vaccine will be through the inhibition parameter η_I, such that the term $\beta V T_s$ is converted to the term $(1-\eta_I)\beta V T_s$. We assume that the vaccine exhibits prophylactic behaviour. The model also considers that $\eta_I = 1$ implies that there is complete inhibition of the virus by the vaccine while when $\eta_I = 0$, inhibition fails [90]. Due to the introduction of the inhibition parameter, η_I, the reproduction number $\mathcal{R}_0$ will be modified to become the control reproduction number, $\mathcal{R}_0^c$. The modified HPV vaccination model is given by the following differential equation system

$$\begin{aligned}
T_s' &= \Lambda + \phi L - \left[\frac{(1-\eta_I]\beta V}{(\gamma + T_s)} + \mu\right] T_s, \\
L' &= \frac{(1-\eta_I)\beta V T_s}{(\gamma + T_s)} - (\mu + \psi + \phi)L, \\
I_1' &= \psi L - (\epsilon + \mu + \theta K) I_1, \\
I_2' &= \epsilon I_1 + r\epsilon I_2 - (\mu + \theta K) I_2, \\
V' &= N_2 \mu (I_1 + I_2) - \delta V, \\
K' &= \sigma I_2 K - \nu K.
\end{aligned} \tag{3.89}$$

The control reproduction number, $\mathcal{R}_0^c$, for the model is given by

$$\mathcal{R}_0^c = \frac{(1-\eta_I)\beta\Lambda\psi N_2\mu(\mu+\epsilon-r\epsilon)}{\delta(\gamma\mu+\Lambda)(\psi+\phi+\mu)(\mu-r\epsilon)(\epsilon+\mu)}, \tag{3.90}$$

Sensitivity analysis of the vaccination model

We carry out sensitivity analysis of the parameters that affect the control reproduction number $\mathcal{R}_0^c$. We use the Latin Hypercube sampling technique to compute the PRCC values and their corresponding P-values in Rstudio. Table 3.9 presents the PRCC values and the corresponding P-values. The results indicate that parameters, β, ψ, ϕ, δ and η_I are the most influential. Increasing or decreasing these parameters has a significant effect on the reproduction number $\mathcal{R}_0^c$.

Table 3.9: Table of PRCC significance (for FDR-adjusted P-values)

Parameter	**PRCC**	**P-value**	**Significant?**
β	0.3808	0	$True$
Λ	0.0528	0.1187	$False$
μ	-0.1063	1.475×10^{-3}	$True$
γ	-0.1012	2.229×10^{-3}	$True$
ψ	0.5646	0	$True$
ϵ	-0.0403	0.2258	$False$
r	-0.0335	0.2925	$False$
ϕ	-0.5137	0	$True$
δ	-0.5932	0	$True$
N_2	0.0860	9.268×10^{-3}	$True$
η_I	0.4737	0	$True$

We also perform a pairwise comparison of the parameters that have P-values less that 0.05 and affect the reproduction number, $\mathcal{R}_0^c$. From the comparisons it can be seen that the natural death of epithelial cells are unrelated and not significantly different. The same applies to the natural clearance of HPV infection and the vaccine inhibition rate. The rest of the parameters are significantly different in relation to the spread of HPV in-host.

The tornado plot for the eleven parameters of the control reproduction number, $\mathcal{R}_0^c$, is presented in Figure 3.12. The plot indicates that the important parameters that have a high

Table 3.10: Pairwise PRCC Comparison for unadjusted P-values

	β	μ	γ	ψ	ϕ	δ	N	η_I
β		0	0	1.16×10^{-7}	0	0	1.076×10^{-12}	0
μ			0.9088	0	0	0	3.209×10^{-5}	0
γ				0	0	0	5.264×10^{-5}	0
ψ					0	0	0	0
ϕ						0.0107	0	0.2398
δ							0	0.000194
N								0
η_I								

Table 3.11: Pairwise PRCC Comparison for FDR-adjusted P-values

	β	μ	γ	ψ	ϕ	δ	N	η_I
β		0	0	1.48×10^{-7}	0	0	1.44×10^{-12}	0
μ			0.9088	0	0	0	3.91×10^{-5}	0
γ				0	0	0	6.14×10^{-5}	0
ψ					0	0	0	0
ϕ						0.0116	0	0.2487
δ							0	0.0002173
N								0
η_I								

Table 3.12: Are the parameters different after FDR adjustment?

	β	μ	γ	ψ	ϕ	δ	N	η_I
β		True	True	True	True	True	True	True
μ			False	True	True	True	True	True
γ				True	True	True	True	True
ψ					True	True	True	True
ϕ						True	True	False
δ							True	True
N								True
η_I								

correlation are : $\beta,\ \psi,\ \phi,\ \delta,\ \eta_I$. Of these, $\beta,\ \psi$, when increased will also increase the reproduction number and subsequently increase infection within cells. On the other hand parameters, $\phi,\ \delta,\ \eta_I$, when increased will decrease the reproduction number and subsequently decrease the spread of infection within cells. The introduction of the vaccine to the body increases the immunity against HPV and hence reduces the spread of HPV infection within cells. Figure

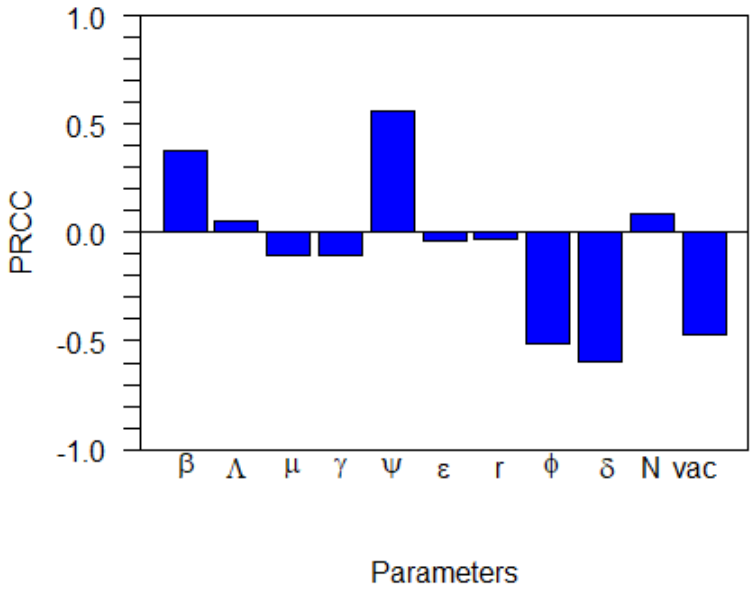

Figure 3.12: Tornado plot for the eleven parameters of the control reproduction number $\mathcal{R}_0^c$ for the HPV in-host vaccination model,where $\eta_I = vac$ and all other parameters as in Table 3.3.

3.13, presents the scatter plots for parameters that have significant PRCC values. To generate these plots, Monte Carlo simulations for the parameters, $\beta,\ \psi,\ \eta_I$ and ϕ, were performed using the Latin Hypercube sampling technique. In each simulation run a 1000 simulations were randomly drawn for each parameter and the scatter plots were plotted in Matlab. The scatter plot indicates that increasing parameters, β, and ψ will monotonically increase, $\mathcal{R}_0^c$, therefore increasing the spread of HPV infection in-host. On the other hand, increasing parameters, η_I and ϕ will monotonically decrease, $\mathcal{R}_0^c$, therefore decreasing the spread of infection in-host. Vaccination is therefore considered an intervention method that is beneficial in the reduction of the spread of HPV in-host.

So to investigate the effect of introducing the vaccine into the model, the numerical simulations for the dynamics of HPV while varying the inhibition parameter are presented. The

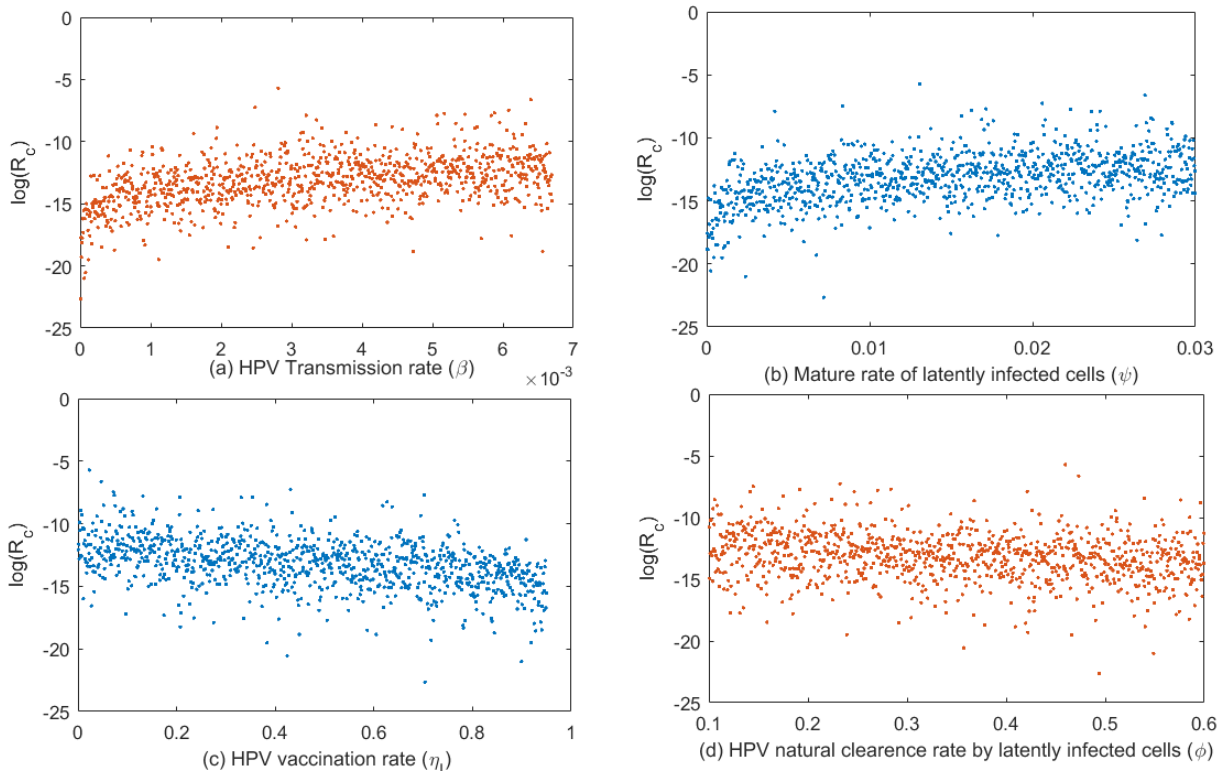

Figure 3.13: The Monte Carlo simulations for parameters with large PRCC magnitude and P-values less than 0.05, using $\mathcal{R}_0^c$, given by equation (3.9) and its associated parameters. Parameters values used for the simulations are taken from Table 3.3. The simulations performed are 1000 per run.

simulations in Figure 3.14 show the dynamics of HPV in the presence of the HPV vaccine. Figure 3.14 (a-d) indicates that the lower the inhibition rate, η_I, the lower the number of healthy susceptible cells and the higher the number of infected cells. The inhibition rate indicates how efficacious the vaccine is. It can be seen that the higher the inhibition rate the higher the reduction in new infections. As explained the HPV vaccine blocks new infections from occurring and this increases the number of susceptible cells and reduces the number of infected cells and HPV virions. It can also be seen that an efficacy rate of about 90% and above will successfully reduce new HPV infection of target cells which means that a vaccine with that level of efficacy will work effectively. This is important because currently HPV vaccines, such as Gardasil, have a high efficacy and are also very expensive making it nearly impossible for the ordinary woman to easily access them. From the simulations, it can be established that, if we lower the efficacy rate to slightly above 85%, we can still achieve the blocking of new HPV infections. We also present a contour plot that shows the effects of varying the vaccine inhibition parameter versus the oncogene expression as indicated by Figure 3.15. The contour plot shows that, to reduce $\mathcal{R}_0$ to below unity, we need to ensure that the vaccine inhibition

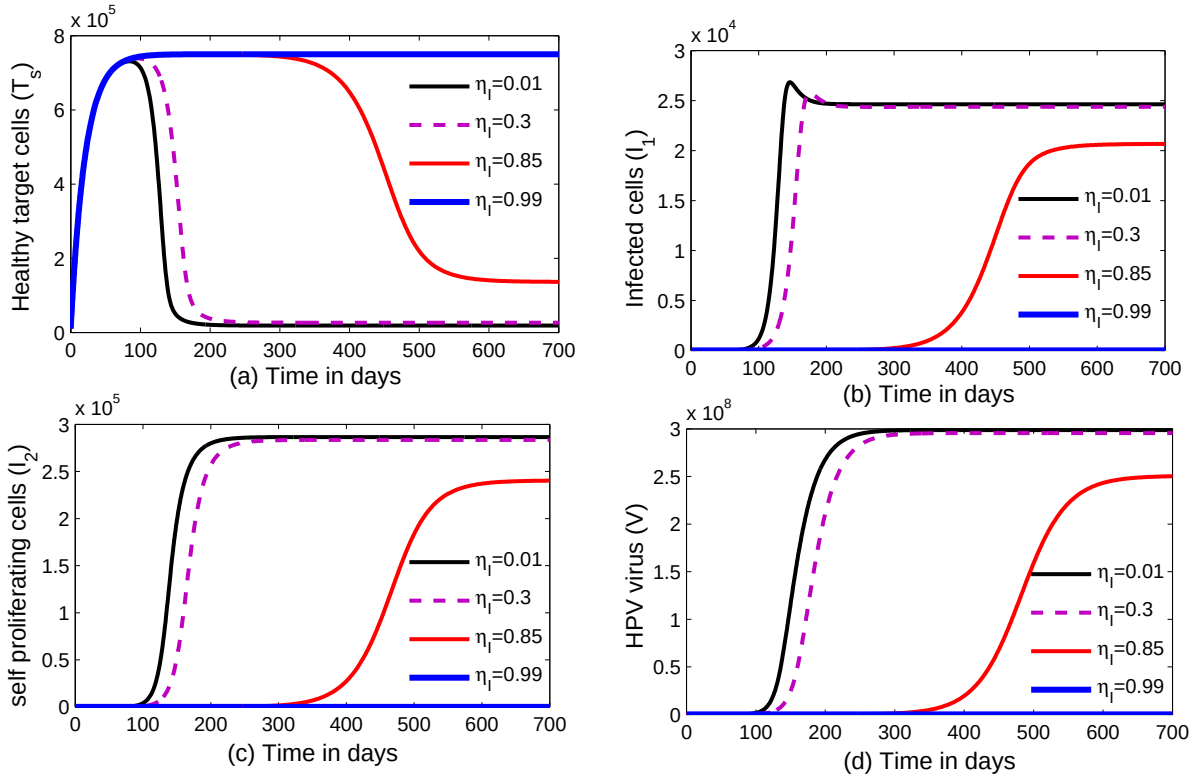

Figure 3.14: Dynamics of HPV infection in the presence of vaccination, for varying inhibition rate η_I and for $\mathcal{R}_0^c > 1$ for $T_s(t), I_1(t), I_2(t), V(t)$ from model system (3.2) and all other parameters as in Table 3.3.

parameter is above 60%. The results also suggest that increasing the inhibition effect of the vaccine will also greatly reduce $\mathcal{R}_0$ to below unity. The combination used (η_I vs ϵ) was chosen as a result of the fact that an increase in the oncogene expression consequently increases the viral load and therefore a good vaccine must be able to inhibit such action. The biological implication of this is that if η_I achieves this threshold value, then HPV can be contained. The results support that Gardasil vaccine has above 90% ability to inhibit high-risk HPV types [72].

We also investigate the effect of inhibition for varying oncogene expression levels on the infected classes I_1 and I_2 as demonstrated by the simulations in Figure 3.16. The simulations presented in Figure 3.16 (a) indicate that, in the presence of low oncogene expression and low inhibition effect, the endemic equilibrium remains stable and we notice that there are more I_1 cells than I_2 cells eventually. This is due to the low self proliferation of the I_1 cells while the inhibition effect of the vaccine is too low to affect the change of the equilibrium point. Figure 3.16 (b) indicates that the presence of high oncogene expression and low vaccine inhibition effect will increase the self proliferation of I_1 cells. Therefore, we observe an evident decline

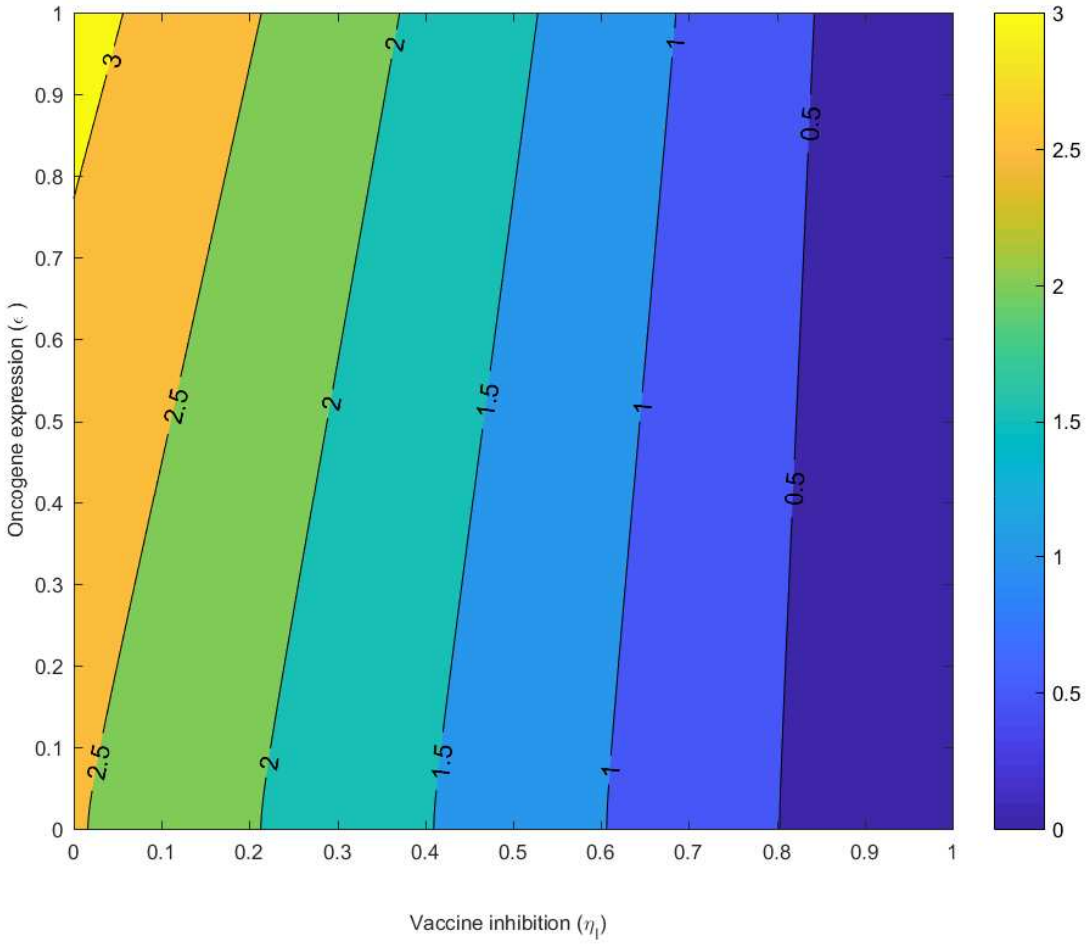

Figure 3.15: Contour plot for the vaccine inhibition rate, (η_1) versus the oncogene expression rate, (ϵ), in relation to the basic reproduction number, $\mathcal{R}_0$, given by equation (3.26) and all other parameters are as in Table 3.3.

in the presence of I_1 cells. The endemic equilibrium however due to this remains stable, as indicated. Figure 3.16 (c) indicates that the presence of low oncogene expression and high inhibition effect causes the endemic equilibrium to become unstable, as both I_1 and I_2 are driven to a disease-free equilibrium due to reduction of $\mathcal{R}_0^c$ to below unity. We observe that a high oncogene expression causes the transition of I_1 to I_2 to increase, such that we have more I_2 cells than I_1 cells as indicated. Figure 3.16 (d) illustrates the dynamics of the I_1 and I_2 cells when both the oncogene expression is high and the vaccine inhibition is high. The results indicate that, though there is a distinct reduction of the I_1 cells as a result of the high oncogene expression, both classes eventually reduce to zero. This makes the endemic equilibrium unstable and reduces $\mathcal{R}_0^c$ to below unity.

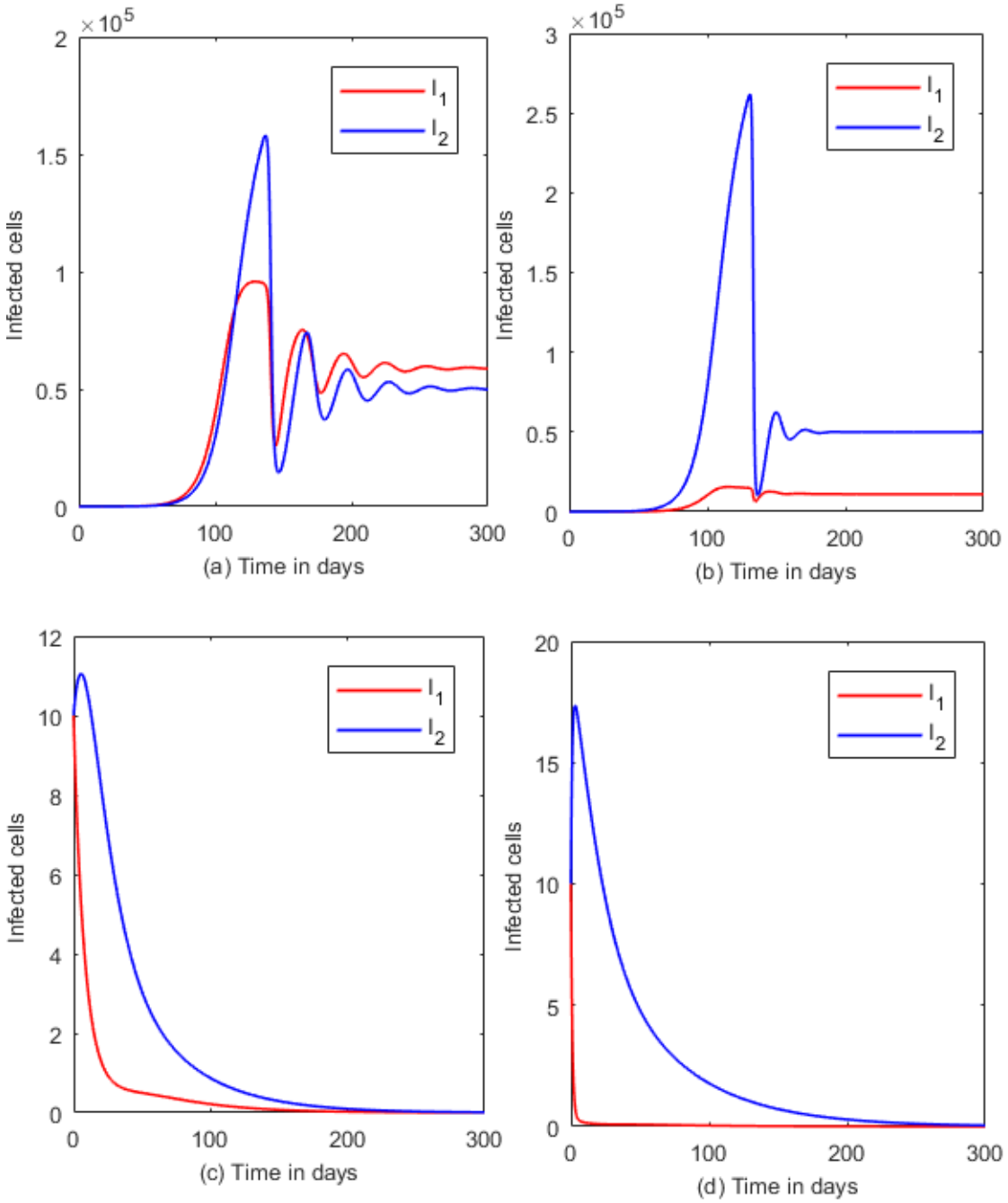

Figure 3.16: Figure (a) illustrates the dynamics of HPV infection for low oncogene expression $\epsilon = 0.1$ and low vaccine inhibition $\eta_I = 0.01$. Figure (b) illustrates the dynamics of HPV infection for high oncogene expression $\epsilon = 0.9$ and low vaccine inhibition $\eta_I = 0.01$. Figure (c) illustrates the dynamics of HPV infection for low oncogene expression $\epsilon = 0.1$ and high vaccine inhibition $\eta_I = 0.9$. Figure (d) illustrates the dynamics of HPV infection for high oncogene expression $\epsilon = 0.9$ and high vaccine inhibition $\eta_I = 0.99$. For all cases all other parameters are as in Table 3.3.

3.7 Discussion and conclusion of the chapter

This chapter looked at the overall dynamics of the basic HPV model in the presence of cell proliferation and immune response. The local and global stability of the disease-free equilibrium was analysed and it was established that the disease-free equilibrium was stable provided that $\mathcal{R}_0 < 1$. The basic model also presented two important endemic equilibrium points, $\mathcal{E}_1^e$ and $\mathcal{E}_2^e$, where the first endemic equilibrium point, $\mathcal{E}_1^e$, was found to be the CTL-inactive endemic equilibrium while the second equilibrium point, $\mathcal{E}_2^e$ was found to be the CTL-activate endemic equilibrium. Based on extensive research on the viral dynamics of HPV by authors such as Stanley *et al.* [92] and Sasagawa *et al.* [82], the first equilibrium point presents the immune evading behaviour of HPV. The stability of this particular equilibrium point was analysed and it was established that a supercritical forward bifurcation existed using a method by Castillo Chavez *et al.*[15]. A supercritical bifurcation ensures that the endemic equilibrium, $\mathcal{E}_1^e$, is locally asymptotically stable whenever $\mathcal{R}_0 > 1$ but close to 1. The global stability of $\mathcal{E}_1^e$ was established using the Lyapunov function approach and it was concluded that the equilibrium point is globally asymptotically stable. The second equilibrium point, $\mathcal{E}_2^e$, for the model was rather complex in nature as it was represented by a quartic polynomial. It was established that there was at least one positive root implying that the endemic equilibrium point was biologically feasible. From the CTL-inactivated endemic equilibrium, we were able to find a special immune response specific reproduction number, $\mathcal{R}_K$ which is also called the CTL reproduction number for the model. The CTL-inactive equilibrium was found to be globally asymptotically stable (implying immune evasion), while when $\mathcal{R}_K > 1$ when $\mathcal{R}_0 > 1$ the CTL activated equilibrium, $\mathcal{E}_2^e$, was found to be globally asymptotically stable. A sensitivity analysis of parameters that form $\mathcal{R}_0$ was performed and the important parameters that affect the reproduction number were established. The PRCCs simulation established that the transmission rate and the mature rate of latently HPV cells were the parameters that increase $\mathcal{R}_0$ when they are increased. The clearance rate was the most important parameter that reduces $\mathcal{R}_0$ when increased. We performed numerical simulations that elaborated the stability of the disease-free and endemic equilibrium points for the model. Results obtained support the theoretical work on the stability analysis of the disease-free and endemic equilibria for respective values of $\mathcal{R}_0$ and $\mathcal{R}_K$. We also presented the extended basic model that included vaccination. In this particular model, we assessed the inhibition effect of the HPV vaccine Gardasil and the simulations indicated that for the vaccine to be efficient in preventing new infections it must have an efficacy of above 85%. The contour plot presented indicated that the vaccination inhibition parameter should be above

60% effective so that the reproduction number, $\mathcal{R}_0$, can be less than unity. The simulations also showed the effects of the vaccine inhibition on the reduction of new infections in the presence of some degree of oncogene expression. A high oncogene expression prompts the immune responses into action due to the presence of unusual cell behaviour and this, coupled with the vaccine effect can eventually promote the clearance of non-persistent infections. Although the immune responses play an important role in the reduction of HPV infection in-host, the research clearly shows that the action of the immune response alone is not sufficient and it is good to advocate for a vaccine for use in countries that are lagging behind. It is envisaged that this work will encourage governments in developing countries to adopt countrywide vaccination of women and girls as a method of reducing the high-risk HPV strains and consequently reduce the cervical cancer burden. In the next chapter, we present the HPV/HIV co-infection model and rigorously analyse the local and global stabilities of the model.

Chapter 4

The in-host HPV/HIV co-infection model

4.1 Introduction

This chapter presents the HPV/HIV co-infection model in the presence of an immune response. The local stability, global stability and numerical simulations for the co-infection dynamics are analysed. We start by presenting the basic in-host model for HIV based on the work by [105]

4.2 The HIV model

We adopt and modify the HIV model by Perelson *et al* [105] because the model presents in-host dynamics that are in line with our scope of work. The model has slight differences from the model [99] as it incorporates latent HIV infection dynamics. HIV viral latency plays a major role in the dynamics of HIV in-host. Due to latency virus, particles manage to evade the immune response though inactively hiding within the genomes of resting CD4+ cells. This results in an increase in difficulty in the elimination of HIV. It is in this regard that we incorporate latency into the model as done by Wang *et. al* [105]. According to Wang *et al.*[105], incorporating latency helps in avoiding the overestimation of infected cells. The model assumes the following; Susceptible target cells denoted by T_h, are recruited at a rate, s and die naturally at a rate, d_1, transmission of infection to healthy target cells is done at a rate, κ. A proportion, ρ, become latently infected cells, L_h upon infection while, $(1-\rho)$, become actively infected cells, I_h. We assume that latently infected cells eventually become actively infectious at a rate, ζ, and the natural death of latently infected cells and actively infectious cells is given by d_2 and d_3

respectively. An actively infectious cell is assumed to burst and release a total of N_1 virions within its entire lifetime and these virions V_h are assumed to degrade at rate c. The model flow diagram for the HIV dynamics is given by

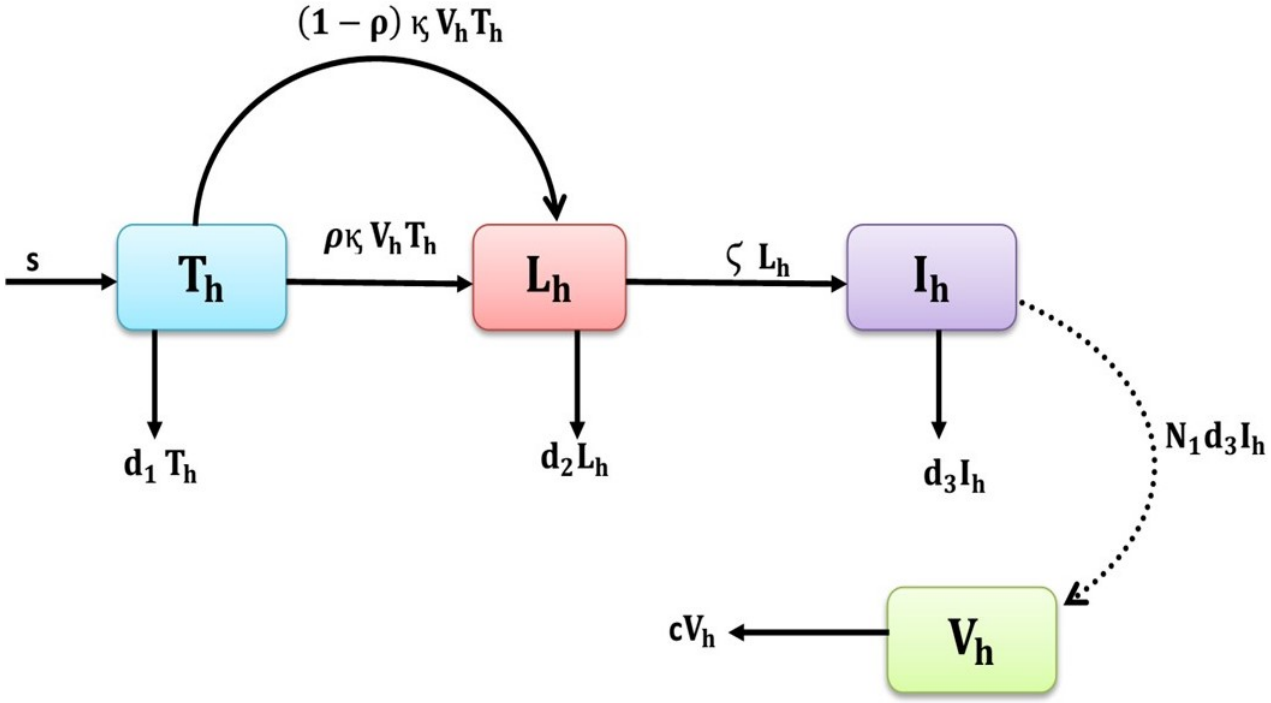

Figure 4.1: In-host dynamics of HIV

This leads to the following differential equations for the basic HIV model without treatment;

$$\begin{aligned} T_h' &= s - \kappa V_h T_h - d_1 T_h, \\ L_h' &= \rho\kappa V_h T_h - (\zeta + d_2) L_h, \\ I_h' &= (1-\rho)\kappa V_h T_h + \zeta L_h - d_3 I_h, \\ V_h' &= N_1 d_3 I_h - c V_h, \end{aligned} \tag{4.1}$$

with initial conditions, $T_h(0) = T_{h0}, L_h(0) = L_{h0}, I_h(0) = I_{h0}, V_h(0) = V_{h0}$. The parameters used in the model are summarized in Table 4.1.

Table 4.1: Table of parameters for the HIV model with latency.

Parameter	**Description**
T_h	Susceptible target cells
L_h	Latently infected cells.
I_h	Actively infected cells that are virus producing.
V_h	HIV free virus particles .
s	Healthy target cell recruitment rate.
κ	HIV infection transmission rate.
d_1, d_2, d_3	Natural death rates for T_h, L_h, I_h respectively.
ρ	Proportion of infections that result in latent infection .
ζ	Progression rate of latently infected cells to the actively infectious class I_h.
N_1	Burst size for an HIV cell
c	Natural death rate of the HIV virus.

4.2.1 Positivity and boundedness of solutions.

Theorem 23 (Positivity and boundedness of solutions for the HIV model.)**.** *For any non-negative initial conditions given by* $(T_{h0}, L_{h0}, I_{h0}, V_{h0})$*, model (4.1) has a unique solution and is bounded for all* $t \geq 0$.

Proof. For model system (4.1) there exists a positively invariant set

$$\Omega_* = \{T_h(t), L_h(t), I_h(t), V_h(t) \in \mathbb{R}^{4+}_{\geq 0} : 0 \leq T_h(t) + L_h(t) + I_h(t) \leq M, V_h(t) \leq M_1\} \qquad (4.2)$$

where M and M_1 are to be established. Using the classical differential equations theory, model (4.1) has a unique solution $T_h(t), L_h(t), I_h(t)$ and $V_h(t)$ on $t \in [0, t_m)$, where $0 < t_m < \infty$. Now $T_h(t)$ is strictly positive $\forall \;\; t \in [0, t_m)$. By contradiction let some $t_1 \in [0, t_m)$, be the first time such that $T_(t_1) = 0$ and $T_h'(t_1) \leq 0$. Using equation (1) from model (4.1) we have $T_h'(t_1) = s > 0$, this contradicts $T_h'(t_1) \leq 0$ and hence $T_h(t) > 0$, $\forall \;\; t \in [0, t_m)$. We also have

$$\begin{aligned} L_h'|_{L_h=0} &= \rho\kappa V_h T_h \geq 0, \\ I_h'|_{I_h=0} &= (1-\rho)\kappa V_h T_h + \zeta L_h \geq 0, \end{aligned} \qquad (4.3)$$

It can clearly be seen that $L_h(t) \geq 0$ and $I_h(t) \geq 0$, $\forall \ \ t[0, t_m)$. Now from the fourth equation we have

$$V_h'(t) = N_1 d_3 I_h - cV_h$$

and hence solving the equation using the integrating factor approach yields

$$V_h(t) = e^{ct}\left[\int_0^t N_1 d_3 e^{cu} I(u)du + V_h(0)\right].$$

Hence $V_h(t) \geq 0$ for all $t \geq 0$ as long as $I_h(t) \geq 0$. To prove the boundedness of solutions, we add up the first three equations of model system (4.1) since they are the target cell compartments as follows and obtain

$$\mathcal{X} = T_h(t) + L_h(t) + I_h(t). \tag{4.4}$$

By substitution we obtain

$$\begin{aligned} \dot{\mathcal{X}}(t) &= s - d_1 T_h - d_2 L_h - d_3 I_h, \\ &\leq s - \mathcal{Q}\mathcal{X}(t), \end{aligned} \tag{4.5}$$

where $\mathcal{Q} = min\{d_1, d_2, d_3\}$. Using the integrating factor approach, we obtain

$$\begin{aligned} \mathcal{X}(t) &= \mathcal{X}(0)e^{-\mathcal{Q}t} + \frac{s}{\mathcal{Q}}(1 - e^{-\mathcal{Q}t}) \\ &\leq \mathcal{X}(0)e^{-\mathcal{Q}t} + \frac{s}{\mathcal{Q}}. \end{aligned} \tag{4.6}$$

Therefore, $\mathcal{X} = T_h(t) + L_h(t) + I_h(t)$ is bounded and thus it follows that $T_h(t), L_h(t), I_h(t)$ are also bounded. Using the same approach, it can be shown that V_h is also bounded since we obtain by the integrating factor approach that;

$$V_h(t) \leq V_h(0) + \frac{N_1 d_3}{c} \parallel I_h \parallel_\infty \tag{4.7}$$

Hence, the proof for boundedness of the set

$$\Omega_h = \{T_h(t), L_h(t), I_h(t), V_h(t) \in \mathbb{R}^{4+}_{\geq 0} : 0 \leq T_h(t) + L_h(t) + I_h(t) \leq M, V_h(t) \leq M_1\} \tag{4.8}$$

where $M = \frac{s}{\mathcal{Q}}$ and $M_1 = \frac{N_1 d_3}{c} \parallel I_h \parallel_\infty$ is completed. □

4.3 Equilibrium analysis for the HIV model

We present the equilibrium points for the HIV and the reproduction number.

4.3.1 The disease-free equilibrium and $\mathcal{R}_{oh}$.

The disease-free equilibrium for the HIV model is given by

$$\mathcal{C}_0 = \left(\frac{s}{d_1}, 0, 0, 0\right).$$

The reproduction number for the HIV model is found using the method by [98]. We only consider the infected classes that is $L_h(t), I_h(t)$ and $V_h(t)$ in the computation of the reproduction number, such that the $\mathcal{F}$ and $\mathcal{V}$ matrices are given by;

$$\mathcal{F} = \begin{pmatrix} 0 & 0 & \frac{s\rho\kappa}{d_1} \\ 0 & 0 & \frac{s(1-\rho)\kappa}{d_1} \\ 0 & 0 & 0 \end{pmatrix}, \mathcal{V} = \begin{pmatrix} (\zeta + d_2) & 0 & 0 \\ -\zeta & d_3 & 0 \\ 0 & -N_1 d_3 & c \end{pmatrix}, \tag{4.9}$$

and therefore the spectral radius $\rho(\mathcal{F}\mathcal{V}^{-1})$ is given by

$$\begin{aligned} \mathcal{R}_{0h} &= \frac{s\kappa N_1 \zeta}{cd_1(\zeta + d_2)} + \frac{s\kappa N_1(1-\rho)d_2}{cd_1(\zeta + d_2)} \\ &= \frac{s\kappa N_1(\zeta + d_2(1-\rho))}{cd_1(\zeta + d_2)} \end{aligned} \tag{4.10}$$

It is important to note that when $\rho = 0$, we have an HIV model with no latent infection and $\mathcal{R}_{0h} = \frac{s\kappa N_1}{cd_1}$, which is the reproduction number for an HIV model without latency.

4.3.2 Endemic equilibrium point

The endemic equilibrium point, $\mathcal{C}_e$, for the HIV model (4.1)

$$\mathcal{C}_e = (T_h^e, L_h^e, I_h^e, V_h^e)$$

is found as follows;

$$T_h^e = \frac{1}{\mathcal{R}_{0h}},\ L_h^e = \frac{\rho(s\mathcal{R}_{0h} - d_1)}{\mathcal{R}_{0h}(\zeta + d_2)},\ I_h^e = \frac{c(s\mathcal{R}_{0h} - d_1)}{N_1 d_3 \kappa},\ V_h^e = \frac{(s\mathcal{R}_{0h} - d_1)}{\kappa}. \tag{4.11}$$

We state the following lemma;

Lemma 6. *The following conditions hold for the HIV model:*

1. *The disease-free equilibrium point is globally asymptotically stable provided that* $\mathcal{R}_{0h} < 1$*and unstable otherwise.*

2. *The endemic equilibrium point for the HIV model is globally asymptotically stable provided that* $\mathcal{R}_{0h} > 1$ *and unstable otherwise*

Using Matlab, we simulate the dynamics of the HIV model presented in model system (4.1) and show the stability of the disease-free and endemic equilibrium points. The simulations that are carried out support the theoretical findings. The parameter values used are sourced from literature and they are given by : $s = 6.2 \times 10^3\ \mu l^{-1}$ per day [102], $\kappa = 5 \times 10^{-8}\ \mu l$ per viron per day (Estimated), $d_1, d_2, d_3 = 0.01, 0.001, 1$ respectively per day [105, 99], $\zeta = 0.1$ per day [105], $\rho = 0.02$ [105], $N_1 = [1000 - 1250]$ virions per cell[105, 3], $c = [20 - 23]$ per day [105, 3, 99]. Figure 4.2 presents the dynamics of the disease-free equilibrium point. Figure 4.2

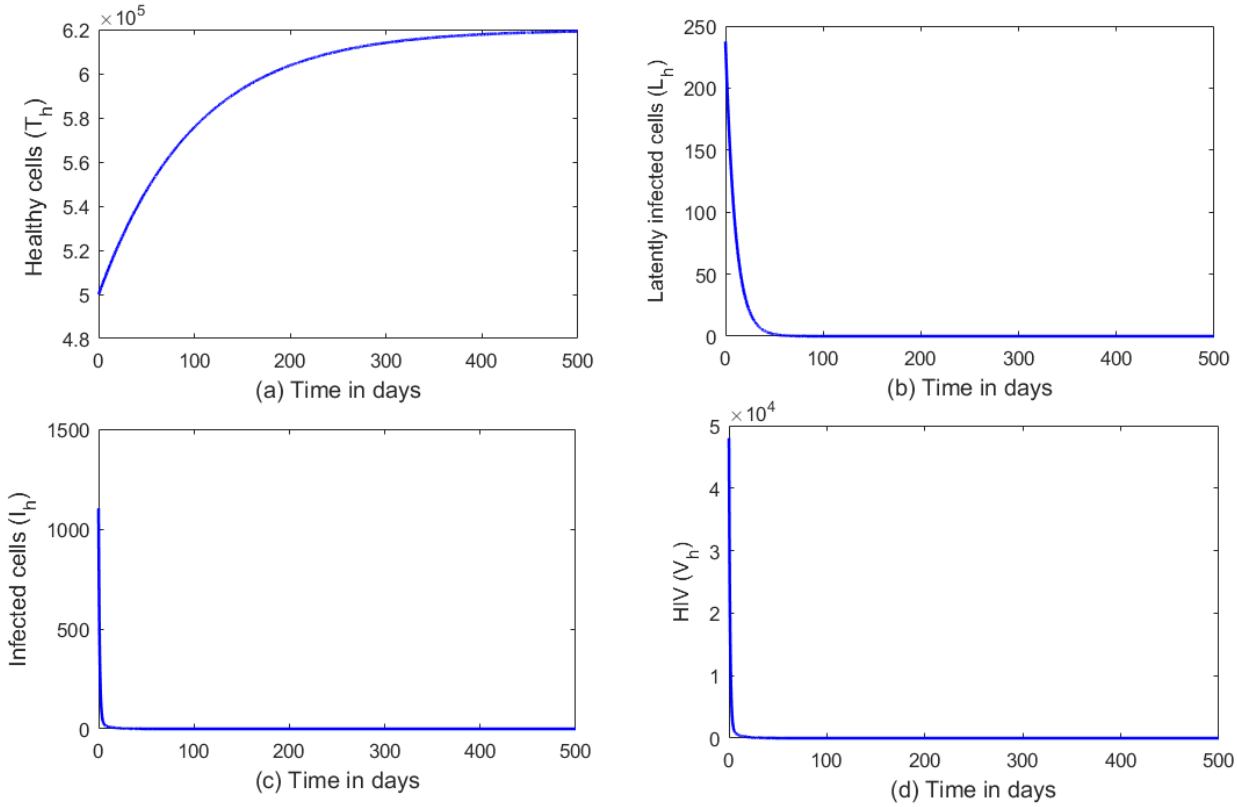

Figure 4.2: In-host dynamics of the HIV model system (4.1) for classes $T_h(t), L_h(t), I_h(t), V_h(t)$, $\mathcal{R}_{0h} = 0.1348 < 1$, and all other parameters as indicated and $\kappa = 5 \times 10^{-8}$. The dynamics presented indicate that the disease-free equilibrium is stable provided $\mathcal{R}_{0h} < 1$.

supports the theoretical work on the HIV model with viral latency which states the disease-free equilibrium is globally asymptotically stable provided that $\mathcal{R}_{0h} < 1$. As seen by Figure 4.2, in the absence of infection, the healthy target cells will gradually increase up to a peak value

that is stable while the latently infected cells and actively cells gradually decrease to zero. Due to a very low viral load the HIV virus will also gradually decline to zero. Hence, model system (4.3) approaches the disease-free equilibrium point given by $\mathcal{C}_0 = [6.191 \times 10^5, 0, 0, 0]$. The endemic equilibrium point, $\mathcal{C}_e$, is simulated and shown in Figure 4.3. The simulations indicate that when $\mathcal{R}_{0h} > 1$, the endemic equilibrium point is globally asymptotically stable hereby supporting the theoretical work done on the model. As HIV is introduced into the system, we observe that the susceptible population declines to a certain constant value while the latently infected cells, $L_h(t)$, gradually increase till they reach a peak constant value which becomes stable. The infected cells will initially increase to a peak value between $[0 - 30]$ days after which it becomes stable. This is due to an increase in the viral load at the beginning of infection. We observe some oscillatory behaviour in all the classes between $[35 - 50]$ days. Thus, for $\mathcal{R}_{0h} > 1$, model system (4.3) approaches the endemic equilibrium point given by $\mathcal{C}_e = [4.605 \times 10^5, 319.9, 1624, 7.075 \times 10^4]$.

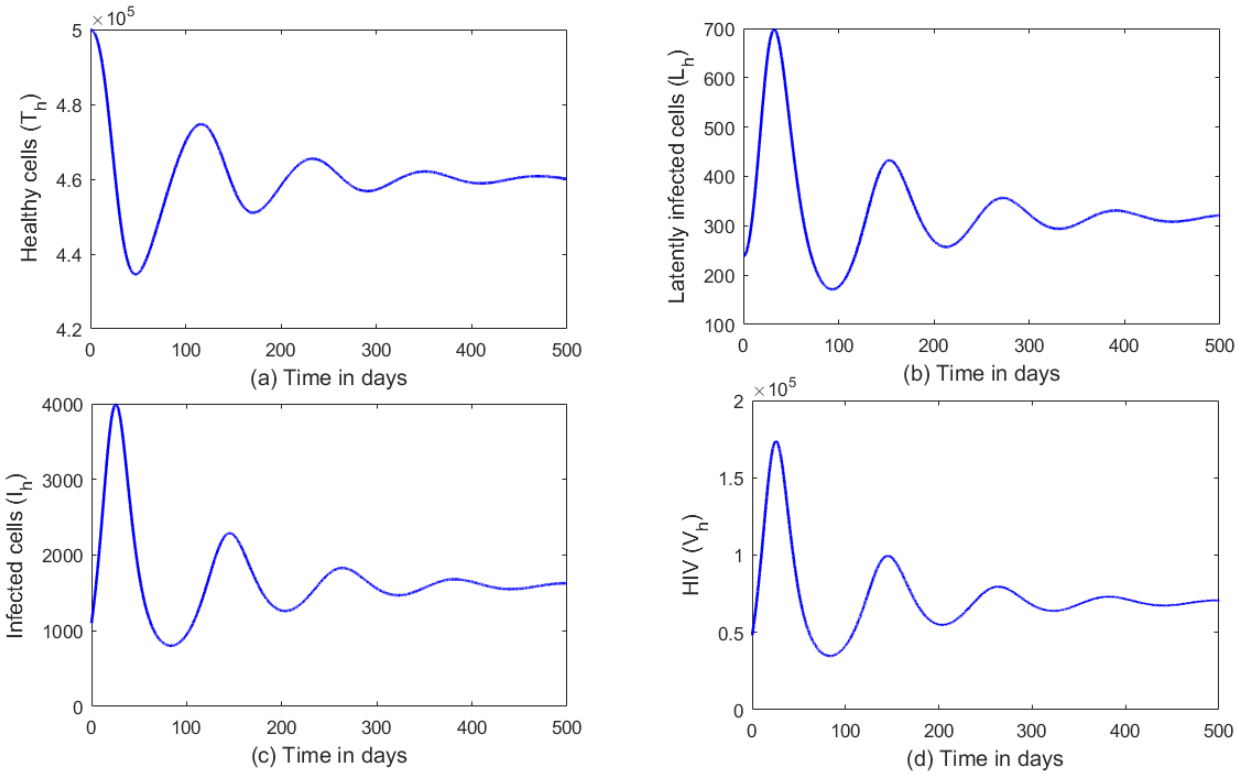

Figure 4.3: In-host dynamics for the HIV model system (4.1), for classes, $T_h(t), L_h(t), I_h(t), V_h(t)$, $\mathcal{R}_{0h} = 1.3476 > 1$ and all other parameters as indicated . The dynamics presented indicate that the endemic equilibrium is stable provided $\mathcal{R}_{0h} > 1$.

In the next section, we extend the model to analyse the dynamics of the HPV/HIV co-infection model.

4.4 The HPV/HIV co-infection model

The co-infection dynamics of HIV/HPV remain poorly understood with not much mathematical modelling done so far. Normally, women who are HIV-positive are at risk of acquiring HPV due to immunodeficiency as a result HIV. A mathematical model for the co-infection dynamics of HIV/HPV based on the work done by Verma *et al.* [99] is developed. In their work, they outline the role of HIV-1 *tat* protein in the proliferation of HPV infected cells. HIV weakens the immune system and makes it easy for infections such as HPV to spread rapidly within cells. This activates HIV to release *tat* protein which increases the production of HPV oncoproteins $E6$ and $E7$. These oncoproteins are responsible for cell proliferation in infected HPV epithelial cells and they promote persistence of HPV infection which is crucial in the development of cancer cells. In the presence of immune suppression, latently infected HPV cells may be reactivated into actively infected cells and also into cancer cells if not cleared by the immune system. HIV-1 *tat* protein is a gene regulatory protein (a protein that normally influences the regions of a DNA molecule that is transcribed by RNA during transcription). In other words, it is a protein that enhances viral transcription and causes the disruption of epithelial tight junctions making the entry of viruses such as HPV into the epithelium through abrasion very easy. *Tat* protein is secreted from the intra-epithelial immune cells and it disrupts the epithelial tight junctions that seal adjacent epithelial cells and restrict the easy flow of viruses such as HPV [5, 97, 99].

HIV *tat* protein has been found to be an enhancer of the self proliferation of infected cells and it has also been established as the main cause of the expression of HPV oncogenes $E6$ and $E7$ in infected individuals [47] . Research affirms that individuals that are HIV-positive are at a higher risk of acquiring HPV [47] as compared to HIV-negative individuals. This because the $E7$ proteins released as a result of $HPV16/18$ increase the permeability of the genital mucosa. A mucosa is defined as a membrane that lines various parts of the body and it is made up of epithelial cells which make it highly susceptible to HPV infection [44, 109]. Transmission of HPV can occur through the oral mucosa, genital mucosa and the intestinal mucosa [47]. The study by Verma *et al.* looked at HIV/HPV co-infection dynamics within the oral mucosa only, while in this particular research we consider the transmission dynamics within the genital mucosa. The primary focus of our research is on heterogeneous sexual transmission of HPV. Verma *et al.* studied how HIV influences HPV infection and but however did not consider how HPV influences HIV infection. This is a subject for future research. The new model will take

into account the role of both latent HIV and HPV infections as omitted by the work done by Verma *et al.*. It is envisaged that the results of this particular model will yield interesting facts about co-infection dynamics.

The total available susceptible epithelial cells are now assumed to be recruited at a rate, $\Lambda(1+\eta V_h)$, as a result the presence of *tat* protein [28], where η is the effect of *tat* protein secreted by an HIV virion, V_h. The model assumes that $0 \leq \eta \leq 1$ such that when $\eta = 0$ the recruitment of susceptible cells remains Λ and when $\eta = 1$ there is an increase in the recruitment of susceptible epithelial cells [99] . *Tat* protein initiates the disruption of epithelial tight junctions and therefore causes I_1 cells to proliferate faster into I_2 cells. Thus, the model equations for the co-infection model are presented as follows;

$$
\begin{aligned}
T_h'(t) &= s - \kappa V_h T_h - d_1 T_h, \\
L_h'(t) &= \rho\kappa V_h T_h - (\zeta + d_2) L_h, \\
I_h'(t) &= (1-\rho)\kappa V_h T_h + \zeta L_h - d_3 I_h, \\
V_h'(t) &= N_1 d_3 I_h - c V_h, \\
T_s'(t) &= \Lambda(1+\eta V_h) + \phi L - \left[\frac{\beta V}{(\gamma + T_s)} + \mu\right] T_s, \\
L'(t) &= \frac{\beta V T_s}{(\gamma + T_s)} - (\mu + \psi + \phi) L, \\
I_1'(t) &= \psi L - (\epsilon + \mu + \theta K) I_1, \\
I_2'(t) &= \epsilon I_1 + r\epsilon I_2 - (\mu + \theta K) I_2, \\
V'(t) &= N_2 \mu (I_1 + I_2) - \delta V, \\
K'(t) &= \sigma I_2 K - \nu K,
\end{aligned}
\tag{4.12}
$$

with initial conditions given by, $T_h(0) = T_{h0}, L_h(0) = L_{h0}, I_h(0) = I_{h0}, V_h(0) = V_{h0}, T_s(0) = T_{s0}, L(0) = L_0, I_1(0) = I_{10}, I_2(0) = I_{20}, V(0) = V_0, K(0) = K_0$.

4.5 Equilibrium points for the model

The co-infection model exhibits three equilibrium points: the disease-free equilibrium point E_0, the CTL-inactive endemic equilibrium point, E_1, and the CTL-active endemic equilibrium point, E_2. In this particular model we are considering the case where an HIV-positive individual develops HPV due to an increase in *tat* protein. This is because *tat* protein increases the susceptibility of epithelial cells. So, the HIV equilibrium point is given by $(\bar{T}_h, \bar{L}_h, \bar{I}_h, \bar{V}_h)$, where $\bar{T}_h$ is the initial concentrations of CD4+ target cells, $\bar{L}_h$, are latently infected target cells, $\bar{I}_h$, are infected target cells and $\bar{V}_h$, is the concentration of HIV virions for an infected individual who progresses to acquire HPV as a result of immune suppression. In this chapter, the effect of *tat* protein is [presented by the term ηV_h as indicated by Verma *et al.* [99], $\eta\bar{V}_h = 1$ implies the doubling effect and $\eta\bar{V}_h = 2$ implies a tripling effect and so on. This simplifies the co-infection model to

$$\begin{aligned}
T_s'(t) &= \Lambda(1+\eta V_h) + \phi L - \left[\frac{\beta V}{(\gamma + T_s)} + \mu\right] T_s, \\
L'(t) &= \frac{\beta V T_s}{(\gamma + T_s)} - (\mu + \psi + \phi)L, \\
I_1'(t) &= \psi L - (\epsilon + \mu + \theta K) I_1, \\
I_2'(t) &= \epsilon I_1 + r\epsilon I_2 - (\mu + \theta K) I_2, \\
V'(t) &= N_2\mu(I_1 + I_2) - \delta V, \\
K'(t) &= \sigma I_2 K - \nu K,
\end{aligned} \tag{4.13}$$

and yields a disease-free equilibrium given by

$$E_0 = \left(\frac{\Lambda(1+\eta\bar{V}_h)}{\mu}, 0, 0, 0, 0, 0\right). \tag{4.14}$$

4.5.1 The basic reproduction number for the co-infection model

The reproduction number for model system (4.13) is found using the next generation approach [98] and we only consider the infection and viral production classes such that the $\mathcal{F}$ and $\mathcal{V}$ are

matrices are;

$$\mathcal{F} = \begin{bmatrix} 0 & 0 & 0 & \dfrac{\Lambda(1+\eta\bar{V_h})\beta}{(\gamma\mu+\Lambda(1+\eta\bar{V_h}))} \\ 0 & 0 & 0 & 0 \\ 0 & 0 & 0 & 0 \\ 0 & 0 & 0 & 0 \end{bmatrix} \tag{4.15}$$

and

$$\mathcal{V} = \begin{bmatrix} (\psi+\phi+\mu) & 0 & 0 & 0 \\ -\psi & (\epsilon+\mu) & 0 & 0 \\ 0 & -\epsilon & (\mu-r\epsilon) & 0 \\ 0 & -N_2\mu & -N_2\mu & \delta \end{bmatrix} \tag{4.16}$$

and the inverse of $\mathcal{V}$ is given by

$$\mathcal{V}^{-1} = \begin{bmatrix} \dfrac{1}{(\psi+\phi+\mu)} & 0 & 0 & 0 \\ \dfrac{\psi}{(\epsilon+\mu)(\mu+\psi+\phi)} & \dfrac{1}{(\epsilon+\mu)} & 0 & 0 \\ q_1 & \dfrac{\epsilon}{(\mu-r\epsilon)(\epsilon+\mu)} & \dfrac{1}{\mu-r\epsilon} & 0 \\ q_2 & q_3 & \dfrac{N_2\mu}{\delta(\mu-r\epsilon)} & \dfrac{1}{\delta} \end{bmatrix} \tag{4.17}$$

where $q_1 = \dfrac{\epsilon\mu}{(\epsilon+\mu)(\mu-r\epsilon)(\mu+\psi+\phi)}$, $q_2 = \dfrac{N_2\mu\psi(\mu+\epsilon-r\epsilon)}{\delta(\mu-r\epsilon)(\epsilon+\mu)(\mu+\psi+\phi)}$ and $q_3 = \dfrac{N_2\mu(\mu+\epsilon-r\epsilon)}{\delta(\mu-r\epsilon)(\epsilon+\mu)}$.

The reproduction number is the spectral radius of the product of $(\mathcal{F}\mathcal{V}^{-1})$ where

$$\mathcal{F}\mathcal{V}^{-1} = \begin{bmatrix} \frac{\Lambda(1+\eta\bar{V_h})\beta q_2}{w_1} & \frac{\Lambda(1+\eta\bar{V_h})\beta q_3}{w_1} & \frac{N_2\mu\Lambda(1+\eta\bar{V_h})\beta}{\delta(\mu-r\epsilon)w_1} & \frac{\Lambda(1+\eta\bar{V_h})\beta}{\delta w_1} \\ 0 & 0 & 0 & 0 \\ 0 & 0 & 0 & 0 \\ 0 & 0 & 0 & 0 \end{bmatrix} \tag{4.18}$$

with

$$w_1 = (\gamma\mu + \Lambda(1+\eta\bar{V^*})). \tag{4.19}$$

The eigenvalues of the matrix $(\mathcal{F}\mathcal{V}^{-1})$ are found to be

$$\lambda_i = \left[\frac{\beta N_2\mu\psi\Lambda(1+\eta\bar{V_h})(\mu+\epsilon-r\epsilon)}{\delta(\mu-r\epsilon)(\mu+\epsilon)(\mu+\psi+\phi)(\Lambda(1+\eta\bar{V_h})+\gamma\mu)}, 0, 0, 0\right] \tag{4.20}$$

for $i = 1, 2, 3, 4$. Therefore, the reproduction number for the HPV model in the presence of HIV is given by

$$\mathcal{R}_0 = \frac{\beta N_2\mu\psi\Lambda(1+\eta\bar{V_h})(\mu+\epsilon-r\epsilon)}{\delta(\mu-r\epsilon)(\mu+\epsilon)(\mu+\psi+\phi)\left[\Lambda(1+\eta\bar{V_h})+\gamma\mu\right]}. \tag{4.21}$$

As indicated in the work by Verma *et al.* the effects of *tat* vary from individual to individual which also affects the dynamics of HPV in-host.

4.6 Local stability of the disease-free equilibrium point

To establish the stability of the disease-free equilibrium, E_0, we state and prove the following theorem;

Theorem 24. *The disease-free equilibrium for the co-infection model system (4.13) is locally asymptotically stable provided that* $\mathcal{R}_0 < 1$ *and unstable otherwise.*

Proof. The Jacobian matrix for model (4.13) evaluated at the disease-free equilibrium is found

to be;

$$J(E_0) = \begin{bmatrix} -\mu & \phi & 0 & 0 & -p_1 & 0 \\ 0 & -p_2 & 0 & 0 & p_1 & 0 \\ 0 & \psi & -p_3 & 0 & 0 & 0 \\ 0 & 0 & \epsilon & -p_4 & 0 & 0 \\ 0 & 0 & N_2\mu & N_2\mu & -\delta & 0 \\ 0 & 0 & 0 & 0 & 0 & -\nu \end{bmatrix}, \tag{4.22}$$

where $p_1 = -\dfrac{\Lambda(1+\eta\bar{V_h})\beta}{\gamma\mu + \Lambda(1+\eta\bar{V_h})}$, $p_2 = (\mu+\psi+\phi)$, $p_3 = (\epsilon+\mu)$, $p_4 = (\mu - r\epsilon)$.

To establish the local stability of the model system (4.13) we find the determinant and the trace as follows;

$$\begin{aligned} Det\ J(E_0) &= -\nu\left[N_2\mu^2\psi p_1(\mu - r\epsilon) + N_2\mu^2\psi p_1\epsilon - \delta\mu(\mu+\psi+\phi)(\epsilon+\mu)(\mu-r\epsilon)\right], \\ &= \delta\mu(\mu+\psi+\phi)(\epsilon+\mu)(\mu-r\epsilon)\left[1-\mathcal{R}_0\right]. \end{aligned} \tag{4.23}$$

If $\mathcal{R}_0 < 1$ then $Det\ J(E_0) > 0$ and the trace of the Jacobian is given by

$$Trace\ J(E_0) = -\mu - (\mu+\phi+\psi) - (\mu+\epsilon) - (\mu - r\epsilon) - \delta - \nu < 0, \tag{4.24}$$

since all parameters are positive and $(\mu - r\epsilon) > 0$. Therefore, the disease-free equilibrium is locally asymptotically stable when $\mathcal{R}_0 < 1$. This completes the proof. □

4.7 Global stability analysis of the disease-free equilibrium for the co-infection model.

To ensure effective viral elimination for both HPV and HIV, we prove the global stability of the disease-free equilibrium point, E_0. We state and prove the following theorem.

Theorem 25. *The disease-free equilibrium for the co-infection model (4.13) is globally asymptotically stable provided that* $\mathcal{R}_0 < 1$.

Proof. To prove the global stability of the co-infection model (4.13), we let $\mathcal{X} = T_s \in \mathbb{R}$ be the susceptible healthy epithelial cell population and $\mathcal{Z} = (L, I_1, I_2, V)$ be the infected population. We rewrite model system (4.13) as follows;

$$\begin{aligned} \frac{d\mathcal{X}}{dt} &= F(\mathcal{X}, \mathcal{Z}), \\ \frac{d\mathcal{Z}}{dt} &= G(\mathcal{X}, \mathcal{Z}), \quad G(\mathcal{X}, 0) = 0, \end{aligned} \tag{4.25}$$

where

$$F(\mathcal{X}, \mathcal{Z}) = \Lambda(1 + \eta\bar{V_h}) + \phi L - \left[\frac{\beta V}{(\gamma + T_s)} + \mu\right] T_s,$$

$$G(\mathcal{X}, Z) = \begin{bmatrix} \dfrac{\beta V T_s}{(\gamma + T_s)} - (\mu + \psi + \phi)L, \\ \psi L - (\epsilon + \mu + \theta K)I_1, \\ \epsilon I_1 + r\epsilon I_2 - (\mu + \theta K)I_2, \\ N_2\mu(I_1 + I_2) - \delta V \end{bmatrix}. \tag{4.26}$$

The disease-free equilibrium point, for the system is given by $\mathcal{U}_0 = (\mathcal{X}^*, 0)$ where

$$\mathcal{X}^* = \left(\frac{\Lambda(1 + \eta\bar{V_h})}{\mu}, 0, 0, 0, 0, 0\right).$$

So, it follows that

$$\frac{d\mathcal{X}}{dt}|_{\mathcal{Z}=0} = \Lambda(1 + \eta\bar{V_h}) - \mu\mathcal{X}, \tag{4.27}$$

this yields the equilibrium point, $\mathcal{X}^* = \dfrac{\Lambda(1 + \eta\bar{V_h})}{\mu}$, that is globally asymptotically stable. Solving differential equation (4.27) yields

$$T_s(t) = \frac{\Lambda(1 + \eta\bar{V_h})}{\mu} + \left[T_s(0) - \frac{\Lambda(1 + \eta\bar{V_h})}{\mu}\right] \exp^{-\mu t}. \tag{4.28}$$

It can be seen that as $t \to \infty$, $T_s \to \mathcal{X}^*$. To guarantee global stability of model system (4.13), we state the following three conditions

1. For $\dfrac{d\mathcal{X}}{dt} = F(\mathcal{X}, 0)$, $\mathcal{X}^*$ is globally asymptotically stable,

2. $G(\mathcal{X},\mathcal{Z}) = \mathcal{A}\mathcal{Z} - \hat{G}(\mathcal{X},\mathcal{Z})$, $\hat{G}(\mathcal{X},\mathcal{Z}) \geq 0$ for $(\mathcal{X},\mathcal{Z}) \in \Omega$,

3. $\mathcal{A} = D_{\mathcal{Z}}G(\mathcal{X}^*, 0)$ is an M-matrix whose off diagonal elements are non-negative and Ω is the region where the model is biologically feasible.

Based on these conditions, we linearise $G(\mathcal{X},\mathcal{Z})$ and obtain the following matrix

$$\mathcal{A} = \begin{bmatrix} -(\mu+\phi+\psi) & 0 & 0 & \dfrac{\beta\Lambda(1+\eta\bar{V_h})}{\gamma\mu+\Lambda(1+\eta\bar{V_h})} \\ \psi & -(\epsilon+\mu) & 0 & 0 \\ 0 & \epsilon & -(\mu-r\epsilon) & 0 \\ 0 & N_2\mu & N_2\mu & -\delta \end{bmatrix} \tag{4.29}$$

and

$$\mathcal{A}\mathcal{Z} = \begin{bmatrix} \dfrac{\beta V\Lambda(1+\eta\bar{V_h})}{\gamma\mu+\Lambda(1+\eta\bar{V_h})} - (\mu+\psi+\phi)L, \\ \psi L - (\epsilon+\mu)I_1, \\ \epsilon I_1 - (\mu-r\epsilon)I_2, \\ N_2\mu(I_1+I_2) - \delta V \\ \sigma I_2 K - \nu K. \end{bmatrix} \tag{4.30}$$

and therefore

$$\hat{G}(\mathcal{X},\mathcal{Z}) = \mathcal{A}\mathcal{Z} - G(\mathcal{X},\mathcal{Z}) = \begin{bmatrix} \dfrac{\beta V\gamma(T_{s0}^* - T_s)}{(\gamma+T_{s0}^*)(\gamma+T_s)}, \\ \theta K I_1, \\ \theta K I_2, \\ 0 \end{bmatrix}. \tag{4.31}$$

Provided that $I_1 \geq 0, I_2 \geq 0, K \geq 0$ and $T^*_{s0} \geq T_s$, it follows that $\hat{G}(\mathcal{X}, \mathcal{Z}) \geq 0$. Then from theorem (25), the disease-free equilibrium is globally asymptotically stable whenever $\mathcal{R}_0 < 1$. This concludes the proof. □

4.8 The endemic equilibrium points E_1 and E_2

The co-infection model has two endemic equilibrium points that is, the CTL-inactive equilibrium, E_1 and the CTL-active equilibrium point, E_2. We define the CTL-inactive equilibrium point, E_1, as an equilibrium point where the immune response is absent and immune evasion by HPV is successful and the CTL-active endemic equilibrium, E_2, is where the immune response is active. The HIV only model has an endemic equilibrium given by $(T^e_h = \bar{T_h}, L^e_h = \bar{L_h}, I^e = \bar{I_h}, V^e_h = \bar{V_h})$ and the equilibrium values are obtained from clinical trial estimates, [99, 58]. We are interested in the effect of *tat* protein in the subsequent increase in the number of susceptible epithelial cells and consequently its effect on the dynamics of HPV in the presence of HIV. The CTL-inactive equilibrium point, E_1, for the HPV model in the presence of HIV is found to be

$$T^e_s = \frac{\Lambda}{\mu} - \frac{\Lambda(1+\eta\bar{V_h})(\mathcal{R}_0-1)\left[\gamma\mu + \Lambda(1+\eta\bar{V_h})\right]}{\mu A_1}, L^e = \frac{\Lambda(1+\eta\bar{V_h})(\mathcal{R}_0-1)(\gamma\mu+\Lambda(1+\eta\bar{V_h}))}{(\mu+\psi)A_1},$$

$$I^e_1 = \frac{\Lambda(1+\eta\bar{V_h})\psi(\mathcal{R}_0-1)\left[\gamma\mu + \Lambda(1+\eta\bar{V_h})\right]}{(\mu+\psi)(\epsilon+\mu)A_1}, I^e_2 = \frac{\Lambda(1+\eta\bar{V_h})\psi\epsilon(\mathcal{R}_0-1)\left[\gamma\mu + \Lambda(1+\eta\bar{V_h})\right]}{(\mu+\psi)(\mu-r\epsilon)(\epsilon+\mu)A_1},$$

$$V^e = \frac{N_2\mu\psi\Lambda(1+\eta\bar{V_h})(\mu+\epsilon-r\epsilon)[\Lambda(1+\eta\bar{V_h})+\gamma\mu][1-\mathcal{R}_0]}{\delta(\mu-r\epsilon)(\mu+\epsilon)(\mu+\psi)A_1}, K^e = 0, \tag{4.32}$$

where

$$\begin{aligned} A_1 &= [\mathcal{R}_0\gamma\mu + \Lambda(1+\eta\bar{V_h})(\mathcal{R}_0-1)], \\ \mathcal{R}_0 &= \frac{\beta N_2\mu\psi\Lambda(1+\eta\bar{V_h})(\mu+\epsilon-r\epsilon)}{\delta(\mu-r\epsilon)(\mu+\epsilon)(\mu+\psi+\phi)(\Lambda(1+\eta\bar{V_h})+\gamma\mu)}. \end{aligned} \tag{4.33}$$

The CTL-active endemic equilibrium point, E_2, is found to be

$$
\begin{aligned}
T_s^{ee} &= \frac{\Lambda\sigma\epsilon\psi - \nu\Phi_0(\Phi_1+\theta K^{ee})(\Phi_2+\theta K^{ee})}{\sigma\epsilon\psi\mu}, \\
L^{ee} &= \frac{\nu(\Phi_1+\theta K^{ee})(\Phi_2+\theta K^{ee})}{\sigma\epsilon\psi}, \quad I_1^{ee} = \frac{\nu(\Phi_2+\theta K^{ee})}{\sigma\epsilon}, \quad I_2^{ee} = \frac{\nu}{\sigma}, \\
V^{ee} &= \frac{N_2\nu\mu(\Phi_4+\theta K^{ee})}{\delta\sigma\epsilon}, \quad K = K^{ee},
\end{aligned}
\tag{4.34}
$$

where K^{ee} is a solution of the quartic polynomial equation given by

$$
f(K) = c_0K^4 + c_1K^3 + c_2K^2 + c_3K + c_4 = 0, \tag{4.35}
$$

with

$$
\begin{aligned}
c_0 &= \theta^4\delta\Phi_0\Phi_3\nu^2 > 0, \\
c_1 &= \theta^3\left[2\delta\nu^2\Phi_0\Phi_3(\Phi_1+\Phi_2) - \delta\Phi_0\beta N_2\mu\nu^2\right], \\
c_2 &= \theta^2\Big[\delta\Phi_0\nu^2\Phi_3(\Phi_1^2+4\Phi_1\Phi_2+\Phi_2^2) - \beta\mu\nu^2N_2\Phi_0(\Phi_1+\Phi_2+\Phi_4), \\
&- \nu\psi\Phi_3(\delta\epsilon\sigma\Lambda+\gamma\mu)\Big], \\
c_3 &= \theta\Big[(\Phi_1+\Phi_2)\left(2\Phi_0\delta\nu^2\Phi_3\Phi_1\Phi_2(-\delta\epsilon\Lambda\nu\sigma\psi\Phi_3 - \beta\mu\nu^2N_2\Phi_0\Phi_4\right) \\
&+ \beta\mu\nu N_2(\Lambda\sigma\psi\epsilon - \nu\Phi_0\Phi_1\Phi_2)\Big] - \gamma\mu\nu\psi\Phi_3(\Phi_1+\Phi_2), \\
c_4 &= \Big[\delta\nu\Phi_1\Phi_2\Phi_3(\Lambda\epsilon\sigma\psi + \nu\Phi_0\Phi_1\Phi_2) + \Phi_4\beta\mu\nu N_2(\Lambda\epsilon\sigma\psi - \nu\Phi_0\phi_1\Phi_2)\Big] \\
&- \gamma\mu\nu\psi\Phi_1\Phi_2, \Phi_3
\end{aligned}
\tag{4.36}
$$

and

$$
\Phi_0 = (\mu+\psi),\ \Phi_1 = (\epsilon+\mu),\ \Phi_2 = (\mu - r\epsilon),\ \Phi_3 = (\mu+\psi+\phi),\ \Phi_4 = (\mu+\epsilon-r\epsilon),\ \Phi_5 = (1+\eta V_h).
\tag{4.37}
$$

The polynomial (4.35), is complex to solve and so we use the Descartes' rule of signs to establish the nature of the endemic equilibrium points. We state the following lemma

Lemma 7. *The quartic polynomial function*

$$f(K) = c_0K^4 + c_1K^3 + c_2K^2 + c_3K + c_4 = 0$$

is subject to the following conditions;

1. *It has only one unique positive root provided that either* $c_0 > 0, c_1 < 0, c_2 < 0, c_3 < 0$ *and* $c_4 < 0$, *or* $c_0 > 0, c_1 > 0, c_2 < 0, c_3 < 0$ *and* $c_4 < 0$, *or* $c_0 > 0, c_1 > 0, c_2 > 0, c_3 < 0$ *and* $c_4 < 0$, *or* $c_0 > 0, c_1 > 0, c_2 > 0, c_3 > 0$ *and* $c_4 < 0$,

2. *It has no positive roots provided that* $c_0 > 0, c_1 > 0, c_2 > 0, c_3 > 0$ *and* $c_4 > 0$,

3. *More than one positive root otherwise.*

4.8.1 The CTL reproduction number, $\mathcal{R}_K^*$, for the co-infection model

Due to the presence of immune response as a result of HPV infection, we calculate the CTL reproduction number, $\mathcal{R}_K^*$, as follows;

$$\mathcal{R}_K^* = \frac{\sigma I_2^e}{\nu} = \frac{\sigma\Lambda(1+\eta\bar{V_h})\psi\epsilon(\mathcal{R}_0-1)\left[\gamma\mu+\Lambda(1+\eta\bar{V_h})\right]}{\nu(\mu+\psi)(\mu-r\epsilon)(\epsilon+\mu)A_1}, \tag{4.38}$$

$$A_1 = [\mathcal{R}_0\gamma\mu + \Lambda(1+\eta\bar{V_h})(\mathcal{R}_0-1)],$$

$$\mathcal{R}_0 = \frac{\beta N_2\mu\psi\Lambda(1+\eta\bar{V_h})(\mu+\epsilon-r\epsilon)}{\delta(\mu-r\epsilon)(\mu+\epsilon)(\mu+\psi+\phi)(\Lambda(1+\eta\bar{V_h})+\gamma\mu)}. \tag{4.39}$$

From the computation of the CTL reproduction number for the co-infection model, $\frac{1}{\nu}$, is the average life of a CTL immune response cell and I_2^e is the number of infected cells at endemic equilibrium E_1. $\mathcal{R}_K^*$ represents the average number of immune cells that are activated by each I_2 cell. We state the following conditions governing the CTL-inactivated/ activated endemic equilibrium ;

1. If $\mathcal{R}_0 > 1$ and $\mathcal{R}_K^* \leq 1$, then the CTL-inactivated endemic equilibrium point, E_1, is globally asymptotically stable.

2. If $\mathcal{R}_0 > 1$ and $\mathcal{R}_K^* \geq 1$, then the CTL-inactivated endemic equilibrium point, E_1, is unstable while the CTL activated equilibrium E_2 is globally asymptotically stable.

The stability of these endemic equilibrium points is proved in the following sections.

4.9 Local stability of the endemic equilibrium point E_1

In the presence of persistent HIV infection given by $\mathcal{R}_0 > 1$, we want to find out when the CTL-inactive endemic equilibrium point, E_1, is stable or unstable. To prove the local stability of the endemic equilibrium point, E_1, we use the bifurcation theory explained in chapter 3. We state and prove the following theorem;

Theorem 26. *Model system (4.13) has a stable unique CTL inactivated endemic equilibrium point given by E_1 whenever $\mathcal{R}_0 > 1$ and is unstable otherwise.*

Proof. To establish the existence of a forward bifurcation, we use the Center Manifold theory [15] outlined in chapter 3 and we re-define model system (4.13) as follows

$$\begin{aligned}
\dot{x}_1 &= f_1 = \Lambda(1+\eta\bar{V_h}) + \phi x_2 - \left[\frac{\beta x_5}{(\gamma + x_1)} + \mu\right] x_1, \\
\dot{x}_2 &= f_2 = \frac{\beta x_5 x_1}{(\gamma + x_1)} - (\mu + \psi + \phi)x_2, \\
\dot{x}_3 &= f_3 = \psi x_2 - (\epsilon + \mu + \theta x_6)x_3, \\
\dot{x}_4 &= f_4 = \epsilon x_3 + r\epsilon x_4 - (\mu + \theta x_6)x_4, \\
\dot{x}_5 &= f_5 = N_2\mu(x_3 + x_4) - \delta x_5, \\
\dot{x}_6 &= f_6 = \sigma x_4 x_6 - \nu x_6,
\end{aligned} \tag{4.40}$$

where $T_s = x_1,\ L = x_2,\ I_1 = x_3,\ I_2 = x_4,\ V = x_5,\ K = x_6$. We consider the case where the bifurcation parameter of interest is the transmission rate $\beta = \beta^*$ and by solving for β^* given that $\mathcal{R}_0 = 1$ yields

$$\beta = \beta^* = \frac{\delta(\mu - r\epsilon)(\mu + \epsilon)(\mu + \psi + \phi)\left[\gamma\mu + \Lambda(1+\eta\bar{V_h})\right]}{N_2\mu\psi\Lambda(1+\eta\bar{V_h})(\mu + \epsilon - r\epsilon)}. \tag{4.41}$$

The Jacobian for system (4.13) evaluated at the disease-free equilibrium is given

$$J(E_{\mathcal{R}_0=1}) = \begin{bmatrix} -\mu & \phi & 0 & 0 & -p_0 & 0 \\ 0 & -p_1 & 0 & 0 & p_0 & 0 \\ 0 & \psi & -p_2 & 0 & 0 & 0 \\ 0 & 0 & \epsilon & -p_3 & 0 & 0 \\ 0 & 0 & N_2\mu & N_2\mu & -\delta & 0 \\ 0 & 0 & 0 & 0 & 0 & -\nu \end{bmatrix}, \tag{4.42}$$

where $p_0 = -\dfrac{\beta^*\Lambda(1+\eta\bar{V_h})}{\gamma\mu + \Lambda(1+\eta\bar{V_h})}$, $p_1 = (\mu+\psi+\phi)$, $p_2 = (\epsilon+\mu)$, $p_3 = (\mu - r\epsilon)$ and β^* is the bifurcation parameter. Based on the local stability theorem in the Section (4.6) when $\mathcal{R}_0 = 1$, the Jacobian, $J(E_{\mathcal{R}_0=1})$ has a zero eigenvalue and all other eigenvalues have negative real parts provided the conditions stated are met, so the Center Manifold theory can be applied. The right eigenvalues for $J(E_{\mathcal{R}_0=1})$ are given $\mathbf{w} = (\omega_1, \omega_2, \omega_3, \omega_4, \omega_5, \omega_6)$, where

$$\omega_1 = -\frac{1}{(\mu+\psi)}, \quad \omega_2 = \frac{1}{\psi}, \quad \omega_3 = \frac{1}{(\mu - r\epsilon)}, \quad \omega_4 = \frac{1}{\epsilon}, \quad \omega_5 = \frac{(\mu+\psi+\phi)(x_1^*+\gamma)}{\psi\beta^* x_1^*}, \quad \omega_6 = 0, \tag{4.43}$$

and $x_1^* = \dfrac{\Lambda(1+\eta\bar{V_h})}{\mu}$. The left eigenvalues for $J(E_{\mathcal{R}_0=1})$ are given by $\mathbf{u} = (u_1, u_2, u_3, u_4, u_5, u_6)$ where

$$\begin{aligned} &u_1 = 0, \quad u_2 = \frac{\psi}{(\mu+\epsilon-r\epsilon)(\mu+\psi+\phi)}, \quad u_3 = \frac{1}{(\mu+\epsilon-r\epsilon)}, \quad u_4 = \frac{1}{(\epsilon+\mu)}, \\ &u_5 = \frac{\beta^*\psi x_1^*}{\delta(\gamma+x_1^*)(\mu+\psi+\phi)(\mu+\epsilon-r\epsilon)}, \quad u_6 = 0. \end{aligned} \tag{4.44}$$

The associated bifurcation parameters for model system (4.13) are given by

$$\begin{cases} a &= \displaystyle\sum_{k,i,j=1}^{n} v_k\omega_i\omega_j \frac{\partial^2 f_k}{\partial x_i \partial x_j}(0,0), \\ b &= \displaystyle\sum_{k,i=1}^{n} v_k\omega_i \frac{\partial^2 f_k}{\partial x_i \partial \phi}(0,0). \end{cases} \tag{4.45}$$

Therefore, the non-zero partial derivatives for f_i for $i = 1, 2, ...6$ are given by

$$\frac{\partial^2 f_2}{\partial x_1 x_5} = \frac{\partial^2 f_2}{\partial x_5 x_1} = \frac{\beta^* \gamma}{(\gamma + x_1^*)^2}, \quad \frac{\partial^2 f_2}{\partial x_5 \beta^*} = \frac{\partial^2 f_2}{\partial \beta^* x_5} = \frac{x_1^*}{\gamma + x_1^*} \tag{4.46}$$

Computing the bifurcation coefficients a and b yields

$$a = -\frac{N_2 \mu \psi}{\delta(\mu + \epsilon)(\mu - r\epsilon)(\mu + \psi + \phi)(\mu + \psi)} < 0$$

$$b = \frac{N_2 \mu \psi \Lambda (1 + \eta \bar{V_h})}{\delta(\mu - r\epsilon)(\mu + \epsilon)(\mu + \phi + \psi)\left[\gamma\mu + \Lambda(1 + \eta \bar{V_h})\right]} > 0. \tag{4.47}$$

We state the following theorem

Theorem 27. *Provided that $a < 0$ and $b > 0$, the model system (4.13) will undergo a transcritical bifurcation at $\mathcal{R}_0 = 1$. The bifurcation exhibited is a forward transcritical bifurcation. In such a bifurcation, the exchange of the disease-free and endemic equilibrium states guarantees that the endemic equilibrium point, E_1, is locally asymptotically stable when $\mathcal{R}_0 > 1$ but close to 1.*

Since it can be seen that $a < 0$ and $b > 0$, it is evident that a transcritical bifurcation exists such that there is an exchange in stability when $\mathcal{R}_0^* > 1$ but close to 1. This means that when $\mathcal{R}_0^* \leq 1$, the disease-free equilibrium point is the only extremum that exists and is globally asymptotically stable while when $\mathcal{R}_0^* > 1$ but close to 1, the endemic equilibrium is the only extremum that exists and is locally stable. Therefore the existence of a supercritical bifurcation implies that reducing the reproduction number, $\mathcal{R}_0^*$ to below unity will lead to the elimination of the endemic equilibrium state and give rise to the control of HPV in HIV-infected individuals. □

4.10 Global stability of the CTL-inactive endemic equilibrium point E_1

To prove global stability of the CTL-inactive endemic equilibrium for the co-infection model, we state and prove the following theorem;

Theorem 28. *The CTL-inactive endemic equilibrium point, E_1, is globally asymptotically stable provided that $\mathcal{R}_0^* > 1$, $\mathcal{R}_K^* \leq 1$ and unstable otherwise.*

Proof. To prove the global asymptotic stability of the endemic equilibrium, E_1, we define a Lyapunov function of the form

$$\begin{aligned}\mathcal{W} &= T_s - T_s^e - T_s^e \ln \frac{T_s^e}{T_s} + L - L^e - L^e \ln \frac{L^e}{L} + I_1 - I_1^e - I_1^e \ln \frac{I_1^e}{I_1} + I_2 - I_2^e - I_2^e \ln \frac{I_2^e}{I_2} \\ &+ V - V^e - V^e \ln \frac{V^e}{V} + \frac{\theta}{\sigma} K. \end{aligned} \tag{4.48}$$

Differentiating $\mathcal{W}$ yields

$$\mathcal{W}' = T_s'(1 - \frac{T_s^e}{T_s}) + L'(1 - \frac{L^e}{L}) + I_1'(1 - \frac{I_1^e}{I_1}) + I_2'(1 - \frac{I_2^e}{I_2}) + V'(1 - \frac{V^e}{V}) + \frac{\theta}{\sigma} K'. \tag{4.49}$$

and by substitution of $T_s', L', I_1', I_2', V', K'$ we obtain

$$\begin{aligned}\mathcal{W}' &= \left[\Lambda(1+\eta V_h) + \phi L - \left(\frac{\beta V}{(\gamma + T_s)} + \mu\right) T_s\right] \left(1 - \frac{T_s^e}{T_s}\right) + \left[\frac{\beta V T_s}{(\gamma + T_s)} - (\mu + \psi + \phi) L\right] \\ &\times \left(1 - \frac{L^e}{L}\right) + [\psi L - (\epsilon + \mu + \theta K) I_1] \left(1 - \frac{I_1^e}{I_1}\right) + [\epsilon I_1 + r\epsilon I_2 - (\mu + \theta K) I_2] \left(1 - \frac{I_2^e}{I_2}\right) \\ &+ [N_2 \mu (I_1 + I_2) - \delta V] \left(1 - \frac{V^e}{V}\right) + \frac{\theta}{\sigma} [\sigma I_2 K - \nu K]. \end{aligned}$$

$$\begin{aligned}&= \Lambda(1+\eta V_h) + \phi L - \mu T_s - \frac{\Lambda(1+\eta V_h) T_s^e}{T_s} - \frac{\phi L T_s^e}{T_s} + \frac{\beta V T_s^e}{\gamma + T_s} + \mu T_s^e - (\mu + \psi + \phi) L \\ &- \frac{\beta V T_s L^e}{(\gamma + T_s) L} + (\mu + \psi + \phi) L^e + \psi L - (\epsilon + \mu + \theta K) - \frac{\psi L I_1^e}{I_1} + (\epsilon + \mu + \theta K) I_1^e + \epsilon I_1 + r\epsilon I_2 \\ &- (\mu + \theta K) I_2 - \frac{\epsilon I_1 I_2^e}{I_2} - r\epsilon I_2^e + (\mu + \theta K) I_2^e + N_2 \mu (I_1 + I_2) - \delta V - \frac{N - 2\mu(I_1 + I_2) V^e}{V} + \delta V^e \\ &+ \theta I_2 K - \frac{\theta \nu}{\sigma}. \end{aligned} \tag{4.50}$$

At the endemic equilibrium, we have

$$\begin{cases} \Lambda(1+\eta V_h) = \mu T_s^e + (\mu + \psi) L^e, \\ \dfrac{\beta V T_s^e}{\gamma + T_s^e} = (\mu + \psi + \phi) L^e, \\ \psi L^e = (\epsilon + \mu) I_1^e, \\ \epsilon I_1^e = (\mu - r\epsilon) I_2^e, \\ N_2 \mu (I_1^e + I_2^e) = \delta V^e. \end{cases} \tag{4.51}$$

We further obtain at the endemic equilibrium

$$\begin{aligned}\mathcal{W}' &= \mu T_s^e + (\mu+\psi)L^e + \pi L - \mu T_s - (\mu T_s^e + (\mu+\psi)L^e)\frac{T_s^e}{T_s} - \frac{\phi L T_s^e}{T_s} + \frac{\beta V T_s^e}{\gamma + T_s}\ \mu T_s^e - (\mu+\psi+\phi)L \\ &- \frac{\beta V T_s L^e}{(\gamma+T_s)L} + (\mu+\psi+\phi)L^e + \psi L - (\mu+\epsilon+\theta K)I_1 - \frac{\psi L I_1^e}{I_1} + (\mu+\epsilon+\theta K)I_1^e + \epsilon I_1 + r\epsilon I_2 \\ &- (\mu+\theta K)I_2 - \frac{\epsilon I_1 I_2^e}{I_2} - r\epsilon I_2^e + (\mu+\theta K)I_2^e + N_2\mu(I_1+I_2) - \delta V - \frac{N_2\mu(I_1+I_2)V^e}{V} \\ &+ N_2\mu(I_1^e+I_2^e) + \theta I_2 K - \frac{\theta\nu}{\sigma}. \end{aligned} \tag{4.52}$$

Collecting like terms and simplifying equation (4.52) yields

$$\begin{aligned}\mathcal{W}' &= \mu T_s^e\left[2 - \frac{T_s}{T_s^e} - \frac{T_s^e}{T_s}\right] + \mu L^e\left[2 - \frac{T_s^e}{T_s} - \frac{L}{L^e}\right] + \psi L^e\left[2 - \frac{T_s^e}{T_s} - \frac{L I_1^e}{L^e I_1}\right] \\ &+ \mu I_2^e\left[1 + \frac{I_1^e}{I_2^e} - \frac{I_1}{I_2^e} - \frac{I_2}{I_2^e}\right] + \frac{\beta V T_s^e}{\gamma+T_s}\left[1 - \frac{T_s L^e}{T_s^e L}\right] + \epsilon I_1^e\left[1 - \frac{I_1 I_2^e}{I_1^e I_2}\right] + r\epsilon I_2^e\left[1 - \frac{I_2}{I_2^e}\right] \\ &+ N_2(I_1^e+I_2^e)\left[1 - \frac{V}{V^e}\right] + N_2\mu(I_1+I_2)\left[1 - \frac{V^e}{V}\right] + \theta K\left[I_2^e - \frac{\nu}{\sigma}\right]. \end{aligned} \tag{4.53}$$

Since the arithmetic mean is greater than the geometric mean it follows that

$$2 - \frac{T_s}{T_s^e} - \frac{T_s^e}{T_s} \leq 0, \quad 2 - \frac{T_s^e}{T_s} - \frac{L}{L^e} \leq 0, \quad 2 - \frac{T_s^e}{T_s} - \frac{L I_1^e}{L^e I_1} \leq 0$$

and for the CTL-inactive endemic equilibrium state we have $\mathcal{R}_K^* < 1$ whenever $\mathcal{R}_0 > 1$. Then it means that the condition $(I_2^e - \frac{\nu}{\sigma} \leq 0)$ must be satisfied so that $\mathcal{W}' \leq 0$. We also note that $\mathcal{W}' = 0$ for $T_s = T_s^e,\ L = L^e,\ I_1 = I_1^e,\ I_2 = I_2^e,\ V = V^e$, thus, the largest compact invariant set $\{T_s^e,\ L^e,\ I_1^e,\ I_2^e,\ V^e \in \Omega : \mathcal{W}' = 0\}$, is the singleton $\{E_1\}$. Therefore by LaSalle's invariance principle [50], the CTL-inactive endemic equilibrium is globally asymptotically stable provided that $\mathcal{R}_0^* > 1$ and $\mathcal{R}_K^* < 1$. This completes the proof. □

Stability analysis of the CTL-active equilibrium, E_2, will be demonstrated using numerical simulations.

4.11 Model extension

This work aims to model the dynamics of HIV/HPV co-infection in the presence of intervention measures such as Combined Antiretroviral Therapy (cART) and HPV vaccination. The effect of HPV vaccination in HIV-positive women remains an interesting area of research that has little supporting data. HIV reduces the effectiveness of most vaccines and the HPV vaccine is

among the list of such vaccines. Normally the initiation of cART/HAART in HIV-positive patients clears or reduces opportunistic infections that arise due to HIV infection. cART/HAART has a marginally positive effect on the well-being of infected persons if administered early and meticulously. Shretha *et al.* in a clinical trial established that cART/HAART does not have an immediate effect on the reduction of HPV infections in 100 naive HIV-positive adolescents [87], Fife *et al.* in a similar study also observed the effects of cART/HAART on HPV in HIV naive patients over a period of 24 months and established that prevalence of high-risk HPV decreased from 62% to 39% [30]. Other researches of similar nature that support the reduction of HPV through long adherence to cART/HAART include that of Minkoff *et al.*[61], Adler *et al.* [1] and Konopnicki *et al.* [48]. It has also been established through clinical trials that the HPV vaccine favours HIV-positive women with low viral loads less than 50 copies/ml [48]. It is therefore recommended that HIV-positive women who intend to take the HPV vaccine should try to reduce their HIV viral load first through strict adherence to cART.

Lacey in his work on HPV vaccination in HIV infected individuals, reiterates that HIV reduces the effectiveness of the HPV vaccine while he proposes that more clinical trials need to be done to ascertain the effectiveness of the HPV vaccine within HIV-positive women [51]. We therefore, propose the following model extension that incorporates the role of cART/HAART and the HPV vaccine in the reduction of HPV in women. The model takes into account the inhibition effect of cART/HAART through the reverse transcriptase and protease inhibitors and also the effect of the inhibition through the HPV vaccine. We extend the model by Verma *et al.* [99] to include the effects of HIV in the latently infected cells and the effects of the inhibition of the HPV vaccine. These are effects that Verma *et al.* did not include in their model. We therefore, introduce constant HIV treatment through the reverse transcriptase inhibitor (RTI) parameter given by ε_R which is responsible for inhibiting the contact of an infected cell and a susceptible healthy cell. It also inhibits the contact between HIV and a susceptible healthy cells. The protease inhibitor (PI) given by ε_P, is responsible for preventing the bursting of an infected cell or the production of virions. In the model, ε_R and ε_P are the drug efficacies that come as a result of cART/HAART. We introduce the effects of the RTIs by converting the term $\kappa V_h T_h$ to $(1-\varepsilon_R)\kappa V_h T_h$ where $\varepsilon_R = 0$ indicates no treatment effect and $\varepsilon_R = 1$ indicates that the reverse transcriptase inhibitor has 100% efficacy. The PIs are introduced into the model by converting the term $N_1 d_3 I_h$ to $N_1 d_3 (1-\varepsilon_P) I_h$, where $\varepsilon_P = 0$ indicates no treatment effect and $\varepsilon_P = 1$ indicates that the protease inhibitor has 100% efficacy. Inhibition as a result of the HPV vaccine Gardasil is modelled using the parameter, ϵ_I. As stated earlier the HPV vaccine

does not clear existing infections but blocks new infections from occurring. Thus, the term $\frac{\beta V T_s}{\gamma + T_s}$ is converted to $\frac{(1-\epsilon_I)\beta V T_s}{\gamma + T_s}$. The extended model is given below;

$$\begin{aligned}
T_h'(t) &= s - (1-\varepsilon_R)\kappa V_h T_h - d_1 T_h, \\
L_h'(t) &= \rho(1-\varepsilon_R)\kappa V_h T_h - (\zeta + d_2) L_h, \\
I_h'(t) &= (1-\rho)(1-\varepsilon_R)\kappa V_h T_h + \zeta L_h - d_3 I_h, \\
V_h'(t) &= N_1 d_3 (1-\varepsilon_P) I_h - c V_h, \\
T_s'(t) &= \Lambda(1+\eta \bar{V_h}) + \phi L - \left(\frac{(1-\epsilon_I)\beta V}{\gamma + T_s} + \mu \right) T_s, \\
L'(t) &= \frac{(1-\epsilon_I)\beta V T_s}{\gamma + T_s} - (\mu + \psi + \phi) L, \\
I_1'(t) &= \psi L - (\epsilon + \mu + \theta K) I_1, \\
I_2' &= \epsilon I_1 + r\epsilon I_2 - (\mu + \theta K) I_2, \\
V'(t) &= N_2 \mu (I_1 + I_2) - \delta V, \\
K'(t) &= \sigma I_2 K - \nu K.
\end{aligned} \tag{4.54}$$

The control/effective reproduction number for model system (4.54) is given by

$$\mathcal{R}_T = \frac{\beta(1-\epsilon_I)(1-\epsilon_R)(1-\epsilon_P) N_2 \mu \psi \Lambda (1+\eta \bar{V_h})(\mu + \epsilon - r\epsilon)}{\delta(\mu - r\epsilon)(\mu + \epsilon)(\mu + \psi + \phi)\left[\Lambda(1+\eta \bar{V_h}) + \gamma\mu\right]}. \tag{4.55}$$

4.12 Numerical Simulations

The simulations presented consider the impact of vaccination of girls and women who are living with HIV and undergoing cART/HAART. McClymont *et al.* [57] in their clinical trial looked at the effects of vaccination on girls and women living with HIV and compared the results with those of women living with HIV who had not been vaccinated. The clinical trial enrolled 479 participants of which only 279 participants were eligible for the study. These eligible participants were given more than one dose of the quadrivalent vaccine Gardasil. The study had 41.9%

black participants, 36.2% white participants and 21.9% were participants from other races. The participants had on average six (6) lifetime sexual partners and the average number of years since diagnosis with HIV was found to be eight (8). The initial CD4+ T-cell count at the start of the study was found to be 500 cells/mm^3 while the HIV viral load suppression was less than 50 copies/ml. Only 10 participants had not started cART/HAART at the time of the clinical trial while the rest were either on some regimen or had defaulted. 266 participants received three doses of the vaccine, 7 received only two doses while 6 received only one dose. The results obtained indicated that breakthrough infections were high among participants who originally had high-risk HPV upon enrolment, followed by those who did not have high-risk HPV at enrolment. These participants had received only one dose of the vaccine and had one follow-up done throughout the study. It was also established that, though there were breakthrough infections among those who had received three doses of the vaccine, these were lower than those who had received one or two doses of the vaccine. So the study concluded that vaccine failure was higher among women living with HIV as compared to those without HIV. However, vaccination also proved beneficial in the reduction of the rate of acquisition of new HPV infections.

There are also other follow up clinical trials that support the benefits of vaccination in women living with HIV given by [51, 57, 58]. We present numerical simulations that model the dynamics of HPV in the presence of vaccination for women living with HIV. The numerical simulations for the co-infection model will make use of the parameters sourced from literature in Table 4.2. We make use of initial HIV concentrations as follows: $\bar{T_h} = 5 \times 10^5$ cells/ml [58], $\bar{L_h} = 237.62$ cells/ml (calculated), $\bar{I_h} = 1.04 \times 10^3$ cells/ml (calculated), $\bar{V_h} = 4.8 \times 10^4$ cells/ml [99], $\kappa = 5 \times 10^{-8}$ virions per day (calculated) and $s = 6.2 \times 10^3$ cells/ml/day (calculated), where

$$\bar{L_h} = \frac{\rho\kappa\bar{V_h}\bar{T_h}}{\zeta + d_2}, \quad \bar{I_h} = \frac{c\bar{V_h}}{N_1 d_3}, \quad \kappa = \frac{c(\zeta + d_2)}{\bar{T_h} N_1 \left[\zeta + d_2(1-\rho)\right]}, \quad s = (\kappa\bar{V_h} + d_1)\bar{T_h} \tag{4.56}$$

We present simulations that show the stability of the disease-free and endemic equilibrium points for varying reproduction number values. We compare two scenarios, in the presence of HIV (i.e there is the action of *tat* protein, $\eta > 0$ which means an increase in the susceptibility of the epithelial cells within the genital mucosa) and in the absence of HIV (i.e there is no effect of tat protein, $\eta = 0$.)

Table 4.2: Table of parameters for the HIV/HPV co-infection model.

Parameter	**Value**	**Description**	Source
s	6.2×10^3/ml/day	Recruitment rate of infected $CD4^+$ target cells.	Calculated
κ	5×10^{-8} /ml/ day	HIV transmission rate.	Calculated
d_1, d_2, d_3	[0.03,0.001,1]/ml/ day	Natural death rate of susceptible, latently infected and infected target cells.	[105],[99]
ζ	0.1 per ml per day	Progression rate of latently infected cells to the actively infected class.	[105]
ρ	0.02 per ml per day	Proportion of infections that result in latent infections where $0 \leq \rho \leq 1$.	[105]
N_1	[1000-1250]/ml/day	Burst size of an HIV cell.	[105], [99]
c	[20-23]/ml/day	Natural death rate of the HIV virus.	[105], [99],[99]
η	varied	*tat* protein effect	varied
Λ	36000 cells/ml/day	$CD4^+$ Epithelial cell recruitment rate	[63]
β	0.0067 virions per day	HPV infection rate.	[99]
δ	0.05 cells per day	Virion death rate.	Est.
μ	0.048 per day	Cells death rate.	[64]
N_2	1000 virions per cell	HPV burst size.	[99]
θ	0.01 per day	HPV clearance rate.	[90]
γ	10^6	Epithelial cell concentration for infection half maximal.	[64]
ψ	0.03	Mature rate of latently infected cells.	[40]
σ	0.001 cells per ml	CTL expansion rate.	Est.
ν	0.5 cells per ml	CTL death rate.	Est.
ϵ	varied between $[0-1]$	Oncogene expression.	[64]
r	0.01	Transit amplifying cells recruitment rate.	[64]
ϕ	0.6	Natural clearance of HPV as a result of healing of cells.	[40]
ϵ_I	varied	HPV vaccine inhibition rate	varied
η_P	varied	Protease inhibition rate	varied
η_R	varied	Reverse transcriptase inhibition rate	varied

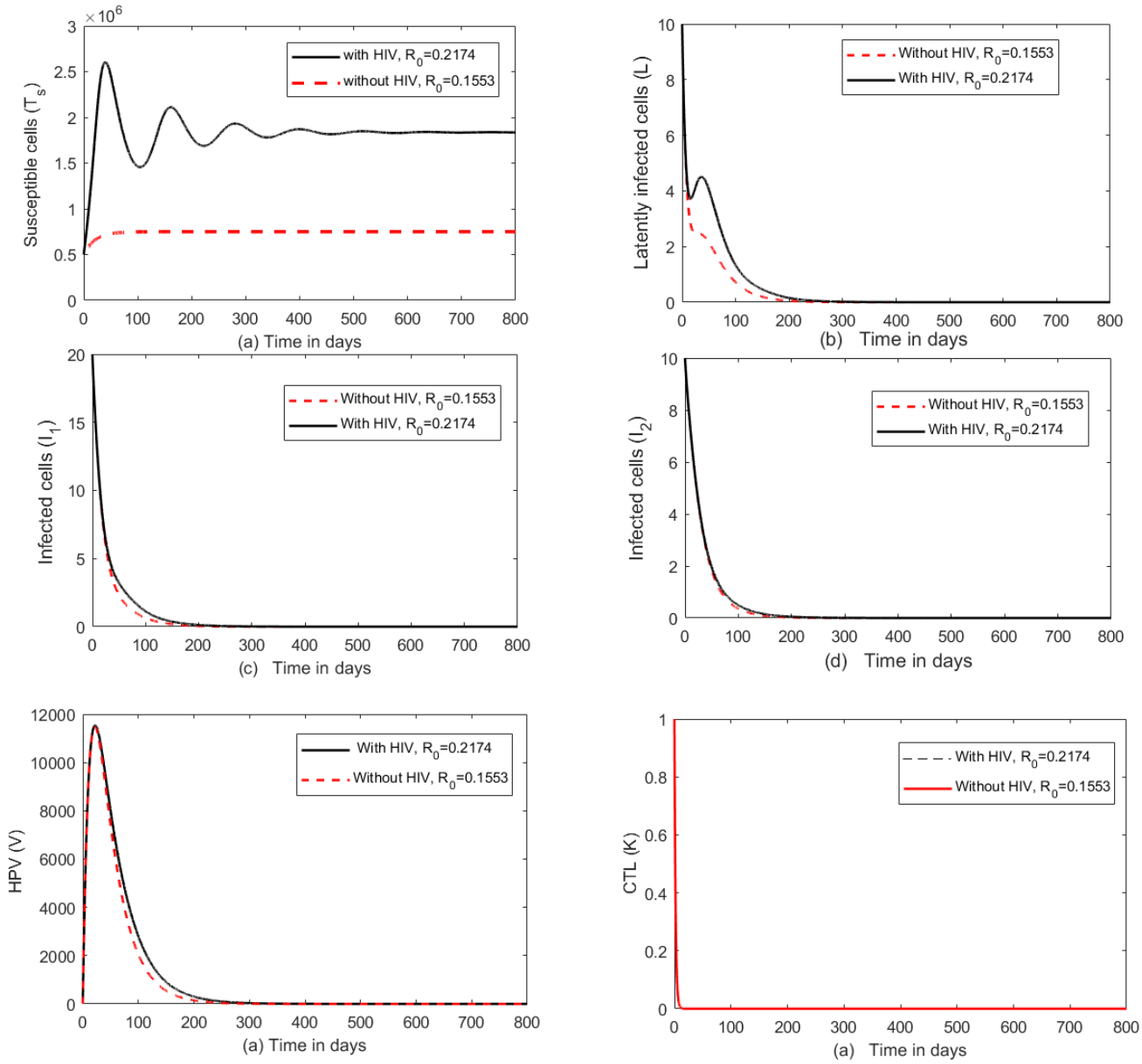

Figure 4.4: Dynamics of HIV/HPV co-infection model (4.13), showing the stability of the disease-free equilibrium for $\mathcal{R}_0 = 0.1553 < 1$, (without HIV) and $\mathcal{R}_0 = 0.2174 < 1$ (with HIV), where 'without HIV' is for $\eta = 0$ and"with HIV" is for $\eta = 2.0833 \times 10^{-5}$ and with $\beta = 0.00067$, $\sigma = 0.00001$, $\epsilon = 0.01$ and all other parameters are as in Table 4.2. Initial conditions used are $T_s(0) = 500000$, $L(0) = 100$, $I_1(0) = 200$, $I_2(0) = 100$, $V(0) = 100$, $K(0) = 1$.

The simulations in Figure 4.4 support the theoretical work presented such that when $\mathcal{R}_0 < 1$ the model approaches the disease-free equilibrium despite the introduction of HPV for the cases "without HIV" and "with HIV" . The model approaches the equilibrium points $E_0 = (1.837 \times 10^6, 0, 0, 0, 0, 0)$ for, $\eta > 0$ and $E_0 = (7.5 \times 10^5, 0, 0, 0, 0, 0)$ for, $\eta = 0$. Figure 4.4 also shows that in the presence of *tat* protein ($\eta > 0$) we have more susceptible cells , more latently infected cells, more infected cells that progress into self-proliferating cells and also more of

the virus as compared to the case where there is no *tat* protein ($\eta = 0$). The CTL-inactive endemic equilibrium is presented in Figure 4.5. It can be seen that for $\mathcal{R}_0 = 22.3414 > 1$ and $\mathcal{R}_K^* = 0.1957 < 1$, the model approaches the first endemic equilibrium given by $E_1 = (2.765 \times 10^5, 1, 114 \times 10^6, 5.76 \times 10^5, 1.20 \times 10^5, 6.68 \times 10^8, 0)$. The results support the theoretical work that the CTL-inactive endemic equilibrium is globally asymptotically stable provided that $\mathcal{R}_0 > 1$ and $\mathcal{R}_K^* < 1$. The stability dynamics of the CTL-active equilibrium are presented in

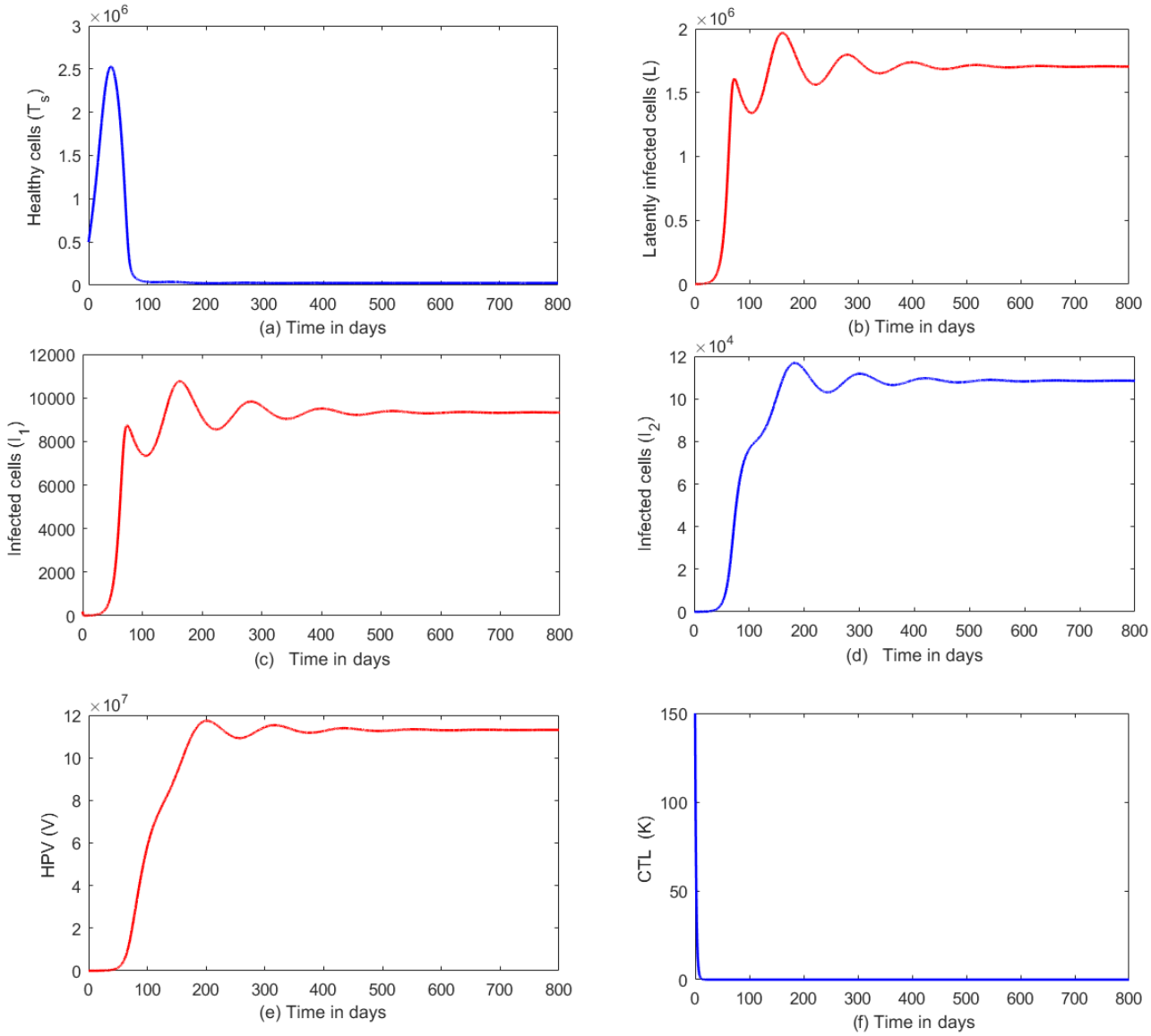

Figure 4.5: Dynamics of HIV/HPV co-infection model (4.13), showing the stability of the CTL-inactive endemic equilibrium point, E_1, for $\mathcal{R}_0 = 22.3414 > 1$ and $\mathcal{R}_K^* = 0.1957 < 1$ and with $\beta = 0.067,\ \sigma = 0.000001,\ \eta = 2.0833E-5$ and all other parameters are as in Table 4.2. Initial conditions are $T_s(0) = 500000,\ L(0) = 100,\ I_1(0) = 200,\ I_2(0) = 100,\ V(0) = 100,\ K(0) = 150$.

Figure 4.6. The simulations clearly support the theoretical work that the endemic equilibrium

E_2 is globally stable provided that $\mathcal{R}_0 > 1$ and $\mathcal{R}_K^* > 1$. The simulations also indicate that within the period (0-100) days there is a delay in the blocking of new infections by the immune response. So, we see an increase in the I_2 cells and HPV within the period. Thereafter a decline in the infected cells is observed after 100 days, as immune response is activated and begins to dock and kill the infected cells. The simulation dynamics approach the equilibrium point $E_2 = (3.45 \times 10^5, 1.403 \times 10^6, 4433, 5000, 9.064 \times 10^6, 40.3)$.

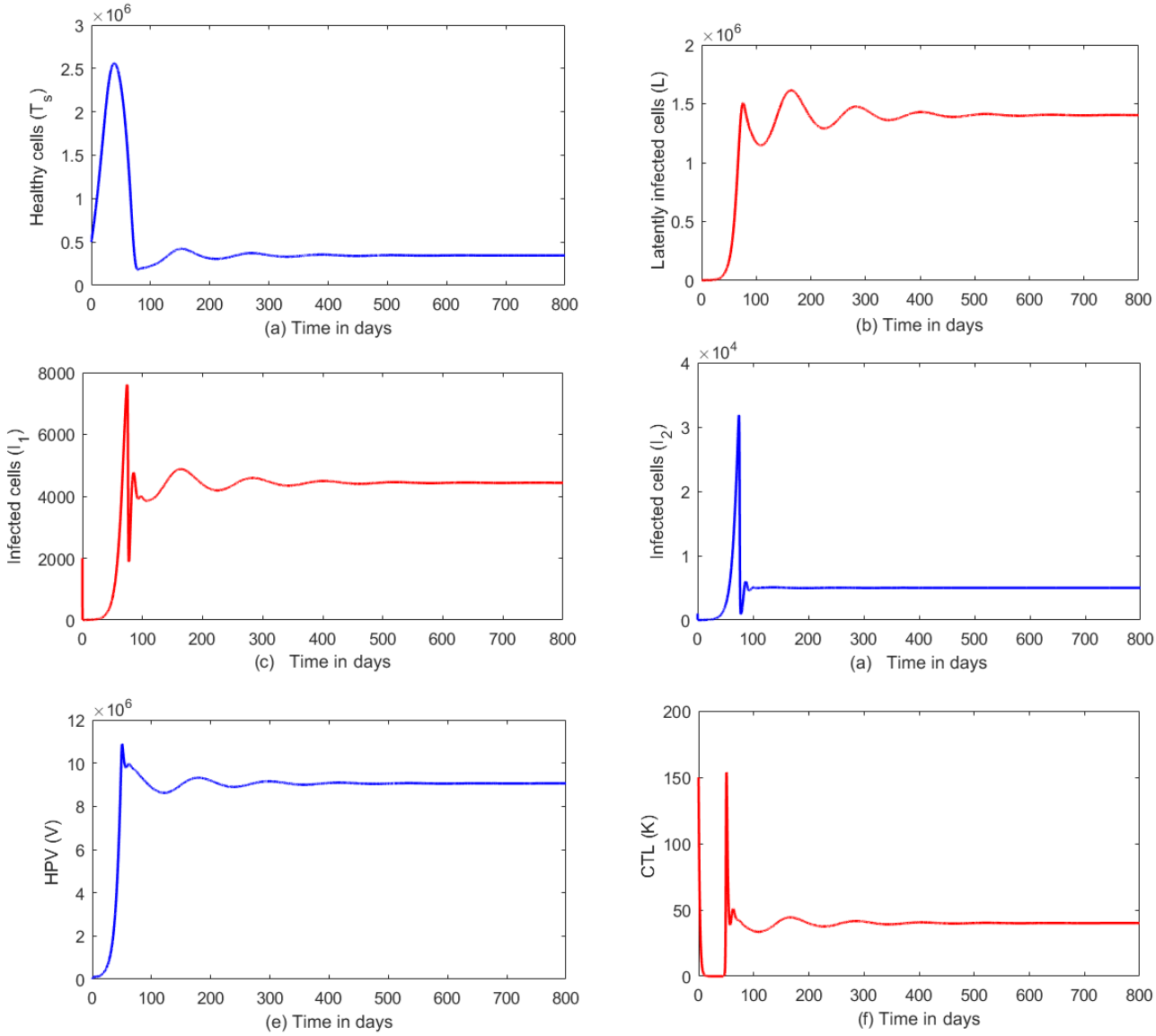

Figure 4.6: Dynamics of HIV/HPV co-infection model (4.13), showing the stability of the CTL-active endemic equilibrium, E_1, for $\mathcal{R}_0 = 24.0351 > 1$ and $\mathcal{R}_K^* = 17.6668 > 1$ and with $\beta = 0.0067$, $\sigma = 0.00001$, $\eta = 2.0833E - 5$ and all other parameters are as in Table 4.2. Initial conditions are $T_s(0) = 500000$, $L(0) = 1000$, $I_1(0) = 2000$, $I_2(0) = 1000$, $V(0) = 1000$, $K(0) = 150$.

4.12.1 Simulating the effects of vaccination on the dynamics of HPV/HIV co-infection

We further simulate the effect of HIV on HPV in the presence of vaccination. The main assumption is that *tat* protein has a doubling effect on the susceptibility of epithelial cells as indicated by the work by [99]. Therefore in all our simulations, we consider the cases $\eta\bar{V_h} = 0$ (there is not *tat* protein effect) and $\eta\bar{V_h} = 1$ (there is *tat* protein effect). The first set of simulations in (Figure 4.7(a-e)) compare the following cases:

1. The case where there is HIV/HPV co-infection and no vaccination (i.e $\eta\bar{V_h} = 1$ and $\epsilon_I = 0$).

2. The case where there is HIV/HPV co-infection and vaccination (i.e $\eta\bar{V_h} = 1$ and $\epsilon_I = 0.90$).

It is observed from the simulations that vaccination is beneficial in blocking new HPV infections even in the presence of HIV. There is a significant increase in susceptible cells and a decline in the infected cells and the virus when the vaccine is 90% efficacious. The effects of *tat* protein are evidently seen in the simulation because *tat* protein increases susceptibility of epithelial cells as mentioned in literature. Figure 4.7 supports that HIV promotes the persistence of HPV as a result of immune suppression. The infected cell dynamics indicate that for the HPV/HIV model the absence of vaccination evidently increases the number of infected cells I_1 (blue dashed line) while the presence of vaccination results in a sharp reduction in I_1 cells (red dashed line). However, we notice that the I_1 cells do not approach the disease-free equilibrium because $\mathcal{R}_0 > 1$ and the HPV vaccine does not clear existing infections as indicated in literature.

The transit amplifying cells, I_2, follow the behaviour of the I_1 cells because they are formed through the proliferation of I_1 cells. So, in Figure 4.7(d) we observe that when there is HPV/HIV co-infection in the absence of vaccination, we have more I_2 cells because there is increased self proliferation of cells due to immune suppression. When vaccination is introduced we see a reduction of these cells. It is observed that vaccination is beneficial in the reduction of new infections. The I_2 cells approach some endemic equilibrium value eventually.

The dynamics of HPV in the presence of HIV is analysed in Figure 4.7 (e). It is observed that in the absence of vaccination we have a sharp rise in HPV within the system due to a production of more I_1 and I_2 cells as indicated by Figures 4.7(c) and (d). The results support

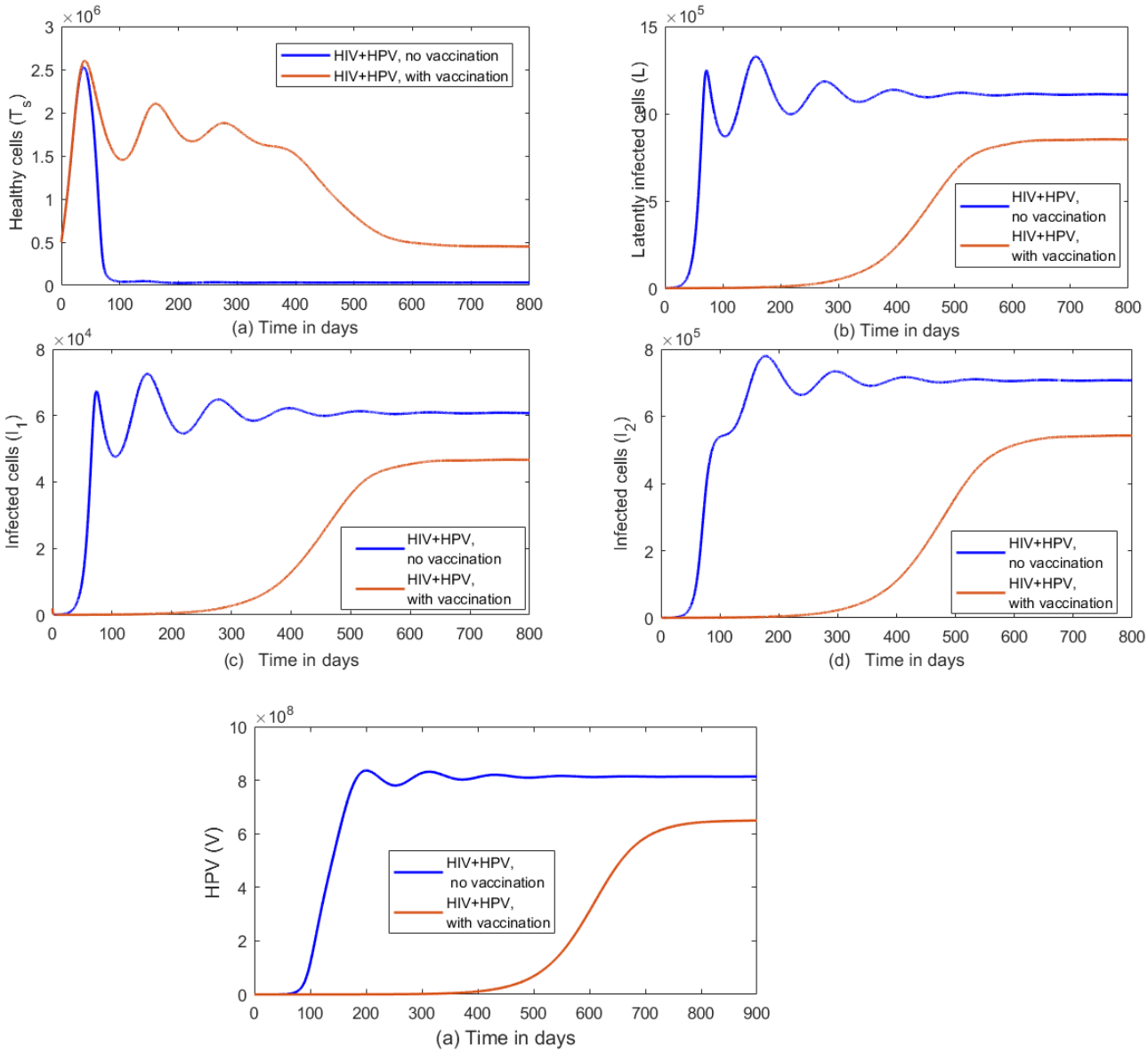

Figure 4.7: Effects of vaccination on the HPV/HIV co-infection model (4.13) , for the cases (i) $\eta\bar{V_h} = 1, \epsilon_I = 0$, (ii) $\eta\bar{V_h} = 1, \epsilon_I = 0.90$, where $\mathcal{R}_0 > 1$ and $\mathcal{R}_K^* < 1$ and all other parameters are taken from Table 4.2. The initial conditions are $T_s(0) = 1000,\ L(0) = 100, I_1(0) = 200,\ I_2(0) = 100,\ V(0) = 100, K(0) = 150$.

that in the absence of vaccination HIV increases the chances of HPV viral burst and hence a high viral load is observed. These dynamics change when vaccination is introduced into the system as we see a distinct decline in HPV produced. For all simulations, we assume that $t = 0$ is the start of the vaccination. The simulations presented in Figure 4.7 help us to recommend vaccination of women and girls living with HIV as a measure to reduce the high-risk HPV burden as supported by literature. The only problem noted is that there is a need to use a

vaccine that blocks a wide range of high-risk and low-risk types of HPV as this might be the only factor that can cause vaccine failure.

From the clinical trial done by Konopnicki *et al.*, it was observed that the occurrence of high-risk HPV in HIV-positive women decreased with an increase in the CD4+ T-cell count [48]. The main possible reason for this was that the higher the CD4+ T-cell count, the healthier an HIV-infected individual is. Also HPV need T-cells for B-cellactivation and anti-HPV antibody production. According to HIV.org a healthy individual should have a CD4+ T-cell count within the ranges of > 500 cells/μl, a chronic HIV patient has a CD4+ T cell count within the ranges of $< 500 - > 200$ cells/μl and an AIDS patient has a CD4+ T-cell count of < 200 cells/μl [96]. We use the data from the study by Konopnicki *et al.* to analyse, using the mathematical model, the dynamics of HIV/HPV co-infection as the CD4+ T-cell count increases. We assume that the healthy CD4+ T-cell count for the model is 8×10^5 cells/ml, the chronic HIV stages are 4×10^5 cells/ml and 2.5×10^5 cells/ml respectively and the chronic AIDS stage is 10^5 cells/ml. The major assumption is that for the case where the CD4+ T cell count is > 500 cells/μl, we assume that $\eta \bar{V_h} = 0$, [99] because of the assumption that *tat* protein does not affect this stage. All stages where the CD4+ T-cell count is such that < 500 cells/μl we consider the action of *tat* protein to be such that $\eta \bar{V_h} = 1$. The simulation dynamics are presented in Figure 4.8.

In Figure 4.8(a), we notice a rise in the number of I_1 cells with a decrease in CD4+ T-cell count for the first 50 days. Figure 4.8(b) supports the dynamics of Figure 4.8(a) since a rise in the number of I_1 cells as the CD4+ T-cell count decreases, also exacerbates the production of I_2 cells. Figure 4.8 (c) shows the dynamics of HPV with changes in the CD4+ T cell count and the results indicate that, as the CD4+ T cell count increases, the HPV viral production decreases. This can indicate that the healthier an HIV-infected individual is, the more the action of the immune response against infections such as HPV. A distinct reduction in HPV viral production is seen when the CD4+ T cell count is above 500 cells/μl. The effect of immune response is also simulated and it is observed that, during the first 50 days, there is a delay in the immune response due to probable immune evasion and because of this, we see a sharp rise in infected cells and the HPV viral load in Figures 4.8(a-c). After 50 days the immune response is activated, we notice a gradual reduction in the infected cells till they reach an equilibrium value. The immune response is also influenced by the changes in the CD4+ T-cell counts, the higher the CD4+ T-cell count the lower the immune response because there are fewer HPV cells to trigger faster immune response.

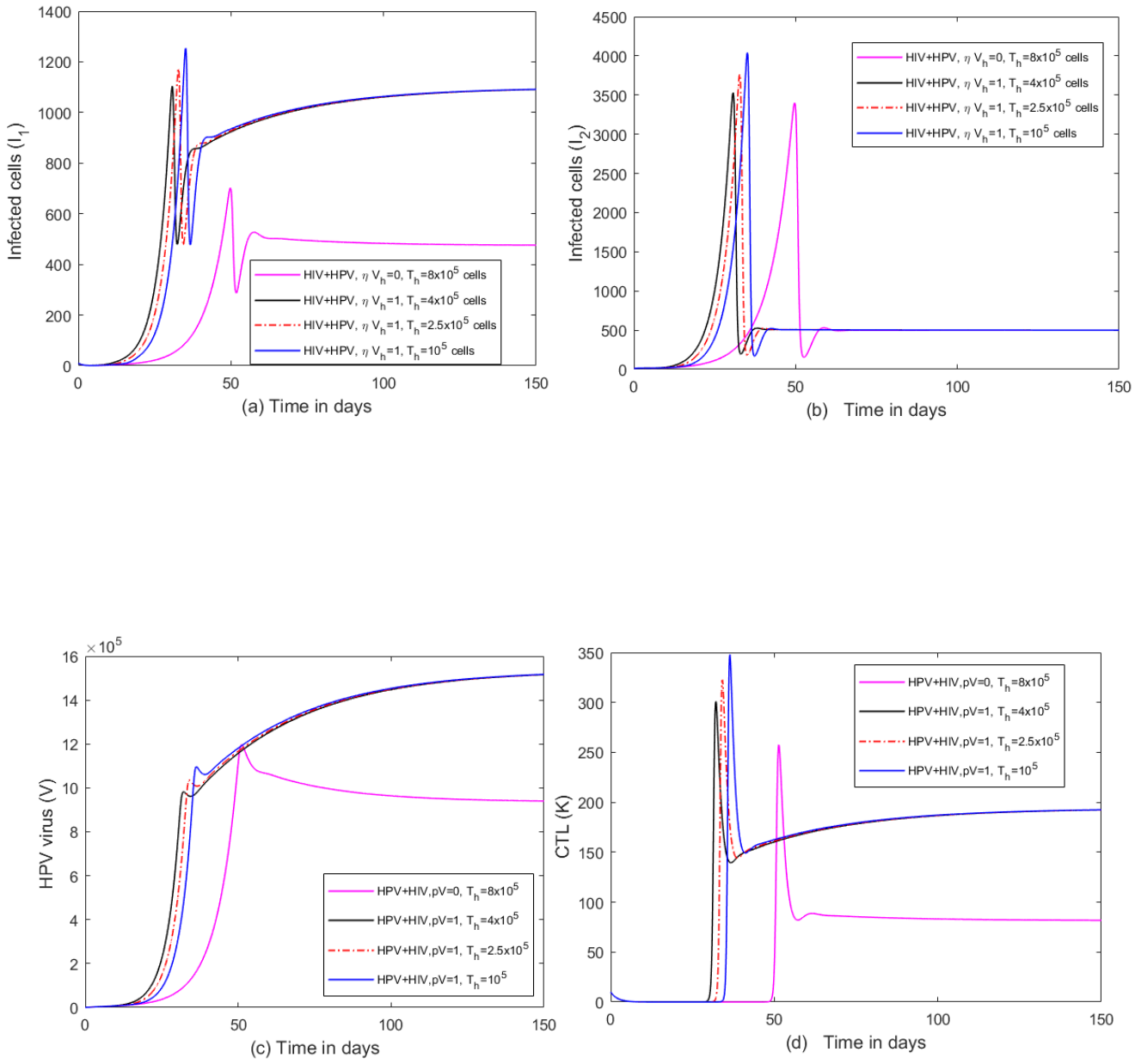

Figure 4.8: Dynamics of HPV/HIV co-infection model (4.13), for the cases (i) $T_h = 8 \times 10^5,\ \eta\bar{V_h} = 0$, (ii) $T_h = 4 \times 10^5,\ \eta\bar{V_h} = 1$ (iii) $T_h = 2.5 \times 10^5,\ \eta\bar{V_h} = 1$ (iv)$T_h = 10^5,\ \eta\bar{V_h} = 1$ with $\mathcal{R}_0 > 1$ and all other parameters are taken from Table 4.2.

4.12.2 Modelling the effects of cART on HIV/HPV co-infection

The dynamics of introducing cART to the model are simulated. The main assumption made is that all individuals are adherent to cART. This because adherence is important in the reduction of HPV infection in HIV-positive women. Minkoff *et al.* in their work looked at the effects of adherence to cART on the reduction of oncongenic HPV. The study enrolled 286 individuals and considered adherence as following cART above 95% [61].

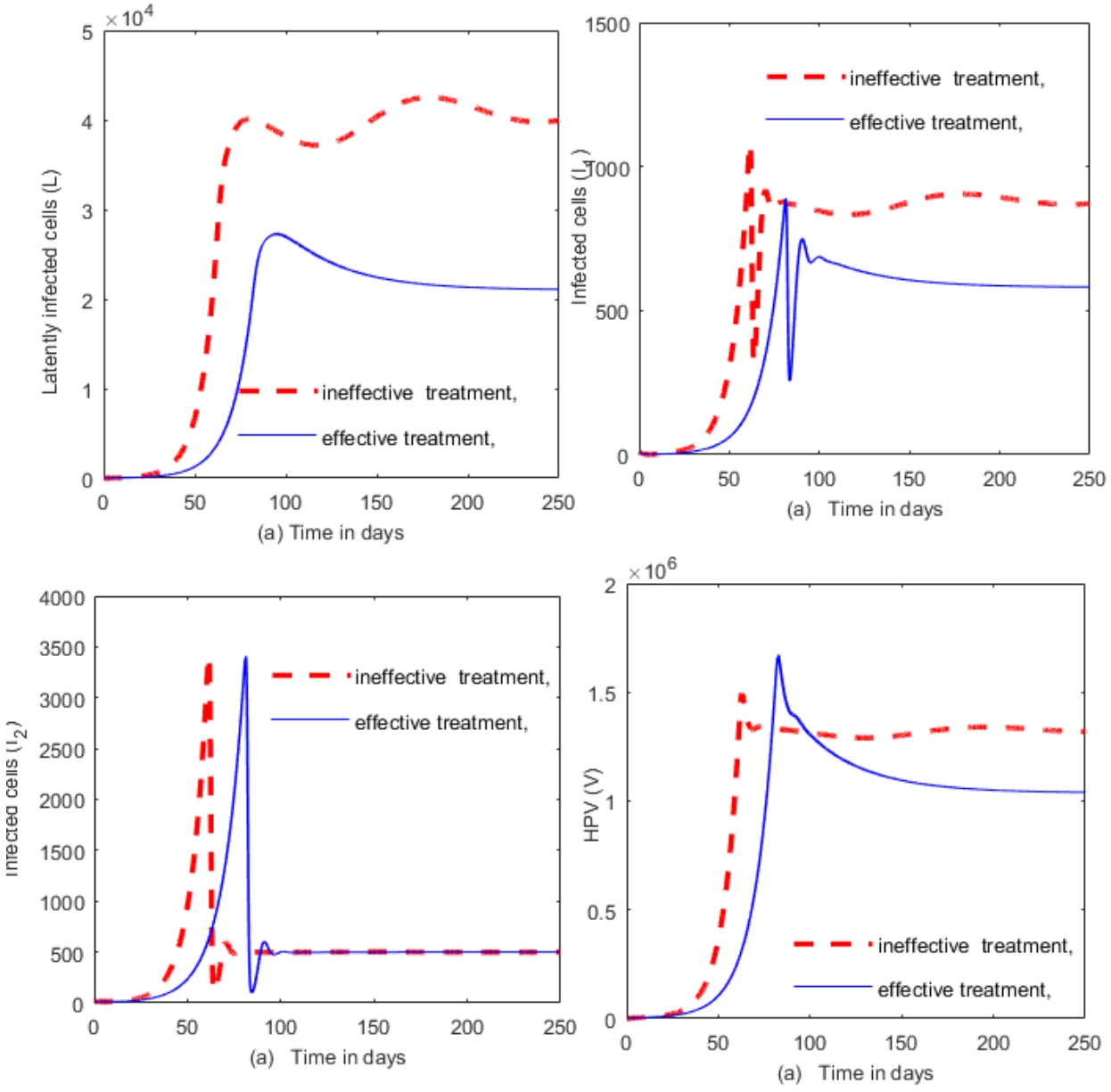

Figure 4.9: Dynamics of HIV/HPV co-infection model (4.13) in the presence of cART with parameters from Table 4.2 and with "ineffective cART" with efficacies $\varepsilon_P = 0,\ \varepsilon_R = 0.01$ and "effective cART" with efficacies $\varepsilon_P = 0.5,\ \varepsilon_R = 0.95$.

The study also looked at the effectiveness of the cART regiments and therefore classified treat-

ment as "effective cART" and "ineffective cART". The results the study showed that strict effective adherence to cART reduced the HPV prevalence in women from 20% before cART to 14% after the start of cART. It was also observed that ineffective cART had an increase in HPV prevalence from 22% before cART initiation to 24% after initiation. Therefore, the study concluded that only effective and adherent cART resulted in the reduction of HPV prevalence in HIV-positive women [61]. Verma *et al.* further quantified "effectiveness" through setting parameter values for the efficacy of HIV treatment at $\epsilon_{PI} = 0$, $\epsilon_{RT} = 0.2$ for "ineffective cART" and $\epsilon_{PI} = 0.5$, $\epsilon_{RT} = 0.95$ for "effective" cART [99]. The results of this particular study validated the results by Minkoff *et al.* that cART helps in the reduction of HPV. Based on this we model the effects of HPV/HIV co-infection in the presence of cART assuming that individuals adhere to treatment[99]. The present model (4.13), presents the effects of latently infected cells on the dynamics of HPV. Figure 4.9 presents the model dynamics for the infected classes and HPV class in the presence of cART. The simulations are done for two cases: case 1, "ineffective case" ($\varepsilon_P = 0, \varepsilon_R = 0.01$) and case 2 "effective case" ($\varepsilon_P = 0.5, \varepsilon_R = 0.95$). The simulations indicate that cART with adherence can reduce HPV prevalence significantly. This motivates us to recommend the education of HIV-positive women and girls on the effects of adherence to cART, in relation to the reduction of sexually transmitted infections such as HPV.

4.12.3 Discussion and conclusion on the chapter

In this chapter we formulated an HPV/HIV co-infection model adopted from the work by Verma *et al.* [99]. The model looked at the effects of including the latent HIV and HPV classes. We believe that the results presented are a better representation of the real situation. The local and global stability analysis of the disease-free and endemic equilibrium points was presented and analysed in depth. The model also exhibited two endemic equilibrium points, E_1 and E_2. The first endemic equilibrium point, E_1, represented the case where the immune response was inactive and the second equilibrium point, E_2, endemic equilibrium point represented the case where the immune response was active. The local and global stability of the equilibrium points was analysed and the conditions for stability and instability were established. It was established that the stability of the equilibrium states was dependent on the reproduction number $\mathcal{R}_0$ and the immune response reproduction number $\mathcal{R}_K^*$. Bifurcation analysis for the model was carried out and it was established that the model exhibits a forward bifurcation whenever $\mathcal{R}_0 > 1$ but close to 1. Sensitivity analysis using the normalized forward sensitivity index approach and the PRCC approach was carried out to establish parameters that affect $\mathcal{R}_0$ and the results obtained

indicated that parameters such as the transmission rate, β, had a positive correlation with $\mathcal{R}_0$. Increasing the transmission rate meant an increase in $\mathcal{R}_0$. Numerical simulations carried out modelled the dynamics of HIV/HPV co-infection in the presence of vaccination only and then in the presence of cART/HAART. Results obtained indicated that anti-HPV vaccination of HIV-infected individuals is beneficial in the reduction of the prevalence of HPV cases provided that the efficacy of the vaccine is above 60%. Results also indicated that cART/HAART was beneficial in the reduction of HPV infection, provided that there was treatment adherence.

Chapter 5

Conclusion and recommendations

5.1 Conclusion

In this thesis, we used mathematical models to investigate the dynamics of HPV in the presence of latent infection and immune response. Chapter one presented the general background to the problem and our objectives for the study. It also gave a brief description of the virology of HPV and the classifications of HPV. In chapter 2, we reviewed the basic model formulated by Verma *et al.* [99] and from the review, we were able to formulate the HPV basic model with adjustments and improvements. The basic HPV model formulated in chapter 3 incorporated latency and immune response. The model was effectively analysed and it was established that there were three equilibrium points of interest, that is the disease-free equilibrium, the CTL-inactive equilibrium and the CTL-active equilibrium. It was also established two two associated reproduction numbers: the basic reproduction number, $\mathcal{R}_0$ and the CTL-reproduction number, $\mathcal{R}_K$, where the latter represented the number of infected cells each immune response cell can address. The conditions for stability of the disease-free and endemic equilibrium were stated based on $\mathcal{R}_0$ and $\mathcal{R}_K$. The local stability of the disease-free equilibrium was established using the Routh Hurwitz criterion method. Bifurcation analysis using the Center Manifold theory was carried out and it was established that the model exhibited a forward transcritical bifurcation indicating that the CTL-inactive endemic equilibrium was locally asymptotically stable provided that $\mathcal{R}_0 > 1,\ \mathcal{R}_K < 1$. We formulated suitable Lyapunov functions to prove the global stability of the two endemic equilibrium points. Sensitivity analysis for parameters that affect $\mathcal{R}_0$ was done using the PRCC method by [35] and Tornado plots and the results indicated that the transmission rate, β and the mature rate of latently infected cells, ψ, had a significant effect on the reproduction number, $\mathcal{R}_0$. Reduction of these parameters significantly reduced $\mathcal{R}_0$.

Numerical simulations presented supported the theoretical work presented. Parameter values used were sourced from literature.

In numerical simulations, we considered the effects of oncogene expression on the dynamics of HPV and established that, the higher the oncogene expression the higher the amplification of infected cells into self-proliferating cells, and, consequently, the higher the production of HPV. The simulations indicated that, though reduction of oncogene expression is key in the reduction of infection, it is not sufficient. Due to this, we extended the model to incorporate vaccination. The results of simulations from the vaccination model indicated that vaccination is beneficial in the reduction of infections, especially if the efficacy of the vaccine is above 60% as indicated by the contour plots presented. However, the most ideal efficacy of the vaccine that gave a total clearance of infection was above 90%, as indicated by the simulations presented.

Chapter 4 presented the dynamics of HPV in the presence of HIV. A lot of clinical studies have been carried out looking at these dynamics. We presented the co-infection model based on the work by Verma *et al.*. A preliminary analysis of the model was done. The reproduction numbers for the model were the co-infection basic reproduction number, $\mathcal{R}_0$ and the CTL-reproduction number $\mathcal{R}_K^*$. The model also exhibited three equilibrium points, that is, the disease-free equilibrium, the CTL-inactive endemic equilibrium and the CTL-active endemic equilibrium. The conditions for stability of these three equilibrium points based on $\mathcal{R}_0$ and $\mathcal{R}_K^*$ analysed and established. Bifurcation analysis indicated that there exists a forward transcritical bifurcation indicating that the CTL-inactive endemic equilibrium point, E_1, was locally asymptotically stable whenever $\mathcal{R}_0 >$ but close to 1. The numerical simulations used parameters from literature especially those from the clinical trials conducted on the HIV/HPV subject matter. We established that HIV does have an effect on an increase in the transmission dynamics of HPV due to the effect of *tat* protein supporting the work by Verma *et al.* [99]. However, vaccination was shown to be beneficial in the reduction of HPV infection in HIV-infected women provided that it was above 90% efficacious. We also simulated the dynamics of the co-infection model in the presence of antiretroviral therapy (HAART) and the results from the simulation indicated that HAART is beneficial in the reduction of HPV infections provided that there is adherence and the healthy CD4+ T-cell count is high.

In general, the study established that while immune response is important in the eradication of infections, it is not sufficient in the elimination and control of infections such as HPV.

Other intervention methods need to be taken up to boost or complement the function of the immune system. At the moment vaccination is the best intervention method that is used to reduce HPV infection. However, in developing countries with poor economies, not all women and girls can access the HPV vaccine because it is expensive. There is not enough education on the importance of vaccination within such nations and therefore the high cervical cancer prevalence in such regions. The researchers envisage that more can be done to enable the easy access of HPV vaccines by women, girls and probably boys in developing countries that are ravished by high HIV transmission.

5.2 Recommendations from the study

From the study we have the following recommendations;

- Early administration of the HPV prophylactic vaccine is recommended as it blocks the acquisition and occurrence of HPV. It is in this regard that we also recommend that HPV vaccination be made mandatory to reduce the prevalence of HPV.
- Vaccination of HIV positive women and girls should be encouraged as it reduces the occurrence of HPV in immune compromised individuals.
- To reduce HPV infection among HIV infected women there is need for an effective use of a combination of RTIs and PIs (cART) drugs as evidenced by the study presented.
- Adherence to cART among HIV-infected women needs to be carefully monitored and cART to be initiated early to reduce HPV infections.

5.3 Future work on HPV in-host dynamics

Real-life infection dynamics in-host are more stochastic than deterministic, especially when referring to dynamics of infections such as that of HPV. This is because of the random fluctuations that occur during the interaction of cells and the virus. Stochastic model results tend to be more useful as compared to deterministic model results because stochastic models produce a distribution of possible outcomes while deterministic models provide single outcomes. In relation to modelling stochasticity in-host several research papers have been produced on the subject matter especially in line with HIV dynamics as indicated in [20, 112, 22, 85, 104, 54] just to name a few. Latency is stochastic and the above studies present the perturbation dynamics

of HIV in-host. However, the models presented did not look at the dynamics of infection in the presence of cell proliferation and immune response which is an aspect we will consider in our future work on the stochasticity of HPV.

Ryser *et al.* [80], in their work on HPV, outlined the importance of stochasticity on the dynamics of HPV. They explained that clearance of HPV infection is highly dependent on an alert immune response system but it is also important to consider the potential contribution of "chance". A lot of randomness surrounds cell dynamics of an infected epithelium and due to this stochastic perturbations are assumed to occur within the basal layer and these contribute to the clearance of new infections. Ryser *et al.* formulated a stochastic model that was based on the theory of branching processes. The model was combined with mechanistic models that used epidemiological data at population level and the results suggested that "chance" played a critical role in the clearance of HPV [80]. The study further went on to reveal that within immune-competent individuals, the immune response can clear about 20% of infections while the rest 80% are taken care of by stochastic proliferation dynamics within the basal layer [80]. We propose for future research the creation of an in-host model for HPV with stochastic perturbations to ascertain the role of "chance" on the dynamics of HPV especially in HIV-positive women and girls.

We also recommend the extension of the basic model to include the effect of antibodies on the dynamics of HPV, so far the only consideration has been that of the antibodies induced by the vaccine. So the modified model can, in addition to the CTLs, also include neutralising antibodies. Finally the model can be extended to include optimal control strategies that can effectively reduce the burden of HPV.

Bibliography

[1] Adler, D. H., Kakinami, L., Modisenyane, T., Tshabangu, N., Mohapi, L., De Bruyn, G., Martinson, N. A., and Omar, T. Increased regression and decreased incidence of human papillomavirus-related cervical lesions among HIV-infected women on HAART. *AIDS (London, England) 26*, 13 (2012), 1645.

[2] Allali, K. Stability analysis and optimal control of hpv infection model with early-stage cervical cancer. *Biosystems 199* (2021), 104321.

[3] Allali, K., Danane, J., and Kuang, Y. Global analysis for an HIV infection model with CTL immune response and infected cells in eclipse phase. *Applied Sciences 7*, 8 (2017), 861.

[4] Amador-Molina, A., Hernández-Valencia, J., Lamoyi, E., Contreras-Paredes, A., and Lizano, M. Role of innate immunity against human papillomavirus (HPV) infections and effect of adjuvants in promoting specific immune response. *Viruses 5*, 11 (2013), 2624–2642.

[5] András, I. E., Pu, H., Deli, M. A., Nath, A., Hennig, B., and Toborek, M. HIV-1 Tat protein alters tight junction protein expression and distribution in cultured brain endothelial cells. *Journal of neuroscience research 74*, 2 (2003), 255–265.

[6] Arbyn, M., Weiderpass, E., Bruni, L., de Sanjosé, S., Saraiya, M., Ferlay, J., and Bray, F. Estimates of incidence and mortality of cervical cancer in 2018: a worldwide analysis. *The Lancet Global Health 8*, 2 (2020), e191–e203.

[7] Arriola, L., and Hyman, J. Lecture notes, forward and adjoint sensitivity analysis: with applications in dynamical systems. *Linear Algebra and Optimisation Mathematical and Theoretical Biology Institute, Summer* (2005).

[8] Asih, T. S. N., Lenhart, S., Wise, S., Aryati, L., Adi-Kusumo, F., Hardianti, M. S., and Forde, J. The dynamics of HPV infection and cervical cancer cells. *Bulletin of mathematical biology 78*, 1 (2016), 4–20.

[9] Ault, K. A. Epidemiology and natural history of human papillomavirus infections in the female genital tract. *Infectious diseases in obstetrics and gynecology 2006* (2006).

[10] Bai, F., Huff, K. E., and Allen, L. J. The effect of delay in viral production in within-host models during early infection. *Journal of biological dynamics 13*, sup1 (2019), 47–73.

[11] Bhunu, C., Garira, W., and Mukandavire, Z. Modeling HIV/AIDS and tuberculosis coinfection. *Bulletin of mathematical biology 71*, 7 (2009), 1745–1780.

[12] Burd, E. M. Human papillomavirus and cervical cancer. *Clinical microbiology reviews 16*, 1 (2003), 1–17.

[13] Carter, J. R., Ding, Z., and Rose, B. R. HPV infection and cervical disease: a review. *Australian and New Zealand Journal of Obstetrics and Gynaecology 51*, 2 (2011), 103–108.

[14] Castell-Rodríguez, A., Piñón-Zárate, G., Herrera-Enríquez, M., Jarquín-Yáñez, K., and Medina-Solares, I. Dendritic cells: Location, function, and clinical implications. In *Biology of Myelomonocytic Cells*. IntechOpen, 2017.

[15] Castillo-Chavez, C., and Song, B. Dynamical models of tuberculosis and their applications. *Mathematical biosciences and engineering 1*, 2 (2004), 361–404.

[16] Chomiczewska, D., Trznadel-Budźko, E., Kaczorowska, A., and Rotsztejn, H. The role of langerhans cells in the skin immune system. *Polski merkuriusz lekarski: organ Polskiego Towarzystwa Lekarskiego 26*, 153 (2009), 173–177.

[17] Chow, L. T., Broker, T. R., and Steinberg, B. M. The natural history of human papillomavirus infections of the mucosal epithelia. *Apmis 118*, 6-7 (2010), 422–449.

[18] Clifford, G. M., Goncalves, M. A. G., Franceschi, S., HPV, study group, H., et al. Human papillomavirus types among women infected with HIV: a meta-analysis. *Aids 20*, 18 (2006), 2337–2344.

[19] Cobo, F. *Human papillomavirus infections: From the laboratory to clinical practice*. Elsevier, 2012.

[20] Conway, J. M., and Coombs, D. A stochastic model of latently infected cell reactivation and viral blip generation in treated hiv patients. *PLoS computational biology 7*, 4 (2011), e1002033.

[21] Corey, L., Wald, A., Celum, C. L., and Quinn, T. C. The effects of herpes simplex virus-2 on HIV-1 acquisition and transmission: a review of two overlapping epidemics. *JAIDS Journal of Acquired Immune Deficiency Syndromes 35*, 5 (2004), 435–445.

[22] Dalal, N., Greenhalgh, D., and Mao, X. A stochastic model for internal HIV dynamics. *Journal of Mathematical Analysis and Applications 341*, 2 (2008), 1084–1101.

[23] Derrick, W. 5.1. grossman. 1976. elementary differential equations with applications.

[24] Du, P. Human papillomavirus infection and cervical cancer in HIV+ women. In *HIV/AIDS-Associated Viral Oncogenesis*. Springer, 2019, pp. 105–129.

[25] Elbasha, E. H. Impact of prophylactic vaccination against human papillomavirus infection. *Contemporary Mathematics 410* (2006), 113–128.

[26] Elbasha, E. H. Global stability of equilibria in a two-sex HPV vaccination model. *Bulletin of Mathematical Biology 70*, 3 (2008), 894.

[27] Elbasha, E. H., Dasbach, E. J., and Insinga, R. P. Model for assessing human papillomavirus vaccination strategies. *Emerging infectious diseases 13*, 1 (2007), 28.

[28] Erwin, S. H. *Mathematical Models of Immune Responses to Infectious Diseases*. PhD thesis, Virginia Tech, 2017.

[29] Fedrizzi, E. N., Laureano, J. K., Schlup, C., Campos, M. O., and Menezes, M. E. Human papillomavirus (HPV) infection in HIV positive women of florianópolis, state of santa catarina, brazil. *DST-J bras Doenças Sex Transm 23*, 4 (2011), 210–214.

[30] Fife, K. H., Wu, J. W., Squires, K. E., Watts, D. H., Andersen, J. W., and Brown, D. R. Prevalence and persistence of cervical human papillomavirus infection in hiv-positive women initiating highly-active antiretroviral therapy. *Journal of acquired immune deficiency syndromes (1999) 51*, 3 (2009), 274.

[31] Franco, E. L., and Harper, D. M. Vaccination against human papillomavirus infection: a new paradigm in cervical cancer control. *Vaccine 23*, 17-18 (2005), 2388–2394.

[32] Freitas, B. C., Suehiro, T. T., Consolaro, M., and Silva, V. Hpv infection and cervical abnormalities in HIV positive women in different regions of Brazil, a middle-income country. *Asian Pac J Cancer Prev 16*, 18 (2015), 8085–8091.

[33] Gatenby, R. A., and Gawlinski, E. T. The glycolytic phenotype in carcinogenesis and tumor invasion: insights through mathematical models. *Cancer research 63*, 14 (2003), 3847–3854.

[34] Giuliano, A. R., Lu, B., Nielson, C. M., Flores, R., Papenfuss, M. R., Lee, J.-H., Abrahamsen, M., and Harris, R. B. Age-specific prevalence, incidence, and duration of human papillomavirus infections in a cohort of 290 US men. *The Journal of infectious diseases 198*, 6 (2008), 827–835.

[35] Gomero, B. Latin hypercube sampling and partial rank correlation coefficient analysis applied to an optimal control problem.

[36] Gravitt, P., and Winer, R. Natural history of HPV infection across the lifespan: Role of viral latency. *Viruses 9*, 10 (2017), 267.

[37] Gurmu, E. D., Kumsa, B., and Koya, P. R. Optimal control strategy on human papilloma virus (HPV) model with backward bifurcation analysis.

[38] Hernandez, B. Y., Wilkens, L. R., Zhu, X., Thompson, P., McDuffie, K., Shvetsov, Y. B., Kamemoto, L. E., Killeen, J., Ning, L., and Goodman, M. T. Transmission of human papillomavirus in heterosexual couples. *Emerging infectious diseases 14*, 6 (2008), 888.

[39] Huibregtse, J. M., and Beaudenon, S. L. Mechanism of HPV E6 proteins in cellular transformation. In *Seminars in cancer biology* (1996), vol. 7, Elsevier, pp. 317–326.

[40] Hunt, S. D. *Modelling the Spread of the Human Papillomavirus on the Cervix*. PhD thesis, 2015.

[41] InformedHealth.org [Internet]. Cologne, G. I. f. Q., and in Health Care (IQWiG), E. The innate and adaptive immune systems.

[42] Jafari, M., and Ansari-Pour, N. Why, when and how to adjust your p values? *Cell Journal (Yakhteh) 20*, 4 (2019), 604.

[43] Kassa, S. M., Njagarah, J. B., and Terefe, Y. A. Analysis of the mitigation strategies for COVID-19: from mathematical modelling perspective. *Chaos, Solitons & Fractals 138* (2020), 109968.

[44] Keele, B. F., and Estes, J. D. Barriers to mucosal transmission of immunodeficiency viruses. *Blood 118*, 4 (2011), 839–846.

[45] Kermark, M., and Mckendrick, A. Contributions to the mathematical theory of epidemics. Part i. *Proc. r. soc. a 115*, 5 (1927), 700–721.

[46] Kojic, E. M., Rana, A. I., and Cu-Uvin, S. Human papillomavirus vaccination in HIV-infected women: need for increased coverage. *Expert review of vaccines 15*, 1 (2016), 105–117.

[47] Konopnicki, D., De Wit, S., and Clumeck, N. HPV and HIV coinfection: a complex interaction resulting in epidemiological, clinical and therapeutic implications. *Future Virology 8*, 9 (2013), 903–915.

[48] Konopnicki, D., Manigart, Y., Gilles, C., Barlow, P., de Marchin, J., Feoli, F., Larsimont, D., Delforge, M., De Wit, S., and Clumeck, N. Sustained viral suppression and higher CD4+ T-cell count reduces the risk of persistent cervical high-risk human papillomavirus infection in HIV-positive women. *The Journal of infectious diseases 207*, 11 (2013), 1723–1729.

[49] Korostil, I. A., Peters, G. W., Cornebise, J., and Regan, D. G. Adaptive Markov chain Monte Carlo forward projection for statistical analysis in epidemic modelling of human papillomavirus. *Statistics in medicine 32*, 11 (2013), 1917–1953.

[50] La Salle, J. P. An invariance principle in the theory of stability.

[51] Lacey, C. J. HPV vaccination in HIV infection. *Papillomavirus Research 8* (2019), 100174.

[52] Li, M. Y. *An introduction to mathematical modeling of infectious diseases*, vol. 2. Springer, 2018.

[53] Lissouba, P., Van de Perre, P., and Auvert, B. Association of genital human papillomavirus infection with HIV acquisition: a systematic review and meta-analysis. *Sexually transmitted infections 89*, 5 (2013), 350–356.

[54] Liu, J., Wang, Y., Liu, L., and Zhao, T. A stochastic hiv infection model with latent infection and antiretroviral therapy. *Discrete Dynamics in Nature and Society 2018* (2018).

[55] Maglennon, G. A., and Doorbar, J. Suppl 2: The biology of papillomavirus latency. *The open virology journal 6* (2012), 190.

[56] Marino, S., Hogue, I. B., Ray, C. J., and Kirschner, D. E. A methodology for performing global uncertainty and sensitivity analysis in systems biology. *Journal of theoretical biology 254*, 1 (2008), 178–196.

[57] McClymont, E., Lee, M., Raboud, J., Coutlée, F., Walmsley, S., Lipsky, N., Loutfy, M., Trottier, S., Smaill, F., Klein, M. B., et al. The efficacy of the quadrivalent human papillomavirus vaccine in girls and women living with human immunodeficiency virus. *Clinical Infectious Diseases 68*, 5 (2019), 788–794.

[58] McClymont, E., Ogilvie, G., Albert, A., Johnston, A., Raboud, J., Walmsley, S., Lipsky, N., Loutfy, M., Trottier, S., Smaill, F., et al. Impact of quadrivalent HPV vaccine dose spacing on immunologic response in women living with HIV. *Vaccine* (2020).

[59] McLaughlin-Drubin, M. E., and Meyers, C. Evidence for the coexistence of two genital HPV types within the same host cell in vitro. *Virology 321*, 2 (2004), 173–180.

[60] Meyer, C. D. *Matrix analysis and applied linear algebra*, vol. 71. Siam, 2000.

[61] Minkoff, H., Zhong, Y., Burk, R. D., Palefsky, J. M., Xue, X., Watts, D. H., Levine, A. M., Wright, R. L., Colie, C., D'Souza, G., et al. Influence of adherent and effective antiretroviral therapy use on human papillomavirus infection and squamous intraepithelial lesions in human immunodeficiency viruspositive women. *The Journal of infectious diseases 201*, 5 (2010), 681–690.

[62] Moscicki, A.-B. Natural history of hpv infection latency and clearance. *Indian Journal of Gynecologic Oncology 19*, 3 (2021), 1–4.

[63] Murall, C. L. *The ecology within: health implications of within-host ecology.* PhD thesis, 2013.

[64] Murall, C. L., Bauch, C. T., and Day, T. Could the human papillomavirus vaccines drive virulence evolution? *Proc. R. Soc. B 282*, 1798 (2015), 20141069.

[65] Myers, E. Mathematical models as research tools for HPV disease. *PAPILLOMAVIRUS REPORT 13*, 5 (2002), 141–144.

[66] Ngina, P., Mbogo, R. W., and Luboobi, L. S. The in vivo dynamics of HIV infection with the influence of Cytotoxic T Lymphocyte cells. *International scholarly research notices 2017* (2017).

[67] Ngina, P., Mbogo, R. W., and Luboobi, L. S. Modelling optimal control of in-host HIV dynamics using different control strategies. *Computational and mathematical methods in medicine 2018* (2018).

[68] Ngina, P. M., Mbogo, R. W., and Luboobi, L. S. Mathematical modelling of in-vivo dynamics of HIV subject to the influence of the CD8+ T-cells. *Applied Mathematics 8*, 8 (2017), 1153–1179.

[69] Njagarah, J. B., Nyabadza, F., Kgosimore, M., and Hui, C. Significance of antiviral therapy and CTL-mediated immune response in containing hepatitis B and C virus infection. *Applied Mathematics and Computation 397* (2021), 125926.

[70] Omame, A., Okuonghae, D., Umana, R., and Inyama, S. Analysis of a co-infection model for hpv-tb. *Applied Mathematical Modelling 77* (2020), 881–901.

[71] on the Evaluation of Carcinogenic Risks to Humans, I. W. G., on the Evaluation of Carcinogenic Risks to Humans. Meeting, I. W. G., Organization, W. H., and for Research on Cancer, I. A. *Human papillomaviruses.* World Health Organization, 2007.

[72] Organization, W. H., et al. Human papillomavirus vaccines: WHO position paper, May 2017–Recommendations. *Vaccine 35*, 43 (2017), 5753–5755.

[73] Passmore, J.-A. S., and Williamson, A.-L. Host immune responses associated with clearance or persistence of human papillomavirus infections. *Current Obstetrics and Gynecology Reports 5*, 3 (2016), 177–188.

[74] Perelson, A. S., Kirschner, D. E., and De Boer, R. Dynamics of hiv infection of cd4+ t cells. *Mathematical biosciences 114*, 1 (1993), 81–125.

[75] Perelson, A. S., and Nelson, P. W. Mathematical analysis of HIV-1 dynamics in vivo. *SIAM review 41*, 1 (1999), 3–44.

[76] Perko, L. *Differential equations and dynamical systems*, vol. 7. Springer Science & Business Media, 2013.

[77] Pourbashash, H., Pilyugin, S. S., De Leenheer, P., and McCluskey, C. Global analysis of within host virus models with cell-to-cell viral transmission. *Discrete Contin. Dyn. Syst. Ser. B 19* (2014), 3341–3357.

[78] Ribassin-Majed, L., and Lounes, R. A SIS model for human papillomavirus transmission.

[79] Ribassin-Majed, L., Lounes, R., and Clémençon, S. Deterministic modelling for transmission of Human Papillomavirus 6/11: impact of vaccination. *Mathematical medicine and biology: a journal of the IMA 31*, 2 (2014), 125–149.

[80] Ryser, M. D., Myers, E. R., and Durrett, R. HPV clearance and the neglected role of stochasticity. *PLoS computational biology 11*, 3 (2015), e1004113.

[81] Sanchez, A. Y. C., Aerts, M., Shkedy, Z., Vickerman, P., Faggiano, F., Salamina, G., and Hens, N. A mathematical model for HIV and hepatitis C co-infection and its assessment from a statistical perspective. *Epidemics 5*, 1 (2013), 56–66.

[82] Sasagawa, T., Takagi, H., and Makinoda, S. Immune responses against human papillomavirus (HPV) infection and evasion of host defense in cervical cancer. *Journal of Infection and Chemotherapy 18*, 6 (2012), 807–815.

[83] Sasvári, Z. *Positive definite and definitizable functions*, vol. 2. Vch Pub, 1994.

[84] Schiffman, M., Clifford, G., and Buonaguro, F. M. Classification of weakly carcinogenic human papillomavirus types: addressing the limits of epidemiology at the borderline. *Infectious agents and cancer 4*, 1 (2009), 8.

[85] Shaikhet, L., and Korobeinikov, A. Stability of a stochastic model for HIV-1 dynamics within a host. *Applicable Analysis 95*, 6 (2016), 1228–1238.

[86] Sharomi, O., Podder, C., Gumel, A., and Song, B. Mathematical analysis of the transmission dynamics of HIV/TB coinfection in the presence of treatment. *Mathematical Biosciences and Engineering 5*, 1 (2008), 145.

[87] Shrestha, S., Sudenga, S. L., Smith, J. S., Bachmann, L. H., Wilson, C. M., and Kempf, M. C. The impact of highly active antiretroviral therapy on prevalence and incidence of cervical human papillomavirus infections in HIV-positive adolescents. *BMC infectious diseases 10*, 1 (2010), 295.

[88] Shuai, Z., and van den Driessche, P. Global stability of infectious disease models using Lyapunov functions. *SIAM Journal on Applied Mathematics 73*, 4 (2013), 1513–1532.

[89] Silins, I., Avall-Lundqvist, E., Tadesse, A., Jansen, K. U., Stendahl, U., Lenner, P., Zumbach, K., Pawlita, M., Dillner, J., and Frankendal, B. Evaluation of antibodies to human papillomavirus as prognostic markers in cervical cancer patients. *Gynecologic oncology 85*, 2 (2002), 333–338.

[90] SMITH, R. J., LI, J., MAO, J., and SAHAI, B. Using within-host mathematical modelling to predict the long-term outcome of human papillomavirus vaccines.

[91] Srivastava, P., Banerjee, M., and Chandra, P. Modeling the drug therapy for hiv infection. *Journal of Biological Systems 17*, 02 (2009), 213–223.

[92] Stanley, M. Immune responses to human papillomavirus. *Vaccine 24* (2006), S16–S22.

[93] Steben, M., and Duarte-Franco, E. Human papillomavirus infection: epidemiology and pathophysiology. *Gynecologic oncology 107*, 2 (2007), S2–S5.

[94] Tarfulea, N. A mathematical model for CTL effect on a latently infected cell inclusive HIV dynamics and treatment. In *AIP Conference Proceedings* (2017), vol. 1895, AIP Publishing LLC, p. 070005.

[95] Toots, M., Ustav Jr, M., Männik, A., Mumm, K., Tämm, K., Tamm, T., Ustav, E., and Ustav, M. Identification of several high-risk HPV inhibitors and drug targets with a novel high-throughput screening assay. *Plos pathogens 13*, 2 (2017), e1006168.

[96] Tsibris, A. M., and Hirsch, M. S. Antiretroviral therapy for human immunodeficiency virus infection. *Mandell: Mandell, Douglas, and Bennetts Principles and Practice of Infectious Diseases. 1st ed. London: Churchill Livingstone* (2009), 1833–54.

[97] Tugizov, S. M., Herrera, R., Chin-Hong, P., Veluppillai, P., Greenspan, D., Berry, J. M., Pilcher, C. D., Shiboski, C. H., Jay, N., Rubin, M., et al. HIV-associated disruption of mucosal epithelium facilitates paracellular penetration by human papillomavirus. *Virology 446*, 1-2 (2013), 378–388.

[98] Van den Driessche, P., and Watmough, J. Reproduction numbers and subthreshold endemic equilibria for compartmental models of disease transmission. *Mathematical biosciences 180*, 1-2 (2002), 29–48.

[99] Verma, M., Erwin, S., Abedi, V., Hontecillas, R., Hoops, S., Leber, A., Bassaganya-Riera, J., and Ciupe, S. M. Modeling the mechanisms by which HIV-associated immunosuppression influences hpv persistence at the oral mucosa. *PloS one 12*, 1 (2017), e0168133.

[100] Vivier, E., Tomasello, E., Baratin, M., Walzer, T., and Ugolini, S. Functions of natural killer cells. *Nature immunology 9*, 5 (2008), 503–510.

[101] Wang, J. W., and Roden, R. B. Virus-like particles for the prevention of human papillomavirus-associated malignancies. *Expert review of vaccines 12*, 2 (2013), 129–141.

[102] Wang, L., and Li, M. Y. Mathematical analysis of the global dynamics of a model for HIV infection of CD4+ T cells. *Mathematical Biosciences 200*, 1 (2006), 44–57.

[103] Wang, X., and Wang, J. Modeling the within-host dynamics of cholera: bacterial–viral interaction. *Journal of biological dynamics 11*, sup2 (2017), 484–501.

[104] Wang, Y., Jiang, D., Hayat, T., and Ahmad, B. A stochastic HIV infection model with T-cell proliferation and CTL immune response. *Applied Mathematics and Computation 315* (2017), 477–493.

[105] Wang, Y., Liu, J., and Liu, L. Viral dynamics of an HIV model with latent infection incorporating antiretroviral therapy. *Advances in Difference Equations 2016*, 1 (2016), 1–15.

[106] Wang, Y., and Zhou, Y.-c. Mathematical modeling and dynamics of HIV progression and treatment. *Chinese Journal of Engineering Mathematics 27*, 3 (2010), 534–548.

[107] Wester, T. Analysis and simulation of a mathematical model of Ebola virus dynamics in vivo. *Society for Industrial and Applied Mathematics 8* (2015), 236–256.

[108] Wilson, R., and Laimins, L. A. Differentiation of HPV-containing cells using organotypic raft culture or methylcellulose. In *Human Papillomaviruses*. Springer, 2005, pp. 157–169.

[109] Xu, H., Wang, X., and Veazey, R. S. Mucosal immunology of HIV infection. *Immunological reviews 254*, 1 (2013), 10–33.

[110] Yang, D. Y., and Bracken, K. Update on the new 9-valent vaccine for human papillomavirus prevention. *Canadian Family Physician 62*, 5 (2016), 399–402.

[111] Zhang, K., Wang, X. W., Liu, H., Ji, Y. P., Pan, Q., Wei, Y. M., and Ma, X. Mathematical analysis of a human papillomavirus transmission model with vaccination and screening. *Mathematical Biosciences and Engineering 17*, 5 (2020), 5449–5476.

[112] Zhao, Y., and Jiang, D. The behavior of an SVIR epidemic model with stochastic perturbation. In *Abstract and Applied Analysis* (2014), vol. 2014, Hindawi.